A X-RAY SCANNING MACHINE FOR IMAGING ATOMIC ELEMENTS

A.G.R. FENELON

A THESIS FOR THE DEGREE OF

MASTER OF SCIENCE

PRESENTED TO

THE NATIONAL COUNCIL FOR EDUCATIONAL AWARDS

THE SCHOOL OF PHYSICAL SCIENCES

NATIONAL INSTITUTE FOR HIGHER EDUCATION, DUBLIN

RESEARCH SUPERVISOR

JOSEPH FRYAR

MAY 1988

DECLARATION

This thesis is based on my own work.

ABSTRACT

X-ray computer axial tomography is a well established technique for producing images which show the spatial variation of X-ray linear attenuation coefficient within an object. X-ray differential K absorbtion edge tomography is the application of computer axial tomography to form images of selected atomic elements within an object, and these images show the distribution of specific atomic element concentration.

The technique is to measure the attenuation of X-rays on either side of the K absorbtion edge of an atomic element with an energy dispersive X-ray detector, and then reconstruct an image of the location and concentration of that element in an object by means of a computer algorithm for display on a colour monitor. This method is able to image several atomic elements in one X-ray scan only of the object, in particular, consecutive elements in the Periodic Table of the Elements.

One atomic element only within the object may be better selected by correcting for the X-ray attenuation of all the other elements, the matrix of the object, by extrapolating the measurements to the K absorbtion edge, thus measuring accurately the absorbtion coefficient of the analyte element only. The concentration of analyte element may be measured down to about $1 kg/m^3$ in a water like matrix with a total of 10^8 photons.

Herein is described the construction of an X-ray machine as a differential K absorbtion edge spectrometer, and the application of this technique to image three chosen atomic elements, 46Palladium, 47Silver, and 48Cadmium using the spectrometer. Experiments which showed that this technique works, and possible further development of the spectrometer, are also described.

CONTENTS

FIGURE INDEX

PLATE INDEX

TABLE INDEX

CHAPTER I

RESUME AND HISTORICAL REVIEW

This work is a way of forming images of the internal structure of objects by means of X-rays. It is a a study of method of imaging atomic elements within an object, and the construction of an X-ray scanning machine for carrying it out. The work consists of three interdependent parts: theory and planning, experimental method and instruments, and image reconstruction of detected elements. The part herein is primarily in relation to experimental method and instruments.

The formal description of this work may be stated as a method and scanning machine for imaging atomic elements by differential X-ray absorbtion edge tomography and computer axial tomography.

X-rays were applied to medical and industrial radiography within a year of their discovery by W.K. Rontgen [1] in November 1895. A photographic plate, which has been placed behind an object and irradiated with X-rays, on development shows a shadow of all planes parallel to the plate within the object in the path of the X-rays as image density variations. Focal plane tomography, invented in 1921 by E.M. Bocage, is a technique which attempts to form a clear image of a particular plane within an object without superimposed images of all the other planes on the photographic plate.

Modern tomography, or computer axial tomography, made possible by the invention of the computer was applied to medical imaging in 1971 by G.N. Hounsfield [2]. The E.M.I. scanning machine which he built was the first manufactured machine for scanning the head for medical diagnosis. The mathematical method for image reconstruction of an object scanned with X-rays had been developed by A.M. Cormack [3,4] in 1963.

There have been four generations of computer axial tomography scanning machines, illustrated in Figure 1.1, developed since the first one made in 1973 by E.M.I.. The first scanning machine had a single Sodium iodide detector and multiplier phototube, and a single collimated beam of X-rays scanned the stationary patients head in 160 linear beam steps and 180 x 1° rotations, in a disc 15mm thick taking about 4 minutes for one complete scan. The step size was 3mm using a X-ray beam 3mm x 15mm. The reconstructed image was displayed in an 80 x 80 pixel grid.

The second generation scanning machine was similar to Hounsfield's machine but had several detectors and a collimated narrow fan X-ray beam. N detectors counting X-ray photons simultaneously at each linear step could be rotated through N° instead of 1°, so that scanning time was reduced to about 20 seconds. The third generation scanning machines did not make linear steps, only angular steps and a collimated fan X-ray beam wide enough to irradiate the whole disc of the patient's head was detected by many detectors arranged on an arc, centre the X-ray beam collimator. The X-ray source and detectors rotate in steps around the patient and the X-ray photons are detected at each angular step. The fourth generation scanning machines have stationary detectors set equidistant in a 360° ring around the

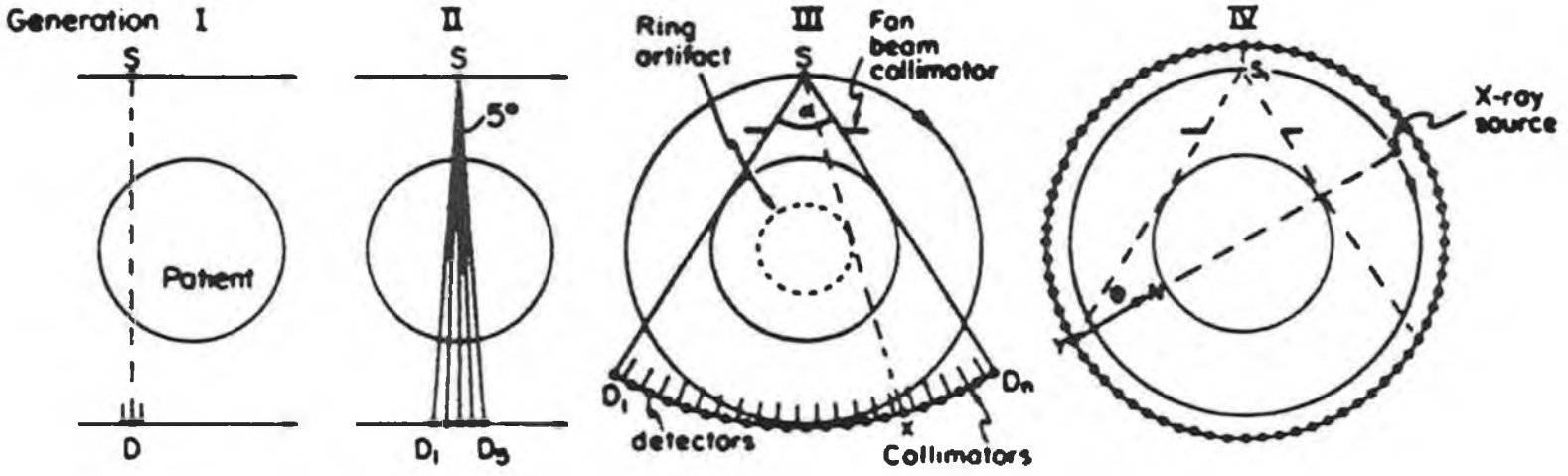

Computer axial tomography.

Schematic diagram to illustrate the development of computer axial tomography scanning machines. [H.E. Johns and J.R. Cunningham, The Physics of Radiology].

FIGURE 1.1

patient, and the X-ray source rotates around the patient to complete a scan in less than 2 seconds. Many consecutive discs can be scanned because the X-irradiation time is so short.

Computer axial tomography can show images of a plane within an object and differentiate between density variations of less than 1% in water like objects. It can differentiate qualitatively between heavy and light atomic elements, and thus help to identify a heavy element within a matrix of light elements. It cannot differentiate between elements close together in the Periodic Table of the Elements, in particular, consecutive elements.

The characteristic X-ray K absorbtion edges of the atomic elements were discovered by C.G. Barkla and C.A. Sadler [5] in 1909. In 1925 R. Glocker and W. Frohnmayer [6] first used differential K absorbtion edge spectroscopy to measure the quantity of an element in a uniform mixture of elements.

The characteristic X-ray K absorbtion edge energy of an atomic element is unique to every element and identifies that element like a fingerprint.

The X-ray K absorbtion edge is an abrupt change in absorbtion of X-rays by an atomic element at a well defined X-ray photon energy due to a quantum of energy being absorbed by the K electron shell of an atom when one of the electrons is ejected from the atom. The energy state of the atom is increased by a unique quantity characteristic of an atomic element and the energy to do this is absorbed from an incident beam of X-rays. A continuum X-ray spectrum which irradiates an atomic element has its transmitted intensity reduced for photon

energies at and above the K absorbtion edge of the absorbing element. The X-ray photons are absorbed by a K electron of the atom, and the incident photon energy is divided between the atom and the kinetic energy of the ejected K electron. At X-ray photon energies below the K absorbtion edge, the attenuation of X-rays gradually decreases with increasing energy, because the penetration of X-rays increases with photon energy. The shape of the attenuation curve is shown in Figure 2.5, and this is an empirical curve. The amount of attenuation is proportional to the number of attenuating atoms intercepted by the incident X-ray beam, so that the fraction of photons removed from the beam can be used to measure the concentration in kilograms per cubic metre of attenuating atoms.

S.J. Riederer and C.A. Mistretta [7] showed theoretically that it is possible to image selectively by computer axial tomography a 53Iodine analyte within a water like matrix using a broad band of X-rays with mean energy just below the K absorbtion edge of Iodine and one or two broad bands with mean energy above it. The object was irradiated with three filtered beams of X-rays, one with a mean energy on either side of the K absorbtion edge at 33.17keV of 53Iodine and a third beam at a slightly higher energy. The Iodine was selectively imaged using transmission measurements for every X-ray beam path through the object consisting of an annular phantom disc made by the computer simulation. The image was reconstructed from the simulated scan by Filtered Backprojection. The analyte element in this method must be known, and the K absorbtion edges of the elements in the matrix of the object must be absent or their absorbtion small within the X-ray pass bands used. It would not be possible to image elements close together or consecutive in the Periodic Table of the Elements with this method.

L. Grodzins [8,9] discussed theoretically the limitations on the sensitivity of differential absorbtion edge spectroscopy using a narrow pass band of X-rays from a synchrotron source for analyte concentration and size and type of object.

In 1984, A.C. Thompson et al [10] used a synchrotron source of X-rays, the photon energy of which could be repeatedly fine tuned above and below the K absorbtion edge of 53Iodine as analyte element to image Iodine within an excised pig heart, a water like matrix.

The work herein was originally to have been a method of identifying atomic elements within an object by measurement of the X-ray fluorescence from analyte elements. Each atomic element irradiated with sufficiently energetic X-rays emits characteristic X-ray lines, K, L, M, N, which can be used to identify the analyte element by detecting the X-ray fluorescence with an energy dispersive detector and sorting the X-ray photon pulses counted according to energy with a multichannel analyser. This method is used for surface analysis of materials, but the intensity of the isotropically radiated fluorescence X-rays is too low for transmission analysis because there is too much absorbtion of the fluorescence X-rays in a thick object.

X-rays are electromagnetic radiation at the short wavelength high energy end of the Electromagnetic Spectrum. Each region of the spectrum interacts with matter differently, and in regions where absorbtion is low, then matter is transparent or has a window for that region. In general, for X-rays, the lower the atomic number of an element, or the less dense a material is, then the more transparent the element or material is to X-rays of a particular photon energy or

wavelength. Conversely, for elements of high atomic number or materials of high density, shorter wavelength or more energetic photons are more readily transmitted than long wavelength or less energetic photons. Thus X-rays can be used to form an image of materials of varying density or varying atomic number on a detector such as a photographic plate or a fluorescent screen, these materials having a window in the X-ray region, but not necessarily in the visible or other regions of the Electromagnetic Spectrum. Materials which are opaque to some regions of the spectrum can be investigated by another region of the spectrum, or alternatively another form of energy may be used.

The X-ray spectral region of interest herein is in the photon energy range 10keV to 60keV corresponding to a wavelength of about 0.12nm to 0.02nm, detectable by the detector and X-ray machine used. This energy range can be used to detect the atomic elements 32Germanium to 68Erbium.

The method is to use the X-ray K absorbtion edge unique to each atomic element to detect and to measure the equivalent thickness of the element, the analyte, within a material, the matrix. An X-ray machine, or a radioactive X-ray emitter, is the source of X-rays of chosen energy and intensity. The matrix containing the analyte element is scanned with a collimated narrow beam of X-rays of energy overlapping the K absorbtion edge of the analyte element and the transmitted beam is intercepted by an energy dispersive X-ray detector. The scanning method employed is to move the matrix containing the analyte element transversely of the X-ray tube in consecutive small steps through the narrow X-ray beam, pausing for a

chosen time at each step and counting and recording the number of photons detected in a narrow energy band on each side of the K absorbtion edge of the analyte element. At each end of a transverse linear scan, the object is rotated through a small chosen angle, and another linear scan is made. The scanning is repeated until the object has rotated through 180°.

The scanning machine is a (x,z,ϕ) scanning coordinate table on which the object to be analysed is mounted in the X-ray beam, and is controlled automatically by means of a computer. Counting and recording of detected X-ray photons, and calculating the magnitude of absorbtion is also done by computer. This X-ray photon count data is then used to reconstruct an image of the linear absorbtion coefficient or the concentration of the object in the path of the narrow beam of X-rays, which may be shown on a colour monitor, or printed on paper. The image which is reconstructed from the data is a digital contour map or representation of the X-ray absorbtion in an axial disc through the object. The image reconstruction is done by means of a computer algorithm. Concentration of analyte elements may be measured down to a few kilograms per cubic metre with a total of about 10^8 photons.

The image reconstruction transforms radially measured radiation data through a disc in the (x,y) plane in the object to an image. The coordinate convention chosen herein is shown in Figure 3.1 in which x is the direction of the linear scanning, -y is the direction of the X-ray beam, and z is the normal to the axial planes in the object being scanned. ϕ is the rotation of the angular scanning steps.

The intensity of the X-ray beam, the beam power per unit area is referred to in the theory and in the BASIC computer programs as I_o for the incident intensity and I for the intensity of the beam after transmission through a scanned object. The flux of X-ray photons detected and counted is referred to as N_o and N for the incident and transmitted beams in the experiments: I_o and N_o, and I and N are equivalent.

The BASIC computer programs which make this work possible are listed in Annexe D in the order in which they are called, and they are referred to by their file names. They are the most recent programs developed during this work, and each is prefaced by a synopsis of what the program does, followed by a description of how it works, in some cases in detail. The experimental method and the computer programs were similar for the 20 x 20 scanning and the 40 x 40 scanning of the objects analysed.

The imaging technique convention chosen herein is that computer axial tomography forms an image of varying density proportional to the integrated linear attenuation coefficient of an object for X-rays, and differential absorbtion edge tomography forms an image of density which is proportional to the concentration of an analyte element, the X-rays being absorbed by a K absorbtion edge; it is an element-specific technique described in Chapter 3.

The very first table top absorbtion edge scanning machine which demonstrated the principle and use of K absorbtion edge spectroscopy to identify and to measure the concentration of 55Caesium, the analyte element in a 20mm diameter cork matrix, was made and operated in July 1985.

CHAPTER II

X-RAYS

X-rays are part of the Electromagnetic Spectrum shown in Figure 2.1 traditionally and informally specified by wavelength of about 10nm to 0.001nm which corresponds to a photon energy of about 120 to 1.2×10^6 electron volts, and overlaps with the ultra violet region at the low energy side and the y-ray region at the high energy side, of the spectrum. y-rays are produced as a result of energy changes taking place when the nucleus of an atom re-arranges itself, the wavelength range being from about 0.01nm to 0.0001nm corresponding to a photon energy of about 1.2×10^5 to 1.2×10^7 electron volts. Atomic X-rays are produced as a result of energy changes taking place in the whole atom due to change in energy state of bound electrons. Electrically charged particles emit electromagnetic radiation when they change velocity, and the greater the rate of change of velocity the greater is the energy change of the particle, and thus the more energetic or shorter the wavelength of the photons. When electrons are decelerated, bremsstralung or braking radiation is emitted by them, so that it is possible to produce electromagnetic radiation of shorter wavelength than y-rays which is sometimes called X-rays, but could be called bremsstralung or synchrotron radiation. Thus an X-ray tube produces bremsstralung, and may also produce atomic X-rays.

ELECTROMAGNETIC SPECTRUM.

	(Hz)	(joules)	(eV)
0.00003nm	10^{22}	6.63×10^{-12}	4.15×10^{7}
0.0003nm	10^{21}	" $\times 10^{-13}$	4.15×10^{6}
0.003nm	10^{20}	" $\times 10^{-14}$	4.15×10^{5}
0.03nm	10^{19}	" $\times 10^{-15}$	4.15×10^{4}
0.3nm	10^{18}	" $\times 10^{-16}$	4150
3nm	10^{17}	" $\times 10^{-17}$	415
30nm	10^{16}	" $\times 10^{-18}$	41.5
300nm	10^{15}	" $\times 10^{-19}$	4.15
3.0 μ	10^{14}	" $\times 10^{-20}$	0.415
30 μ	10^{13}	" $\times 10^{-21}$	0.0415
300 μ	10^{12}	" $\times 10^{-22}$	0.00415
3.0 mm	10^{11}	" $\times 10^{-23}$	4.15×10^{-4}
30 mm	10^{10}	" $\times 10^{24}$	" $\times 10^{-5}$
30 cm	10^{9}	" $\times 10^{-25}$	" $\times 10^{-6}$
3.0 m	10^{8}	" $\times 10^{-26}$	" $\times 10^{-7}$
30 m	10^{7}	" $\times 10^{-27}$	" $\times 10^{-8}$
300 m	10^{6}	" $\times 10^{-28}$	" $\times 10^{-9}$
3.0 km	10^{5}	" $\times 10^{-29}$	" $\times 10^{-10}$
30 km	10^{4}	" $\times 10^{-30}$	" $\times 10^{-11}$
300 km	10^{3}	" $\times 10^{-31}$	" $\times 10^{-12}$

FIGURE 2.1

Experiments show that X-rays are produced when electrons strike a solid material, they travel in straight lines, are not deflected by magnetic or electric fields, can travel through objects which are opaque to light, and can discharge electrically charged objects due to ionisation by the X-radiation of the surrounding air.

When an electron strikes the target of an X-ray tube it is decelerated by the nuclei of the atoms in or near the surface of the target. A photon of bremsstralung is emitted at each deceleration, as illustrated in Figure 2.2 in which an electron changes direction in the Coulomb electric field of the nucleus of an atom. In general this is true for any moving positively or negatively charged particle of mass m and charge Ze. The particle is deflected from its straight line path by the electric field of the target nucleus, atomic number Z, into a curve of radius r, and centre the nucleus. By Coulomb's Law, the force on the particle is

$$\text{force} = [k(Ze)(ze)]/r^2 \qquad (2.1)$$

$$\text{and the deceleration} = [Zz/m][ke^2/r^2] \qquad (2.2)$$

where e is the charge on the electron and k is a constant.

The rate of loss of energy E of the particle with distance x, is given by

$$-\frac{dE}{dx} \propto (Zz/m)^2 \qquad (2.3)$$

This is also proportional to the energy of the particle.

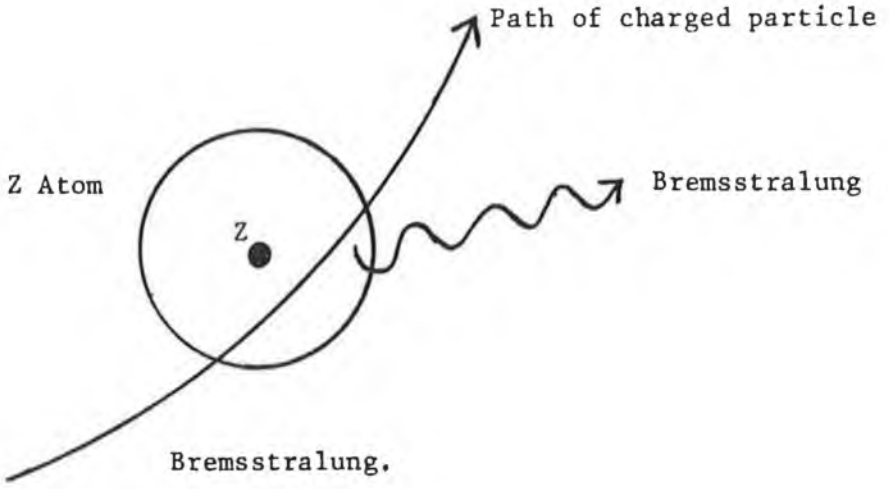

FIGURE 2.2

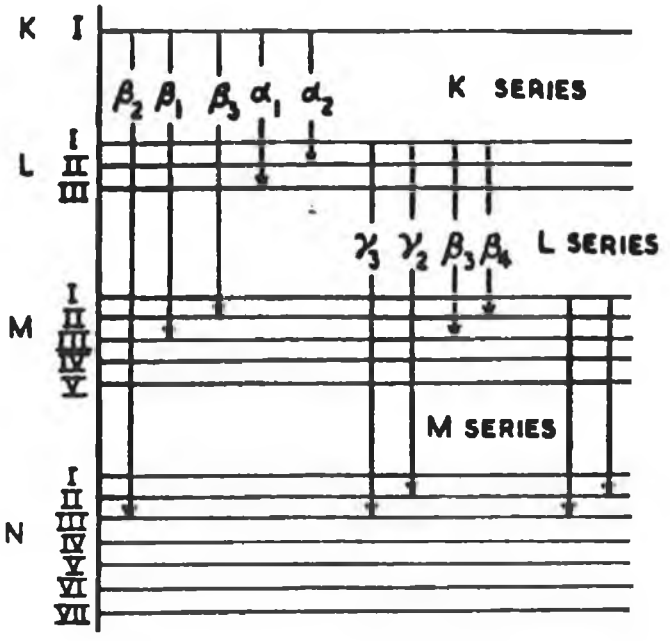

Inner orbital electron transitions.

The energy levels occupied by the inner orbital electrons of an atom and some of the transitions which produce characteristic X-rays.

[J. Yarwood, Volume II Atomic Physics].

FIGURE 2.3

Thus $$-\frac{dE}{dx} \propto E(Zz/m)^2. \qquad (2.4)$$

The X-ray spectral region available for this work is of wavelength about 1.2nm to about 0.02nm which corresponds to an energy range of 1keV, set by the lower limit of detectability of the EG & G Ortec Si(Li) detector, to 60keV, set by the Si(Li) detector upper limit and the maximum voltage of 60kV of the X-ray tube. This energy range corresponds to the energy range of the K absorbtion edges of the atomic elements 11Sodium to 68Erbium.

X-rays, like all electromagnetic radiation, have a dual wave-particle nature, the manifestation of which depends on the interaction with matter, or the experiment. The wave nature of X-rays is involved with coherent scattering, diffraction, polarisation, reflection, wavelength dispersion, and the wave and group velocity with which the X-rays are propagated. Their particle nature applies to incoherent scattering, photoelectric absorbtion, ionisation in gases, liquids, and solids, scintillation, and energy dispersion of X-ray photons. The particle nature of X-rays pertains to this work because the X-radiation beam is absorbed in materials being investigated mainly by photoelectric absorbtion, and the unabsorbed radiation is detected by an energy dispersive detector, also by photoelectric absorbtion; and because the beam is collimated, detection of scattered radiation is minimised.

There are four physical quantities which specify X-radiation: wavelength which is measured in nanometers, 1nm = 10^{-9}m; frequency , measured in Hertz, 1Hz = s^{-1}; the energy of the photon, measured in electron volts, 1eV is the energy change of an electron when it travels through an electric potential difference of 1 volt,

kiloelectron volts, keV, or megaelectron volts, MeV; and the intensity I, which is the radiation energy per unit area per second, the power per unit area. The relation between wavelength and frequency is $\nu\lambda = c$, where $c = 2.99793 \times 10^{8} ms^{-1}$ is the velocity of electromagnetic radiation in a vacuum.

The energy of the photon of electromagnetic radiation is given by $E = h$, where $h = 6.625 \times 10^{-34}$ joule.second. The relation between energy in electron volts and wavelength in nanometres is given by

$$E_{eV} \approx 1239.6/\lambda \qquad (2.5)$$

The intensity I_j in joules of a monochromatic photon of wavelength is measured as the count rate I_c given by $I_c = I_j/hc$

An atom of an element consists of a small, $\approx 10^{-15}$m diameter, dense central nucleus made up of Z protons, the atomic number of the element, and an approximately equal $(A-Z) \geq Z$ number of neutrons, where A is the atomic mass number of the element, and Z electrons arranged around the nucleus in groups or shells so that the total energy of the electrically neutral atom is a minimum. The atomic number Z is the fundamental constant of an element, not the mass number A; or the atomic weight. The electron shells are designated K, L, M, N, O, and the maximum number of electrons allowed in each shell is $2n^2$, where n is the principal quantum number, n = 1, 2, 3, 4, 5, 6.

The two electrons for which n = 1 are in the K shell. For n = 2 there are 8 electrons, in the L shell; and for n = 3, the 18 electrons are in the M shell. The closer a shell is to the nucleus, the greater the binding energy of its electrons, and the more negative potential

energy such electrons contribute to the atom. The electrons in the outermost shell are the valency electrons, and are involved in formation of molecules by covalent bonding in which two or more atoms share electrons, or ionic bonding in which one atom more electropositive than another donates one or more electrons to an acceptor atom to form an ionic molecule made up of positive and negative ions. The total energy of the molecule is thus less than that of the separately existing atoms, the energy being emitted as heat or light because the atomic energy changes are of the order of a few tenths of an electron volt to a few electron volts. The more energy that is emitted on formation of the molecule the more stable it is, or chemically inert. There are four more quantum numbers which describe the atom, and no two electrons can have identical quantum numbers. The azimuthal quantum number l describes the orbital angular momentum, determines the shape of the orbital and has values 0, 1, 2, ... (n-1). The magnetic quantum number, m = 0, ± 1, ± 2, ...± l, determines the orientation of the orbital, and so of the atom, in an external magnetic field. The spin quantum number s has values ±0.5 and describes the rotational direction of the electron. The precession quantum number is $\underline{j} = \underline{l} + \underline{s}$ where the electron spin can add to the magnetic quantum number in parallel or in antiparallel. This model of the atom and its interaction with energy was developed by spectrometry, and scattering of charged particles by the nucleus of the atom.

When an atom of an element is irradiated with charged particles or with electromagnetic radiation, an electron in the atom may be excited to a higher energy level, or the electron may be knocked out of the atom to produce a positive ion. When an electron falls to a lower,

more tightly bound energy level of the atom, or if an electron is captured by a positive ion, the atom radiates energy in the infra red, visible, ultra violet, or X-ray region of the spectrum. The energy of the photon is equal to the difference between the energy of the atom in the upper energy level or in the free state, and its energy in the lower energy level. If incident radiation is sufficiently energetic, an electron may be knocked out of an inner electron shell of a multi shell atom, and when an electron falls from an outer shell into the vacant site, a photon of radiation is emitted of a wavelength in the X-ray region of the spectrum.

When a K shell vacancy is created in an atom an electron falls from any allowed higher energy level by a spontaneous transition within 10^{-12} second of the vacancy being created, and the new vacancy is then filled by an electron in a shell further out still. Electron transitions in a large number of atoms excited by primary bombarding electrons or primary incident X-radiation produce secondary X-ray spectral lines of definite photon energy and discrete wavelength which are characteristic of the emitting element, and are radiated isotropically. This is the characteristic X-ray line spectrum of the elements discovered by C.G. Barkla [11,12] in 1906. The characteristic X-ray emission or fluorescence is superimposed in the continuum spectrum of the irradiated elements and appears as sharp peaks. The most intense X-ray spectral lines are the K_α and K_β lines which are due to electron transitions to the K shell from the L shell, and to the K shell from the M shell, respectively. Thus the photon energy of the K_β line is greater than that of the K_α line. The K_α and K_β lines for 42Molybdenum are shown in Figure 2.8 of wavelength 0.071nm and 0.063nm. All electron transitions to the K, L, M ... energy levels

further out in the atom, produce the K, L, M ... spectral lines respectively, the atom having one more electron shell than the number of spectral series.

All of the lines in a series are due to transitions to the same shell. The higher energy levels have smaller energy differences between them, so that the wavelength of the K, L, M.... lines becomes progressively longer. Because the transitions occur within 10^{-12} second, the L, M, N.... transitions for one atom and emission of the corresponding photons effectively occur in coincidence with the K shell being filled. Figure 2.3 is an energy level diagram showing some of the electron transitions from a higher energy level to a lower one, which is equivalent to a transition of the whole atom from an initial quantum state to a final quantum state. There is a maximum of two electrons in the K shell, and because n = 1, l = 0 there is only one K energy level. For the L shell n = 2, so l = 0, ± 1 and there are three possible energy sublevels for this shell, LI, LII and LIII. The $K_{\alpha 1}$, $K_{\alpha 2}$ lines are due to the electron transitions LIII, LI to the K shell. The transitions in this model of the atom are governed by selection rules, which are $\triangle N = 0$, $\triangle l = \pm 1$, and $\triangle j = 0, \pm 1$, and so allow only certain transitions. There is no transition LI to the K shell because in this case $\triangle l$ would be zero. The $K_{\beta 1}$, $K_{\beta 2}$ lines are due to transitions from the MIII and NII levels to the K shell. The $L_{\alpha 1}$, $L_{\alpha 2}$ lines are due to transitions from the MV, NIV levels to the LIII energy level. The transitions with the greatest probability of occurring result in the most intense spectral lines; the $\alpha 1$ lines for which $\triangle n = 1$ are the strongest. The normal X-ray spectra are due to singly ionised atoms in the K, L, M, N ... states, and when the energy levels are sharply defined, the spectral lines are very narrow. The

inner shells of an atom are electrically screened by the outer shells so that they are little influenced by the physical or chemical state of the atom, as are the valency electrons.

The frequency ν of a characteristic X-ray spectral line of wavelength λ increases regularly with the atomic number Z of the elements, expressed by Moseley's Law,

$$\sqrt{\nu} = k(Z - b) \quad \text{or more simply} \quad \lambda \alpha \quad 1/Z^2 \qquad (2.6)$$

where k and b are constants which are different for each spectral line K, L, M, N. Figure 2.4 shows Moseley's Law for the K and L spectral lines. The nearly linear dependance of the X-ray photon energy, $E = h\nu$ on the square of the atomic number Z shows a fundamental relation between characteristic X-ray emission and the positive nuclear charge which determines the chemical properties of atomic elements. The nucleus of the atom is electrostatically screened by the second electron in the K shell which effectively reduces the atomic number Z by b = 1. The value of k is greater for the K_β line than for the K_α line because the energy of the K_β photon is greater. The intensity of characteristic emission lines depends on the concentration of an element irradiated with X-rays or charged particles.

ABSORPTION AND SCATTERING OF X-RAYS.

All forms of energy interact with matter so as to result in four primary macroscopic effects; reflection, absorbtion, scattering, and transmission, which depend on the form of the energy, the physical properties of matter, and the four interactions occur simultaneously.

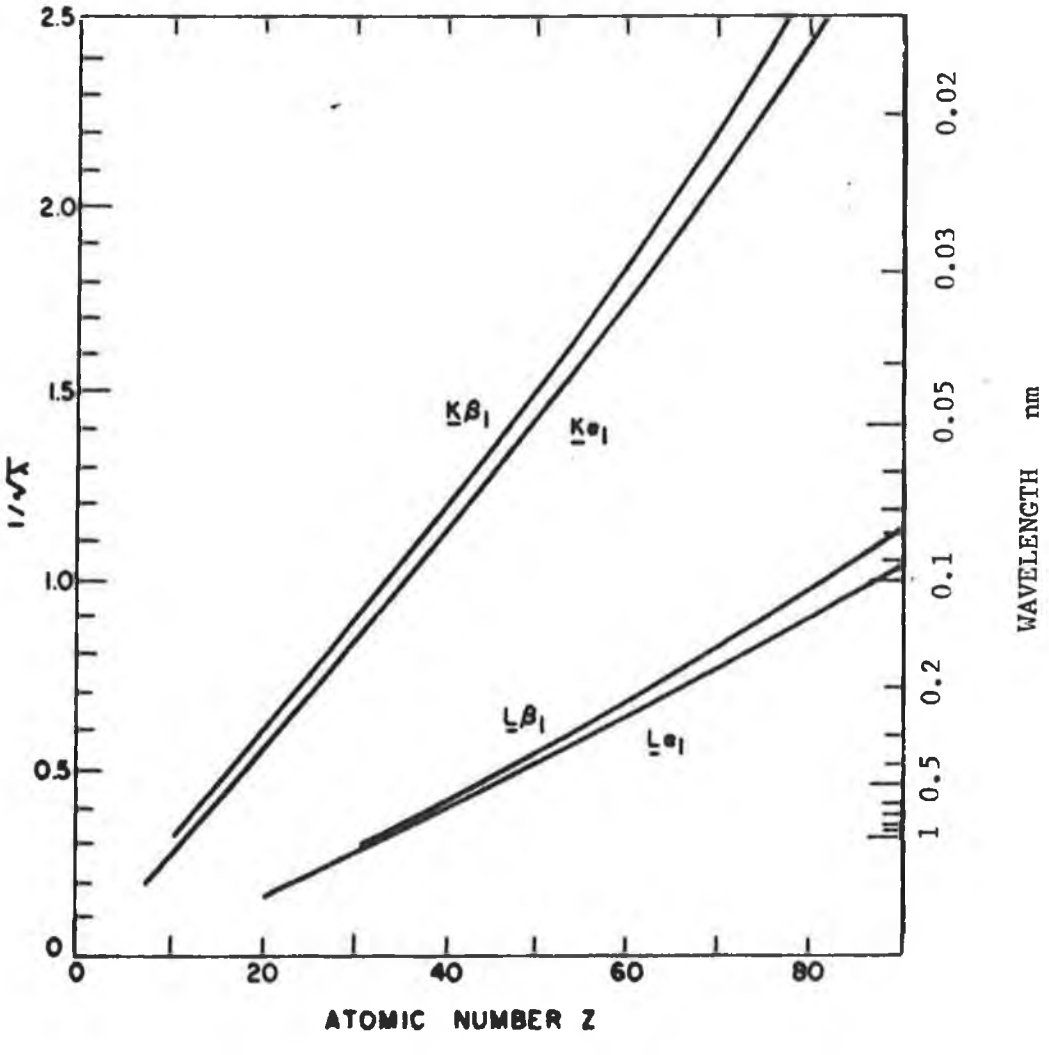

Moseley's Law.

Curves for selected X-ray spectral lines.
[E.P. Bertin, Principles and Practice of X-ray Spectrometric Analysis].

FIGURE 2.4

The macroscopic effect of scattering of X-rays is isotropic reflection for low energy radiation and partially directional reflection for high energy radiation.

The ability of an element to attenuate X-rays depends on the energy of the photon, and experiment shows that generally attenuation decreases with increasing photon energy. Attenuation of X-rays also increases with increasing atomic number of the element, the attenuation is proportional to Z^4 due to the increasing concentration of electrons. When the X-ray photon has sufficient energy to knock an electron out of the K shell of an atom, absorbtion of X-rays abruptly increases. Other electron shells give similar abrupt increases in the absorbtion of X-rays; the K and L shells being the most important, and require more energetic X-ray photons than the electron shells further out from the nucleus of the atom.

The increase in absorbtion of X-rays at a definite photon energy is an absorbtion edge of an element, and is the minimum photon energy which can expel an electron from an electron shell of the atom. The absorbtion edges are characteristic of a particular atomic element, and uniquely identify the element.

The general form of the change in the mass attenuation coefficient with X-ray photon energy, and the change in the intensity I of the transmitted X-ray beam for an atomic element are the curves shown in Figure 2.5. The lightest element which has a K absorbtion edge is 4Beryllium, of photon energy 115eV and 10.8nm wavelength in the ultrasoft X-ray region of the spectrum. The K absorbtion edge energy of the elements progressively increases with increasing atomic number,

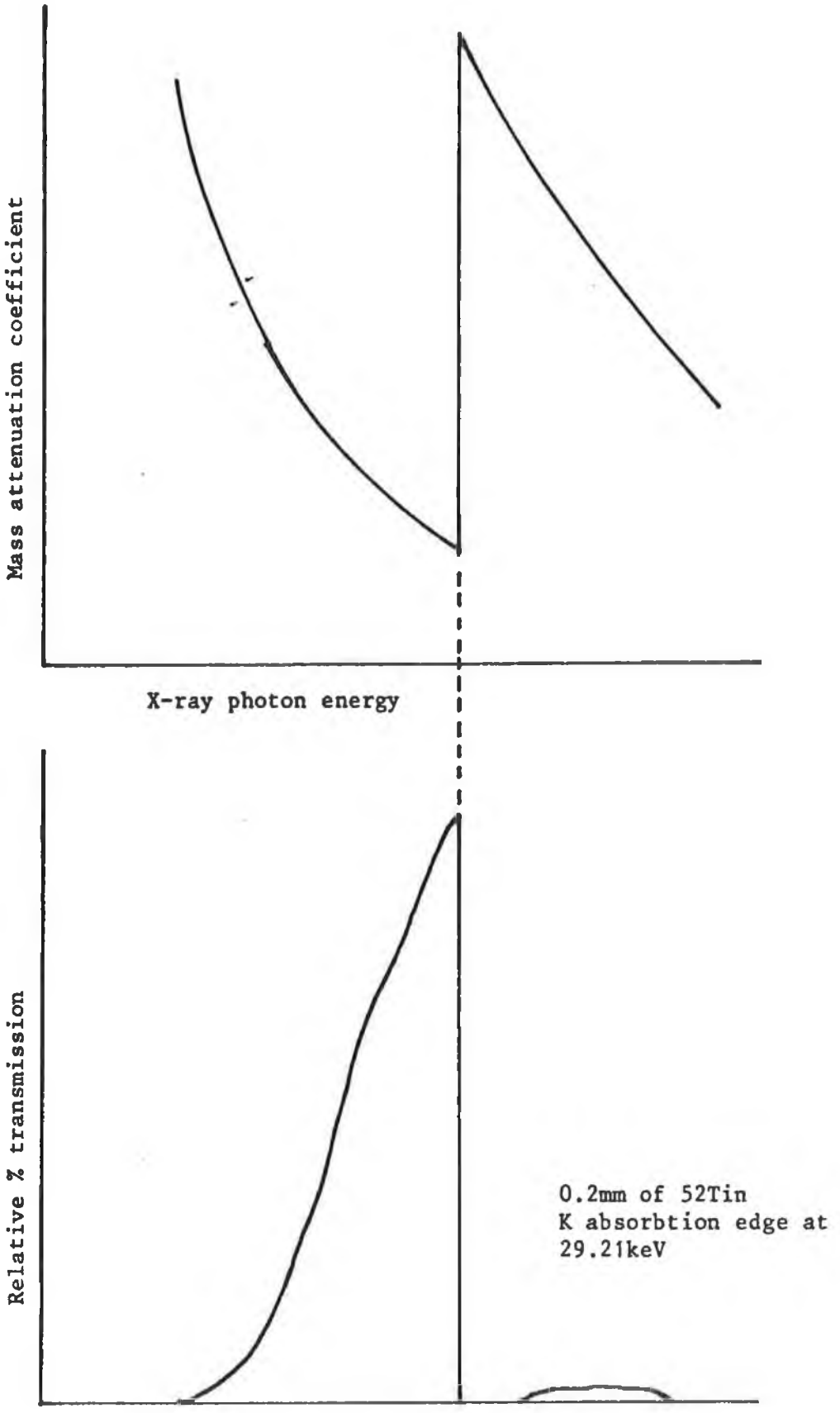

Attenuation of X-rays by an atomic element.

The change in the mass attenuation coefficient of an element, and the relative % transmission with X-ray photon energy near an absorbtion edge.

FIGURE 2.5

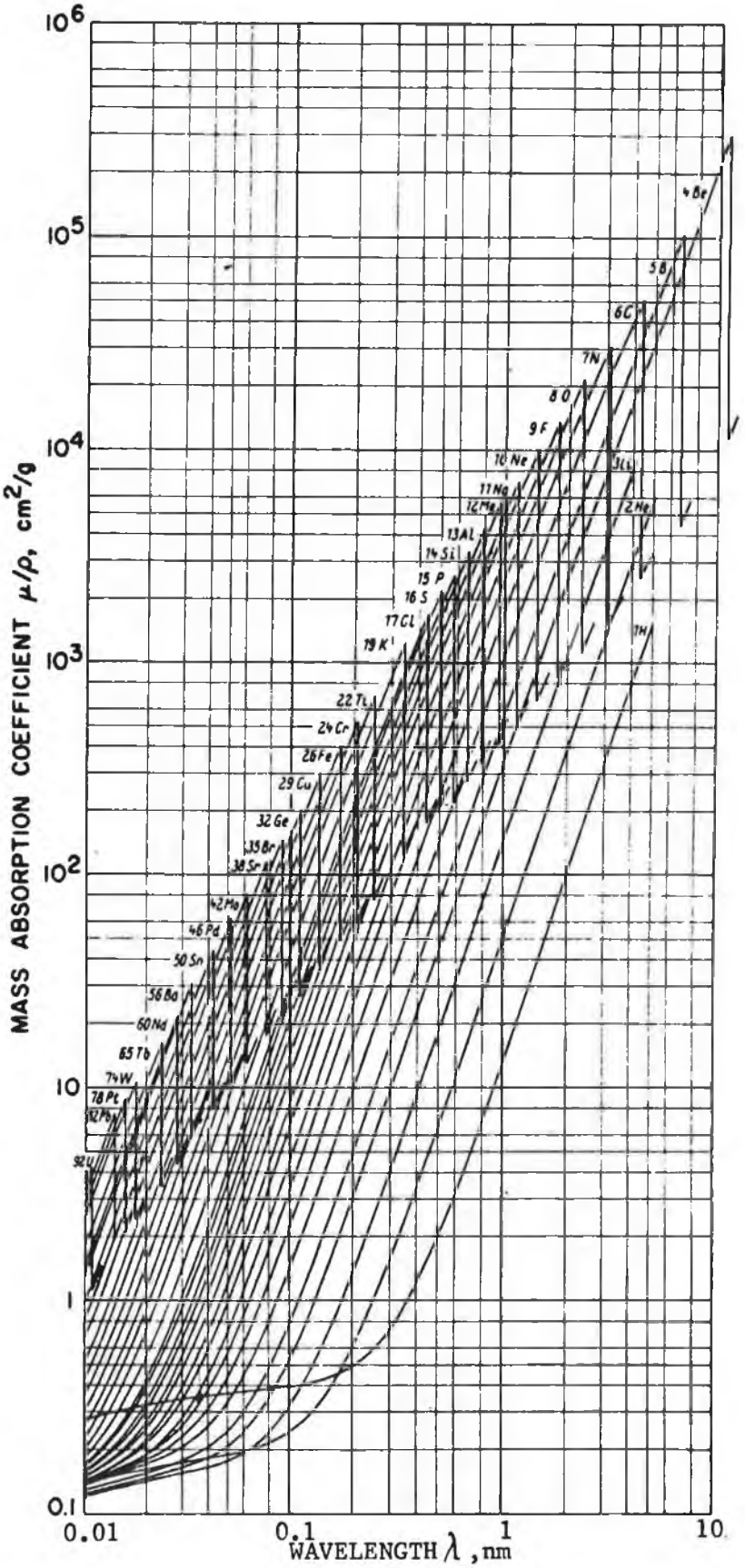

X-ray K absorbtion edges of the atomic elements.

[E.P. Bertin, Principles and Practice of X-ray Spectrometric Analysis].

FIGURE 2.6

so that for 92Uranium, the K absorbtion edge photon energy is 116keV and has a wavelength of 0.01nm. The LI absorbtion edge energies range from 62eV for 12Magnesium to 22keV for 92Uranium. Figure 2.6 shows the X-ray K absorbtion edges of the atomic elements.

The main difference between X-ray and optical spectra, illustrated in Figure 2.7, is that X-ray spectra are due to energy changes in the inner electron shells of atoms, and optical spectra are due to energy changes in the valency electrons. Optical absorbtion spectral lines shown in B occur at the same wavelength as the corresponding optical emission spectral lines because the same energy must be absorbed by a valency electron from a photon to raise it to a higher energy level as the electron emits as a photon when the electron falls to the lower level. Similar X-ray absorbtion spectral lines shown at A do not occur because the next outer electron shell of an atom is filled with electrons, and so inner shell electrons can only be ejected from the atom by a sufficiently energetic photon or particle. For Hydrogen and Helium the H_α and He_α optical spectral lines correspond to the K_α X-ray spectral lines of the other elements.

The characteristic X-ray spectral lines of a series from one element always have less photon energy than the energy of the absorbtion edge of the element, so that they are always on the long wavelength side of the absorbtion edge as shown in Figure 2.7. The absorbtion edge is the minimum energy required to eject an electron from an atom, whilst the characteristic spectral lines associated with that edge are due to transitions from higher energy levels to fill the electon vacancy which gave rise to that absorbtion edge. Thus 74Tungsten K_α lines of energy 58.5keV cannot excite Tungsten K_α lines, because the K

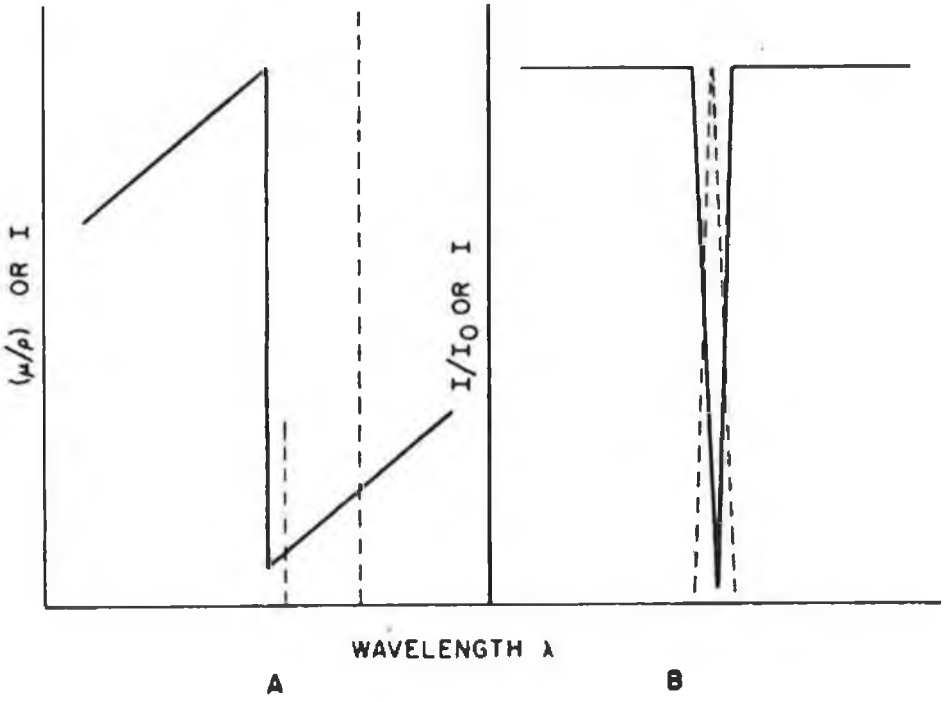

Comparison of X-ray and optical spectra.

A. The X-ray absorbtion edge is located at a higher energy and shorter wavelength than the corresponding X-ray emission spectral lines.B. The optical absorbtion and emission spectral lines occur at the same energy and wavelength.

[E.P. Bertin, Principles and Practice of X-ray Spectrometric Analysis].

FIGURE 2.7

absorbtion edge is 70keV. Tungsten is fairly transparent to its own spectral lines because absorbtion is less on the long wavelength side of the absorbtion edge than on the short wavelength side.

The absorbtion edges also have fine structure due to small differences in the energy state of the whole atom, and because of atomic isotopes, and neighbouring atoms. Fine structure occurs within about 200eV on both sides of an absorbtion edge.

If a monochromatic collimated beam of X-rays is incident on a material medium part of the beam is absorbed, part scattered out of the direction of the incident beam, and part is transmitted. The intensity I of the transmitted beam is always less than the intensity I_o of the incident beam. Due to scattering, the deflection of X-rays interacting with matter, the transmitted beam intensity is lower than that caused by absorbtion alone. Absorbtion is the reduction in the intensity of X-rays due to energy conversion by the photoelectric effect in the medium. The attenuation of the X-ray beam is the reduction in intensity due to absorbtion and scattering. Thus matter is an absorber and an attenuator, and the absorbtion is less than the attenuation. Similarly the coefficients used to measure absorbtion and attenuation of X-rays by materials, hereinafter defined, are different. In practise in the X-ray photon energy range and the experimental method used herein, the absorbtion coefficient and the attenuation coefficient of atomic elements are taken to be the same and their numerical values are taken from tables of attenuation coefficients.

A material is referred to herein as an X-ray absorber even if it includes X-ray scattering, that is an attenuator.

Attenuation of X-rays by matter is due to their effects on the atoms of the matter intercepting the X-ray photons. The intensity of the radiation is the energy per second passing through unit area normal to the direction of the beam. If a colinear beam of monochromatic X-rays of wavelength λ and intensity i is incident on a thin section of thickness dy of an absorber of uniform material, the decrease in intensity di on crossing the section is proportional to dy and to the intensity i so that

$$di = - \mu_1 i dy \qquad (2.7)$$

where μ_1 is defined as the linear attenuation coefficient of the absorber, or attenuator. If μ_1 is independent of y, then

$$\int \frac{di}{i} = \ln i = \mu_1 y + k \qquad (2.8)$$

At $y = 0$, $i = I_o$, the incident intensity, then $k = \ln I_o$, and so the intensity of the beam after passing through a thickness y of the absorber is

$$I = I_o e^{-\mu_1 y} \quad \text{and} \quad \mu_1 = [\ln(I_o/I)]/y \ \ cm^{-1} \qquad (2.9)$$

The linear attenuation coefficient μ_1 depends on the number and kind of atoms in the attenuating material.

If the material of the attenuator is not of uniform composition so that the linear attenuation coefficient depends on the path which the X-ray beam takes in traversing the object, then

$$\int \frac{di}{i} = - \int \mu_1(y) dy + k' \qquad (2.10)$$

and so $$I = I_o \exp\left(- \int_y \mu_1(y)dy \right) \qquad (2.11)$$

which is the line integral of the linear attenuation coefficient in the y direction resulting in the transmitted X-ray beam intensity I; Beer's law. If the intensity is measured as the flux of X-ray photons then

$$N = N_o \exp\left(- \int_y \mu_1(y)dy \right) \qquad (2.12)$$

The mass attenuation coefficient is $\mu = \mu_1/p$ where p is the density of the attenuator. It is a property of the atoms only, independent of the physical or chemical state of the attenuator, and a function only of X-ray wavelength and attenuator atomic number.

The equivalent thickness t of an X-ray absorber is its mass per unit area, kilograms per square metre, so that attenuators can be directly compared with one another, and p relates μ_1 and μ:

$$I = I_o e^{-\mu_1 y} = I_o e^{-\mu t} \qquad (2.13)$$

because $\mu_1/p = \mu$ and $y \times p = t$.

When the intensity is measured as the flux of X-ray photons, then this equation becomes

$$N = N_o e^{-\mu t} \qquad (2.14)$$

where N, N_o are the transmitted and incident number of photons, the quantities measured in this work.

The half-value thickness is the thickness of an attenuator needed to reduce by one-half the X-ray beam intensity:

$y_{\frac{1}{2}} = 0.693/\mu_1$, and the half-value equivalent thickness is $t_{\frac{1}{2}} = py_{\frac{1}{2}}$

The mass attenuation coefficients for different substances can be compared with one another because it is the attenuation due to unit mass of attenuator, so that the total mass attenuation coefficient for a compound material can be calculated from the values for each element in the compound. The mass attenuation coefficient for a compound substance made up of elements Z_i in weight fractions W_i is their sum, given by

$$\mu = \sum_i W_i(\mu_1/p)_i \qquad (2.15)$$

Thus for an analyte element a within a matrix m, the mass attenuation coefficient is

$$\mu = \mu_1/p = W_a(\mu_1/p)_a + W_m(\mu_1/p)_m = \mu_a W_a + \mu_m W_m \qquad (2.16)$$

The linear attenuation and mass attenuation coefficients are the sum of three separate linear attenuation and mass coefficients due to photoelectric absorbtion,τ, which is the total absorbtion of X-rays and thus emission of spectral lines, mass scattering coefficient,s, and electron pair production coefficient, π, given by

$$\mu = \tau + s + \pi \text{ and } \mu_1/p = \tau/p + s/p + \pi/p. \qquad (2.17)$$

For a well collimated beam of X-rays of energy less than 1.02 MeV $\pi = 0$ and $s << \tau$, so that herein $\mu = \tau$ and $\mu_1/p = \tau/p$.

When X-rays intereact with matter there are four secondary different

processes which may occur simultaneously which are, in the order of increasing photon energy:

Thomson scattering
the photoelectric effect
Compton scattering
electron pair production.

Thomson scattering is also known as classical, elastic, unmodified or incoherent scattering because the wavelength of the scattered photons is the same as that of the incident photons, so there is no loss of photon energy in the scattering interactions. The incident X-rays cause electrons in the atoms of the irradiated material to oscillate in the same direction as that of the electric vector of the photon, and the accelerated electrons radiate secondary X-rays of the same frequency as that of the incident X-rays. Thomson scattering is isotropic, but the scattered radiation can be emitted from crystal planes in a solid in preferential directions by diffraction to cause interference, and the radiation is then coherent, the X-ray photons all being in the same phase. Thomson scattering occurs with greater probability for low energy photons and high atomic number elements.

The photoelectric effect occurs when the energy of an incident photon is sufficiently great to eject a bound electron from an atom of an element. The photon energy must be sufficient to overcome the binding energy of at least the most loosely bound or valency electron in the atom, which is the ionisation potential, or at greater photon energies, the binding energy of more tightly bound electrons. No matter how intense is the irradiation, no electrons are emitted by an atom when the photon energy is less than the ionisation potential.

The photon is totally absorbed by the electron, and the difference in energy between that of the photon and the electron is the kinetic energy, $mv^2 = h\nu - \phi$, of the ejected photoelectron where h is the photon energy, and ϕ is the binding energy. In the X-ray region of the spectrum inner shell electrons are ejected, and in the ultra violet, visible, and infra red regions, outer shell electrons are ejected. It is the photoelectric effect of primary X-rays which is utilised herein.

Compton scattering also called inelastic, modified, or coherent scattering, occurs when an incident X-ray photon ejects a loosely bound electron from an outer electron shell of an atom taking some of the photon's energy with it, and the scattered photon has less energy and so a longer wavelength than the incident photon. The energy and momentum before the interaction is conserved, and the Compton recoil electron and the scattered photon are deflected from opposite sides of the path direction of the incident photon. The increase in wavelength is given by Compton's equation

$$\Delta\lambda = \lambda' - \lambda = [h/m_o c]\ (1 - \cos\phi) \qquad (2.18)$$

where λ', λ are the scattered and incident photon wavelengths, h is Planck's constant, m_o is the electron rest mass, c is the velocity of electromagnetic radiation, and ϕ is the scattering angle of the modified photon. $\Delta\lambda$ is a maximum for $\phi = 180°$ and $h/m_o c = 0.0024$nm is the Compton wavelength. $\Delta\lambda$ is independent of λ and atomic number, so it is the same for all elements and X-ray photon energies. Compton scattering predominates over classical scattering for low atomic number elements, and for high energy photons of energy between 0.2 and 5meV. The Compton effect is a confirmation of the quantum theory of

radiation because of excellent agreement between theory and experiment.

Electron pair production does not occur until the photon energy is at least 1.02MeV, which is the energy mass equivalent of an electron and positron pair which may be produced when a photon goes too close to the nucleus of an atom. The energy of the photon is converted to matter by Einstein's equation $E = mc^2$, where E is the photon energy, $h\nu$, m is the mass of the particles produced, and c is the velocity of electromagnetic radiation, h is Planck's constant, and ν is the photon frequency.

PRODUCTION OF X-RAYS.

The usual way to produce an X-ray spectrum is by accelerating a beam of electrons in a strong electric field in an ultra high vacuum X-ray tube, and then decelerating them as quickly as possible by impact on a target usually made of an element of high melting point such as Tungsten or Molybdenum, to withstand the intense heat produced on impact. A high atomic number element decelerates the electrons more quickly than one of low atomic number. X-rays are emitted from the target in a divergent beam, the shape of which depends on the way in which the electrons are focused on the target. The energy distribution curves for a 74Tungsten target for X-ray tube accelerating potential differences of 20, 25, 30, 40 and 50kV are shown in Figure 2.8. These are continuum spectra which have a continuous range of wavelengths from low energy, overlapping with the visible region of the spectrum to a definite maximum energy which is determined by the high tension electron accelerating potential difference between cathode and anode of the X-ray tube, and occurs

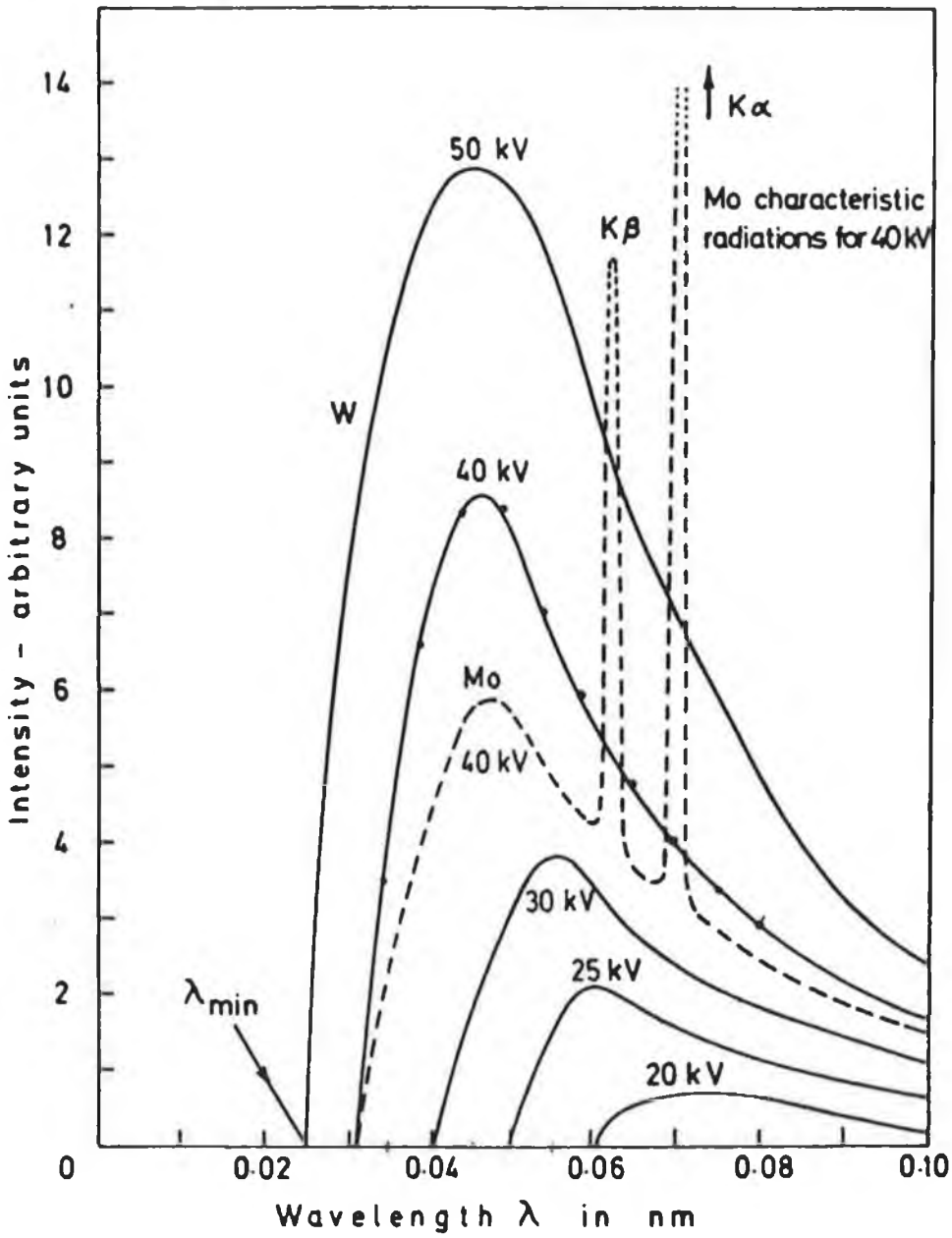

X-ray spectra for 74Tungsten.

Distribution of energy in the X-ray spectrum for different X-ray tube potential differences.

[T.A. Littlefield and N. Thorley, Atomic and Nuclear Physics].

FIGURE 2.8

when the velocity of an electron is reduced to zero on impact with one atom of the target: all of the energy of the electron is converted to a single photon, so that the maximum energy of the X-ray photon in electron volts is the voltage of the accelerating potential. If the electric potential difference between the cathode and anode is V, then the energy of the electron, eV, is converted to a photon of energy $E_\lambda = eV = h\nu = hc/\lambda$, and so $\lambda = hc/eV$, where e is the electric charge on the electron, h is Planck's constant, c is the velocity of electromagnetic radiation, and λ_m is the minimum wavelength of the photon, and V is in volts.

Most electrons are decelerated in stages by impact on several atoms of the target, and at each stage a photon is emitted; the electrons being scattered inelastically and discontinuously by nuclei of the target atoms, and some of their energy at each collision is converted to an X-ray photon. Thus the wavelength of most photons is greater than $_m$. The majority of electron collisions result in the energy being converted to photons which give the spectrum an intensity peak which occurs at about $1.5\lambda_m$, which is taken as the wavelength of the X-ray tube operating at a particular voltage, or the effective wavelength of the continuum. The intensity gradually approaches zero at the longer wavelengths where only a small amount of the electron's energy is converted to photons.

The intensity per unit wavelength interval of the beam from an X-ray tube at wavelengthλor photon energy can be measured experimentally for chosen anode voltages V and chosen current i, or can be calculated by Kramer's formula

$$I \alpha iZ(\lambda/\lambda_{min} - 1)/^2 \qquad (2.19)$$

or Beatty's formula

$$I_w = (1.4 \times 10^{-9}) iZV^2 \qquad (2.20)$$

where Z is the atomic number of the target in the X-ray tube, I is the X-ray intensity at wavelength λ, I_w is the integrated X-ray intensity of the continuum in watts, and λ_{min} is the minimum wavelength of the continuum. The equations show that the intensity of the X-ray beam is proportional to the atomic number of the target element which is equal to the number of its electrons, and to the anode current which is proportional to the number of bombarding electrons, and to the square of the anode voltage. The general shape of the continuum is not changed much for changes in Z and i, but for changes in V the maximum intensity moves towards the short wavelength end of the spectrum and the maximum itself increases in proportion to about V^4 because at higher velocity the electrons can be decelerated in a greater number of steps.

When the anode voltage V is increased so that the energy of the primary electrons is sufficient to knock electrons out of the K shell of the target element, the characteristic X-ray spectral lines of the target element begin to appear superimposed on the continuous spectrum and progressively increase in intensity as V is increased and λ_{min} moves to shorter wavelengths. The k_α and K_β lines superimposed on the 40kV continuum spectrum for a 42Molybdenum target are shown in Figure 2.8. The maximum anode voltage of the X-ray tube used herein is 60kV, which is below the 70keV K_α absorbtion edge but above the 58.5keV K_α lines of the 74Tungsten target, so the spectrum is a continuum.

The high tension electron accelerating voltage may be alternating current in which case the X-ray tube acts as its own diode half-wave

rectifier, and X-rays are produced when the anode is positively charged with respect to the cathode. The accelerating electric potential rises from zero to the maximum and falls again to zero for the positive half of the cycle only. A constant voltage X-ray tube is supplied by a high voltage direct current from a high tension transformer and rectifier and smoothing circuit. Modern X-ray tubes have evolved from the high vacuum X-ray tube invented in 1913 by W.D. Coolidge [13] which had an electrically heated cathode. The current flowing in an X-ray tube is controlled by the temperature of the cathode.

Because the electrons are accelerated in the X-ray tube only by the electric potential difference between anode and cathode it is immaterial which electrode is maintained at ground potential. Thus if the anode is at ground potential it may be water cooled, and the electrons are accelerated from the cathode maintained at a high negative electric potential by the power supply. This is the type of X-ray tube employed herein.

A method for producing X-rays of high energy overlapping with the γ-ray region of the Electromagnetic Spectrum uses a synchrotron. Atomic X-rays are of energy 120eV and wavelength 10nm to 150keV and wavelength 0.008nm, and X-ray machines can produce X-rays of up to 10^{6}eV and 10^{-6}nm wavelength. Electrons moving in a circular path are under constant acceleration in a strong magnetic field in an ultra high vacuum. The energy given to the electrons is supplied by the synchrotron power supply, and radiation is continuously emitted by the electrons, the energy of the photons being proportional to the acceleration of the electrons. Synchrotron radiation has a very broad spectrum the width of which depends on the distribution of the velocities of the electrons.

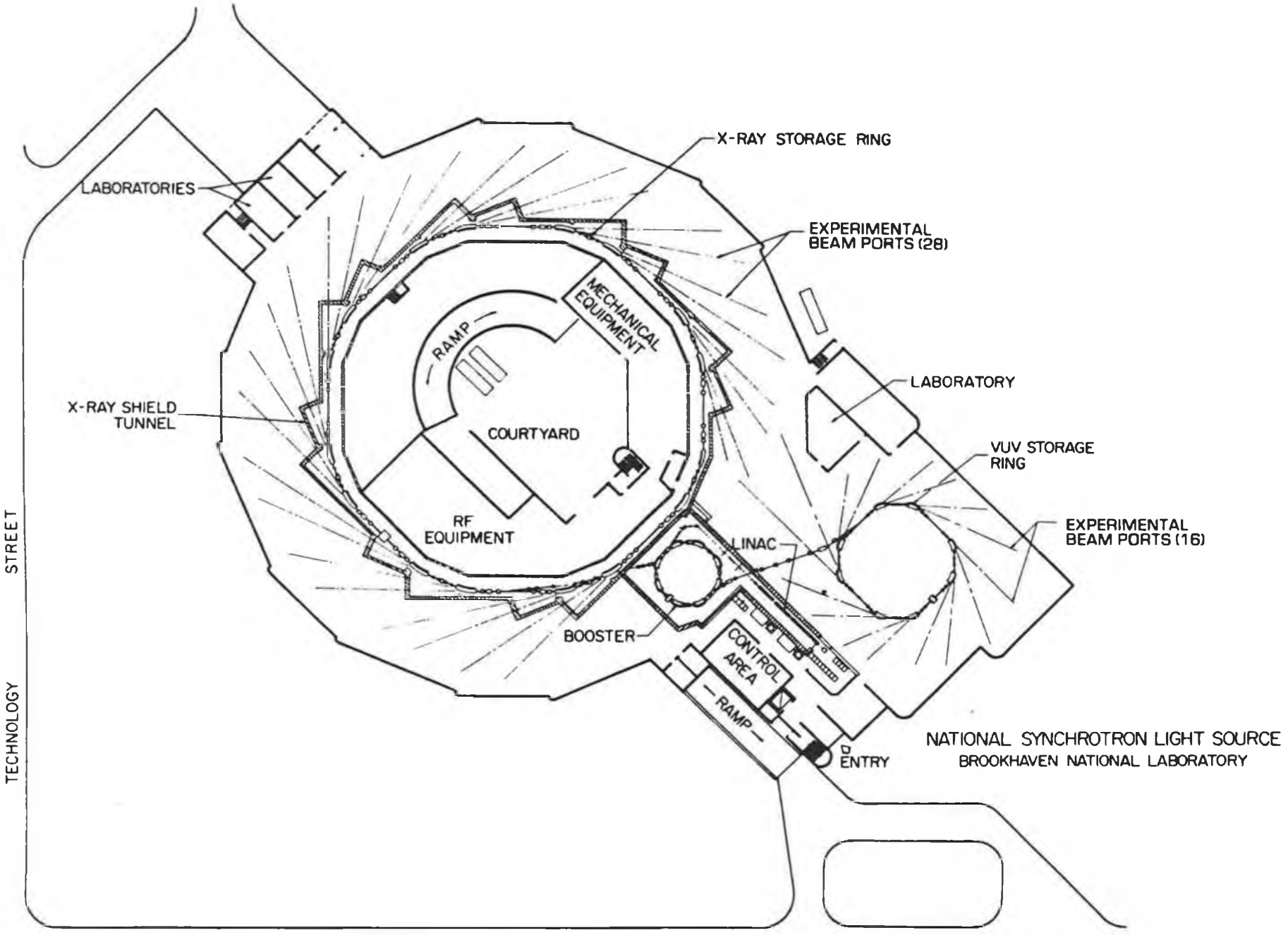

[National Synchrotron Light Source Annual Report 1985].

FIGURE 2.9

Figure 2.9 is a plan of the National Synchrotron Light Source at Brookhaven National Laboratory, New York, U.S.A., which can produce synchrotron radiation of up to 2.5×10^{9}eV and 5×10^{-7}nm.

Other sources of X-rays are radioactive isotopes of atomic elements, and secondary fluorescence X-rays emitted by an element which is irradiated with a primary X-ray beam.

Figure 2.10 shows the Amersham International (241)95Americium variable energy X-ray source type AMC.2084 used in the first experiments of this work. Also shown are the normalised K_{α} and K_{β} fluorescence X-ray spectral lines emitted by the six target elements which may be selected in turn, set in a rotary holder. The target element is irradiated by a 10mCi, 370MBq, 241 Americium primary source of 60keV γ-rays surrounding the 4mm aperture through which the K_{α} and Kβ X-rays from the target are emitted. The half-life of (241)95Americium is 433 years, decaying to (237)93Neptunium with the emission of an α-particle and a 60keV γ-ray.

A 3mCi, 111MBq, (109)48Cadmium source emitting the K_{α} and K_{β} lines of (109)47Silver was used in the experiments for imaging 46Palladium [14]. The transmutation of Cadmium nuclei to Silver nuclei is by electron capture, in which the nucleus of the Cadmium atom captures an electron from the K shell to increase the atomic number by 1, but leaving the mass number unchanged. The K shell vacancy is filled by another electron to emit the 47Silver K_{α} and K_{β} X-ray spectral lines. This source was encapsulated in a radiation shield consisting of a Lead filled Copper container having a 2mm aperture for the exit of the 47Silver X-rays.

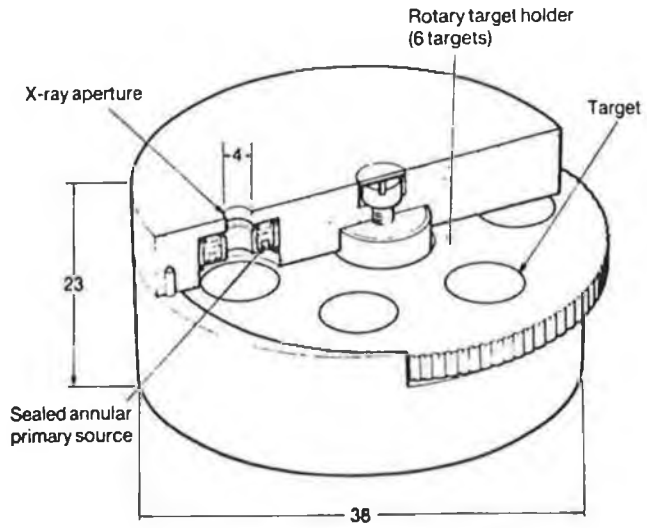

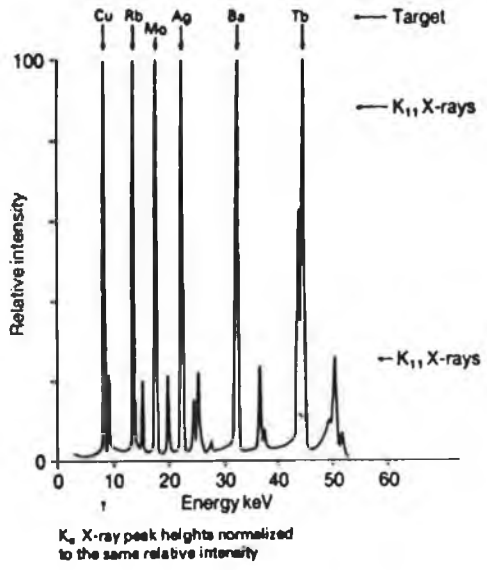

X-ray emission

target selected	energy (keV)[1] Kα	Kβ	photon yield[2] (photons/sec per steradian)
Cu	8·04	8·91	$2{\cdot}5 \times 10^3$
Rb	13·37	14·97	$8{\cdot}8 \times 10^3$
Mo	17·44	19·63	$2{\cdot}43 \times 10^4$
Ag	22·10	24·99	$3{\cdot}85 \times 10^4$
Ba	32·06	36·55	$4{\cdot}65 \times 10^4$
Tb	44·23	50·65	$7{\cdot}6 \times 10^4$

Notes
(1) Weighted mean energies
(2) The photon output is highly collimated limiting emission to ~0·5 steradians.

Primary source
A 10mCi, 370MBq americium-241 source*, consisting of a ceramic active component in a welded stainless steel capsule, with integral tungsten alloy rear shielding.

*activity tolerance −0, +25%

These sources are also available with an iron-55 primary source for lower energy spectrometry.

Recommended working life 15 years

A radioactive X-ray source.

The Amersham International 241(95) Americium variable energy X-ray source type AMC.2084 and its spectral characteristics.

[Amersham International].

FIGURE 2.10

X-RAY DETECTORS.

There are four types of detector for detecting and measuring X-rays: gas detector, scintillation detector, and solid state semiconductor detector, in which X-rays interact with the detector by photoelectric absorbtion, so that an absorbed photon is converted to an electric current pulse which can be measured; and the photographic plate. An insensitive but absolute method of measuring X-ray intensity is to measure the temperature rise of a block of Lead irradiated with X-rays. A solid state semiconductor detector is described in Chapter 4.

The intensity of a beam of X-rays can be measured by the ionisation it causes in a gas in a chamber, illustrated in Figure 2.11. A photon expels a photoelectron from a gas atom with kinetic energy proportional to the photon energy minus the binding energy of the electron. This photoelectron ionises the gas losing about 30eV per ion pair until its energy is expended, so that the number of ion pairs is proportional to the photon energy. The beam enters through a thin X-ray window, and the photons are absorbed in an inert gas at low pressure, such as 18Argon to produce Argon ions and secondary electrons. An electric field is maintained in the chamber by a direct current voltage between two electrodes: a positively charged straight fine wire mounted concentrically with a negatively charged cylindrical cathode. Ions are accelerated towards and collected by the oppositely charged electrode, and the elecric current flowing in the chamber can be measured.

The proportional counter and the Geiger counter are developments of the ionisation chamber, the basic difference in their operation is in the electric field strength between the anode and cathode of the

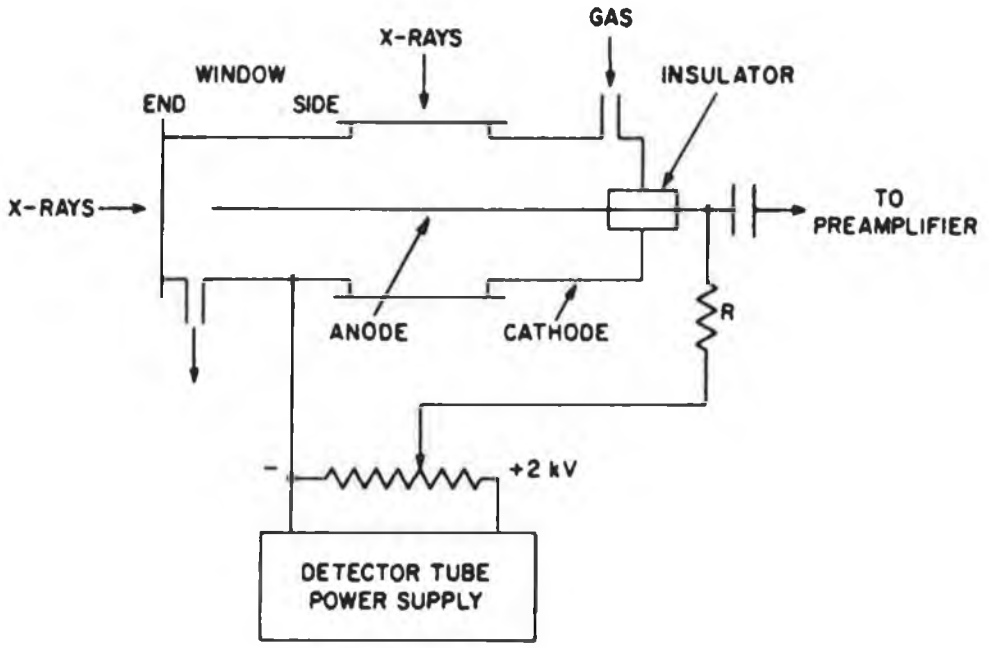

Structure of the gas-filled X-ray detector.

The tube is shown to have both end and side windows for illustration only.

[E.P. Bertin, Principles and Practice of X-ray Spectrometric Analysis].

FIGURE 2.11

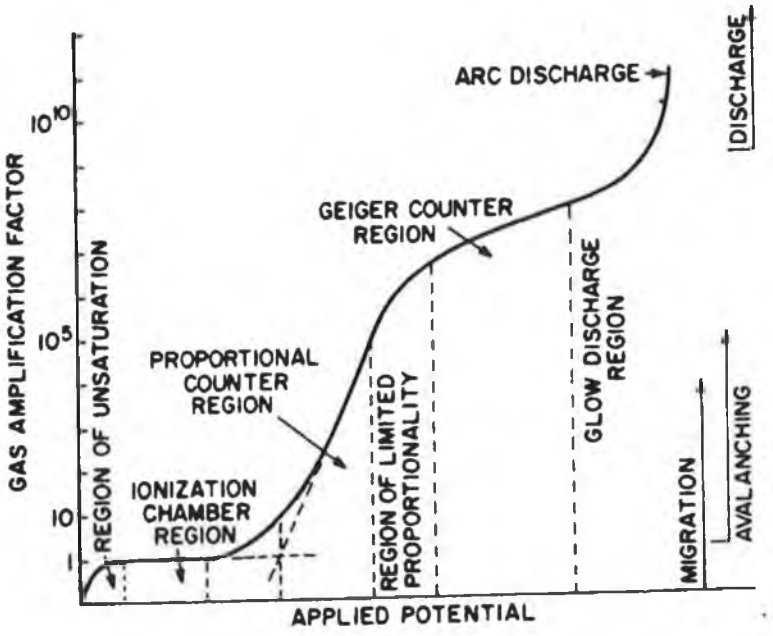

Operation of a gas-filled X-ray detector.

The gas amplification factor as a function of applied electric potential for the gas-filled X-ray detector.

[E.P. Bertin, Principles and Practice of X-ray Spectrometric Analysis].

FIGURE 2.12

chamber, as illustrated in Figure 2.12. When the electric field strength is low some of the secondary electrons have time to combine with positive ions before they reach the anode because they are not accelerated to high enough velocity to be collected. Thus the anode current is unsaturated. The number of secondary electrons collected increases in proportion to the increasing electric field strength, so that the current increases linearly. When all the electrons are collected the current is saturated, and there is no further increase in anode current with increase in field strength until the secondary electrons are accelerated to the ionisation potential of the detector gas just before they reach the anode. This is the ionisation chamber region of operation in which the gas amplification factor, gain G, of the chamber is 1. Further increase in electric field strength accelerates the primary electrons to cause ionisation by collision of the gas to produce secondary electrons. If the photoelectron has energy E, equal to the X-ray photon energy less the photoelectron binding energy, and produces on average N_o primary electrons and positive ions, then $N_o = E/V_i$, where V_i is the effective ionisation potential of the detector gas. V_i is a combination of the ionisation potentials of the gas atom greater than the first ionisation potential, because an atom may be multiply ionised by the primary electrons. The gas gain G is the number of secondary electrons N collected by the anode produced by ionisation of the detector gas by each primary elecron produced by the photoelectron ejected from an atom by the X-ray photon. Thus $G = N/N_o = NV_i/E$, and depends on the electric field strength between anode and cathode of the detector. In the proportional counter the anode current is proportional to the photon energy and G may be 100 to 10^5.

As the anode voltage increases further, ionisation by the primary electrons spreads out from the anode wire and becomes more general, so that in the Geiger region of operation the incident X-ray photon triggers a general discharge of the chamber, giving current pulses much larger than those of the proportional region, so that G is about 10^9. The discharge is stopped quickly by means of a low concentration halogen or organic quenching gas so that the count rate capability of the chamber can be increased by neutralising the positive ions before they reach the cathode.

In a scintillation detector shown in Figure 2.13 the luminescence caused by absorbtion of X-rays by 81Thallium atoms in a crystal of Sodium iodide is detected and amplified by a multiplier phototube, and the current pulses are measured. The photoelectrons ejected from the 53Iodine atoms produce blue light photons, scintillations, on collision with atoms of the crystal. The gain of the scintillation detector is about 10^6.

The Sodium iodide is doped with 10^{-3} mole fraction of 81Thallium which is responsible for the scintillation of the crystal, called an activator. The allowed energy levels, which in an atom are discrete, are energy bands in a crystal having a band gap between the valency band and the conduction band of about 8eV. In a pure crystal incident radiation needs to be sufficiently energetic to raise an electron from the valency band to the normally empty conduction band, and then the electron can move around the crystal lattice leaving a positively charged hole in the valency band. The electron cannot normally be raised to an energy level in between the bands, the forbidden energy band of the crystal. Sodium iodide doped with 81Thallium has energy

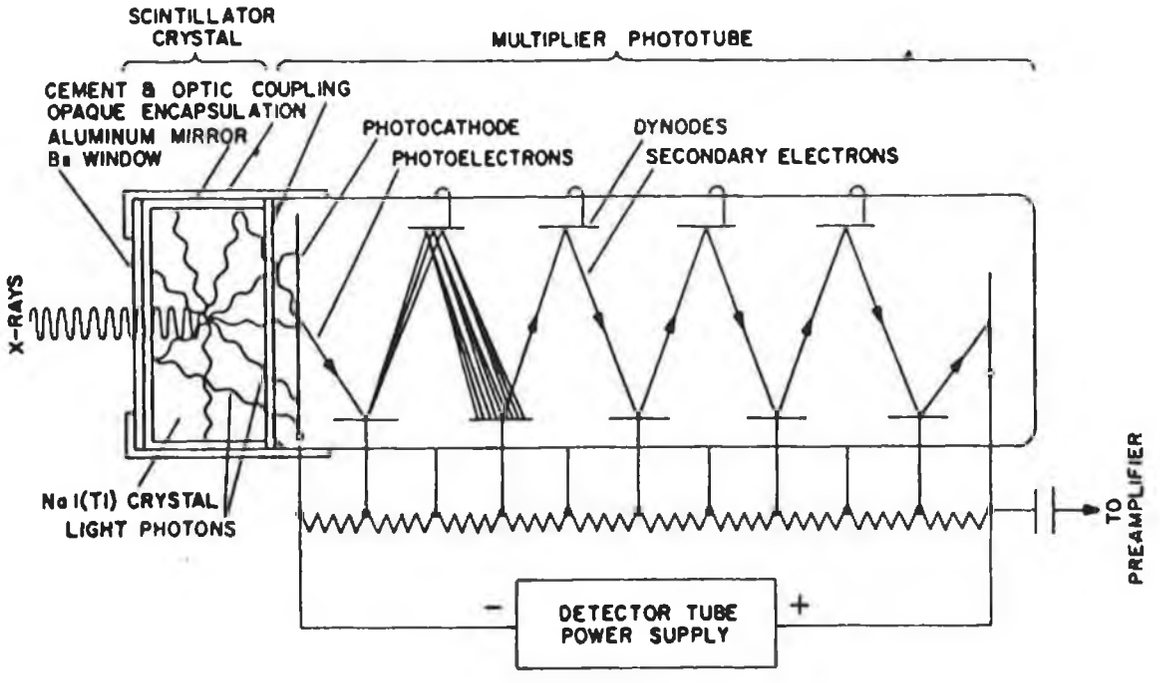

Structure of the scintillation counter.

[E.P. Bertin, Principles and Practice of X-Ray Spectrometric Analysis].

FIGURE 2.13

X-RAY UNITS

QUANTITY AND UNITS	S.I.		C.G.S.	
RADIATION ABSORBED DOSE	GRAY	Joule/kg	RAD	1Gy = 100RAD
DOSE EQUIVALENT	SIEVERT	Joule/kg	REM	1Sv = 100REM
ACTIVITY	BECQUEREL	s^{-1}	CURIE	1Ci = 3.7×10^{7}Bq

FIGURE 2.14

states between the valency and conduction bands of the crystal. Light emitted by Thallium activated Sodium iodide is mainly from electronic transitions in the Thallium, and the peak of the luminescence spectral band is 410nm corresponding to a photon energy of 3eV. This is the most efficient of the inorganic scintillating crystals in which about 12% of the incident X-ray photons cause Thallium luminescence.

UNITS OF X-RADIATION MEASUREMENT.

The rontgen is the S.I. unit of radiation exposure, the quantity of X- or γ-radiation which liberates a charge of 2.58×10^{-4} coulombs per kilogram of air of positive and negative ions. The S.I. units and the corresponding older C.G.S. units units are shown in Figure 2.14.

For safety purposes radiation is measured in absorbed dose and absorbed dose rate. The unit of absorbed radiation dose is the Gray. 1 joule of energy absorbed per kilogram of biological tissue or equivalent, of any kind of ionising radiation is 1 Gray. The unit related to the biological effect is the Sievert, which is the absorbed radiation in Gray multiplied by the relative biological efficiency, a quality factor of the radiation. The quality factor is 1 for electrons and X-rays, and 10 for α-particles, because α-particles produce about 10 times the ionisation in biological tissue as electrons and X-rays. The absorbed dose rate is usually given in Grays per hour. The maximum dose allowed is 0.05 Grays per year, which

in practise is a maximum permissible rate of about 25μG/h. The average background radiation exposure rate at sea level is about 0.5μG/h.

The intensity of a beam of X-rays is defined as the energy flux per unit area per unit time, which is the power per unit area. In X-ray spectrometry intensity is usually given as the number of photons per second passing through unit area. For a particular detector, the area is that of the radiation absorber, so that the intensity is proportional to the photon count rate.

The intensity of a point source of X-rays varies with the inverse square of the distance from the source. A narrow collimated beam of X-rays is used herein in order that the measured intensity depends only on the absorbtion of X-rays before reaching the detector, and not on distance or scattering by the absorber. For monochromatic X-rays the energy flux in joules per unit time is $E=Ihc/\lambda$ watts, where I is the count rate, h is Planck's constant, c is the velocity of electromagnetic radiation and λ is the wavelength of the photons in metres.

CHAPTER III

TOMOGRAPHY

COMPUTER AXIAL TOMOGRAPHY.

An X-ray photograph shows the internal structure of an object as a two dimensional image consisting of the images of all parts of the three dimensional object in one image plane, the density of the images being determined by the intensity of the radiation reaching the photographic plate. Thus an X-ray absorber in a plane in an object further from the photographic plate than an absorber in a plane in the object nearer to it appears in the same plane in the photograph, or the image of one absorber may be superimposed upon that of another, as illustrated in Figure 3.1, with reference to Cartesian coordinates. So it is not clear from the photograph where an absorber is located within an object: the X-ray photograph shows that it lies in the beam of X-rays at a particular place normal to the beam, but gives no information for the beam direction, the y-direction. One or more X-ray photographs taken in the (y,z) or (z,x) planes, or in a plane rotated about the y axis by θ from the (y,z) plane may show the location of an absorber along the X-ray beam direction, so that these photographs may give the (x,y,z) coordinates of an absorber.

Tomography, which means 'written in a cutting or cross section', is a

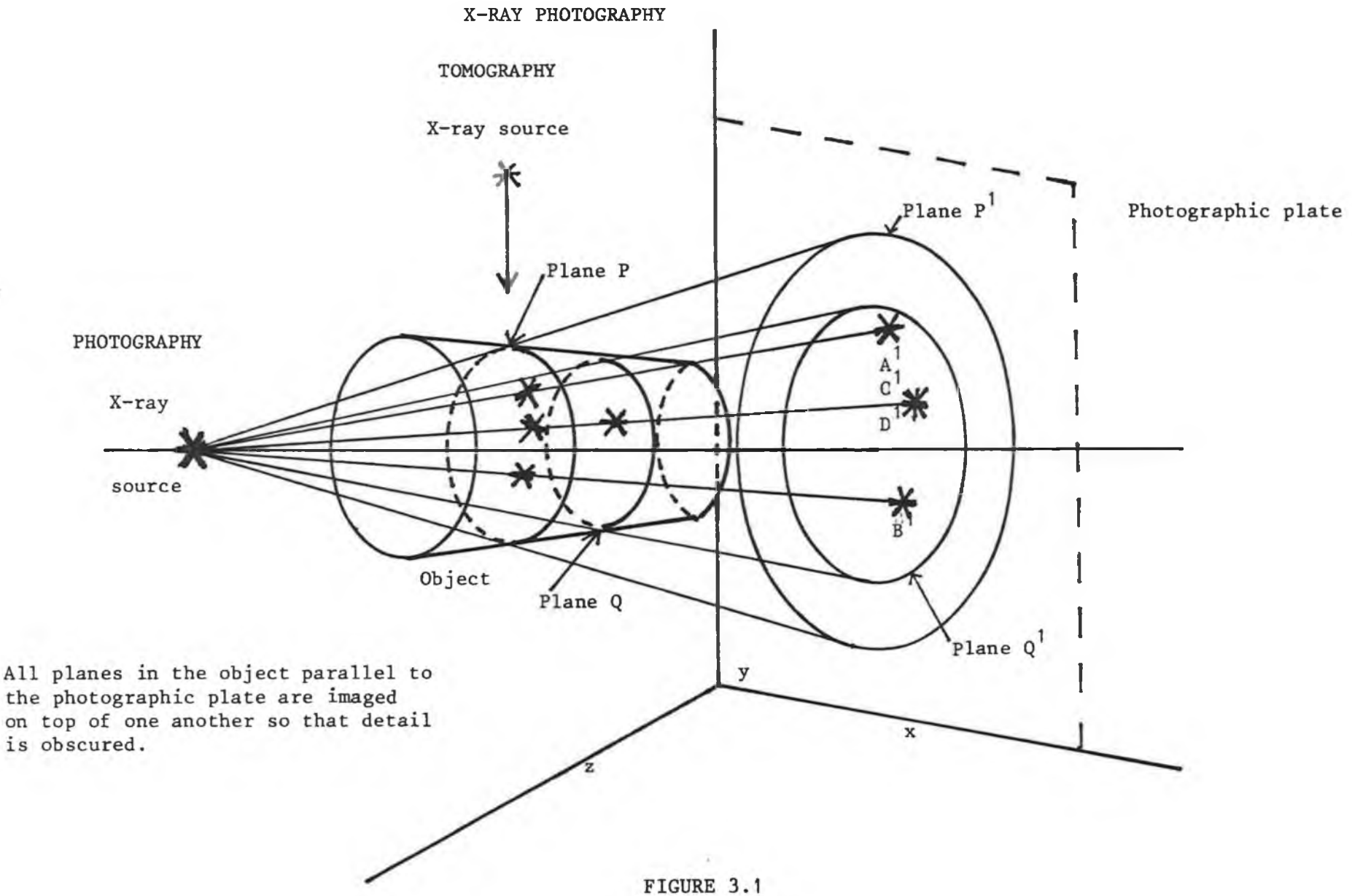
X-RAY PHOTOGRAPHY
TOMOGRAPHY
X-ray source
Plane P
Plane P¹
Photographic plate
PHOTOGRAPHY
X-ray
source
A¹
C¹
D¹
B¹
Object
Plane Q
Plane Q¹
All planes in the object parallel to the photographic plate are imaged on top of one another so that detail is obscured.
y
x
z

FIGURE 3.1

method of making an image of the internal structure of an object at a chosen plane within the object.

There are two methods of making an image of a particular plane in an object using transmission X-rays: focal-plane tomography, and computer axial tomography. Focal-plane tomography is a technique in which a source of X-rays and a photographic plate are moved so that the ratio of their distances from a chosen plane in an object is a constant, so that only this plane produces a well-defined image on the photographic plate. As shown in Figure 3.2 the X-ray tube moves in a straight line parallel to the plane in the object being imaged whilst the photographic plate moves in synchronisation in a straight line in the opposite direction during the photographic exposure. In this way, points in the focal plane of the object stay in fixed positions on the photographic plate to form clear images because they are not smeared, and points out of the focal plane form images on different parts of the photographic plate and so are blurred because they are smeared, and the further they are away from the focal plane the greater is the blurring.

Computer axial tomography, illustrated in Figure 3.3, forms images of absorbers in a chosen plane within an object by laterally irradiating that plane only with X-rays in discrete linear and angular steps, detecting the transmitted X-rays, and by means of a mathematical technique converting the changes in intensity of detected X-rays into an image of that plane. Thus radial measurements on an object are transformed into an axial image plane of the object which is determined by the axial position of the radius chosen in the object, so that all other planes are omitted. The mathematically reconstructed image so

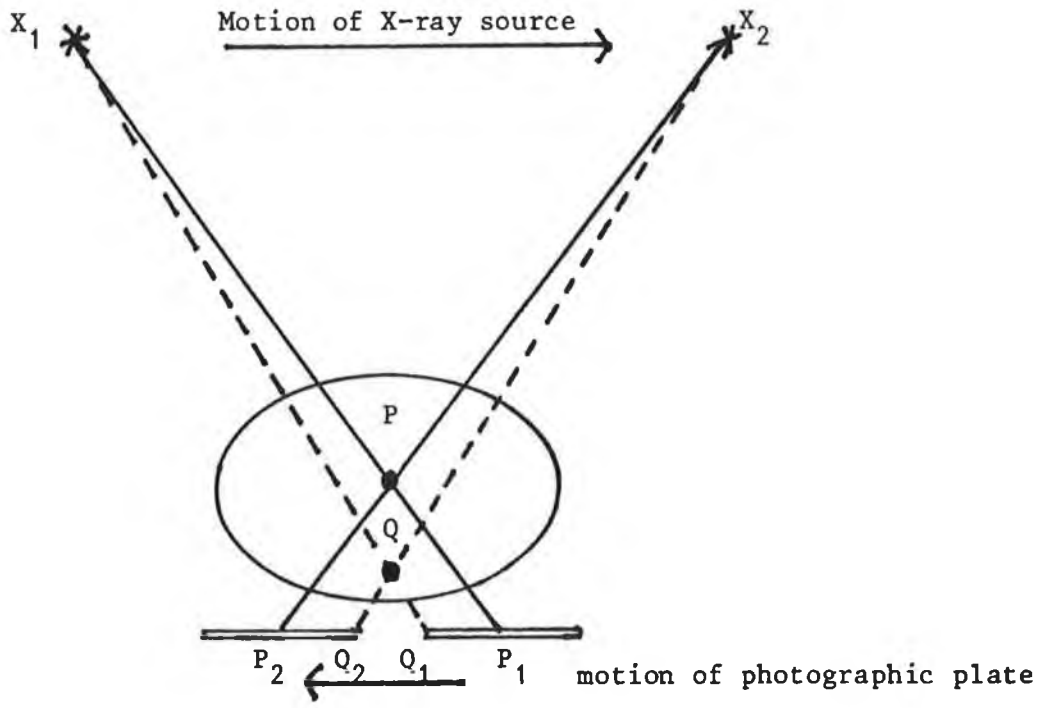

Principle of focal plane tomography.

FIGURE 3.2

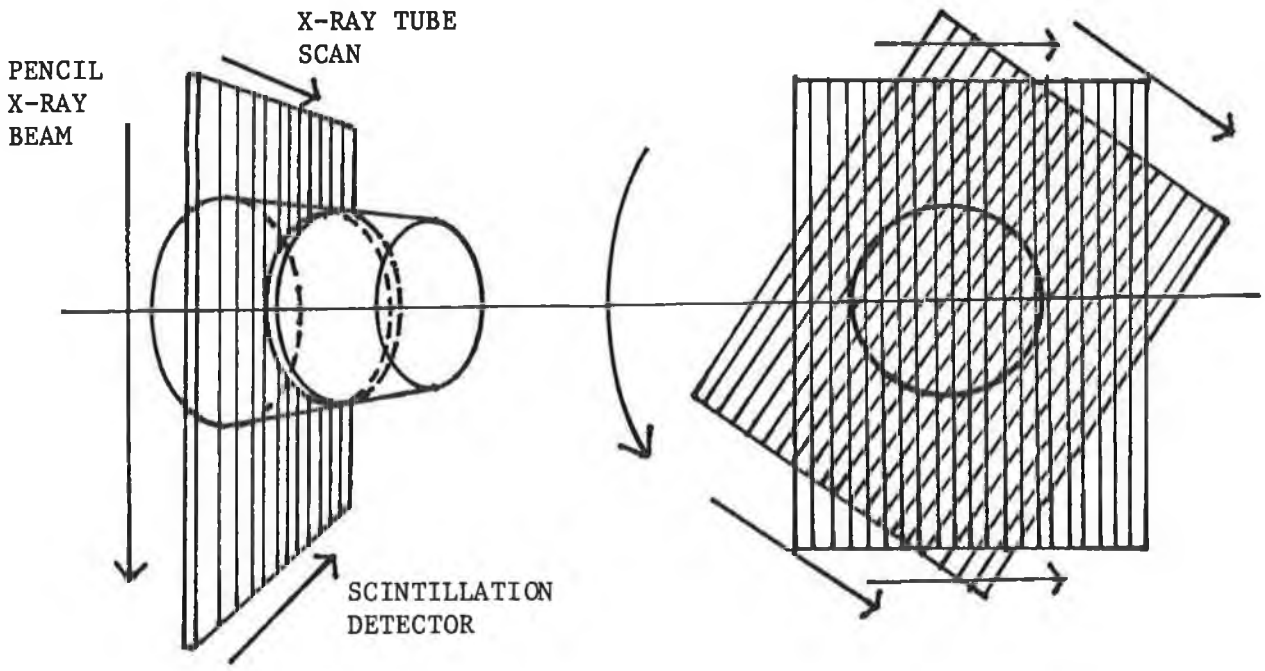

Principle of computer axial tomography.

FIGURE 3.3

formed is a distribution of linear attenuation coefficient, like a contour map. In practise, the image is of a thin axial disc of the object rather than a plane due to the finite width of the X-ray beam, which may be up to 15mm wide: in this work the beam width is chosen to be 1mm or 2mm, so that the disc is 1mm or 2mm thick. Thus the image is a two dimensional representation of the linear attenuation coefficient for X-rays or concentration of the analyte which may be displayed on a colour monitor or printed on paper. The attenuation of the X-ray beam in the radial direction is due to the average attenuation in that direction.

Focal plane tomography effectively forms an axial image of an object plane having some radial changes in order to define that axial plane clearly. In computer axial tomography all measurements are radial in order to select only one axial image plane.

The density of a reconstructed image of a plane in an object scanned by computer axial tomography is determined by the relative attenuation of X-rays in different parts of that plane of the object, which is detected as the relative transmission of the scanning X-rays. The smaller the differences that can be detected with precision, the more sensitive the scanner is in distinguishing between small differences in the X-ray density of the attenuators in the scanning plane.

The total linear attenuation coefficients, μ, of X-ray attenuators in medical computer axial tomography is measured on an arbitrary Hounsfield number scale defined by

$$\frac{\mu_{absorber} - \mu_{water}}{\mu_{water}} \times 1000$$

so that each Hounsfield unit is equivalent to 0.1% of the linear attenuation coefficient of water. This equation defines H = 0 for water, H = -1000 for air, so that the total linear attenuation coefficients of attenuators are compared with that of water.

DIFFERENTIAL K ABSORBTION EDGE TOMOGRAPHY.

Differential K absorbtion edge tomography is a technique for identifying and measuring the concentration of the atomic elements of which an absorber of X-rays is made in a chosen plane within an object, by transverse scanning of an object with a narrow collimated beam of X-rays in an energy band which overlaps the characteristic X-ray absorbtion edges of the elements being analysed, or monochromatic X-rays of energy above and below the K absorbtion edges of those elements. The scanning method is similar to that of computer axial tomography scanning; the essential difference is that an energy dispersive detector absorbs the X-rays transmitted by the object being scanned and the voltage pulses proportional to the energy of the X-ray photons absorbed by the detector are separated and counted according to magnitude. Differential absorbtion of X-rays in a narrow band on either side of an absorbtion edge of an element identifies that element as shown in Figures 2.5 and 2.6 and an image of that element in a plane within an object shows its concentration.

DIFFERENTIAL ABSORBTION OF X-RAYS.

The differential absorbtion of X-rays applied in the method of this work depends on the difference between the absorbtion coefficient of an element at the low energy side and at the high energy side of an

absorbtion edge, in this case of the K absorbtion edge of the element. It is the measurement of this differential which can locate the absorbtion edge on the energy spectrum and so uniquely identify the element and indirectly measure its concentration from the magnitude of the absorbtion.

Suppose a narrow collimated beam of monochromatic X-rays passes through an object consisting of an analyte element, a, within a matrix, m. The transmitted X-ray flux detected is

$$N = N_o e^{-\mu t} \tag{3.1}$$

where N_o is the incident flux, μ is the mass attenuation coefficient of the object, t is its equivalent thickness, and $t = px$ where x is the thickness of the object of density p. The mass attenuation coefficient is the attenuation of X-rays due to unit mass of a particular attenuator, so that the total mass attenuation coefficient is the sum of the mass attenuation coefficients of the constituent elements, and therefore the mass attenuation coefficient of analyte and matrix is

$$\mu = \mu_a W_a + \mu_m W_m \tag{3.2}$$

where W_a, W_m are the weight fractions of the analyte and matrix, and μ_a, μ_m are their mass attenuation coefficients. Thus

$$N = N_o \exp\left[-(\mu_a W_a + \mu_m W_m)t\right] \tag{3.3}$$

Suppose the beam consists of two coexistent colinear monochromatic

X-ray beams, one on each side and close to the K absorbtion edge of the analyte element as shown in Figure 3.4, the transmitted detected flux of each beam is

$$N_l = N_{ol} \exp [- (\mu_{al}W_{al} + \mu_{ml}W_{ml})t] \quad (3.4)$$

$$N_h = N_{oh} \exp [- (\mu_{ah}W_{ah} + \mu_{mh}W_{mh})t] \quad (3.5)$$

where l, h refer to the low and high energy sides of the K absorbtion edge. Thus

$$N_l/N_h = (N_{ol}/N_{oh}) \exp [W_a(\mu_{ah} - \mu_{al})t] \exp [W_m(\mu_{mh} - \mu_{ml})t] \quad (3.6)$$

which rearranged, gives

$$W_at = [\ln (N_l/N_h)(N_{oh}/N_{ol})] /(\mu_{ah}-\mu_{al}) - W_mt [(\mu_{mh} - \mu_{ml})/(\mu_{ah}-\mu_{al})] \quad (3.7)$$

If μ_{mh} is close to μ_{ml} then the second term is zero, and so the equivalent thickness of the analyte element is

$$t_a = W_at = \ln[(N_l/N_h)(N_{oh}/N_{ol})]/(\mu_{ah}-\mu_{al}) \quad (3.8)$$

The difference between the last two equations is

$$t_m (\mu_{mh} - \mu_{ml})/(\mu_{ah} - \mu_{al}) \quad (3.9)$$

which depends on the equivalent thickness of the matrix and its mass attenuation coefficient, and these are unknown in most cases. Thus corrections need to be made to the X-ray photon count data to eliminate the effect of the matrix. Attenuation of X-rays in the matrix of the object reduces the measured value of the equivalent thickness of the

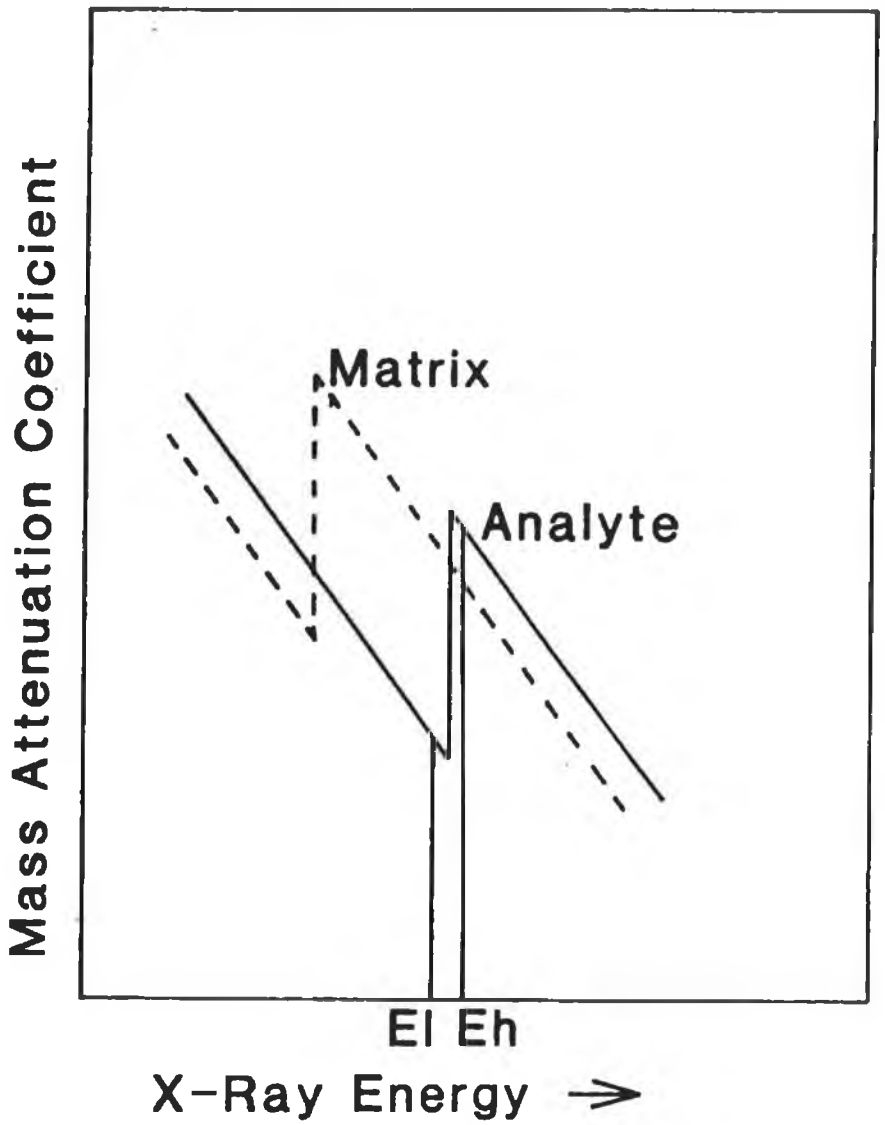

The mass attenuation coefficient.

This shows the variation of the mass attenuation coefficient of analyte element and matrix near the K absorbtion edge of the analyte. The difference in mass attenuation coefficient at energy E_l and at energy E_h is much greater for the analyte element than for the matrix.

[14]

FIGURE 3.4

analyte element because near the K absorbtion edge of the analyte $(\mu_{ah} - \mu_{al})$ is positive and $(\mu_{mh} - \mu_{ml})$ is negative.

The accuracy of measurement of analyte concentration depends on the accuracy with which the X-ray beam flux measurements are made. This depends on the number of photons counted at each step of a scan of an object, and on the effect of the matrix, which ideally would be negligible. Thus $(\mu_{ah} - \mu_{al})$ must be accurately determined, and $(\mu_{mh} - \mu_{ml}) = 0$, which would be so if the energy of the two X-ray beams is at the K absorbtion edge of the analyte element. In practice it is not possible to do this because the absorbtion edge has fine structure, and it is not possible to choose monochromatic beams very close to the K absorbtion edge, which means that $(\mu_{mh} - \mu_{ml}) \neq 0$. Radioactive sources emitting monochromatic X-rays of energies on either side of the absorbtion edge are useable, but the energy of the photons may not be sufficiently near the energy of the K absorbtion edge to make $(\mu_{mh} - \mu_{ml}) = 0$. A synchroton could be used to generate X-rays of energy close to the K absorbtion edge, but not so close as to overlap the fine structure of the absorbtion edge.

One method of correcting for the matrix effect may be used when the analyte can be introduced into the object after a differential scan of the matrix is first made, and then an identical differential scan is made with the matrix containing the analyte. Thus the X-ray beam flux at each step of a scan of the matrix alone is used as if it were the incident X-ray flux for the corresponding step of the scan of the matrix containing the analyte. The measurements are then due to the analyte element as if the matrix was not present. The equation giving the ratio of the detected X-ray intensities for the two monochromatic

collimated beams, or the X-ray energies selected by single channel analyser windows from a continuum spectrum, effectively two narrow X-ray bands, chosen is

$$N_l/N_h = (N_{ol}/N_{oh}) \exp [(\mu_{ah} - \mu_{al})t_a]\exp[(\mu_{mh} - \mu_{ml})t_m] \quad (3.10)$$

where $t_a = W_a t$ and $t_m = W_m t$, the analyte and matrix equivalent thickness.

This equation for the attenuation of X-rays by the matrix only for these two X-ray bands is

$$N_{ml}/N_{mh} = (N_{ol}/N_{oh})\exp [(\mu_{mh} - \mu_{ml})t_m] \quad (3.11)$$

so $$\exp (\mu_{mh} - \mu_{ml})t_m = (N_{ml}/N_{mh})(N_{ol}/N_{oh}) \quad (3.12)$$

and substituted in the equation for the analyte and matrix gives

$$t_a = [\ln(N_l/N_h)(N_{mh}/N_{ml})]/ (\mu_{al}-\mu_{ah}) \quad (3.13)$$

for the equivalent thickness of the analyte element corrected for the effect of the matrix.

The second method of correcting for the presence of the matrix when the analyte and matrix are not separable is to make measurements which can be used to extrapolate the intensity measurements, $\ln(I_o/I)$, to the K absorbtion edge of the analyte element as shown in Figure 3.5, thus ignoring the fine structre in the curve near the absorbtion edge.

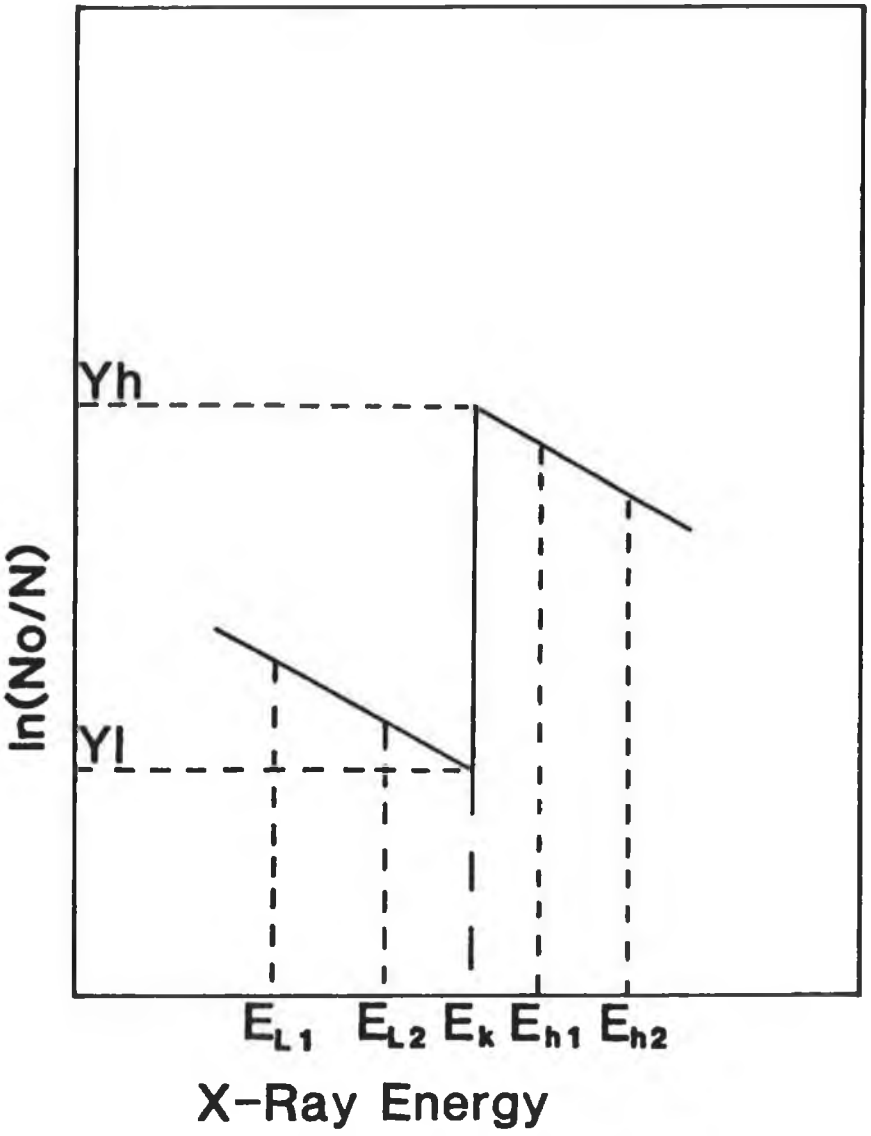

Correction for the effect of the matrix by extrapolation.

Schematic diagram to illustrate the extrapolation of projection data, taken at the four X-ray energies $E_{l1,2}$ and $E_{h1,2}$ to the absorbtion edge at E_k. N_o and N are the incident and transmitted X-ray fluxes respectively. Y_l and Y_h are the extrapolated values of $\ln(N_o/N)$.

[14]

FIGURE 3.5

This method chooses two or more narrow X-ray bands at the low energy side of the absorbtion edge, and two or more at the high energy side. These bands could be four or more narrow collimated coexistent X-ray beams, or a band of X-rays overlapping the absorbtion edge from which four or more single channel analysers, having their windows set to four narrow bands, select the output pulses from an energy dispersive detector. This method scans the object only once. Single channel analysers are needed for selecting the narrow X-ray bands for the X-ray beam overlapping the K absorbtion edge of an analyte element and for the collimated coexistent X-ray beams, and for both methods of correcting for the presence of the matrix.

The flux of X-rays detected for each narrow band or window is

$$N = N_o \exp[-(\mu_a t_a + \mu_m t_m)] \qquad (3.14)$$

so that

$$\ln(N_o/N) = \mu_a t_a + \mu_m t_m \qquad (3.15)$$

When $\ln(N_o/N)$ for each line is extrapolated to the K absorbtion edge, then two equations are obtained.

$$Y_l = \mu_{al} t_a + \mu t_m \qquad \text{for the low energy side} \qquad (3.16)$$

and

$$Y_h = \mu_{ah} t_a + \mu_{mh} t_m \qquad \text{for the high energy side} \qquad (3.17)$$

and Y_l, Y_h are the values of the natural logarithms, at the K absorbtion edge. These equations give the equivalent thickness of the analyte element

$$t_a = (Y_h - Y_l)/(\mu_{ah} - \mu_{al}) \qquad (3.18)$$

because at the absorbtion edge $\mu_{mh} = \mu_{ml}$.
Four narrow X-ray bands provide a straight line extrapolation to the absorbtion edge of an analyte element, but more than four may improve the extrapolation.

A band of X-rays which overlaps the K absorbtion edges of several analyte elements which may be consecutive in the Periodic Table of the Elements can be used to form images of these elements using a multichannel analyser which has two regions of interest or narrow pass bands selected on each side of each element's K absorbtion edge. The complete X-ray spectrum as selected by the multichannel analyser is recorded in its memory, but only the regions of interest are printed out. In this way, three elements of consecutive atomic number may be imaged using eight regions of interest set on the multichannel analyser. To image n elements of consecutive atomic number with a pair of narrow lines on each side of their absortion edges requires 2n+2 regions of interest. Similarly for m narrow lines instead of a pair requires m(n+1) regions of interest.

X-rays are attenuated by the matrix as well as by the analyte element, matrix meaning all elements except the chosen element for analysis, so that if there are several analyte elements present in an object, the matrix includes all analyte elements except the one selected. If an object is irradiated with a broad band of X-rays, the low energy X-rays are absorbed more readily than the high energy or harder X-rays, so that the harder X-rays emerge from the object preferentially. This is known as beam hardening. This work uses nearly monochromatic or narrow band X-rays, and the detector is energy dispersive so that any beam hardening does not affect the measurements.

Due to matrix absorbtion there is a lower limit to the quantity of analyte in a matrix which may be detectable for a particular matrix material and size and the number of photons counted in a full scan of an object. A paper by L. Grodzins [9] examines the theoretical lower limits to differential absorbtion edge tomography using a synchrotron source of X-rays which can be tuned across an absorbtion edge of an analyte element for quantitative measurements of the fraction of analyte element to matrix atoms in an object of given size and material for a given total photon flux for scanning. An equation derived by L. Grodzins in [9] shows that the fraction f of analyte to matrix atoms in an object is inversely proportional to the square root of the total X-ray photon flux:

$$f = \frac{1}{W\mu_m\mu_a A_a \sqrt{\frac{DBC\mu_m}{n_o W}}} \qquad (3.19)$$

where n_o is the total number of incident photons, W is the width of the X-ray beam, D is the diameter of the section in the object being scanned, B is a factor due to the resolution to sensitivity broadening effect of the image reconstruction algorithm taken as 2 in [9], μ_a and μ_m are the mass attenuation coefficients of the analyte element and matrix, and A_a and A_m are the atomic weight of the analyte element and the average atomic weight of the matrix. Grodzin's equation applies to one pixel in the image reconstruction grid.

The maximum fraction of analyte to matrix atoms which is detectable according to L. Grodzin's equation is

$$f_{min} = \text{constant} / \sqrt{N_o} \qquad (3.20)$$

For $n_o = 10^7$, the total number of photons in a complete scan, W = 1mm, D = 40mm, B = 2, gives $f_{min} \approx 3 \times 10^{-5}$. Thus the smallest detectable fraction of analyte to matrix atoms is theoretically about 10^{-5}. so a few kg/m^3 of analyte in a 40mm water like matrix should be measurable. Figure 3.6 shows graphs of f_{min} for various objects scanned with 10^7 X-ray photons in 40 linear steps.

The object is scanned in linear consecutive steps with a narrow collimated beam of X-rays so that at each step the number of photons is counted for a predetermined time to give a set of projection measurements. The object is axially rotated through consecutive angular steps, and at each angle a linear scan is made to give a set of projection measurements corresponding to each angle. An axial image of the concentration of the analyte element in the object can be reconstructed from these measurements or data set using a computer algorithm.

One source of X-rays used in the experiments herein is an Amersham International (241)95Americium variable energy X-ray source shown in Figure 2.10 and the block electric circuit diagram of an experiment is shown in Figure 5.9. The 56Barium K_α and K_β X-rays whose energies are on either side of the 55Caesium K absorbtion edge, detected by the EG & G Ortec Si(Li) detector, are selected by narrow energy windows set in two EG & G Ortec 551 timing single channel analysers, and the differential absorbtion of X-rays is measured. Similarly, the K_α and K_β X-rays from

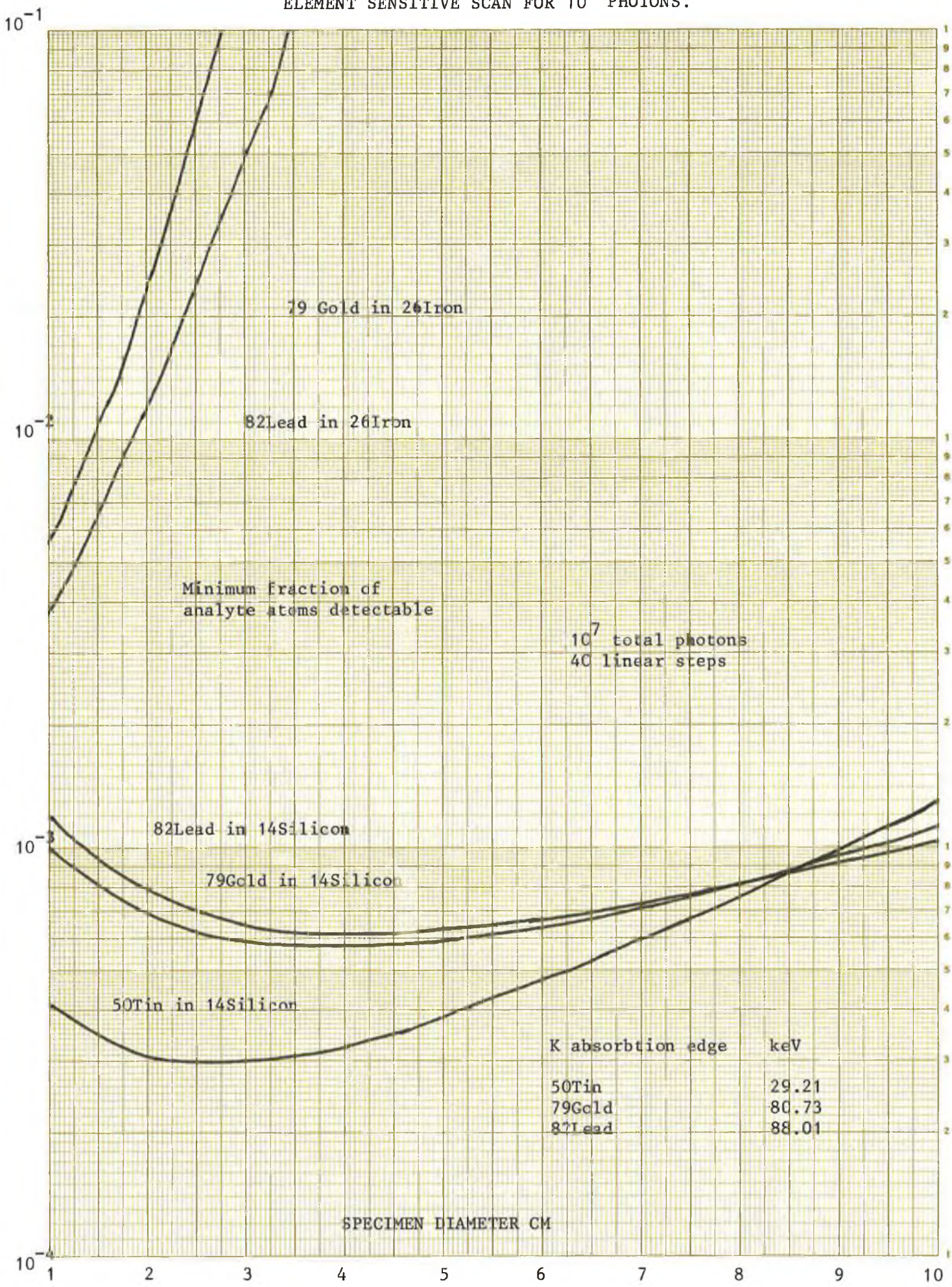
ELEMENT SENSITIVE SCAN FOR 10^7 PHOTONS.
10^{-1}
10^{-2}
10^{-3}
10^{-4}
79 Gold in 26Iron
82Lead in 26Iron
Minimum fraction of analyte atoms detectable
10^7 total photons
40 linear steps
82Lead in 14Silicon
79Gold in 14Silicon
50Tin in 14Silicon
K absorbtion edge keV
50Tin 29.21
79Gold 80.73
82Lead 88.01
SPECIMEN DIAMETER CM
1 2 3 4 5 6 7 8 9 10

FIGURE 3.6

47Silver from a (109)48Cadmium source are differentially absorbed by 46Palladium.

Another source of X-rays is an X-ray tube shown on Plates 4.3 and 4.4 and a block diagram is shown in Figure 6.1. The X-ray tube generates a wide band of X-ray energies which is filtered so as to irradiate the object with a narrow band of X-rays which overlaps the K absorbtion edge of an atomic element. Two single channel analysers with narrow energy windows set on either side of the K absorbtion edge of the element may be used to select X-rays detected by an energy dispersive detector, the EG & G Ortec Si(Li) detector, which are nearly monochromatic, and is thus equivalent to an X-ray source producing two monochromatic X-ray beams of energies on either side of the K absorbtion edge of an analyte element. As with a synchrotron source of X-rays, fine structure does not allow the narrow energy windows to be set too close to the K absorbtion edge, so using two single channel analysers $(\mu_{mh} - \mu_{ml}) \neq 0$. By extrapolating to the K absortion edge of an analyte using four single channel analysers, two on either side of the absorbtion edge,

$$(\mu_{mh} - \mu_{ml}) = 0 \qquad (3.21)$$

The value of $\ln(N_o/N) = \mu t$, where I_o,I are in the X-ray beam intensities, μ is the mass attenuation coefficient and t is the equivalent thickness of the object in the beam path, is independent of the X-ray beam spatial profile, as shown in Annexe B.

The essential scanning measurements for computer axial tomography and differential absorbtion edge tomography are the values of $\ln(N_o/N) = \mu t$ for each step of a scan, where N_o,N are the incident and transmitted X-ray beam fluxes. For computer axial tomography μt is the linear attenuation coefficient of the material in the X-ray beam path of thickness t of the object being scanned. In differential absorbtion edge tomography μt, is the integrated concentrations of the analyte element in the object on either side of its K absorbtion edge for one X-ray beam where t is the equivalent thickness of the analyte element. For the X-ray photon energies used herein and a collimated X-ray beam, the mass attenuation coefficient is close to the mass absorbtion coefficient of the elements, so it is taken as such.

When $\ln(N_o/N) = \mu t$ is extrapolated to the K absorbtion edge of an analyte element then μ is equal to the mass absorbtion coefficient at the absorbtion edge, so that there is an intrinsic correction for scattering of X-rays.

RECONSTRUCTION OF THE IMAGE OF AN OBJECT SCANNED WITH X-RAYS.

Reconstruction of the image through a plane in the object uses a mathematical reconstruction technique which transforms radial digital measurements, the number of photons counted at each scanning step, into an axial digital representation of that plane. There are several possible techniques which may be used; solution of linear simultaneous equations, iterative reconstruction, reconstruction by backprojection, and analyte reconstruction.

Image reconstruction from measurements made in scanning an object by computer axial tomography or differential absorbtion edge tomography consists of two parts: conversion of the line integral of the attenuation of each X-ray beam or of the sum of the concentrations of the analyte elements in a scanning step into image density measurements or representation, and the display of this data as an axial image. The spatial resolution of scanning is approximately the width of the X-ray beam. The image reconstruction is on a square grid in which the number of columns equals the number of linear steps of the scanning, and each element of which is a pixel, a picture element. The first experiments herein had 20 linear steps of 2mm step size and 20 angular steps of 9° increments to give a 20 x 20 grid of 400 pixels. The X-ray beam was 2mm diameter, so that the voxels, volume elements, of the scanning were 2mm cubes. In later experiments there were 40 linear steps of 1mm step size, and 40 angular steps of 4.5° increments with a 1mm diameter X-ray beam to give a grid of 1600 pixels and voxels.

For a scan of 40 steps and 40 rotations there are 1600 linear simultaneous equations in 1600 unknowns, many of which are zero because only some of the pixels and the beams are common for each rotation. In practise the equations are not solved, which would be done by inverting the matrix of overlap areas f_{jk}^{ns} to give each value of the concentration C_{jk} in a pixel, because the number of elements f_{jk}^{ns} is so large, a unique solution does not exist if there are more unknowns than equations, or there may be no solution possible due to errors introduced by noise.

The image reconstruction data may be calculated by computer, using an algorithm, a formula containing a set of steps for carrying out a numerical calculation, instead of solving the simultaneous equations, and two alternative methods are used in this work: an iterative algebraic reconstruction technique, and an analytic filtered backprojection method. The image coded in digital data is then displayed on a colour or grey shade monitor, or printed on paper.

The method herein can be used to produce computer axial tomographs which show X-ray attenuation variations with little or no discrimination between atomic elements, and differential absorbtion edge tomograms which have atomic element identification. All the image reconstruction techniques can produce both computer axial tomographs and differential absorbtion edge tomograms, but only the second can give a quantitative measurement of analyte element concentration.

Calculation of the image reconstruction data array is done herein in two different ways. One is an iterative method, the repeated re-estimation of the concentration of analyte element in each pixel of the reconstruction grid by means of an iterative formula carried out by a computer algorithm which compares calculated equivalent thickness with measured equivalent thickness, the Algebraic Reconstruction Technique. The second method is an example of a transform method in which points located in a plane are changed from polar to Cartesian coordinates, the analytic or Filtered Backprojection method.

THE ALGEBRAIC RECONSTRUCTION TECHNIQUE.

The Algebraic Reconstruction Technique measures the equivalent thickness of the object and compares it with the image which the algorithm has reconstructed.

In the Algebraic Reconstruction Technique a uniform blank starting image of analyte concentration C_{jk} is given to each jk pixel of the reconstruction grid, as shown in Figure 3.12, by means of an initial computer calculation which determines the average equivalent thickness of the analyte element from all the measured values of equivalent thickness. The concentrations C_{jk} of analyte in the pixels are modified for every position of the X-ray beam in the linear scans, and every rotation step from 0° to 180° by the iterative formula

$$C_{jk}(\text{new}) = C_{jk}(\text{old}) + Rf_{jk}^{rs}\epsilon \qquad (3.22)$$

where f_{jk}^{rs} is the fractional overlap of the simulated X-ray beam at the s linear step and r rotation of the scan with the jk pixel of the reconstruction array, and $0 < f_{jk} \leq 1$.

$$\epsilon = \frac{t_{ao}^{rs} - t_{ai}^{rs}}{\sum_{jk} f(jk)^2} \qquad (3.23)$$

is a correction factor in which t_{ao}^{rs} is the equivalent thickness of the analyte in the object measured by the X-ray beam at the s linear step and r rotation, and t_{ai}^{rs} is the postulated equivalent thickness of the analyte in the image calculated for the s linear step and r rotation, which changes at each iteration. $C_{jk}(\text{new})$ is the concentration of the analyte in the jk pixel for the

latest iteration calculated from the previous value C_{jk}(old) modified by the correction factor ϵ. R is an arbitrary relaxation constant, $0 < R \leq 1$, which suppresses oscillations of the concentration values with successive iterations. It is not yet known why this works. The smaller the value of R, the more heavily damped is the oscillation, as shown in Figure 3.7. After one image iteration the image may be shown on the monitor screen, but a better image can be reconstructed after several image iterations, so that the concentration of analyte element in the pixels of the reconstruction grid tends to a limiting value.

The standard deviation in the concentration of analyte in the pixels is given by

$$\sigma^q = \frac{1}{S}\left[\sum_{j,k}\left\{C_{jk}^q - \bar{C}_{jk}^q\right\}^2\right]^{1/2} \qquad (3.24)$$

where q is the iteration number, s is the total number of steps and C_{jk} is the concentration averaged over all the pixels. Iterations are stopped when $\sigma^{q+1} - \sigma^q < (1/N)\sigma^q$ where N is a chosen constant; herein N was chosen as 100, so that the difference between the estimated and measured maximum concentration of analyte element was less than 1%. This means that the number of image iterations required to reconstruct the image can be from 5 to 15 depending on the value chosen for the relaxation constant.

In the Algebraic Reconstruction Technique the areas of overlap between the pixels of the reconstruction grid and the simulated X-ray beam paths were calculated to 0.02 of a pixel in strips parallel to the ordinate. The method of calculation and the BASIC computer program

RELAXATION CONSTANT.

Graph of standard deviation against iteration number for an image of 46Palladium in a 30mm diameter cork matrix, for different relaxation constant R.

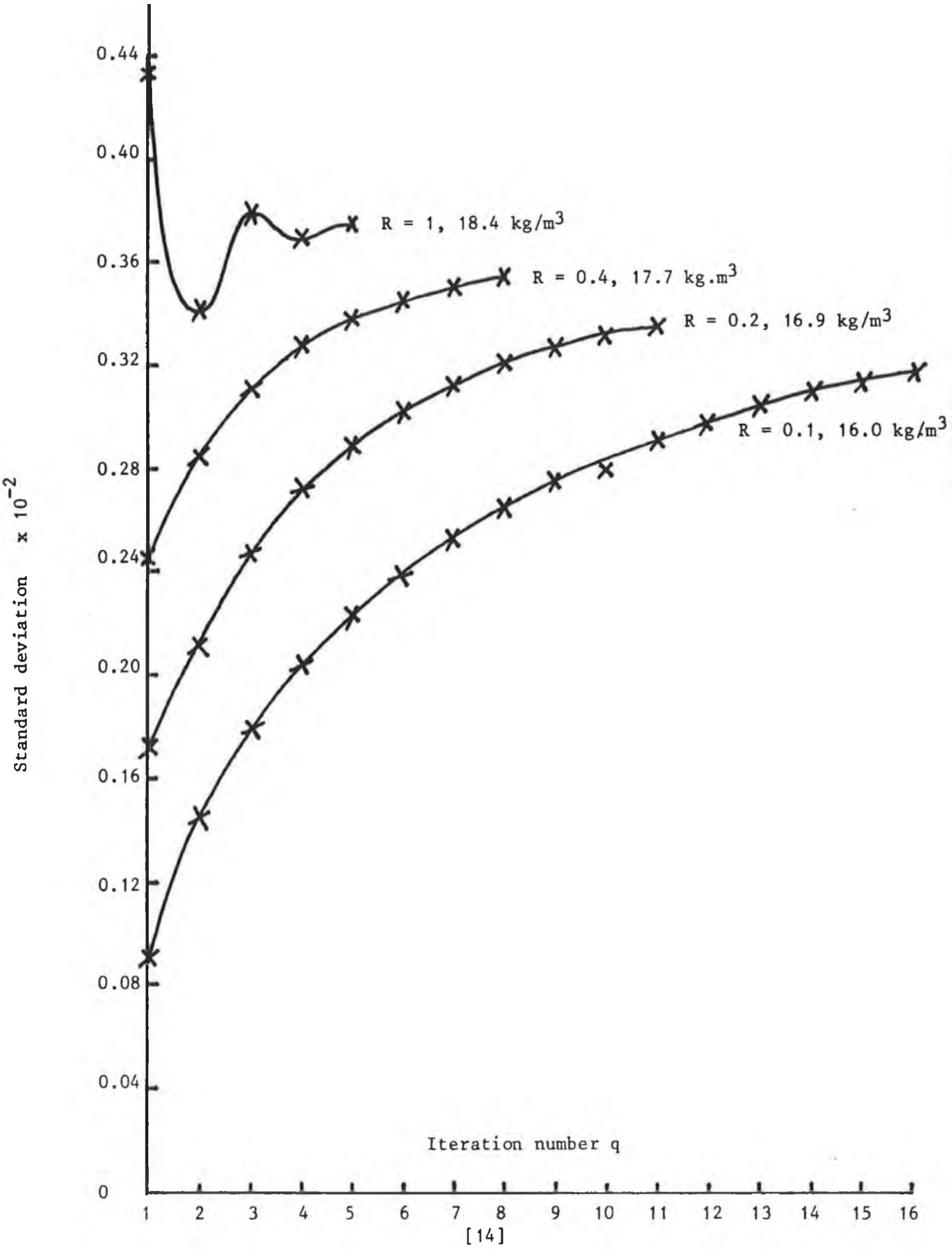

[14]

FIGURE 3.7

RECON40 run on the VAX 11/785 computer is listed in Annexe D. The areas of overlap for the 20 x 20 grid could be stored in the computer whilst the reconstruction programme was being run. For the 40 x 40 grid it was necessary for the overlap areas to be stored on computer disc file and read into the computer one by one whilst the reconstruction programme was being run, because the array was so large; about 132,000 overlap areas.

FILTERED BACKPROJECTION

The simplest method of image reconstruction to implement, it is not simple mathematically, is by means of Backprojection illustrated in Figure 3.8 in which the X-ray scan measurements which are the image projection data or X-ray absorbtion profiles are projected on to the image plane from all the scan angles to build up the image where some of them overlap. The image density in a pixel of the reconstruction grid is the sum of all the integrated linear attenuation coefficients or simulated X-ray beam paths passing through this pixel, and because they extend across the image plane the image density is not zero in pixels not part of the image which results in star artefacts around the edges of the image, or a blurred edge to the image if there is a large number of beam paths. Due to the finite width of the beam path, the scan profile $\ln(N_o/N)$ is a histogram.

The second image reconstruction method used in this work is an analytic method or Filtered Backprojection algorithm in which the image projection data is modified by a mathematical filter function before the image is reconstructed by backprojection. The one used is a Ramachandran filter or convolution function in which the image

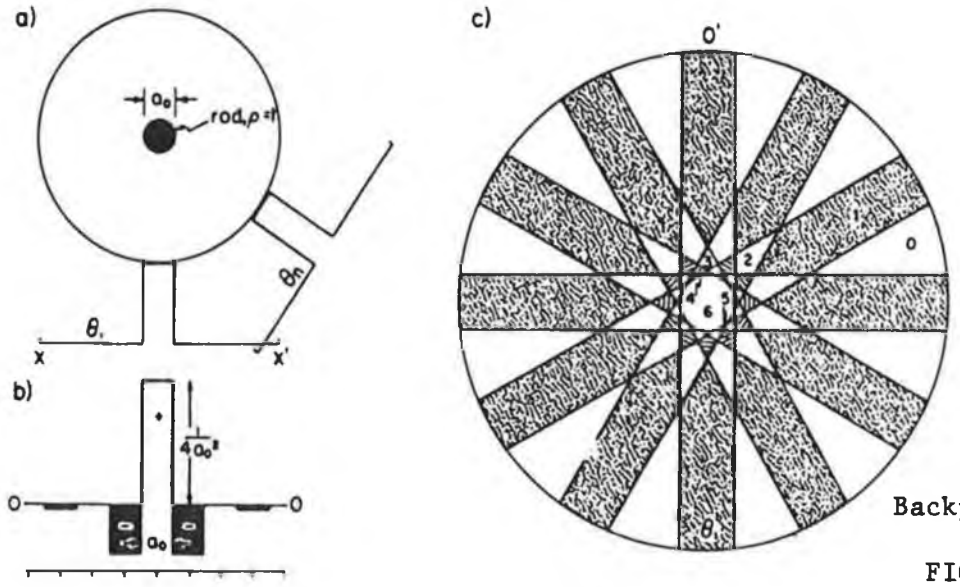

Backprojection.

FIGURE 3.8

a) X-ray transmission profiles at θ_1, θ_n for a rod of density 1 and diameter a_0.
b) Ramachandran filter function.
c) Backprojection of a for 30° angles giving a star pattern.

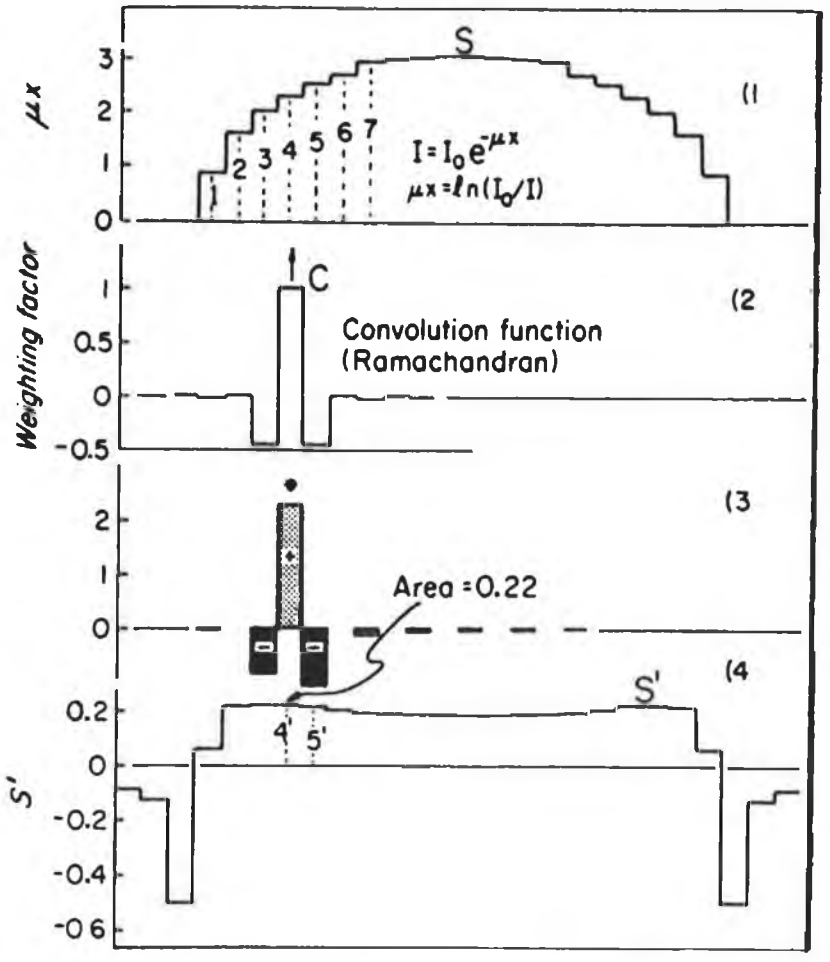

Convolution.

FIGURE 3.11

Convolution. 1) S is a graph of $\ln(I_0/I) = \sum \mu . \Delta x$ for an elliptical object of density 1 irradiated with a vertical X-ray beam.
2) C is a Ramachandran filter function.
3) An intermediate step in the convolution.
4) This is the resultant profile S^1 which is Backprojected.

[H.E. Johns and J.R. Cunningham, The Physics of Radiology].

projection data is convolved with or folded in with the filter so that image artefacts are reduced and an accurate reconstruction image is made.

Reconstruction of an image of an object by backprojection is a linear transformation of detected X-ray photon count data from the object space to the image space in which the projection data measurements, $\ln(N_o/N) = \mu t$, contain the information which is interpreted by an algorithm to reconstruct an image of the object. The image is a projection of the object provided there is a one-to-one correspondence between every point of the image and that of the object. These projection data measurements contain the attenuation of X-rays by an object for computer axial tomography, and the absorbtion of X-rays at the absorbtion edge of an atomic element for differential absorbtion edge tomography.

The flux of detected X-ray photons is given by Beer's Law

$$N = N_o \exp\left[-\int_y \mu(\underline{r})dy\right] \tag{3.25}$$

for each measurement made at a particular step of a scan of an object with X-rays. The linear form of this equation is

$$\ln(N_o/N) = \int_y \mu(\underline{r})dy \tag{3.26}$$

and $\ln(N_o/N)$ is called the Radon transform of $\mu(\underline{r})$ which is the projection data used to reconstruct an image of a plane within the object, by projecting these measurements on to the image plane.

Suppose a quantity varies in a (x,y) image plane so that it is a function of position. The position of any point in the plane may be given in Cartesian or polar coordinates. As shown in Figure 3.9

$$f(r,\phi) = f[(1^2 + z^2)^{\frac{1}{2}} , \Theta + \tan^{-1} (y/1) \tag{3.27}$$

because $r^2 = 1^2 + z^2$

and $\phi = \Theta + \tan^{-1} (z/1)$

The Radon transform of $f(r,\phi)$ is the line integral of $f(r,\phi)$ along a line PL, distance 1 from the origin set at an angle Θ to the y-axis of Cartesian coordinates. If PL is the path of the X-ray beam, then the Radon transform is the integrated linear attenuation coefficient along the beam path, which is the experimental measurement of the Radon transform in the direction of the X-ray beam.

The Radon transform is defined by

$$[Rf](1,\Theta) = \int_{-\infty}^{\infty} f(r,\phi)dz \tag{3.28}$$

where $f(r,\Theta)$ is integrated along the line PL from $-\infty$ to ∞. Thus

$$[Rf](1,\Theta) = \int_{-\infty}^{\infty} f[(1^2 + z^2) , \Theta + \tan^{-1}(z/1)]dz \tag{3.29}$$

for $1 \neq 0$, and

$$[Rf](1,\Theta) = \int_{-\infty}^{\infty} f(z,\Theta + \pi/2)dz \tag{3.30}$$

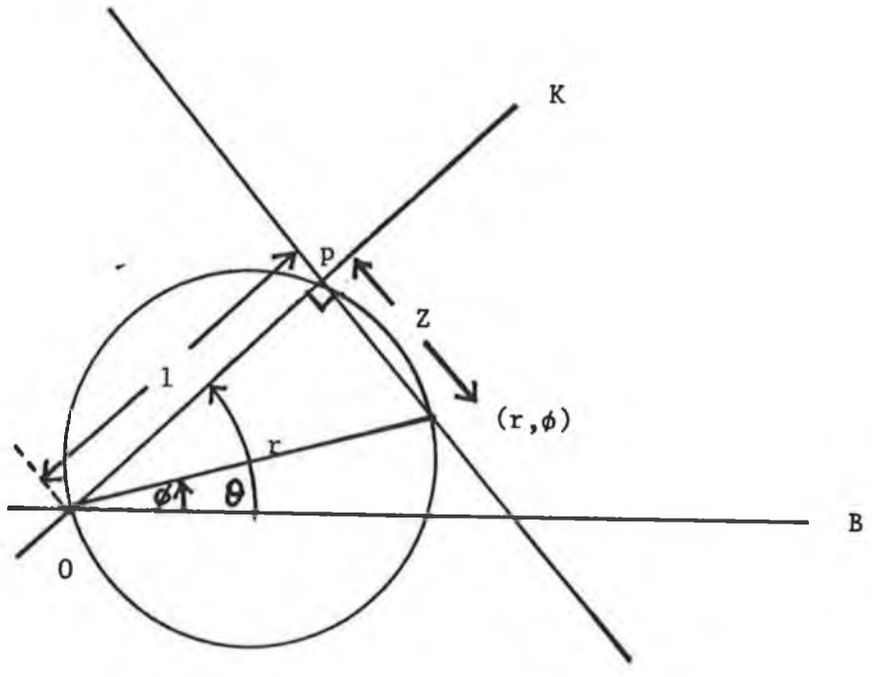

Radon transform R (1,θ) of a function f (r,φ)

FIGURE 3.9

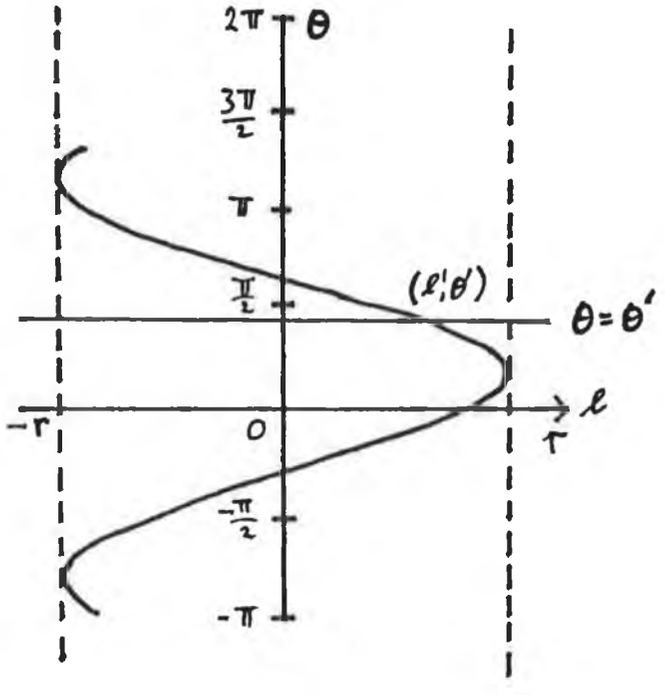

The locus of a set of lines parallel to the line L in Figure 3.9.

FIGURE 3.10

for $l = 0$, which is

$$[Rf](l,\theta) = \int_{-\infty}^{\infty} \mu(r)dz. \qquad (3.31)$$

In practice the integral is along the line between the X-ray source and detector.

In figure 3.10, $l = r\cos(\theta - \phi)$ so that at a particular point (r,ϕ) is constant. The equation gives the locus of the set of points (l,θ) which is a cosine curve of amplitude r and phase angle $-\phi$. If $\theta = \theta'$ is a constant and l varies, the points are on a line parallel to the line L.

In a linear scan of an object at a fixed angle θ' the object moves relative to the X-ray source and detector is parallel steps in a scanning grid. The X-ray photon count at each step gives the X-ray sum at every point of the grid in polar coordinates (l,θ), which is the Radon transform of the linear attenuation coefficient for computer axial tomography, and concentration for differential absorbtion edge tomography at each step i of the scanning grid.

The inverse Radon transform of $f(r_i,\phi_i)$ is

$$R^{-1}\,[Rf(r_i,\phi_i)] = [R_i f](l_i,\phi_i) = f(r_i,\phi_i) \qquad (3.32)$$

a functional, which produces a real number at each step i of the scanning grid, the numerical values of the projection data given by $\ln(N_o/N)$.

The inverse Radon transform is approximated to in Filtered Backprojection wherein a convolution with a Ramachandran filter function is followed by

backprojection. The convolution introduces negative numbers into the reconstruction array which effectively smooths the reconstruction histogram.

The convolution function, illustrated in Figure 3.11 is

$$C = 1/(W^2) \text{ for } k = 0, \quad C = 1/\pi W_k{}^2 \text{ for } k = \pm 1m, \pm 3, \pm 5$$

and C = 0 for k = ±2, ±4, ±6 and W is the width of the pixels in the reconstruction grid. The digital values for C required by the calculation approximate to the curve shown. The calculation is made by the BASIC computer program run on the VAX11/785 computer FILTRECONAV40 listed in Annexe D.

The fractional area of overlap between any pixel in the reconstruction grid with a simulated X-ray beam path is calculated from the geometry of the grid as illustrated in Figure 3.12 using Cartesian coordinates in which the origin is the centre of rotation for the beam paths and the scanning. The method is the same for a 20 x 20 grid and 7.5° angular steps which is a 20 x 24 scan as for a 40 x 40 grid and 4.5° angular steps which is a 40 x 40 scan. The method of calculation and the BASIC computer program RECON40 run on the VAX 11/785 computer are listed in Annexe D: CARLAR40 and FILTRECONAV40.

In the analytic reconstruction method or Filtered Backprojection, each pixel is divided in four equal parts and the X-ray beam path divided in two equal parts in the calculation, and each pixel subdivision is counted as 1 if the centre of a half-beam path passes through it, and 0 if it

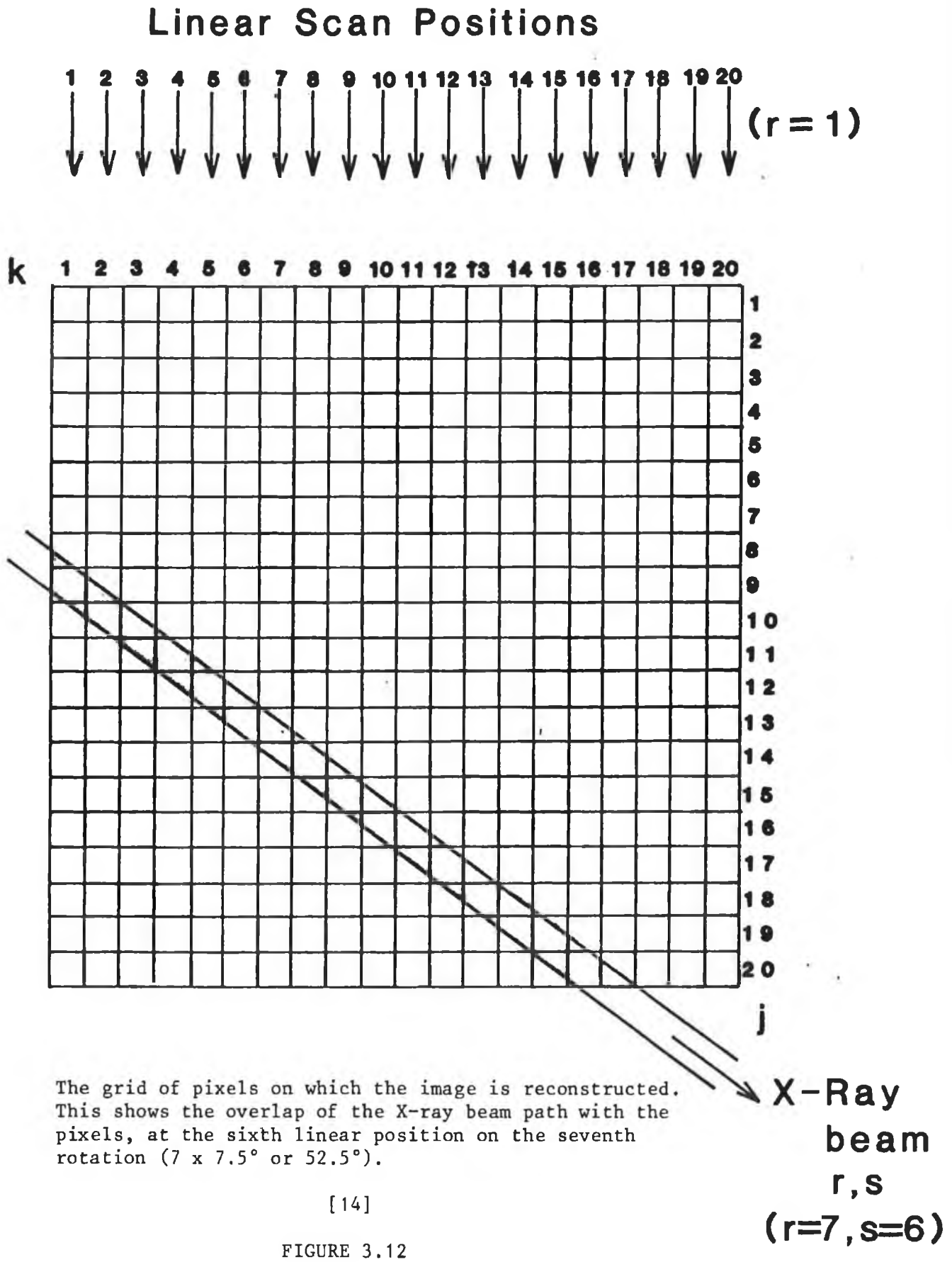

The grid of pixels on which the image is reconstructed. This shows the overlap of the X-ray beam path with the pixels, at the sixth linear position on the seventh rotation (7 x 7.5° or 52.5°).

[14]

FIGURE 3.12

does not. When the calculation is completed the 80 x 80 grid is averaged to a 40 x 40 grid for image display. This method is an improvement on an earlier method in which each pixel is counted as 1 if the centre of the X-ray beam passes through the pixel and 0 if it does not.

THE QUALITY OF A RECONSTRUCTED IMAGE OF AN OBJECT

The number of areas of overlap between the simulated X-ray beam path and the pixels of the reconstruction grid is approximately $2N^3$, where N is the number of linear steps and angular steps. Thus for an 80 x 80 grid there are about 10^6, and about 28 x 10^6 for a 240 x 240 grid. This large number of non-zero overlap areas sets a practical limitation on the spatial resolution of the image reconstruction because of the time required for calculating the image data. To scan an object 240mm across at a 1mm spatial resolution, in practice a realistic scan, requires a very fast computer. This large number of overlap areas corresponds to the N x N pixel grid multiplied by the N angular steps, and there are about twice as many again because the simulated X-ray beam path intercepts the pixels non-orthogonally for all angles except 0° and 90°. The longest beam path across the grid is the diagonal which intercepts about 3N pixels, and the shortest path which is parallel to the diagonal intercepts about 0.4N pixels. The total number of overlap areas including the zeros is about N^4, which corresponds to the (N x N) pixel grid (x N) angular increments, (x N) pixels excluded from the simulated X-ray beam path.

The quality of a reconstructed image of an object made by both kinds of tomography is influenced by artefacts or image distortions which may be introduced at any stage from scanning to display.

Laterally streaked artefacts introduced in the image as shown in Plate 6.2 are due to the X-ray beam being off centre in the linear scan by a small distance, because of an apparent shift of the object as viewed by the X-ray beam and detector. One-to-one correspondence between the object space and the image space is fixed by the centre of rotation, or the ϕ-axis of the scan, being at the centre of the linear scan or the object scanning grid. This artefact may be corrected by shifting the X-ray photon count data in the computer memory array so as to centre the scanning data artifically, but accurate alignment of the X-ray beam with the x-coordinate is the best method to prevent this artefact appearing. The star artefacts or blurred edges around an object which are always introduced in the reconstruction of the image can be reduced by increasing the spatial resolution of the scan. The more scanning steps there are the more this artefact is reduced. Further improvement in image quality is possible using a Ramachandran filter in the reconstruction by Backprojection.

Statistical variations in the X-ray photon count can introduce noise into the image reconstruction, noticeable even with a uniformly attenuating materials. This can be reduced by using a large number of X-ray photons in a complete scan, but the total number may be limited by possible radiation damage done to the object, and by the irradiation time required.

For good image display sufficient colour or grey scale shades are required. Any of the artefacts can occur when the object is rigidly mounted in the scanning coordinate table, and does not move. If the object moves during scanning then streaked or edge distortion of the image may occur. This distortion may be reduced by scanning the object as quickly as possible, for example in medical scanning.

CHAPTER IV

X-RAY MACHINE AND SCANNING INSTRUMENTS

PHILIPS X-RAY MACHINE.

The X-ray machine is part of a Philips PW 1270 automatic simultaneous X-ray spectrometer modified to provide a source of X-rays of chosen energy and intensity of up to 60keV.

The machine consists of a power supply cabinet bolted to an analysing cabinet, which is shown in Figures 4.1 and 4.2. The power supply cabinet has not been modified, and all un-needed wiring inside the analysing cabinet of the spectrometer has been removed. The block wiring diagram of the machine is shown in Figure 4.3. The full electric circuit diagram of the machine is shown in Figure 4.4, and only a small part of this was modified to include the voltage and current monitor lamps, and additional microswitches in the safety shut down circuit. All components in the analysing cabinet of the spectrometer have been removed except the 66kV high tension tank, water cooling supply, and the X-ray tube.

The X-ray machine consists of a Philips PW 2184/00 X-ray tube, a high tension constant voltage generator, high voltage and current control circuits, and switch-on and safety circuits. The X-ray tube target is cooled by a pressurised mains cold water supply, so that the anode is

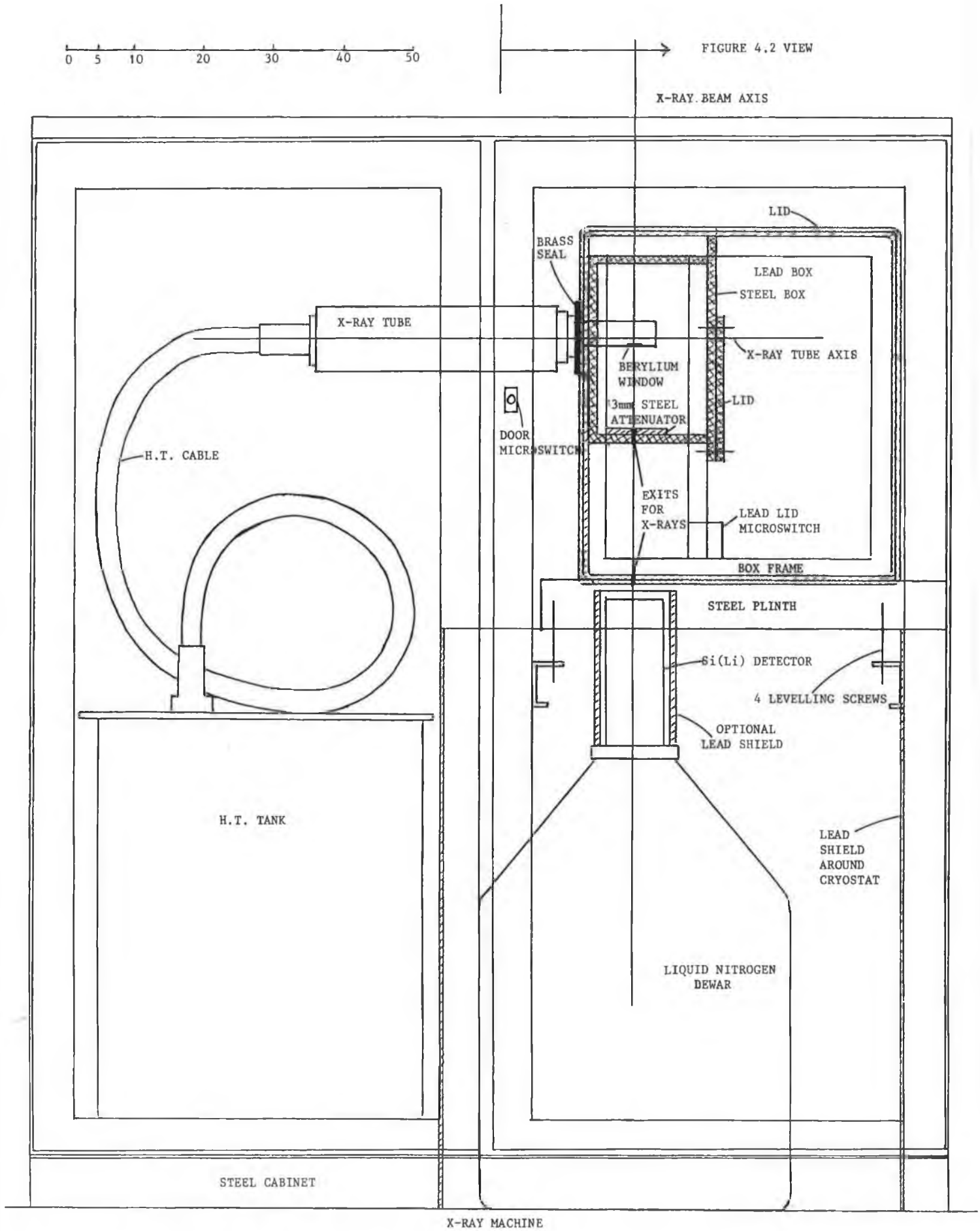
SCALE, centimetres
0 5 10 20 30 40 50
FIGURE 4.2 VIEW
X-RAY BEAM AXIS
LID
BRASS SEAL
LEAD BOX
STEEL BOX
X-RAY TUBE
X-RAY TUBE AXIS
BERYLIUM WINDOW
3mm STEEL ATTENUATOR
LID
DOOR MICROSWITCH
H.T. CABLE
EXITS FOR X-RAYS
LEAD LID MICROSWITCH
BOX FRAME
STEEL PLINTH
Si(Li) DETECTOR
4 LEVELLING SCREWS
OPTIONAL LEAD SHIELD
H.T. TANK
LEAD SHIELD AROUND CRYOSTAT
LIQUID NITROGEN DEWAR
STEEL CABINET
X-RAY MACHINE

FIGURE 4.1

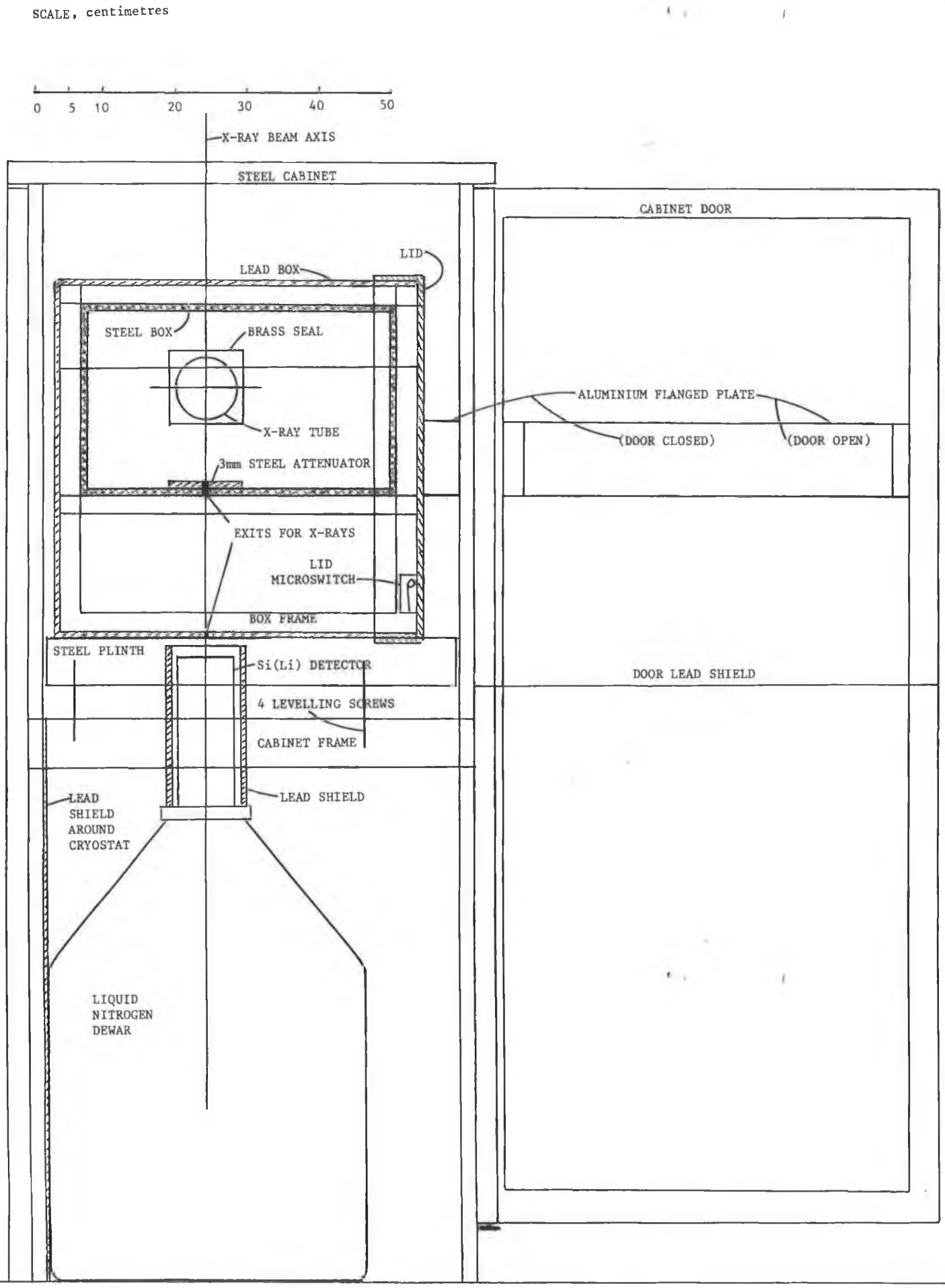

X-RAY MACHINE
FIGURE 4.2

X-RAY MACHINE BLOCK WIRING DIAGRAM.

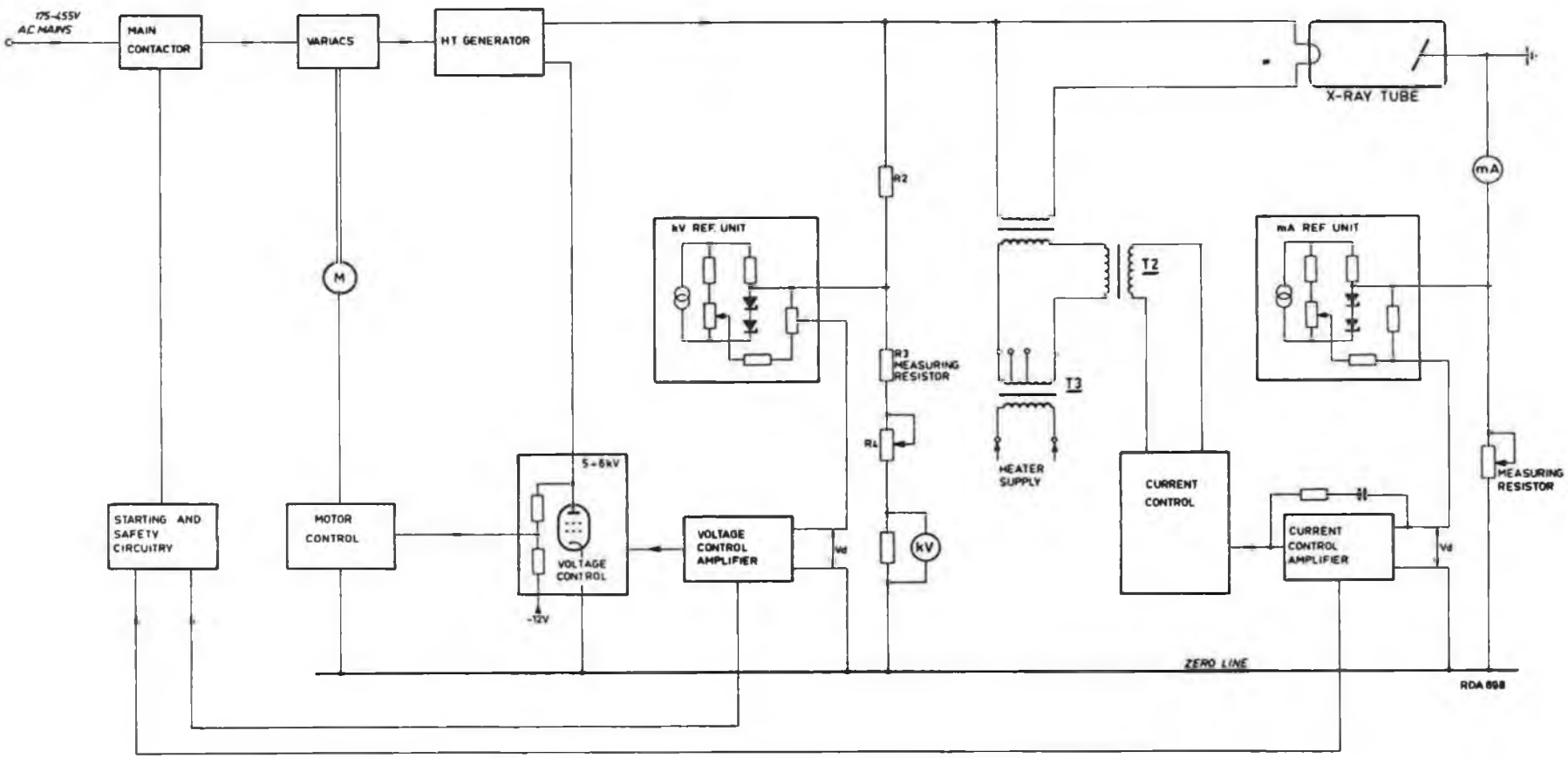

[Philips, Automatic simultaneous X-ray spectrometer PW1279].

FIGURE 4.3

applied to the cathode heater of the X-ray tube. The stability is better than 0.03%.

The high voltage is controlled with reference to a very stable and variable reference voltage V_r, kV REF.UNIT, which is thermostatically controlled. The high voltage is monitored via a voltage divider R_2 R_3 R_4, in the high tension tank, tapped so that a fraction V_m is compared with V_r: the difference $V_d = V_r - V_m$ is applied to the VOLTAGE CONTROL AMPLIFIER stabilised by matched pair transistors to minimise drift whose output is connected to the fast response VOLTAGE CONTROLLER, V.C.. The stabiliser in the voltage controller is a high voltage thermionic valve whose quiescent anode voltage is 5.5kV. The control range is ±4kV so that at 60kV, mains electricity voltage fluctuations of up to 6% are correctable by the fast voltage controller, and which can also correct ripple voltages. The thermionic valve stabilises the negative polarity high tension direct current with reference to the zero line by compensating for voltage fluctuations at the opposite positive polarity terminal of the bridge rectifier by operating as a variable impedance current sink. The 66kV maximum output of the high voltage transformer is -60kV with respect to the zero line, in addition to a maximum of +6 kV on the anode of the thermionic valve with respect to the zero line.

The motor driven variable transformers via the MOTOR CONTROL are used for correcting for voltage changes greater than 6%, and for changing from one high voltage setting to another by the kV selection switch SK1 on the selection and indicator panel S.I.. If the voltage variation is greater than 500 the electric motor M is switched on by the voltage control unit to change the position of the contacts on the variable transformers so that the anode voltage of the valve returns

to its preset value. The X-ray tube high voltage is determined by the voltage of the primary winding of the high voltage transformer as selected by the variable transformers.

The current flowing in the X-ray tube is measured by the potential difference it produces across the very stable wire-wound MEASURING RESISTOR. The difference voltage V_d between this potential difference and a fixed very stable reference voltage in the thermostatically controlled MA REF.UNIT is applied to the CURRENT CONTROL AMPLIFIER which controls the CURRENT CONTROL. There is a resistance condenser feedback filter having a long time constant to smooth 50Hz and 100Hz electricity mains ripples to prevent amplifier oscillation. The current control is effectively a variable resistance whose magnitude depends on its input voltage from the current control amplifier, and the resistance is stepped up by the impedance transformer T2 connected in series with the primary winding of the X-ray tube cathode heater supply transformer T3 connected to the electricity mains. The filament tranformer T2 in the high tension tank GN is a high voltage isolating transformer. The secondary windings of the heater supply transformer T3 and the impedance transformer T2 and the primary winding of the filament transformer T2 are all connected in series. The load for the current control circuit is the filament transformer primary winding, connected to XA16 and XA15 in Figure 4.4. The impedance transformer is a variable impedance in the filament transformer circuit, effectively a potentiometer which controls the current flowing in the load. The impedance of the secondary winding of T2 depends on the voltage in its primary winding and this voltage is supplied by the CURRENT CONTROL which is a variable impedance. When there is no voltage across the primary winding of T2 then the impedance of its secondary winding is very large and effectively an

open circuit, so that the current flowing in the filament transformer is nearly zero. When there is a voltage across the primary winding of T2 then the impedance of its secondary winding drops and the transformer T3 supplies a current to the filament transformer.

The current in mA settings are chosen by changing the measuring resistor on the selection and indicator panel, S.I..

The push button SK4 on the selection and indicator panel is pressed so as to energise the relay RE1 which allows the electricity mains current to flow through the primary section of the auto transformer T7. The secondary section of T7 includes the contacts of the safety circuits in which the electricity mains current flows which must be closed in order to allow relay RE1 to be energised. The safety circuits are the thermostat switch on the power supply cabinet which opens if the temperature reaches 65°C, the cabinet door and analysing chamber microswitches, the X-ray tube high voltage cable security chain microswitch, and the Penn external outlet water flow switch. If any of these contacts are open, then the relay RE1 cannot be energised, or if any should open during machine operation RE1 is de-energised, and the machine shuts down immediately. With relay RE1 energised, the contacts S-V and R-U close to allow electricity mains current to energise the auto transformer T1, the secondary section of which supplies 220 volts electricity mains current to the variable transformers, and to the whole X-ray machine. The blue monitor lamp lights.

The bimetal thermal delay switch B1 heats, and after 45 seconds its contacts close to complete the circuit to energise relay RE11. During this time the contacts of the variable transformers are turned to the

minimum voltage position. The relay RE2 closes its contacts S-V and R-U so that the electricity mains voltage is applied to the primary of the high voltage transformer so that the high voltage is switched on, and the variable transformers' contacts are turned to their selected kV setting. There is another delay of 45 seconds during which the red monitor lamp flashes at 1 Hz, after which time the relay RE15 is energised so that its contacts 5-6 close to supply electricity mains voltage to the cathode heater transformer T2, and its contacts 9-10 open to send an all clear signal to the logic circuits of the machine. Then the red monitor lamp lights continuously and the 'X-RAYS ON' lamp lights. The red lamp flashes whenever the voltage or current settings are changed, and lights continuously when voltage and current are at their selected settings. The X-ray tube current is switched on following voltage switch-on so as not to overload the cathode of the X-ray tube with a momentary heavy current.

The X-ray machine is switched off by pressing the 'OFF' button SK7 which is connected in series with the safety circuit microswitches, and this de-energises the main relay RE1 so as to open its contacts S-V and R-U so switching off the current to the autotransformer A.T.U.. Both cabinets are fitted with red pilot lamps LA1 and LA2 which light when the doors are open for inspection provided the safety circuit interlock door microswitches MS1, MS2, MS4 are defeated by withdrawing the lever in each microswitch.

The X-ray machine has an internal water flow switch in the cooling water circuit which switches off the machine after a delay of 6 seconds if the water flow rate falls below 3 litres per minute. The 6

second delay prevents brief pressure drops in the water supply switching off the machine.

The voltage and current stability of the X-ray machine is better than 0.03% following half an hour's operation for electricity mains voltage variations of -15% to +10%. Stability may be checked by connecting a differential voltmeter between terminals 10 and 11 of the high tension tank for voltage stability, and between the positive terminal of the millimeter and the zero line for current stability.

The specification of the X-ray machine and the X-radiation flux calculations are in Annexe A.

The photographs show further details of the X-ray machine and scanning instruments. Plate 4.1 shows the machine closed ready for scanning an object. The EG & G Ortec pulse counting instruments and detector power supply are placed on top of the X-ray machine, and beside it on the bench are, in order, the (x,z,ϕ) scanning coordinate table controller, the EG & G Ortec 7100 multichannel analyser, the BBC microcomputer and colour monitor. Plate 4.2 shows the X-ray machine opened, and the high voltage transformer, X-ray tube, Lead analysing chamber, and EG & G Ortec Si(Li) detector are visible. Plate 4.3 shows part of the inside of the analysing cabinet in more detail. Plate 4.4 shows the inside of the Lead analysing chamber containing the steel box shield for the X-ray tube and the (x,z,ϕ) scanning coordinate table. An aqueous 48Cadmium sulphate object in a sealed perspex container is mounted on the ϕ-coordinate of the table.

X-ray machine and pulse counting instruments.

PLATE 4.1

The X-ray machine analysing cabinet.

PLATE 4.2

The X-ray tube and high tension tank.

PLATE 4.3

The Lead analysing chamber and coordinate table.

PLATE 4.4

ANALYSING CHAMBER.

The analysing chamber, shown in Figures 4.1 and 4.2 and Plate 4.4 is a 3mm thick Lead box formed of 1.5mm thick sheet Lead on a light box section steel frame, with 7cm wide fully overlapping joints, and fully sealed on the 5 sides. All joints are soldered with Timman's solder using resin as soldering flux, and the solder has penetrated well under the joints. The box is closed with a closely-fitting 3mm thick Lead lid with 7cm flanges formed on and soldered around the edges to a thin steel flanged sheet, which is pushed on to the open side of the box at the front. The external dimensions of the box are 45cm wide by 49cm high by 50cm deep. The box is mounted on a steel frame plinth the height and level of which can be adjusted by four screws attached to the frame of the analysing cabinet. The door of the Lead box is held tightly shut by means of a flanged plate attached to the door of the cabinet, which is secured shut by two hex bolts. A 10mm thick welded steel box external dimensions 17cm wide by 27cm high by 44cm deep is mounted on the frame inside the Lead box, the partially open side of which facing towards the inside of the Lead box is closed with a 10mm thick flat steel plate having a 3cm minimum overlap secured to the flanges on the steel box with 10 hex bolts. The X-ray tube is sealed into the Lead box with a closely fitting 10mm thick brass plate collar which is secured to the Lead and steel boxes with four studs threaded into the brass collar. The exits for the X-ray beam are a 2mm diameter aperture in the steel box, and a 15mm diameter aperture in the Lead box situated vertically below the anode of the X-ray tube. These apertures may be covered with 0.5mm thick Lead plates having exits of up to 2mm diameter to collimate the X-ray beams. Various

kinds of X-ray filters may be placed below the exit in the steel box, held in a slider and frame attached to the bottom of the box. An attenuator made of a 3mm thick piece of mild steel may be attached to the bottom of the steel box to reduce the intensity of the X-ray beam to a level which the detector and pulse counting equipment can measure. The thickness of the Lead is sufficient to absorb X-rays down to the calculated exposure rate level, and below the measured natural background level, even if the lid of the steel box is not in place, or in the absence of the steel box, as shown in Annexe A.

Electric cables to the inside of the Lead box are led in through 100cm long narrow channels folded over and soldered to the top right hand corner of the outside of the Lead box.

The power supply incorporates a shut down safety circuit which includes the door microswitches, all electrically connected in series. A door microswitch is added to the cabinet door for access to the Lead box, and a microswitch is attached to the inside of the Lead box to protect its lid. When the lid of the Lead box is fully closed by the Aluminium flanged plate pressing against it this microswitch clicks closed, and when the two hex bolts on the cabinet door are fully secured, the door microswitch clicks closed. On outlet water flow switch external to the machine is also connected into the safety circuit. Thus if any of these microswitches are open, including the ones already in the machine, such as the cabinet door not fully closed, or open, or the lid of the Lead box not fully closed, or not in place, or the flow of water too low or absent, then the machine will not start; or if already running, it will immediately shut down.

X-RAY TUBE COOLING WATER PRESSURISER.

Production of X-rays by bremsstralung is very inefficient; about 1% of the energy in the electron beam at the energies selected is converted to X-rays, the rest of the energy being converted to heat which must be dissipated. The X-ray tube, high tension tank, power supply cabinet, and analysing cabinet are cooled by a mains cold water supply circuit, which incorporates a fan-convected air cooler, heat exchanger in the high tension tank, and the Copper block anode of the X-ray tube, to sink. More than 3kW of heat needs to be dissipated when the machine is operating at maximum power, and a water flow of at least 3 litres per minute is required. A pressure of about 3.5 bar is needed to achieve this flow rate due to the resistance of the water circuit. The mains cold water supply pressure varies between 1 and 2 bar, so a continuously running water pressuriser is needed to increase the pressure. Figure 4.5 shows a recirculating water pressuriser, which consists of a water inlet valve, a 10-stage high pressure water pump, Stork VCX10, water pressure gauge, outlet pipe to X-ray machine, and a recirculating bypass with gate valve. The mains cold water is turned on at the inlet valve and flows through the pump and gate valve through the X-ray machine, at mains pressure. When the pump is operating the water pressure is raised above that of the mains pressure by partially closing the bypass gate valve; the more fully it is closed, the greater is the pressure of the water. The excess energy added to the water by the 0.5kW electric motor of the pump is dissipated in the gate valve and pump, and causes no noticeable temperature increase of the water.

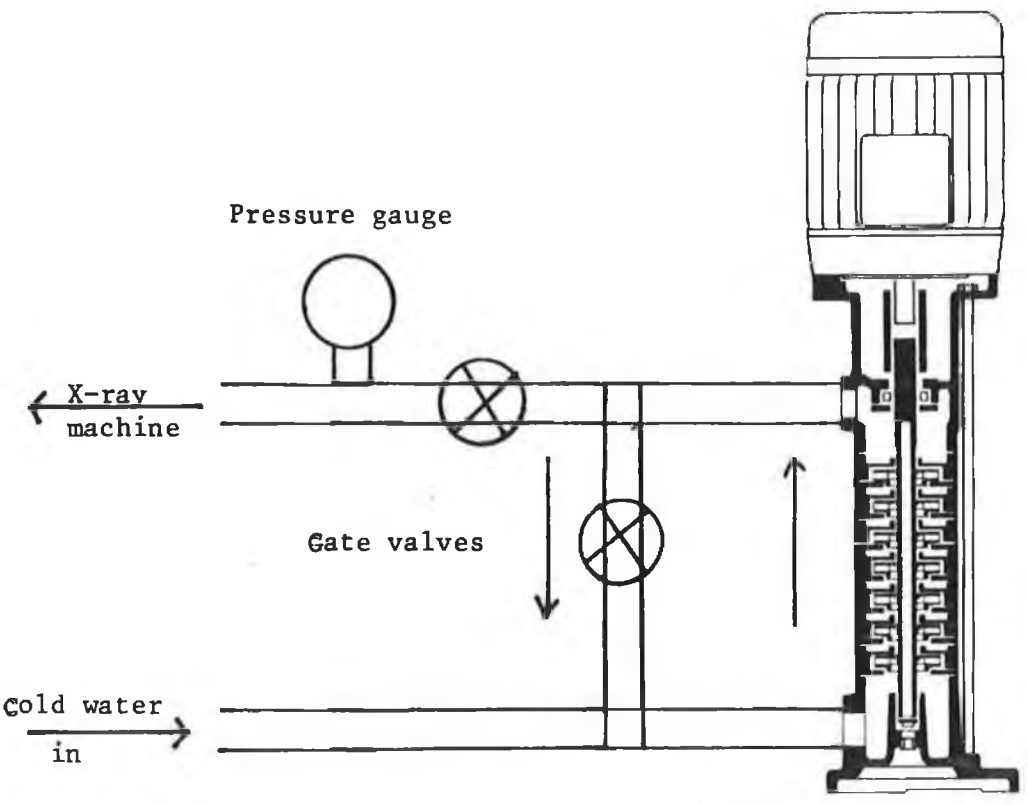

X-ray tube cooling water pressuriser.

FIGURE 4.5

(x,z,ϕ) SCANNING COORDINATE TABLE.

The object to be scanned is mounted in a chuck or secured to a bush wheel on a (x,z,ϕ) scanning coordinate table shown in Plate 6.1 which is modified Feedback CNC 932 computer controlled milling machine. The x and z coordinate movements are made by the stepping motors in the table which rotate lead screws, controlled via an interface by a BBC microcomputer. The x-coordinate motor moves the object transversely across the beam of X-rays for the linear scans, and the z-coordinate motor moves the object axially of the X-ray tube through the beam of X-rays so that a chosen disc of the object can be scanned. The object is rotated in angular steps by a stepping motor mounted on the table and controlled by the BBC microcomputer. The centre of rotation of the ϕ-coordinate must coincide with the centre of the X-ray beam in order to prevent blurred streaked artifacts appearing to one side at the edges of the reconstructed images, and a BBC microcomputer program, MDPOINT was written to do the centering.

The centre of the X-ray beam fixes the centre of the linear scan. The centre of rotation of the ϕ-coordinate, are the two primary reference points in the scanned object. These points match the centre of rotation in the simulated X-ray beam path with the centre of the reconstruction grid for the image, held in an image data array in computer memory or on disc file, to ensure that there is a one to one correspondence between every point of the image and the scanned object. The centering program, MDPOINT, and a synopsis thereof is listed in Annexe D.

X-RAY DETECTOR.

The X-ray detector is placed on the floor of the analysing cabinet below the exit in the Lead box. The detector used herein is an energy dispersive Si(Li) detector which can be used for computer axial tomography as well as differential absorbtion edge tomography, and a scintillation detector which can be used for computer axial tomography. A 1.5mm thick Lead shield attached to the inside walls of the analysing cabinet surrounds the liquid Nitrogen dewar flask below the detector, and the top of this shield is near the bottom of the Lead box. A 1.5mm thick Lead shield covers the inside of the doors of the cabinet.

The detector, illustrated in Figure 4.6 is an EG & G Ortec Lithium drifted Silicon, Si(Li) detector sealed in a vacuum cryostat cooled to 77K by liquid Nitrogen contained in a 30 litre dewar flask. It consists of a p-type Silicon single-crystal semiconductor having an intrinsic or i-type region between p-type and n-type regions, the i-type region being formed with Lithium diffused or drifted into the p-type Silicon. The Lithium compensates for the p-type and n-type dopants and the impurities in the Silicon. The p-type region is on the detector surface, and the n-type region is below. Thin Gold electrodes make ohmic contact with the p-type and n-type layers in the crystal. The n-type layer is connected to a field effect transistor and preamplifier. The p-type layer is covered with a 10μm thick Beryllium window, and the detector is sealed in a capsule to protect it from external contamination and from light. The 77K cryostat reduces electrical noise in the detector and preamplifier and prevents

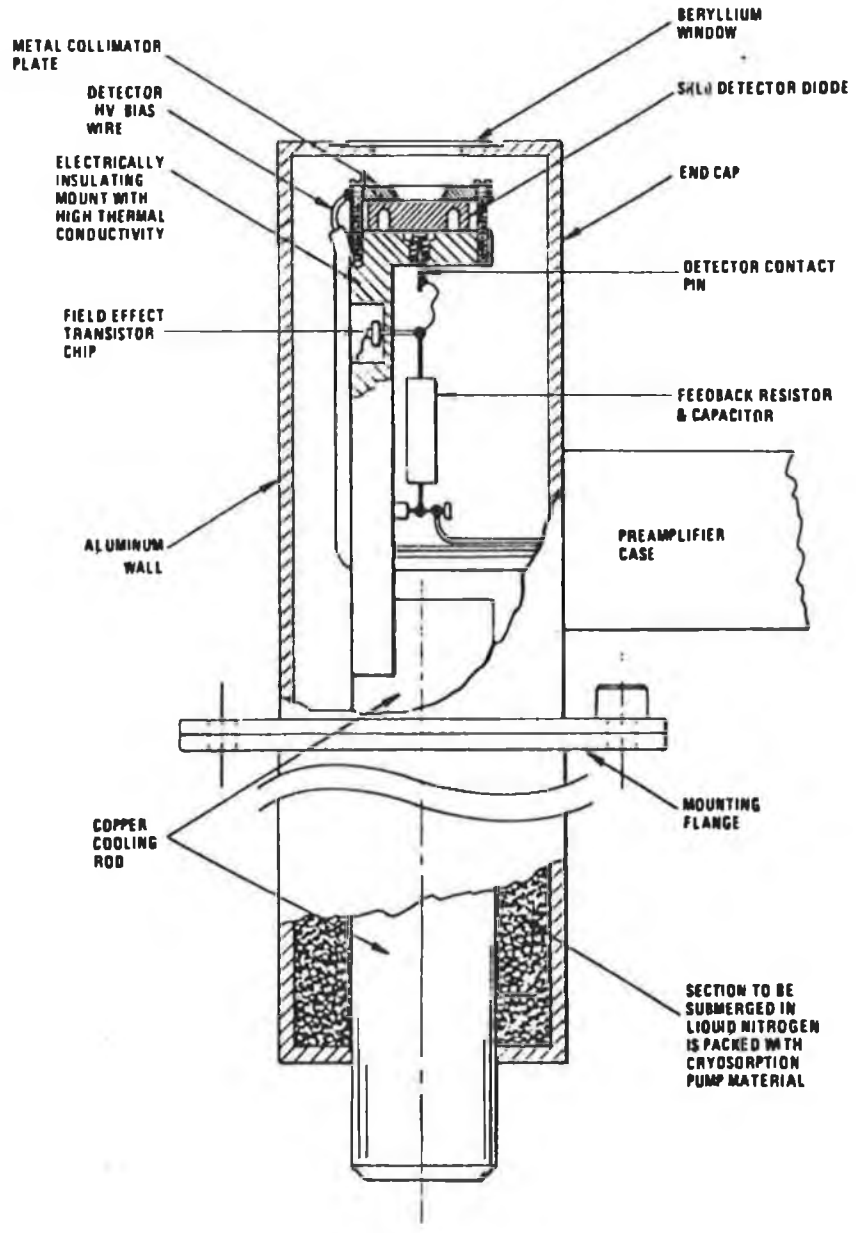

The Lithium drifted Silicon detector.

The mounting is in a 77K liquid Nitrogen cryostat.

[E.G. & G Ortec; R. Jenkins, R.W. Gould, and D. Gedeke, Quantitative X-Ray Spectrometry].

FIGURE 4.6

the Lithium from diffusing through the Silicon when an electric field is applied to the crystal.

A direct current at -1500 volts from a stabilised nuclear instrumentation module power supply is applied across the detector element. Thus the detector is a reverse-biased p-i-n diode, a fast acting photoresistor, in which the i-type region is depleted of free electron-hole pairs, and so has a high electrical impedance. The strong electric field draws the electrons to the p-type region, and the holes to the n-type region of the diode. The active part of the detector is the depletion region, which is 6mm in diameter and 5.47mm deep.

When an X-ray photon enters the depletion region it is absorbed by a Silicon atom giving up all of its energy to a photoelectron ejected from that Silicon atom. This photoelectron ionises the Silicon along its path to produce electron-hole pairs, losing about 3.8eV of energy for each pair produced. Thus the number of pairs produced is proportional to the energy of the photoelectron, which in turn is proportional to the energy of the X-ray photon. The electron-hole pairs are collected by the electrodes of the diode to produce a charge pulse which is integrated by an integrating circuit to an electric current and changed to a voltage pulse, the magnitude of which is proportional to the energy of the X-ray photon. Thus the Si(Li) detector can distinguish between X-ray photons of different magnitude, which is in the range of 3keV to 60keV by the magnitude of the corresponding output voltage pulse. This means that the Si(Li) detector is energy dispersive.

This Si(Li) detector has a count rate capability set at greater than 10^5 counts per second, with a measured energy resolution of about 230eV at 8keV the K_α line of 29Copper and of about 370eV at 22keV the K_α line of 47Silver. The energy resolution of a detector changes a little with the count rate. Figure 4.7 shows the energy resolution performance of a Germanium detector which is a graph of the full width at half maximum resolution in eV against the input count rate for an EG & G Ortec planar high purity 32Germanium detector used with an EG & G Ortec 572 main amplifier. The feedback resistance of $2 \times 10^9 \Omega$ in the charge sensitive loop of the preamplifier is chosen for high count rates. τ is the time constant of the main amplifier. The resolution is decreased as the maximum count rate capability is increased, set by the value of the feedback resistance in the preamplifier and the time constant of the main amplifier. The curves are similar for a Si(Li) detector, but the resolution is a little better than can be obtained with high purity Germanium detectors.

Figure 4.8 shows the variation in percentage detector efficiency for an EG & G Ortec Si(Li) detector in the energy range 1keV to 100keV. The practical detector range is for photons of about 1.5keV to 60keV.

Figure 4.9 compares the spectral resolution capability of the Si(Li) detector, the 54Xenon gas proportional counter, and the 11Sodium iodide scintillation detector for the 22.16keV K_α line from 47Silver with matched amplifier gains.

The Si(Li) detector is protected by a remote shut down circuit which

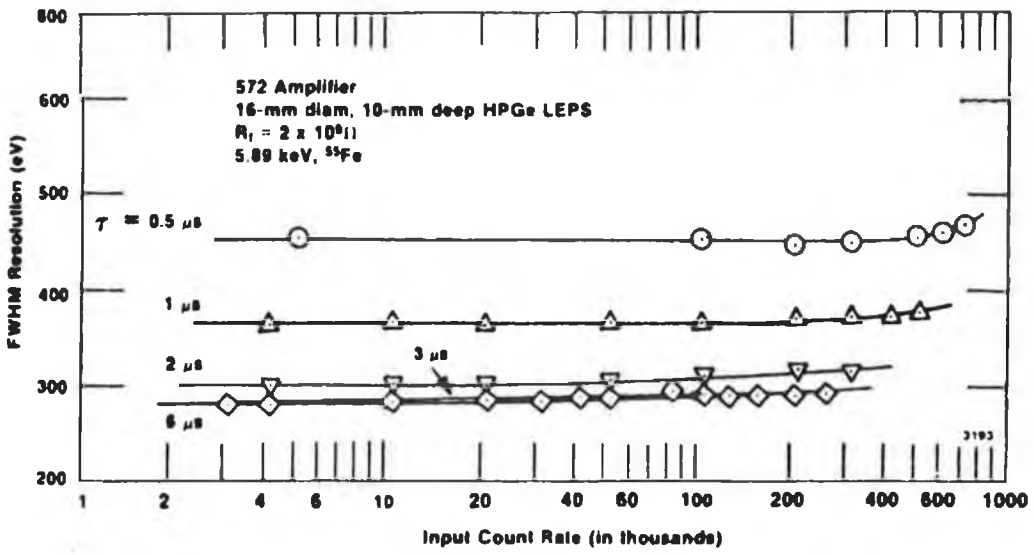

The energy resolution performance of a 32Germanium detector. [E.G. & G.Ortec, Nuclear Instruments and Systems].

FIGURE 4.7

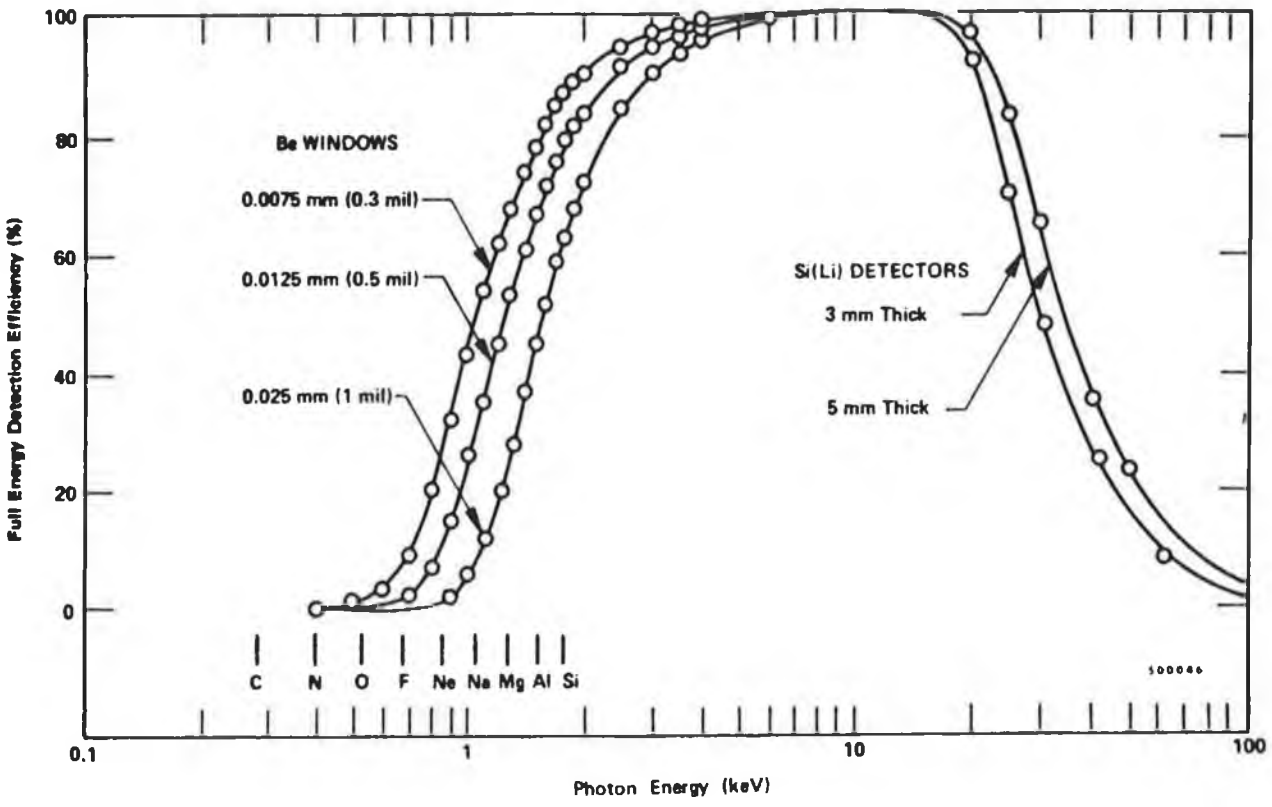

The detection efficiency of a Si(Li) detector. [E.G. & G,Ortec, Nuclear Instruments and Systems].

FIGURE 4.8

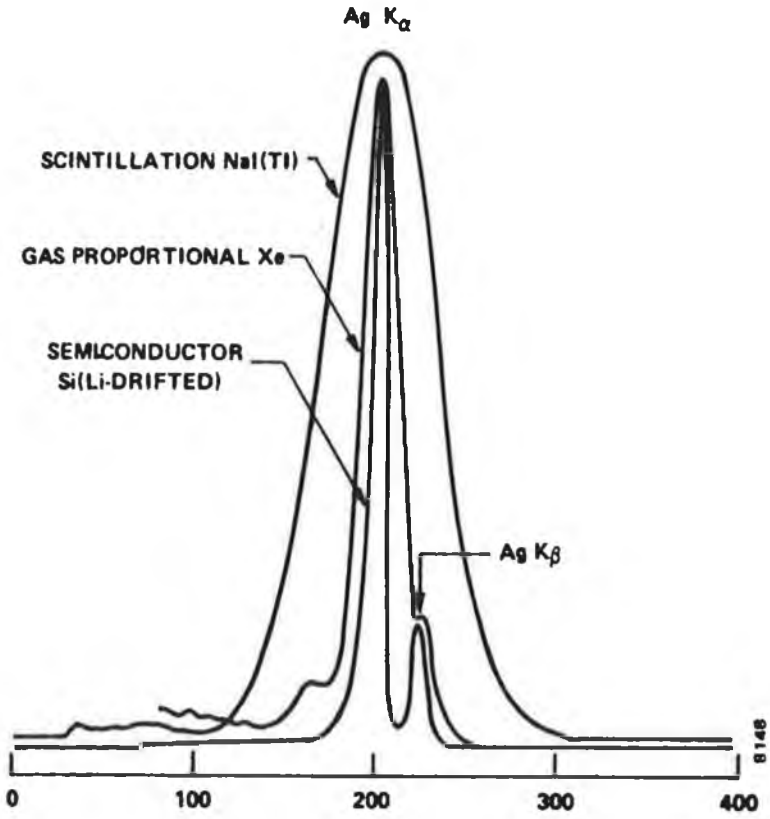

FIGURE 4.9

The spectral resolution capability of three X-ray detectors.

[E.G. & G.Ortec, Experiments in Nuclear Science].

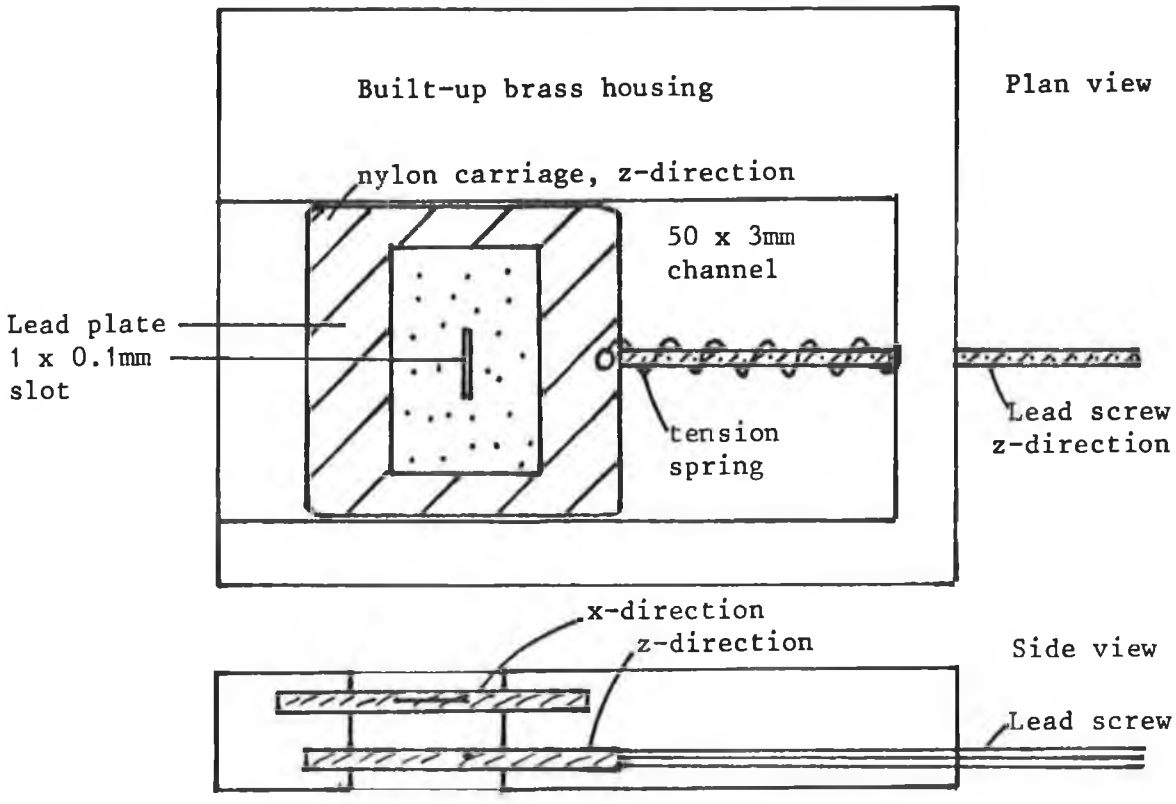

An adjustable collimator.

FIGURE 4.10

switches off the high tension power supply if the temperature of the detector rises above 77K.

X-RAY BEAM COLLIMATORS.

The X-ray beam is collimated with Lead collimators to define the size of the beam equal to the width of the linear scanning steps, and to ensure as far as possible that the X-rays which are detected are photons not scattered by the atoms in the object being scanned. Thus the detected beam should be only the photons not absorbed by the object.

The collimators in the Lead box were aligned with the anode of the X-ray tube by simulating the X-ray beam path using a Helium-Neon laser clamped vertically on a retort stand placed on the floor of the analysing cabinet. The laser was positioned so that its beam passing through the 15mm aperture in the Lead box and the 2mm aperture in the steel box was shining on the centre of the Beryllium window of the X-ray tube. A 1mm diameter collimator of Lead 0.5mm thick was placed on the floor of the steel box; its position was adjusted so that the laser beam was of maximum intensity at the centre of the Beryllium window, and then it was secured to the steel box. In the same manner a 1mm diameter collimator was secured to the floor of the Lead box. The 1.5mm diameter exit of a portable 241 Americium variable energy X-ray source was placed over the collimator in the Lead box, and the Si(Li) detector was moved underneath it until the detected count rate increased to a maximum. Thus the two collimators defined a 1mm

diameter vertical pencil beam through the centre of the Beryllium window of the X-ray tube and the detector.

In practice, alignment of the detector was difficult because a 1mm pencil beam of source to detector distance 450mm through the two collimators to impinge upon the 6mm diameter detector element allowed very little error in placement of the detector. Thus the collimator on the bottom of the Lead box was replaced with a collimator which was adjustable independently transversely and axially of the X-ray tube from outside the X-ray machine, and this made alignment of the X-ray beam and detector easy.

The adjustable collimator is shown in Figure 4.10. It consists of two 0.5mm thick Lead plates 40mm square mounted closely together in the X-ray beam, one above the other. Each plate has a 1mm x 10mm slit cut in the middle thereof, one slit set at right angles to the other. Each Lead plate is enclosed in a nylon carriage, 50mm square and 3mm thick, which slides smoothly in a channel 50mm wide and 3mm deep. The channels which are set at right angles to one another are formed in a built-up brass housing secured by four bolts to the underside of the plinth upon which the Lead box is mounted. The slit in each Lead plate is set crosswise of the channel in which the plate is mounted. The carriage is moved forwards along its channel by means of a lead screw, the head of which presses against the middle of one side of the carriage. A tension spring, surrounding the lead screw, attached to the carriage at one end and soldered into a circular groove in the brass housing at the other end ensures that the head of the lead screw is in contact with the carriage. The uppermost carriage can be moved

through a distance of about 15mm transversely of the X-ray tube, the end of the lead screw being accessible from the rear of the X-ray machine. The lower carriage can be moved about 70mm axially of the X-ray tube by means of the lead screw accessible from the side of the machine. In this way it is possible for the lower carriage to clear the 25mm aperture in the brass housing through which the X-ray beam passes. Thus the two Lead plates can define a 1mm square pencil beam which is movable to any position within a 10mm diameter circle by rotating the lead screws.

The adjustable collimators were preset experimentally. The collimators were removed from the X-ray machine, and the detector was positioned beneath the 15mm diameter aperture in the Lead box. A photographic plate was placed on top of the detector, about 5cm below the aperture in the Lead box, and using the 1mm diameter collimator in the steel box as a pinhole camera, a photograph of the anode inset in the window of the X-ray tube was taken at 40kV, 5mA, 45 seconds exposure time, and which appears as an image illustrated in Figure 4.11. The collimators were then remounted to the underside of the Lead box plinth in the machine.

The adjustable collimators were set at a position corresponding to the middle of the image of the anode by experiment. When scans of the anode of the X-ray tube were done using the two movable slits, the count rate measured by the detector confirmed the size and shape of the image in the photograph. The scan axially of the X-ray tube, with the transverse-motion slit set at the maximum count rate position, is

Graph of Counts/sec against the distance the axial collimator moves in mm for the X-ray tube and scintillation detector.

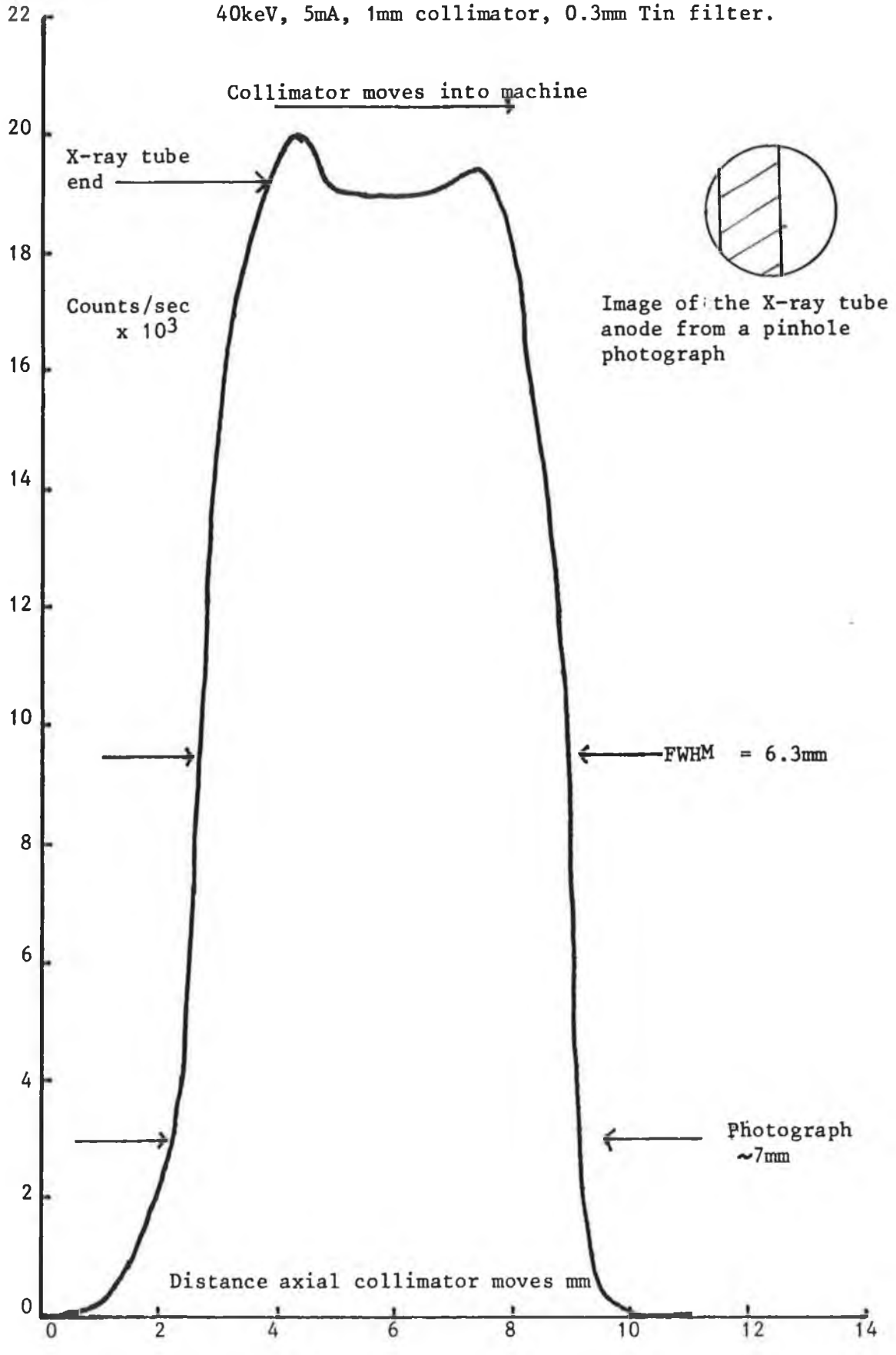

X-ray beam spatial profile.

FIGURE 4.11

shown in Figure 4.11 which is a graph of count rate against position of the collimator slit.

X-RAY PHOTON COUNTING INSTRUMENTS.

The EG & G Ortec 575 main amplifier, connected to the Si(Li) detector and X-ray photon counting instruments, shown in the block diagrams of Figures 5.9 and 6.1 has a low voltage power supply for the preamplifier in the Si(Li) detector. Negative pulses from the preamplifier are conducted by a screened lead to the main amplifier and amplified to standard NIM unipolar pulses, 20μs duration, which range in magnitude from 0 to +10 volts, depending on the input pulse voltage, and the gain of the amplifier which can be set between 10.5 and 501.5. The decay time of the pulses is shortened by adjusting the pole-zero cancellation potentiometer in the amplifier so that the pulse trace viewed on an oscilloscope connected to the output of the amplifier returns to the baseline on the screen of the oscilloscope as quickly as possible without undershooting the baseline. The maximum count rate of the main amplifier is about 1.5×10^5 per second for 5 volt pulses. The gain of the amplifier, which is normally set at 250 herein is determined experimentally: the output pulse magnitudes are to be in the range of 0 to 10 volts for the range of energies of the X-ray photons being counted. The two negative output connections of the main amplifier are each connected to the input connector of a single channel analyser, or alternatively, one output connector is connected to the input of a multichannel analyser.

The EG & G Ortec 550 single channel analysers are used to select amplified voltage pulses from the energy dispersive Si(Li) detector within a chosen range of voltages which correspond to a particular range of X-ray photon energies if the output voltage of the Si(Li) detector and the main amplifier are linearly proportional to the input voltage. The lower energy level is selected by a lower level discriminator which can be adjusted in the range 0 to 10 volts, and the upper energy level is adjusted in the range 0 to 1 volt above the lower level set by an upper level discriminator. As the low level discriminator voltage is raised the upper level discriminator voltage rises with it, of fixed magnitude, thus defining a voltage window which can move along a 0 to 10 voltage range in step with the X-ray photon energy range, the part of which is determined by the gain of the main amplifier. The window of one single channel analyser is set at the high energy side, and the window of the other is set at the low energy side of the absorbtion edge of an analyte element when an object containing the analyte element is being irradiated with a filtered continuum of X-rays which overlaps the K absorbtion edge of the element. Alternatively, if a radioactive source of X-rays is used to irradiate the object instead of a continuum X-ray source, the windows of the two single channel analysers are set on the K_{α} and K_{β} lines of the source on each side of the absorbtion edge of the element. Thus the window of the single channel analyser is an adjustable narrow band pass filter which can be turned into voltage pulses in an adjustable voltage spectrum determined by the 575 amplifier gain, and which corresponds linearly with the energy spectrum of the X-ray photons. The window may be calibrated using photons of known energy, for example the K_{α} and K_{β} lines of 56Barium

by use of a multichannel analyser, or by scanning. The single channel analysers are set on the K_α and K_β Barium X-ray lines by scanning each one with a narrow 10mV window. The width of the peak is found, and the lower level and upper level discriminations are set so that the window encompasses the peak only. For a gain of 250 in the main amplifier the Barium K_α line lower level discriminator is 4.90 volts with a window of 140mV, and the Barium K_β line lower level discriminator is 4.30 volts having a 250mV window.

The EG & G Ortec 551 timing single channel analyser similar to the 550 single channel analyser, has an adjustably delayed output pulse which can range between 0.1 and 11μs.

The EG & G Ortec 7100 multichannel analyser has 1024 channels into which amplified electrical pulses from the Si(Li) detector are selected and stored in internal memory according to the magnitude in an input range between 0 and 10 volts. An analogue to digital converter measures the magnitude of each input pulse and this is represented by an integer number which is the address of a location in the multichannel analyser memory. Each memory address corresponds to a channel, and the numbers of pulses in the channels can be displayed on a monitor. This is a pulse height analysis of the pulses giving a histogram of energy against count intensity. When the conversion gain or resolution of the analogue to digital converter is set at 1024 the full scale range of a 0 to 10 volts is divided into discrete segments of about 10mV wide. The memory of the multichannel analyser can be calibrated in energy so that the cursor can indicate the energy of each channel in keV instead of channel number. Calibration is done

using two monochromatic X-ray sources of known energy, one near the high and one near the low energy ends of the spectral range of choice, and the multichannel analyser internal calibration procedure. The maxima of the two peaks correspond to two channels on the monitor, the numbers of which are then converted to energies in keV to define an energy scale on the multichannel analyser. A lower level discriminator, a circuit which rejects pulses below a chosen amplitude, determines the lower energy limit at which pulses are converted to a number by the analogue to digital converter so that low energy electrical noise, or pulses below a particular energy level can be excluded. The discriminator shapes the accepted pulses to standard amplitude and profile; transistor-transistor logic +5v pulses.

The number of pulses counted in each channel of the multichannel analyser can be transferred to a BBC microcomputer via the serial connector of the multichannel analyser and the RS423 serial connector of the BBC microcomputer.

The multichannel analyser has no energy window. A timing single channel analyser can be used to make a window in the multichannel analyser by first passing the pulses through the single channel analyser so that only those that pass through the voltage window in the single channel analyser appear in the multichannel analyser. Conversely, the multichannel analyser can be used to set the voltage range of the windows for two single channel analysers by adjusting their windows so that the upper and lower level voltages coincide with the edges of the K_α and K_β peaks appearing on the multichannel analyser monitor screen. Figure 4.12 shows a block electric circuit

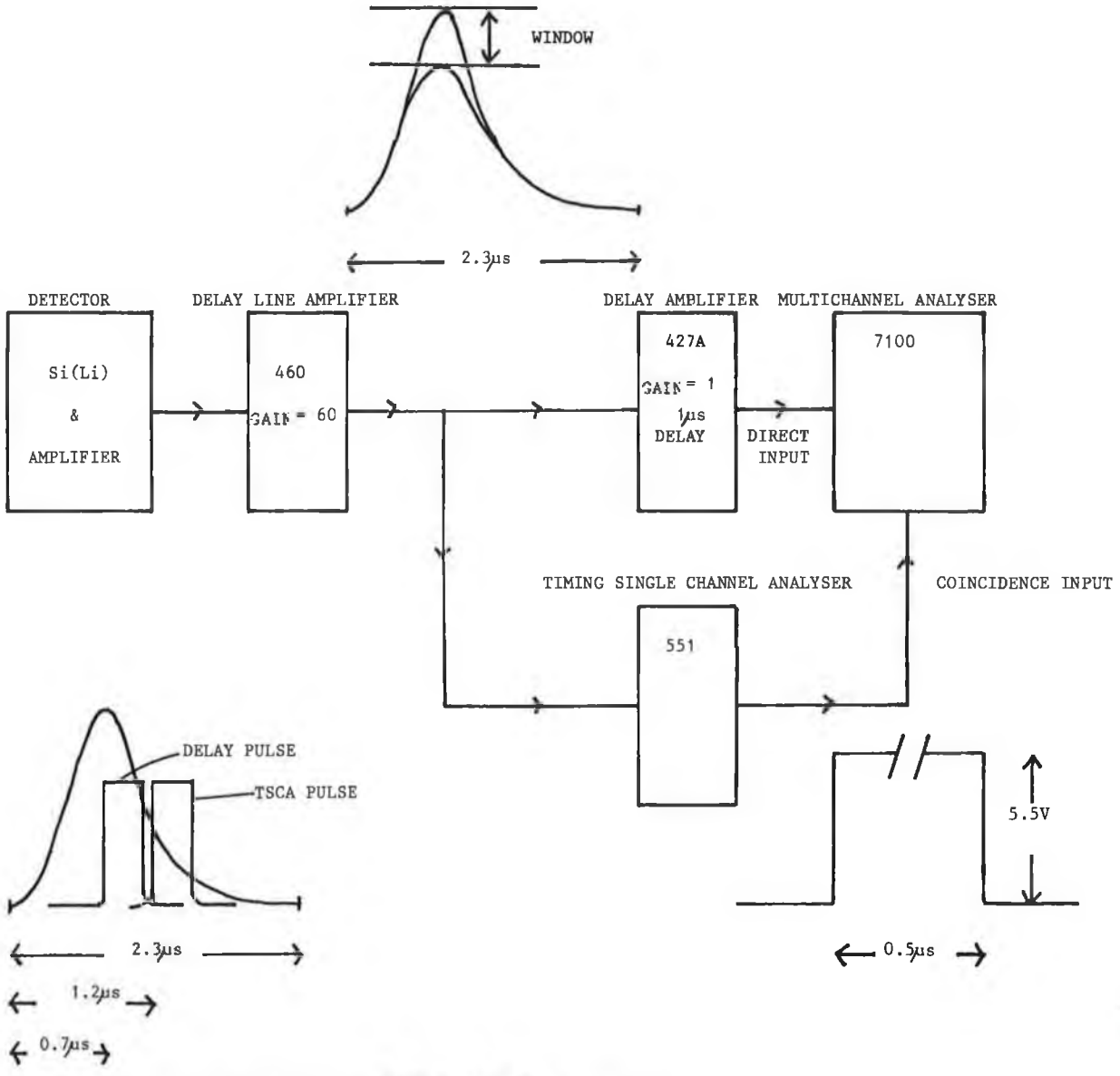

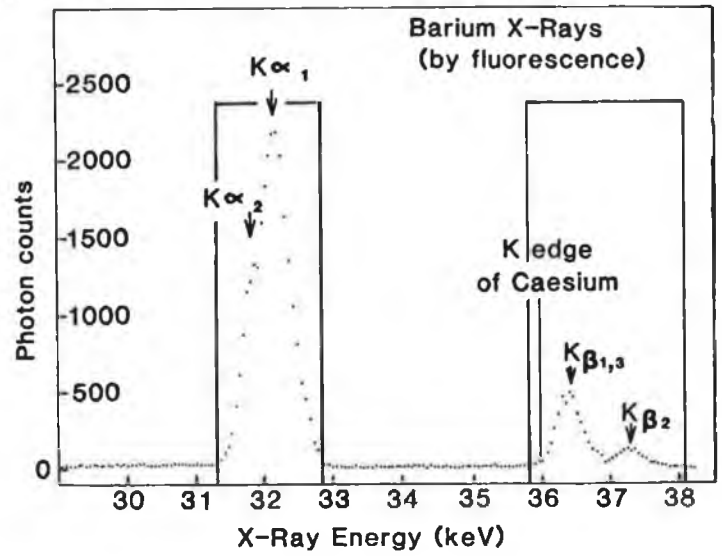

DELAY LINE AMPLIFIER GAIN	= 60
INTEGRATING TIME CONSTANT	= 0.2μs
DELAY AMPLIFIER TIME	= 1μs
TSCA DELAY TIME	= 625ns
TSCA FOR K_{α} LOWER LEVEL	= 4.82V
WINDOW	= 0.25v
PEAK AT CHANNEL NUMBER	= 448
TSCA FOR K_{β} LOWER LEVEL	= 5.37v
WINDOW	= 0.35v
PEAK AT CHANNEL NUMBER	= 507

MULTICHANNEL ANALYSER ENERGY WINDOWS FOR 56BARIUM.

FIGURE 4.12

diagram for making windows in the multichannel analyser, a diagram of the regions of interest, and the pulses. A coincidence circuit in the multichannel analyser allows its analogue to digital converter to be gated, so that only the pulses which pass through the single channel analyser window are recorded in the multichannel analyser. This happens when the multichannel analyser receives a pulse from both input terminals simultaneously; coincident pulses. The output pulse from the single channel analyser occurs at the mid point of the trailing edge of the input pulse, in order to allow its analogue to digital converter to measure the pulse height, in addition to the delay caused by the single channel analyser which is set by the delay control. The EG & G Ortec 426A delay amplifier retards the input pulse so that the coincident input pulse and the direct input pulse are in step to allow the direct input pulse to be recorded by the multichannel analyser. The delay time is adjusted until the two pulses coincide, as viewed on a two channel oscilloscope screen.

The Nuclear Enterprises Scalar Ratemeter SR7 is for counting and analysis of the pulses from radiation detectors; scintillation detectors or Geiger counters, proportional counters or semiconductor detectors. It has a direct current high voltage supply, linear amplifier and pulse analyser, two scalars, with one input terminal each, and digital ratemeters, a timer, and interfaces for a printer and digital recorder.

The high voltage supply for operating a radiation detector can be varied from +10 to +2500 volts in four ranges with a potentiometer

fine adjustment. The setting resolution is 1 volt, and the maximum current is 200μA at 2000 volts.

There are three input terminals; scintillation detector, and Geiger counter which accept negative pulses, and a positive pulse amplifier input terminal.

The pulse analyser has three operational modes: integral, normal, and window mode. In the integral mode all incoming pulses above a voltage threshold, the range of which can be selected from 10mV to 1998 mV, are counted. In the normal mode only the pulses between independent upper and lower levels are counted. In window mode, the fixed window mode moves on top of the lower level. The scalars can register 10^6 counts, with a maximum count rate of 2×10^6 counts per second.

The Scalar Ratemeter SR7 has four operating modes: one cycle in which it counts for a given time and stops; a digital rate mode in which it counts continuously until manually stoped; a periodic count mode in which the counting is done for a preset period and repeats itself, for a maximum of 255 times, after a selected time interval; and a high voltage scan mode in which the high voltage output is peridically decreased in cycles. The operation of the scalar ratemeter is selected by the keyboard on the front panel.

The Scalar Ratemeter SR7 was used in the first experiments for differential absorbtion edge tomography using the EG & G Ortec Si(Li) detector, and for computer axial tomography using a scintillation detector from the Philips PW 1270 spectrometer, as a pulse counter

interface between the EG & G Ortec 551 timing single channel analysers and the BBC mircocomputer. This was necessary because the 551 timing single channel analysers are not accessible by the BBC microcomputer. The block electric circuit diagrams using the Scalar Ratemeter SR7 are shown in Figures 5.7 and 5.9.

X-RAY BEAM TRANSMISSION FILTERS.

The X-ray tube produces a continuum spectrum of photons having a range of energies from a maximum which is the operating potential of the anode of the X-ray tube to a few hundred electron volts of dwindling intensity. The general form of the continuum spectra for 20, 25, 30, 40 and 50kV for a 74Tungsten target is shown in Figure 2.8. The intensity maximum increases with increasing voltage, and the intensity at fixed voltage is proportional to the electric current flowing in the X-ray tube. Most of the spectrum for a particular operating voltage is not needed to scan an object for one or a few atomic elements, and is also unwanted, because every photon which is detected, whatever its energy, adds to the count rate of photons by the counting instruments. To maximise the count rate for a particular range of energies, and in order to maintain it within the count rate capability of the instruments, it is necessary to exclude as much of the continuum outside the required photon energy range as possible. This is done by means of a metal filter placed in the X-ray beam at the exit of the steel box. A filter may be placed anywhere in the beam provided it is sufficiently far in front of the detector so as not to increase the count rate due to scattering by the atoms of the filter, and is preferably located inside the Lead box. The required

X-ray beam intensity is for a maximum count rate of about 10^4 s^{-1} in order to keep the dead-time of the multichannel analyser to less than about 15%. The total number of photons required is 10^6 to 10^8 for a complete scan of an object.

The effect of a particular element and the thickness of that element used for filtering X-rays can be calculated by means of a BASIC program run on a BBC microcomputer, shown in Annexe D. This program, SPECTRA, calculates the intensities of the X-rays transmitted through the filter, the attenuation of the filter, and draws a graph, for a range of energies from 12keV to 50keV, and wavelength from 0.025nm to 0.1nm, in energy increments of 1keV. The computer program uses the equation

$$I = I_o e^{-\mu t} \qquad (4.1)$$

where I is the intensity of the emergent X-ray beam of incident intensity I_o, μ is the mass attenuation coefficient of the filter metal, equivalent thickness t, in the calculations using data input on computer file; incident intensity of X-rays at 1keV intervals, mass attenuation coefficients of the filter element corresponding to these X-ray energies, density and thickness of the filter element. The filter considerably attenuates low energy X-rays, and absorbs nearly all of those above the K absorbtion edge of the element constituting the filter, leaving a pass band of the continuum to emerge from the filter.

The attenuation increases with filter thickness more rapidly than the bandwidth narrows. Thus to choose a particular pass band of energies,

it is necessary to choose a filter element having its K absorbtion edge at the high energy side of the pass band, a filter thickness which gives a bandwidth which includes the absorbtion edges of the elements being analysed, and an attenuation such that the counting instruments are within their count rate capability for a chosen electric current flowing in the X-ray tube. The voltage on the anode of the X-ray tube should be a few to about 10kV greater than the energy of the K absorbtion edge of the filter element. The pass band spectrum for a 0.3mm thick 50Tin filter, calculated and printed by the BBC microcomputer program SPECTRA listed in Annexe D together with the I and I_o integrated intensities, filter attenuation, and attenuation at each energy increment between 12keV and 50keV is shown in Figure 4.13. The shape of the incident X-ray spectrum on a Tin filter of thickness greater than about 0.1mm does not much influence the shape of the pass band spectrum: a spectrum of constant intensity from 12keV to 40keV incident on a 0.3mm thick Tin filter emerges as a pass band spectrum almost identical to that of a continuum from an X-ray tube provided the maximum incident intensities are the same.

The calculated and experimental spectra for 0.3mm thick Tin filters agree very well as shown in Figure 6.6.

Figure 4.14 shows a BBC microcomputer print of the 40keV incident X-ray spectrum I_o, the mass attenuation coefficient as a function of energy for 50Tin, and the filtered spectrum I for a 0.1mm Tin filter.

ENERGY (keV)	WAVELENGHT (A)	Io	I
12	1.033	1.26	2.05113328E-8
13	0.953	1.38	2.71817079E-7
14	0.885	1.83	7.05634016E-6
15	0.826	2.47	1.12746136E-4
16	0.774	3.31	5.25557051E-4
17	0.729	4.19	2.16720001E-3
18	0.688	5.01	6.352454E-3
19	0.652	5.96	1.85254555E-2
20	0.619	6.69	5.21033452E-2
21	0.59	7.42	0.104301353
22	0.563	7.84	0.190393715
23	0.538	8.23	0.30282991
24	0.516	8.43	0.480382207
25	0.495	8.46	0.626766745
26	0.476	8.37	0.754993518
27	0.459	8.2	0.881080886
28	0.442	7.95	1.06303915
29	0.427	7.61	1.18591327
30	0.413	7.02	4.64737987E-4
31	0.399	6.38	7.29696471E-4
32	0.387	5.79	9.81667691E-4
33	0.375	5.11	1.5636998E-3
34	0.364	4.49	2.89009098E-3
35	0.354	3.76	3.83099376E-3
36	0.344	3.03	5.10529327E-3
37	0.335	2.25	6.00093623E-3
38	0.326	1.52	6.14246184E-3
39	0.317	0.67	4.28580206E-3
40	0.309	0	0
41	0.302	0	0
42	0.295	0	0
43	0.288	0	0
44	0.281	0	0
45	0.275	0	0
46	0.269	0	0
47	0.263	0	0
48	0.258	0	0
49	0.252	0	0
50	0.247	0	0

SPECTRUM=144 FILTER=5.70149023 ATTENUATION=3.95936822E-

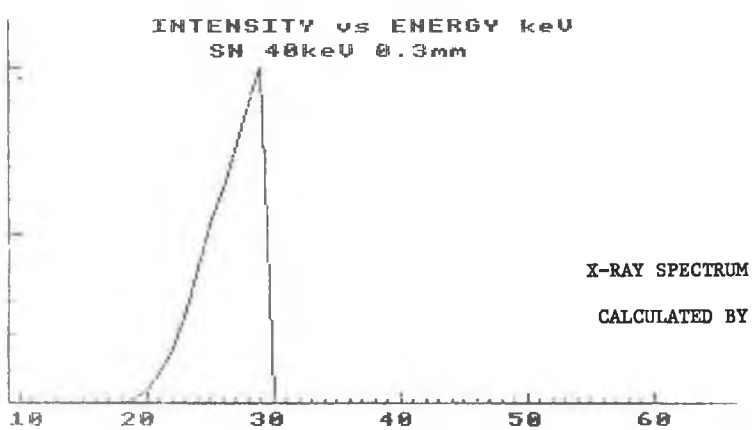

X-RAY SPECTRUM FOR SOTIN

CALCULATED BY SPECTRA.

FIGURE 4.13

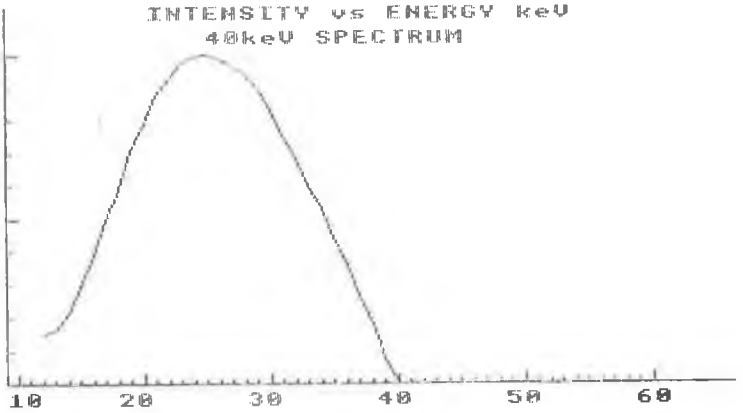
INTENSITY vs ENERGY keV
40keV SPECTRUM
10
20
30
40
50
60

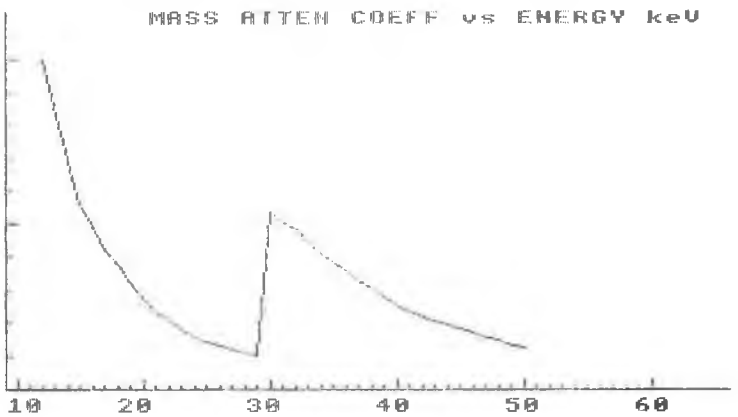
MASS ATTEN COEFF vs ENERGY keV
10
20
30
40
50
60

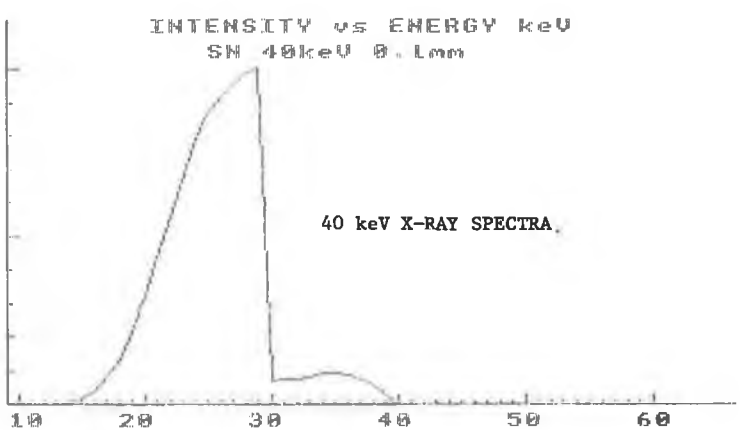
INTENSITY vs ENERGY keV
SN 40keV 0.1mm
40 keV X-RAY SPECTRA
10
20
30
40
50
60

FIGURE 4.14

X-RAY PHOTON COUNTING DEAD-TIME.

The count rate capability of the equipment is limited by the dead-time of the slowest instrument used, the time during which that instrument is unable to count because it is not yet ready for the next count, so that a lower count rate results than the number of photons incident on the detector. The instrument dead-times for N_o, N, N_h, Nl are not the same, and at fast count rates, dead-time becomes important: N_o, N_1 are the incident and detected flux of X-ray photons, and N_h and N_1 are the detected flux at the high and low energy side of an absorbtion edge of an atomic element. If the corrected values for N_o, N are aN_o, bN where a, b are factors dependent on the count rate for a particular counting instrument such as a multichannel analyser for a monochromatic collimated X-ray beam transmitted by the object the equation for the equivalent thickness of the analyte element and matrix

$$\mu_a t_a + \mu_m t_m = \ln(N_o/N) \qquad (4.2)$$

becomes $$\mu_a t_a + \mu_m t_m = \ln(aN_o/bN) \qquad (4.3)$$

so that $$\mu_a t_a + \mu_m t_m = \ln(N_0/N) + \ln(a+b) \qquad (4.4)$$

where t_a, t_m are the equivalent thickness of the anlyte element and matrix, and μ_a, μ_m are their mass attenuation coefficients. The second term ln(a/b) moves $\ln(N_o/N)$ by a variable magnitude on the ordinate axis of a graph of X-ray photon attenuation ratio against energy by an equal amount for all points, but does not change the difference between N_h and N_1. In addition, this does not affect the numerical values of the logarithms, $\ln(N_o/N)$, extrapolated to the absorbtion

edge, hereinafter described, for the equivalent thickness of the analyte element to give the equation

$$t_a = (Y_h - Y_l)/(\mu_{ah} - \mu_{al}) \qquad (4.5)$$

from equation 3.16 and 3.17 and as shown in Figure 6.11.

This prediction was confirmed by experiment.

IMAGE DISPLAY OF A SCANNED OBJECT.

The tomographic image of an object scanned by X-rays may be displayed in colour or grey shades on a monitor screen or printed on paper. For computer axial tomography images as shown in Plate 6.2 and Figure 6.13 the image density variations in the pixels of the reconstruction are proportional to measurements of the integrated linear attenuation coefficient of the object at each step of the scan. For differential K absorbtion edge tomography images, shown in Plates 6.3. 6.4, and 6.5 and in Figure 6.14, 6.15, and 6.16. The image density is proportional to the concentration of analyte element in each pixel of the reconstruction grid.

The image density variations are shown on an eight colour or eight grey shade scale, the limits of which could be chosen in an arbitrary range of 0 to 80. Thus the light colour scale could be selected for an X-ray absorbtion range, so that for example the matrix of the object could be deleted from the image by choosing the lower limit greater than 0, say 20, and the eight colour scale expanded to fit this range. The image density profile at a chosen section of the image could be selected by a movable line cursor on the colour

monitor, and a graph of image density range against linear position along the cursor drawn on the monitor below the image of the object. The concentration of analyte element at a particular location in the object can be displayed as a number above the image by moving a point or one-pixel cursor to that location in the image. The display controls are shown on the monitor beside the image display, and then values are chosen by key on the BBC microcomputer keyboard. The image display program R.DISP4OT is listed in Annexe D.

CHAPTER V

EXPERIMENT.

The experimental work began with a simple manually operated scanning machine to demonstrate the principle and use of K absorbtion edge spectroscopy to identify one atomic element, and was developed to a computer controlled automatic scanning machine which can image consecutive atomic elements in the Periodic Table of the Elements, and which can also do computer axial tomography producing images of integrated linear attenuation coefficient as an alternative method of forming images of the internal structure of an object.

The object to be scanned consisted of a cork matrix containing an analyte element; initially 55Caesium, and later on 55Caesium and 56Palladium formed into 5mm diameter epoxy glue rods. The X-ray source was two coexistent monochromatic collimated beams from a radioactive emitter which was used to scan the object in discrete linear steps and angular steps from 0° to 180°, and the beam was detected with an energy dispersive detector.

The flux of detected X-rays in each monochromatic beam after passing through the object is given by

$$N = N_o e^{-\mu t} \qquad (5.1)$$

where μ is the mass attenuation coefficient of the object and N_o is the incident flux; t is the equivalent thickness of the object. The X-ray flux N_o is measured at the start of a linear scan, the flux N is measured at each step, and the parameter $\ln(N_o/N)$ is used in the reconstruction of the image of an object. In the first experiments the effect of the matrix was ignored. N was measured for each monochromatic beam on either side of the K absorbtion edge of the analyte element. The differential measurement of $\ln(N_o/N)$ at the low and high energy sides of the K absorbtion edge gave a value for the equivalent thickness of the analyte element according to equation 3.8. Later experiments corrected for the effect of the matrix by two different methods. In one method the matrix was scanned alone and the measured X-ray beam fluxes taken as N_o at each step, and an identical scan which included the analyte element with the matrix was made in which the measured X-ray fluxes were N. The second method for matrix effect correction extrapolated the parameter $\ln(N_o/N)$ to the absorbtion edge of the analyte element, to measure its concentration is described in Chapter 6.

The essential measurements are the X-ray photon fluxes N_o and N on each side of the K absorbtion edge of an analyte element in order to give a numerical value to equations 3.8 and 3.18 at each step of the scan. These are the fundamental equations and measurements which the reconstruction algorithm uses as the basic data to make a tomographic image of the object; equation 3.18.

Figure 5.1 shows the X-ray spectra used for imaging 46Palladium in the experiments herein, printed from the EG & G Ortec 7100 multichannel analyser. The K absorbtion edge of 46Palladium at 24.365keV was imaged using the K_α and K_β 47Silver X-rays at 21.991 to 22.163 and

X-RAY SPECTRA FOR IMAGING 46PALLADIUM

The X-rays emitted by electron capture in 109 Cadmium, to image 46Palladium.

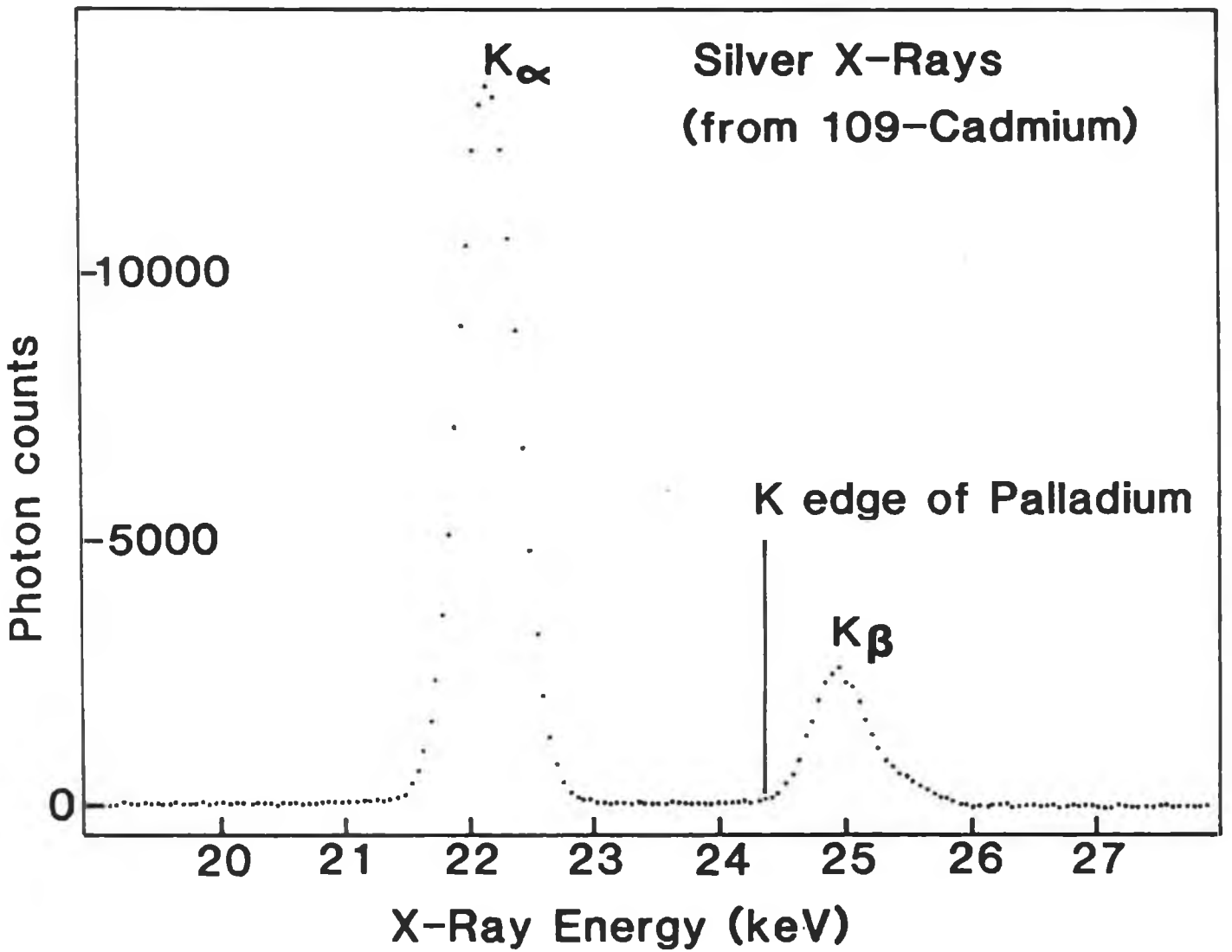

[14]

FIGURE 5.1

X-RAY SPECTRA FOR IMAGING 55CAESIUM

Fluorescence X-rays from 56Barium induced by radiation from 241 Americium, to image 55Caesium.

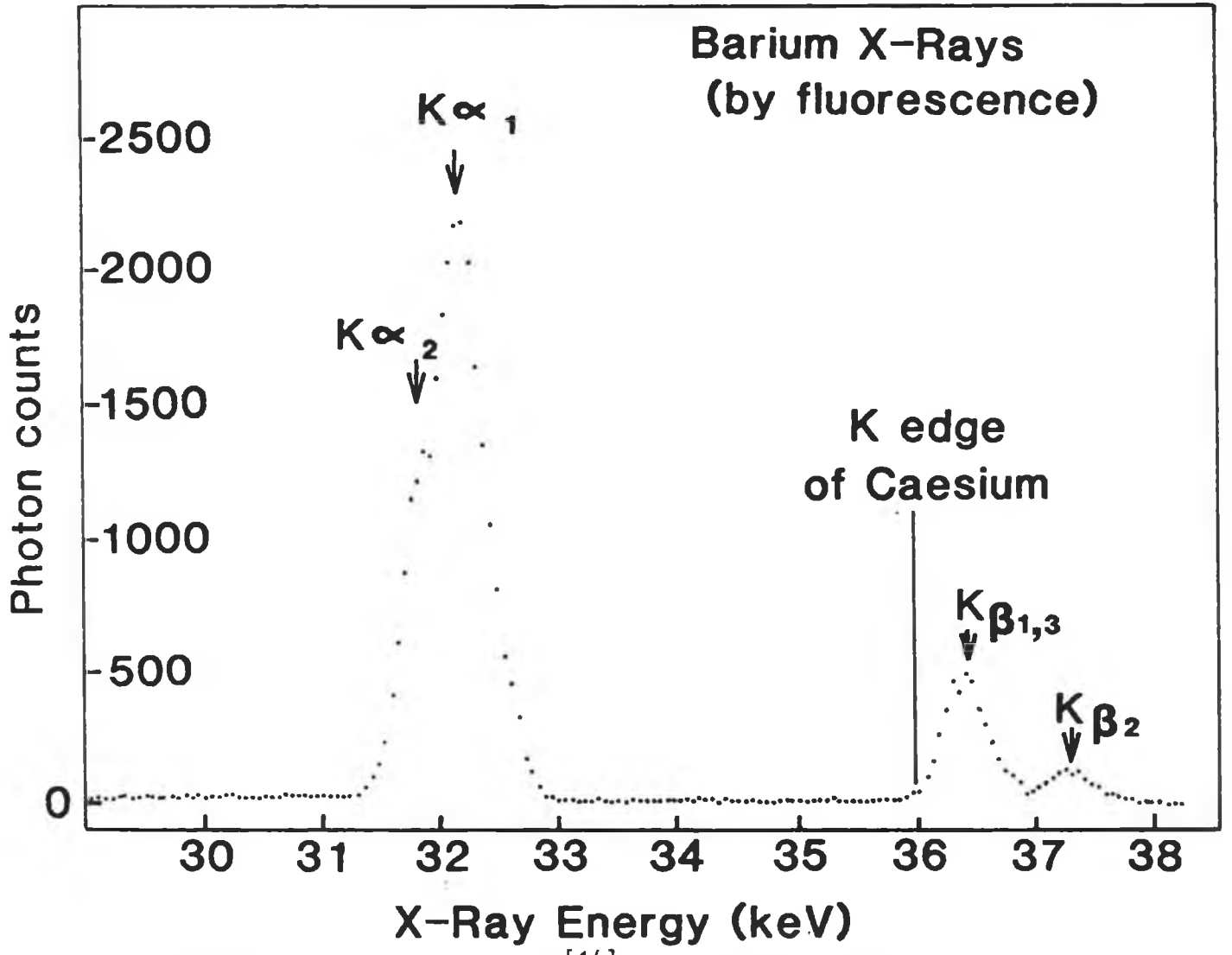

[14]

FIGURE 5.2

24.912 to 25.463keV respectively emitted from a 3mCi, 111MBq, 109 Cadmium source after electron capture of a K electron by the nucleus of the Cadmium atom. 55Caesium was imaged by the K_α and K_β fluorescence lines shown in Figure 5.2 of 56Barium emitted by a 10mCi, 370MBq, Amersham International 241 Americium type AMC.2084 source.

A SIMPLE X-RAY K ABSORBTION EDGE SCANNING MACHINE.

Figure 5.3 is a schematic drawing of the first table top K absorbtion edge scanning machine which was used to show that K absorbtion edge spectroscopy can identify and locate an analyte element, 55Caesium, concealed within a matrix, a cork. The source of X-rays was a 10mCi, 370MBq, Amersham International variable energy X-ray source shown in Figure 2.10 using (241)95Americium 5.48MeV α-particles and 60keV γ-rays to excite 56Barium K_α and K_β X-ray lines by fluorescence. The exit of the source defined a 4mm diameter collimated beam, which was directed vertically downwards to the EG & G Ortec Si(Li) detector via a 1.5mm collimator in a 3mm thick Lead shield placed over the detector. The K_α and K_β X-ray lines of 56Barium of energy 32.19keV and 36.38keV are located on either side of the K absorbtion edge of the 55Caesium analyte element at 35.97keV. The position of the Caesium was to be located within a 20mm diameter cork matrix, and so a reference radius was marked on the end of the cork. The cork was secured to the end of an axle having a degree circle attached, mounted on the carriage of a travelling microscope stand so that the cork could be moved transversely through the X-ray beam. The block electric circuit diagram is shown in Figure 5.4. The energy selection windows of two EG & G Ortec 550 single channel analysers were set on the Barium K_α and K_β lines so that two EG & G Ortec 875 counters

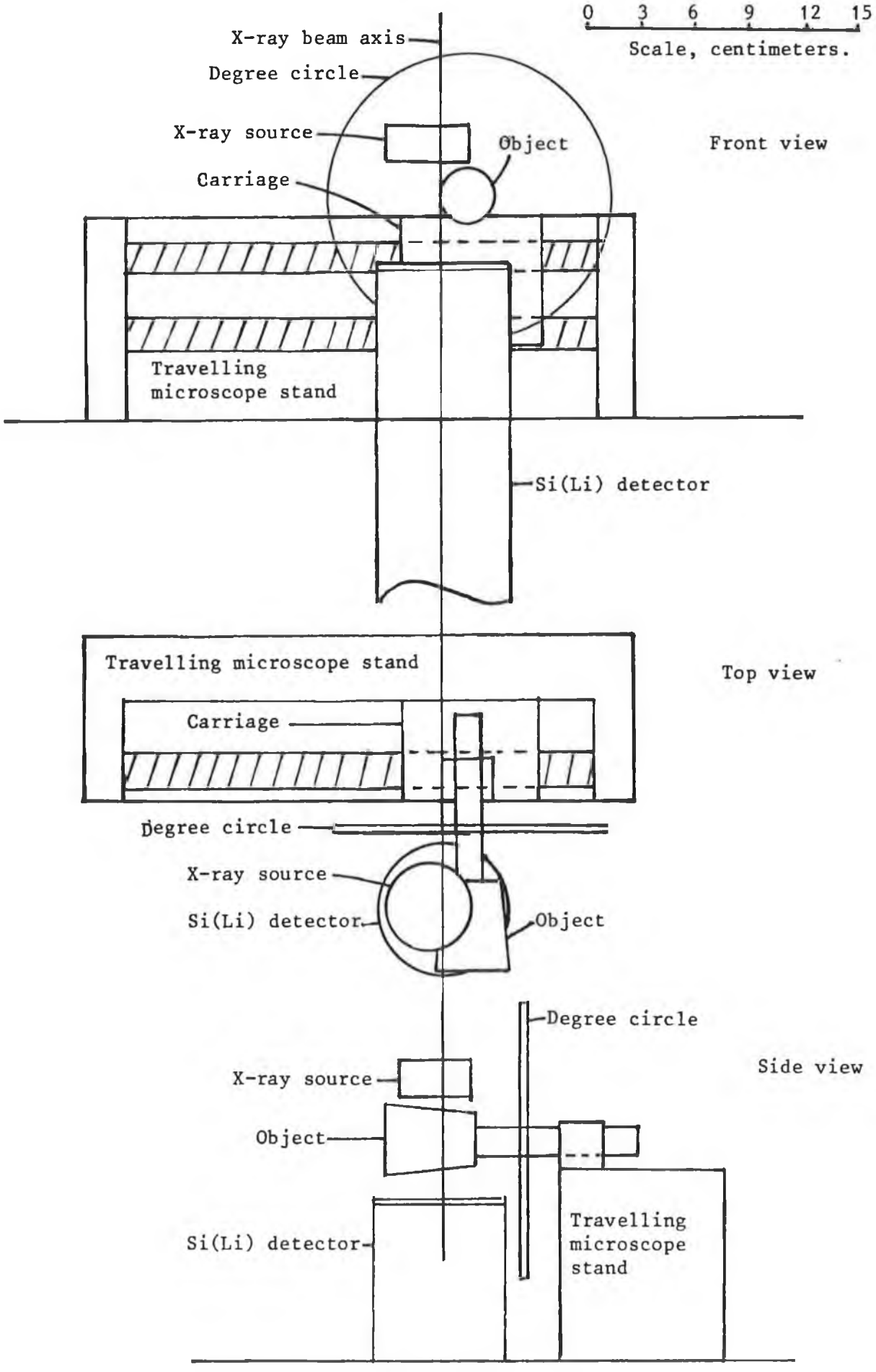

A table top X-ray K absorbtion edge scanning machine.

Figure 5.3

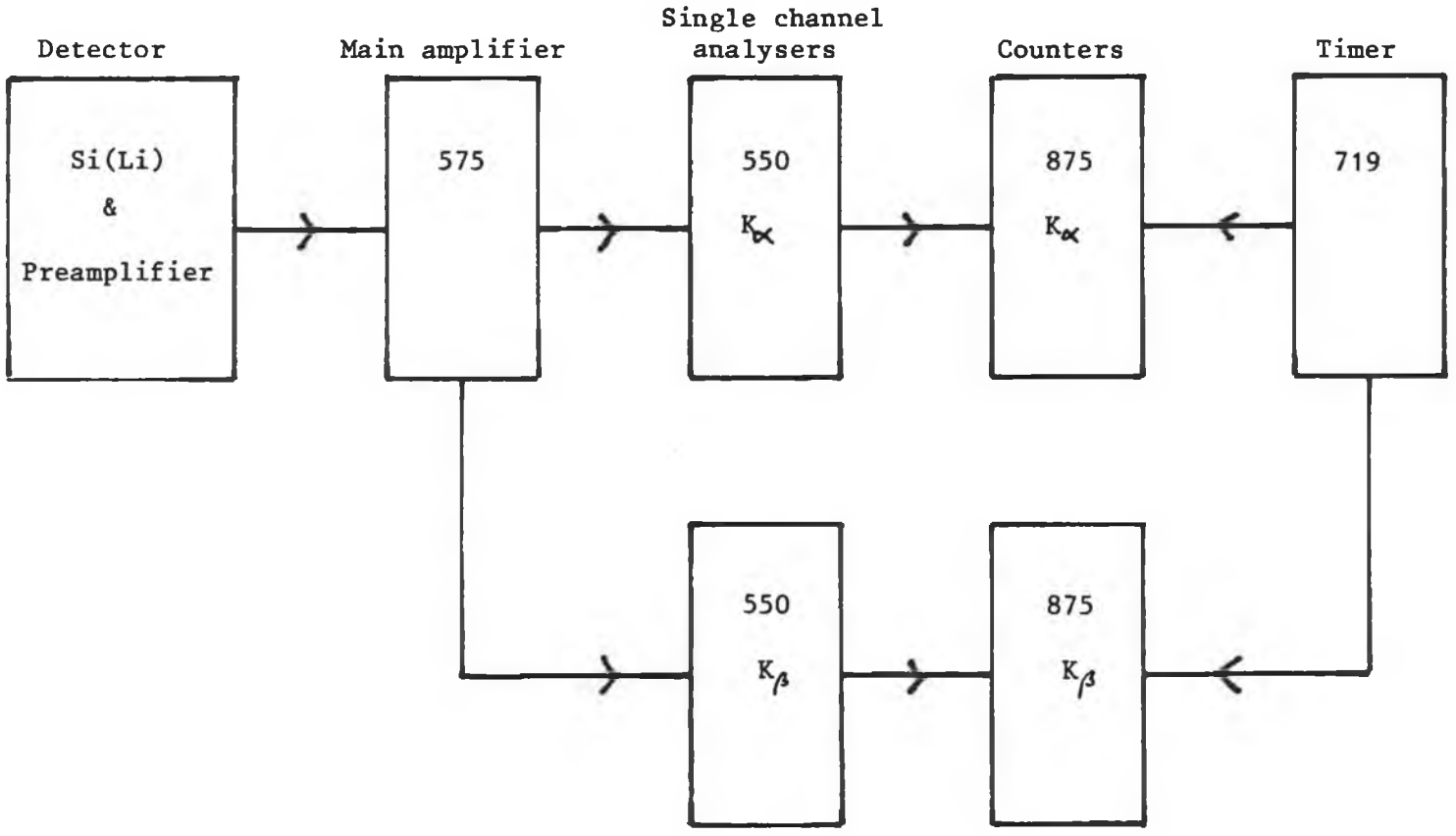

Block electric circuit diagram of the table top scanning machine.

FIGURE 5.4

recorded separately X-ray photons emitted by the source for a predetermined time set by an EG & G Ortec 719 timer to measure the detected count rate for K_α and K_β photons.

Count rates for the 56Barium K_α and K_β lines were measured for 28mm long linear scans of the object having 14 counting positions 2mm apart, and 18 angular steps of 20° between each linear scan from 0° to 360° and the ratio of the K_α to K_β count rates calculated. This ratio increased to a maximum and decreased again as the 55Caesium analyte element absorbed differentially the X-radiation during each linear scan. The counting time was 100 seconds and in the region of 2500 counts for the K_α line, and 400 counts for the K_β line were recorded, so that $K_\alpha/K_\beta \approx 6$ for the cork matrix. Absorbtion of X-rays by the Caesium sample reduced the K_α counts to around 1900 and the K_β counts to around 170, and thus $K_\alpha/K_\beta \approx 11$ for strong absorbtion. This shows that there was an energy-specific differential of about 2 for this Caesium sample.

A graph of horizontal rotation in degrees against horizontal linear scan position in mm for the maximum K_α to K_β ratio in each linear scan, shown in Figure 5.5 marked the locus of the analyte element as it moved through the X-ray beam. Due to the finite width of the beam and of the absorber the locus only approximated to a sin wave. The narrower the absorber and the smaller the diameter of the collimated beam of X-rays, the closer the locus would approximate to a sine curve. From the graph and the direction of rotation of the angular steps it was possible to deduce that the Caesium analyte was located on a circle of diameter 10mm, and 90° anticlockwise of the reference radius. This was confirmed experimentally by scanning the cork to show

Graph of Horizontal anticlockwise rotation degrees against Horizontal linear position.

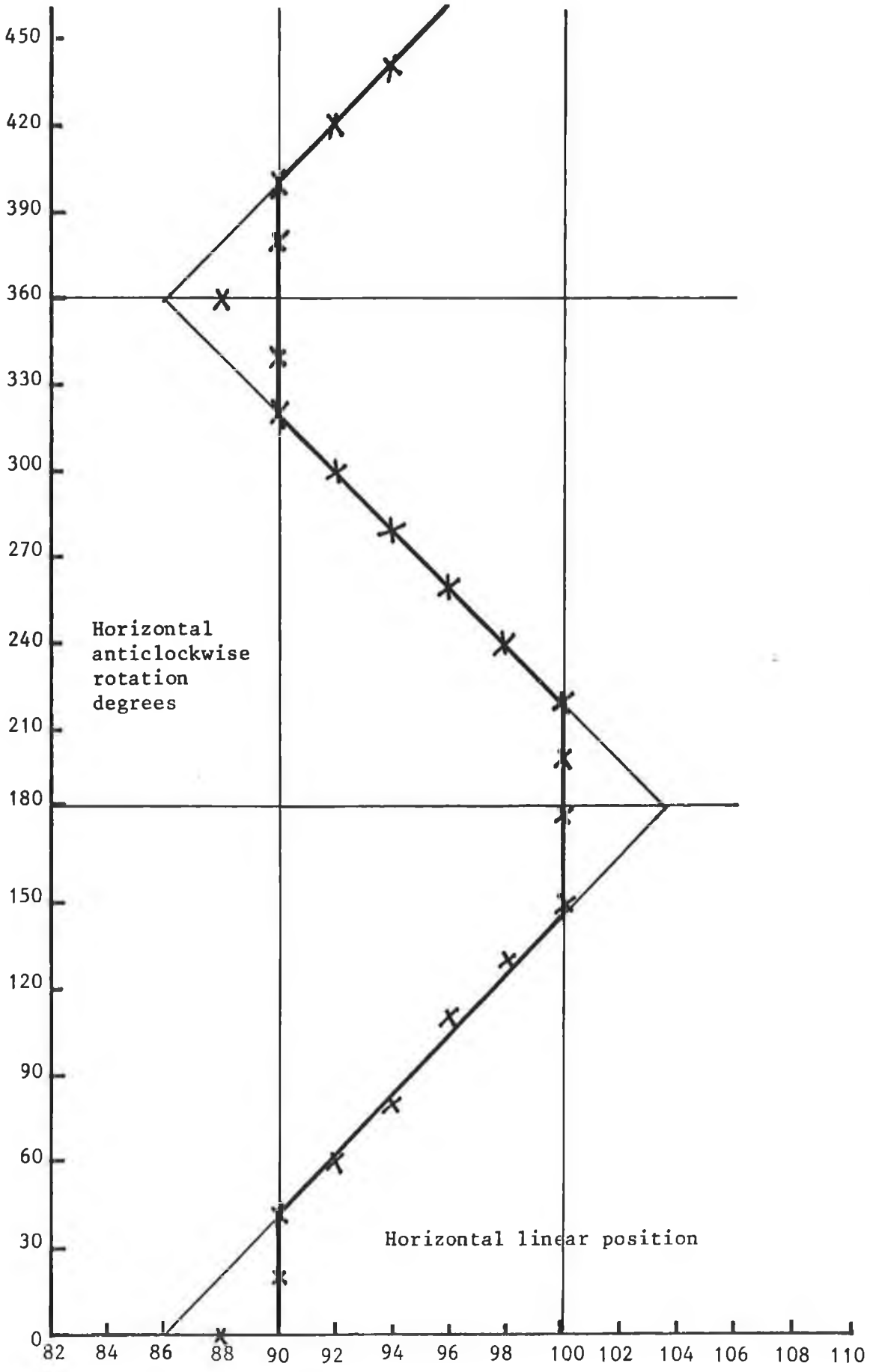

Differential K absorbtion edge tomography of 55Caesium.

Location of maximum absorbtion of X-rays by a 55Caesium sample within a 20mm diameter cork matrix.

FIGURE 5.5

THE CONCENTRATION SHAPE OF A 55CAESIUM ANALYTE.

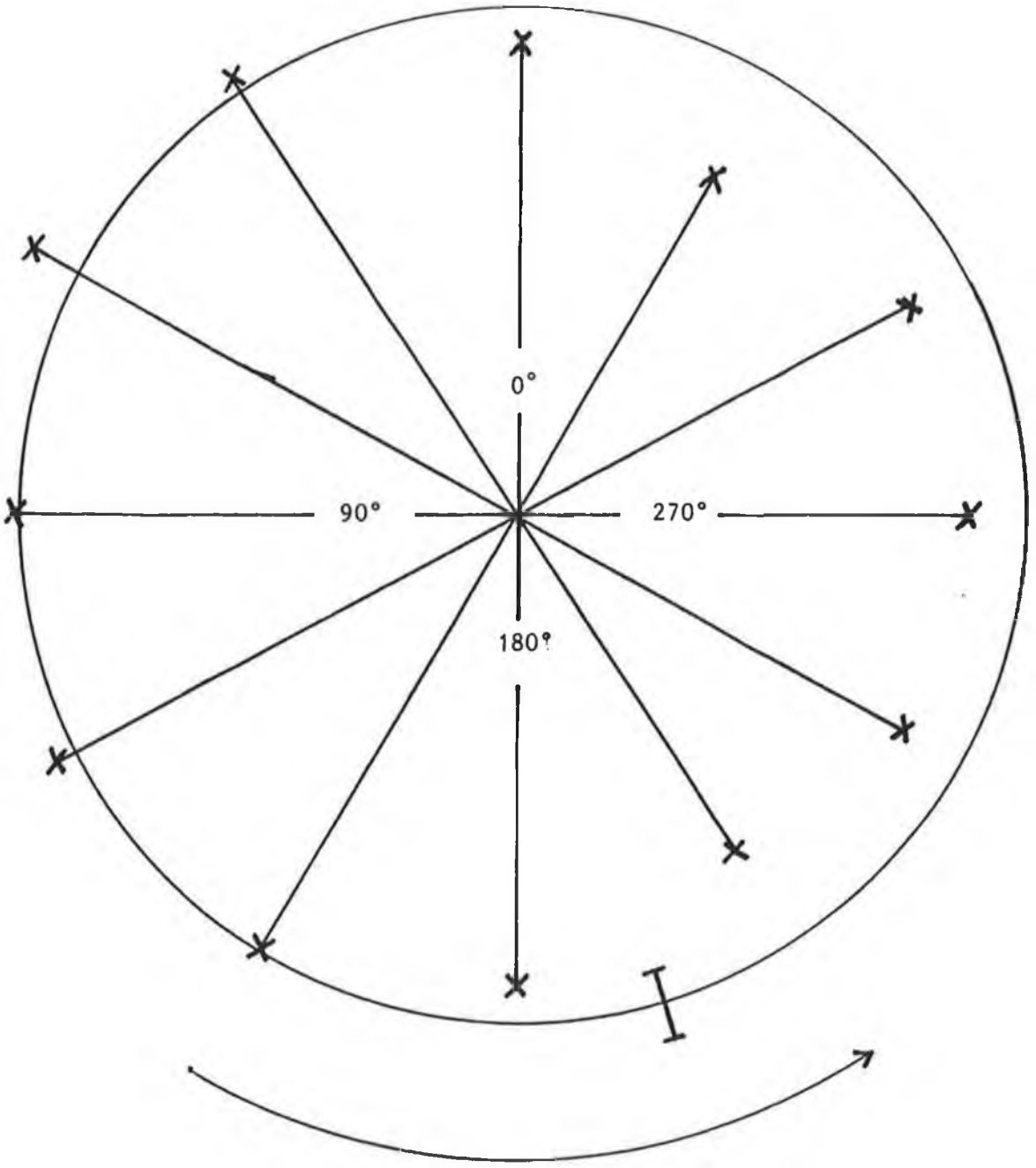

The length of the lines through the centre is a measure of the equivalent thickness t of the 55Caesium analyte in the 20mm diameter cork matrix. The circle is for $t = 0.30 kgm^{-2}$ with an error bar of $0.02 kgm^{-2}$. The arrow shows the direction of the scan rotation.

FIGURE 5.6

that the maximum K_α to K_β ratio was measured when the X-ray beam crossed the marked position of the Caesium analyte and then by cutting the cork transversely through the scanned axial plane.

The 'concentration shape' of the 55Caesium analyte element was also determined by measuring the equivalent thickness at maximum absorbtion of X-rays for 12 angular steps of 30° between 0° and 360° by irradiating the analyte with X-rays under the beam only and calculating the value of the K_α to K_β count of the maximum absorbtion at each angular step. The equivalent thickness was a nearly uniform 0.30 ± 0.02 kg/m^2 showing that if the Caesium was evenly dispersed at its location, then the analyte was circular in shape. The matrix effect of the cork gave a lower concentration of analyte element than should have been measured. The 'concentration shape' of the 55Caesium is shown in Figure 5.6. The counting time was 200 seconds and around 3600 counts for the K_α line and 320 for the K_β line were recorded so that $K_\alpha/K_\beta \approx 11$ for the maximum absorbtion by the 55Caesium analyte element.

A SEMIAUTOMATIC BBC MICROCOMPUTER CONTROLLED SCANNING MACHINE.

The manually operated scanning machine was semiautomated to scan two samples of 55Caesium analyte element concealed within a 30mm diameter cork matrix. Figure 5.7 is a schematic drawing of a scanning machine in which the linear scanning was controlled, and the pulse counting measured and stored semiautomatically by a BBC microcomputer. The object to be scanned was rotated manually.

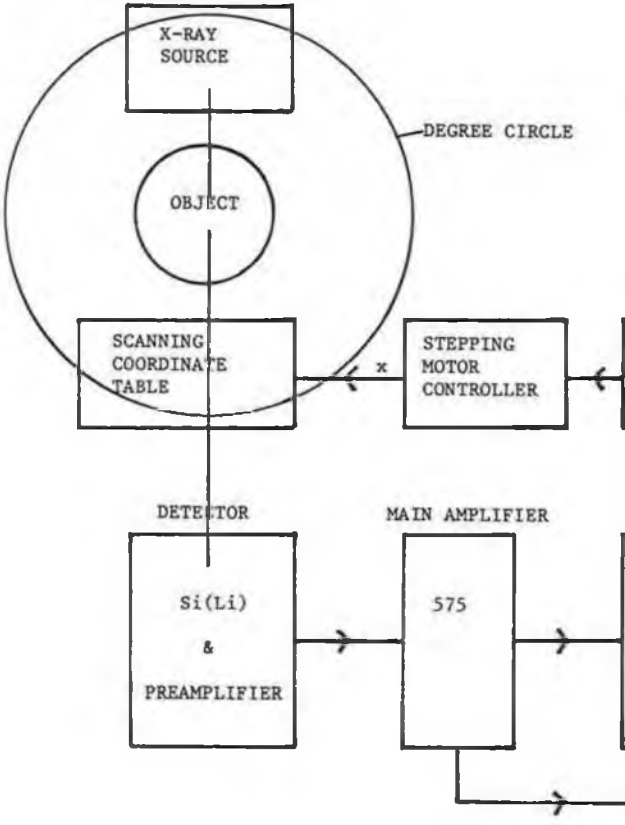

A SEMIAUTOMATIC SCANNING MACHINE

FIGURE 5.7

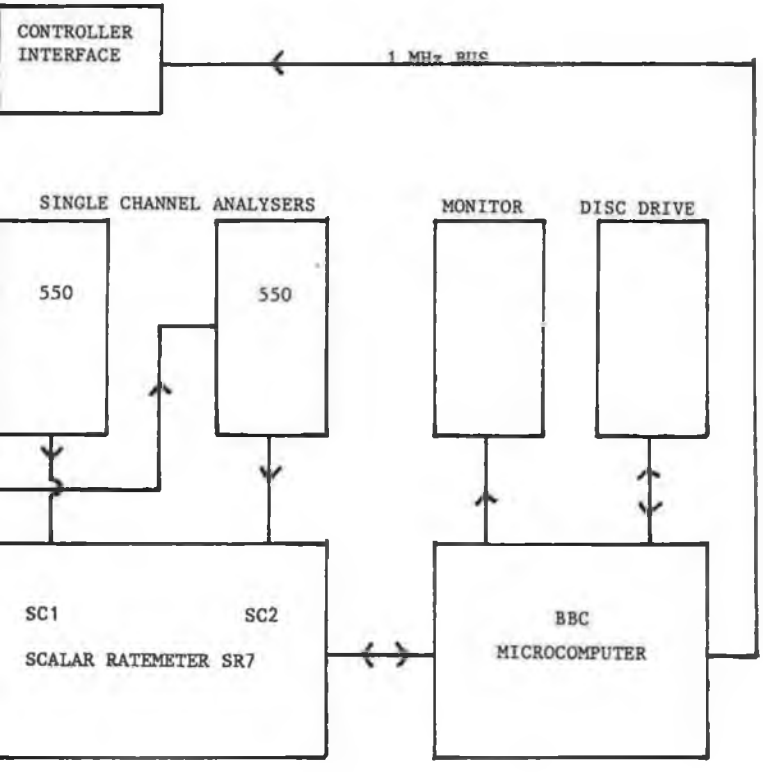
CONTROLLER
INTERFACE
1 MHz BUS
SINGLE CHANNEL ANALYSERS
550
550
MONITOR
DISC DRIVE
SC1
SC2
SCALAR RATEMETER SR7
BBC
MICROCOMPUTER

A semiautomatic scanning machine.

PLATE 5.1

The 46Palladium and 55Caesium analytes in the cork matrix.

PLATE 5.2

Plate 5.1 shows the EG & G Ortec Si(Li) detector protruding through a hole cut in a table with the Feedback CNC 932 computer controlled milling machine used as a (x,z,ϕ) scanning coordinate table placed beside it. The 241 Americium variable energy X-ray source mounted on a retort stand emits 56Barium K_α and K_β X-rays in a vertical 4mm diameter collimated beam downwards which are admitted to the detector through a 1.5mm diameter aperture in a 3mm thick Lead plate. The cork matrix containing the 55Caesium analyte element was secured to the end of an axle having a degree circle attached, mounted on a bracket bolted to the uppermost or x-coordinate table of the milling machine. The distance the linear or x-direction scan moved was measured with a ruler attached to the table. After each scan the starting position had to be preset at a fixed position to allow for backlash in the lead screw of the table. The centre position of the linear scan also had to be aligned with the centre of the X-ray beam. The flat cable connects the milling machine to its controller standing on the bench, and this is connected to the BBC microcomputer.

The scanning coordinate table was moved in the x and z directions using a BASIC computer program run on the BBC microcomputer. This program was similar to POSSCAN listed in Annexe D. The (x,z) coordinates of the table were chosen by using the edit keys of the BBC microcomputer.

The first semiautomatic scans were made with 20 counting positions in 19 steps 2mm wide in the x-direction; the centre position being 9.5 steps from the start. After each linear scan the object was rotated through 9° between 0° and 171° to provide 20 angular steps.

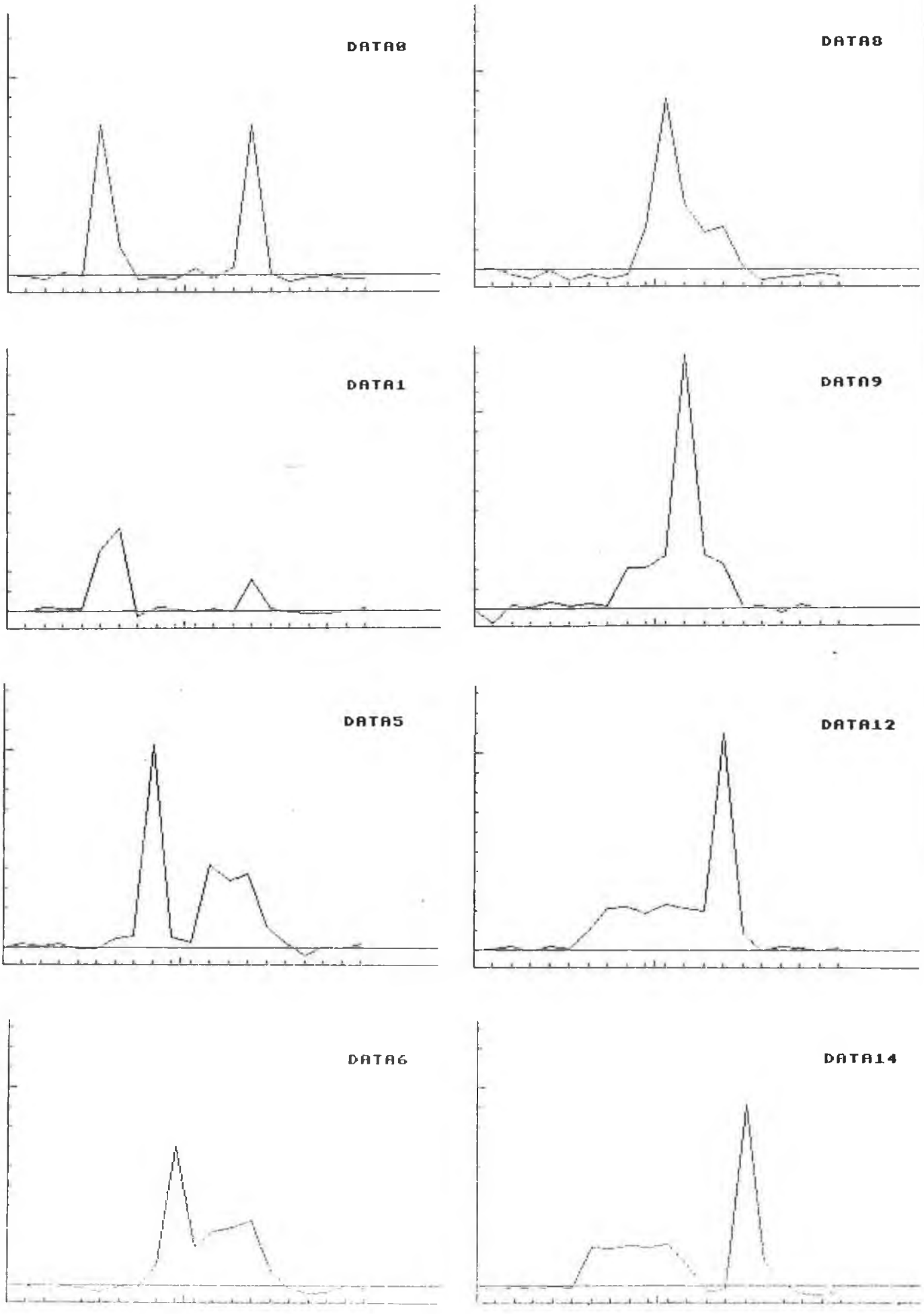

Equivalent thickness profile of 55Caesium in a cork matrix.
Each DATA increment is one 9° angular step.

FIGURE 5.8

A BASIC program similar to the program COUNTER listed in Annexe D run on the BBC microcomputer counted and stored on a disc file the pulses from the Si(Li) detector during a predetermined counting time at each step, and moved automatically the x-coordinate table for each linear scan.

A Nuclear Enterprises Scalar Ratemeter SR7 was used as a pulse counter and store, and computer interface, which unlike the single channel analysers could be accessed by the BBC microcomputer for the X-ray photon count data. The serial data connector of the Scalar Ratemeter SR7 was connected to the RS423 serial connector of the BBC microcomputer and the data transferred from the Scalar Ratemeter SR7 to the BBC microcomputer.

The equivalent thickness profile of the 55Caesium analyte was drawn on a printer as a graph of equivalent thickness against linear scan position for each angular position, and some examples are shown in Figure 5.8. The Caesium was in a flat 1.2mm X1mm and a round 2mm diameter sample of maximum equivalent thickness about 8kg/m^2. The graph scale is 0 to 10kg/m^2.

AN AUTOMATIC SCANNING MACHINE WITH AN X-RAY LINE SOURCE.

This scanning machine was an automatic version of the last one and capable of scanning an object from start to finish in 20 linear steps 2mm wide and 24 angular steps of 7.5°, taking several hours or days to accomplish, [14]. Figure 5.9 shows a schematic drawing of the scanning machine including a block electric circuit diagram. The sources of X-rays used were an Amersham International 241 Americium

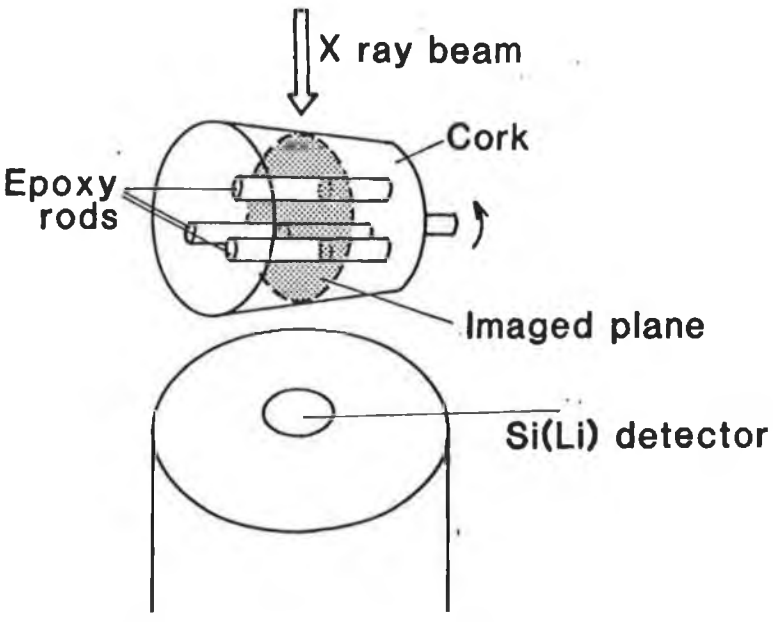

SCHEMATIC DIAGRAM WHICH SHOWS THE RELATIONSHIP OF THE IMAGED PLANE TO THE X-RAY BEAM AND THE DETECTOR.

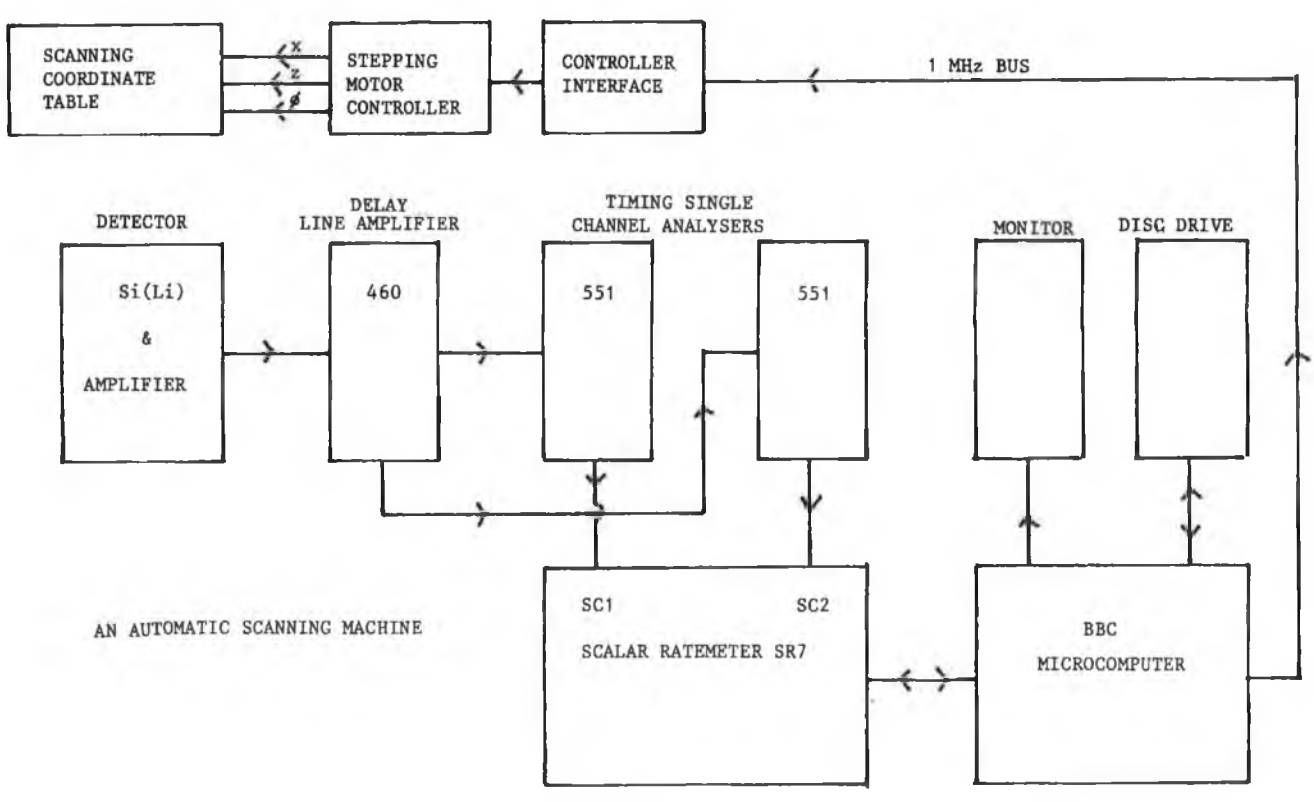

AN AUTOMATIC SCANNING MACHINE

FIGURE 5.9

variable energy X-ray source, emitting 56Barium K_α and K_β X-rays, for imaging 55Caesium, and a 109 Cadmium source emitting 47Silver K_α and K_β X-rays for imaging 46Palladium. Plate 5.2 shows the 46Palladium and 55Caesium analytes in the cork matrix mounted between X-ray source and detector.

A stepping motor having 7.5° angular steps was mounted on a bracket on the uppermost or x-coordinate table of the (x,z,ϕ) scanning coordinate table, and this motor was controlled by the y-axis controller of the Feedback CNC 932 computer controlled milling machine. The x-coordinate table was driven by the x-axis controller during a complete scan of an object.

The (x,z,ϕ) coordinates of the scanning coordinate table could be varied, or chosen, before the start of a complete scan by means of a BASIC program POSSCAN, listed in Annexe D, run on the BBC microcomputer. The (x,z) coordinates were adjusted so that the X-ray beam from an Amersham International 241 Americium variable energy X-ray source was a few mm to one side of the axle of the ϕ-coordinate stepping motor. The centre of the axle was then found using the BASIC program MDPOINT to scan the axle with the X-ray beam, and calculate the x-coordinate position of the ϕ-axis to line the ϕ-axis with the centre of the X-ray beam. The x-coordinate table was moved by the program in 1/12mm steps through the X-ray beam and the number of photons counted for a chosen time at each step. When the X-ray beam was partially intercepted by the axle of the stepping motor the count rate decreased quickly, gradually further decreased to a minimum at the centre of the axle and increased again, to rise quickly when the other side of the axle left the X-ray beam. The edges of the axle

were not sharply defined because the X-ray beam had a finite width and because of fluorescence. The centre of the axle was located by counting the number of small steps between the edges of the axle as defined by the quick decrease in the count rate, and inserting half the number of steps in the program from one edge of the axle, to position the centre of the axle at the centre of the X-ray beam. The program then moved the x-coordinate table to the starting position for a scan. Then the program moved the z-coordinate table by a chosen distance to position the disc in the object to be scanned under the X-ray beam. The program then started the COUNTER program by a CHAIN statement, which controlled the scanning of the object from start to finish, and read the data from the Scalar Ratemeter SR7 into the BBC microcomputer, and then on to disc memory file.

The image of the internal structure of the object was then reconstructed using a BASIC reconstruction program run on the VAX 11/785 computer, and the file containing the areas of overlap of the X-ray beam path with the pixels in the reconstruction grid.

In this experiment the correction for the effects of the matrix was done by adding the analyte element after the preliminary scan of the matrix was done; both scans being identical.

Figure 5.10 shows examples of the equivalent thickness for the differential K absorbtion edge tomography scan of the 46Palladium analyte using the 109 Cadmium K_α and K_β 47Silver X-rays. Figure 5.10a shows a scan of the cork matrix alone which gives a negative result according to the equation

$$N_l/N_h = N_{ol}/N_{oh} \exp [W_a(\mu_{ah}-\mu_{al})t] \exp [W_m(\mu_{mh}-\mu_{ml})t]. \quad (5.2)$$

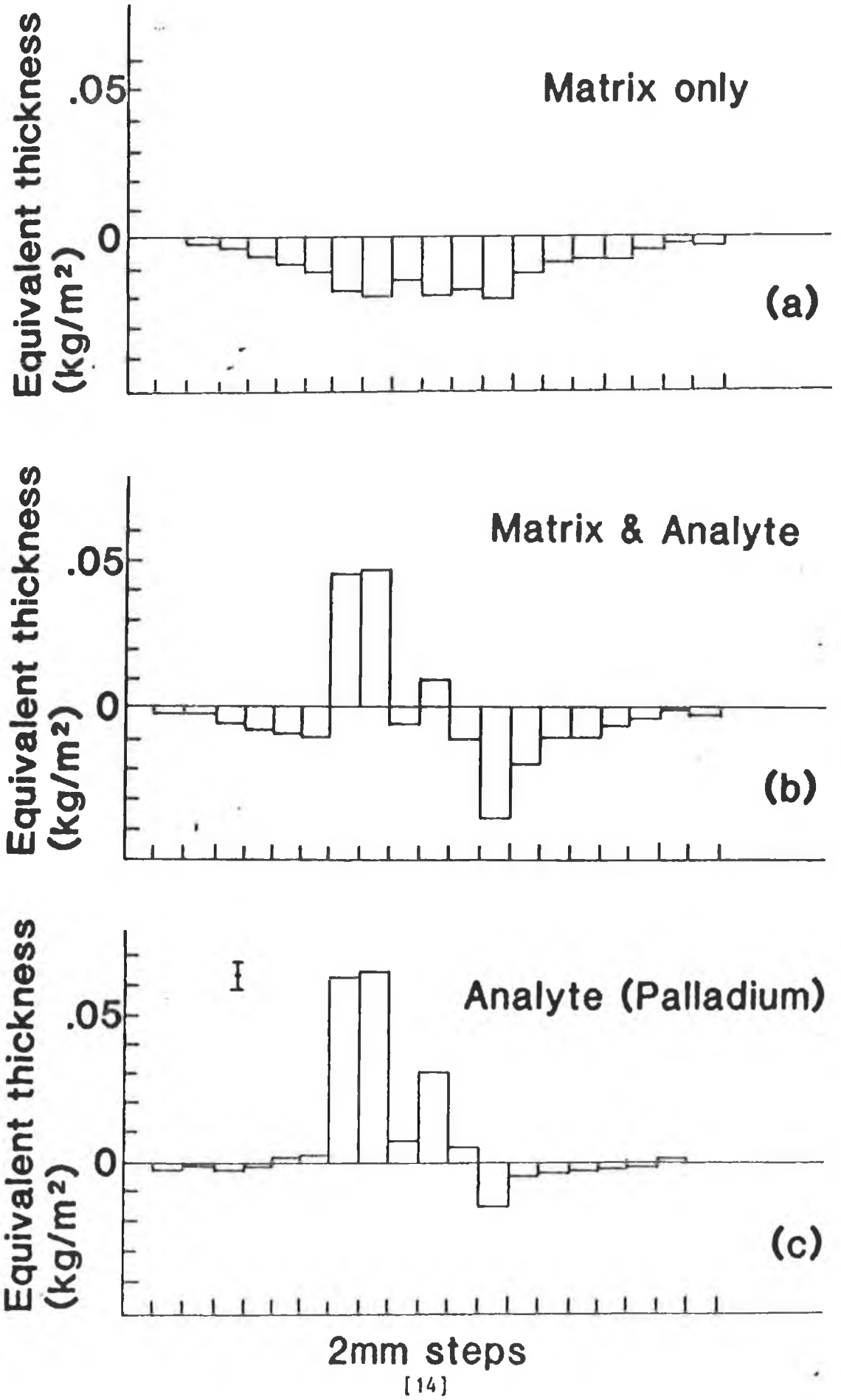

Projection data for 46Palladium.
Examples of the equivalent thickness projection data obtained by scanning the object with Silver X-rays from 109 Cadmium to image 46Palladium.

FIGURE 5.10

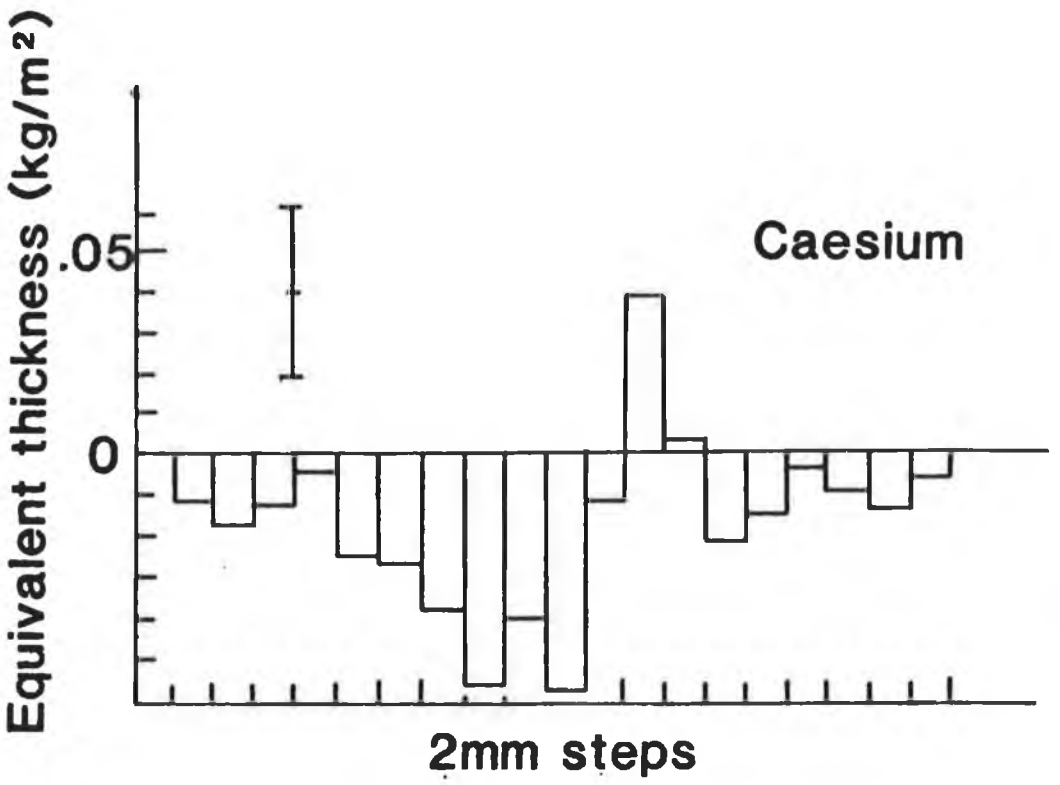

Projection data for 55Caesium.

An example of equivalent thickness projection data obtained by scanning the object with Barium fluorescence K_α and K_β X-rays, the energies of which are on either side of the K absorbtion edge of 55Caesium.

[14]

FIGURE 5.11

Figure 5.10b is a scan in which the 46Palladium and the 55Caesium epoxy glue rods have been put into the cork matrix. The Caesium appears as a negative peak in addition to the negative result for the cork matrix. The 46Palladium rod gives a positive result because of the relatively strong differential absorbtion of the K_α and K_β Silver X-rays. The equivalent thickness of the 46Palladium analyte corrected for the matrix effects, the matrix including the cork and the Caesium, is shown in Figure 5.10c using the scanning data of Figure 5.10a. The effects of the matrix have been corrected for the cork, shown by the base line being restored to zero, but the Caesium shows a small negative value because it was not included in the matrix scan.

Figure 5.11 shows the 55Caesium differential K absorbtion edge scan using K_α and K_β X-rays of 56Barium, but no correction for the effect of the matrix was made because of the poor counting statistics.

Figure 5.12 shows a sequence of reconstructed images photographed from a monochrome monitor screen. The grey shade scale is shown beside the images. Figure 5.12a is a computer axial tomography image reconstructed from the attenuation measurements of the K_α Silver X-rays transmitted by the matrix without the analyte elements. Figure 5.12b is a similar image using K_β Silver X-rays, and both images are nearly the same.

Figure 5.12c and d are images of the cork matrix with the two Palladium and one Casesium epoxy glue rods put into the cork. The differential absorbtion by Palladium is seen in the two photographs. Figure 5.12c is the absorbtion for Silver K_α X-rays and the dominant feature is the rod containing 55Caesium, and the K_α X-rays being below

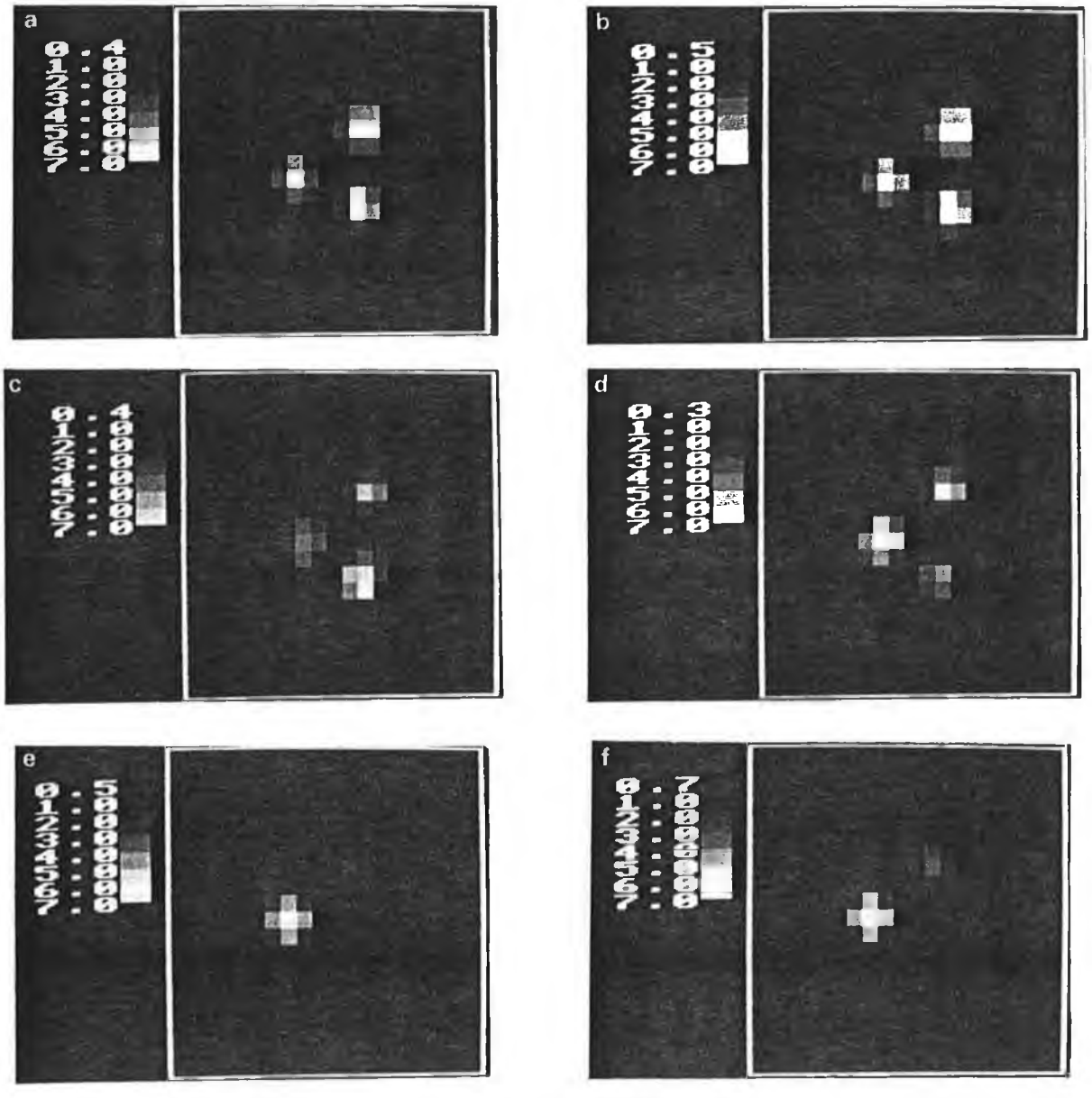

A sequence of reconstructed images which show steps in the imaging of palladium. (a) and (b): Reconstructed images derived from absorption data for Ag K_α (a) and K_β (b) X-rays. Palladium and caesium have not been added. (c) and (d): Reconstructed images derived from absorption data for Ag K_α (c) and K_β (d) X-rays. Palladium and caesium have been added. Note the change in emphasis is from caesium to palladium on going from the lower energy K_α to the higher energy K_β X-rays. (e) and (f): Reconstructed images of palladium. (e) has not been corrected for matrix effects (maximum concentration: 14.1 kg/m^3). (f) has been corrected (maximum concentration: 16 kg/m^3).

Reconstructed images of 46Palladium.

FIGURE 5.12

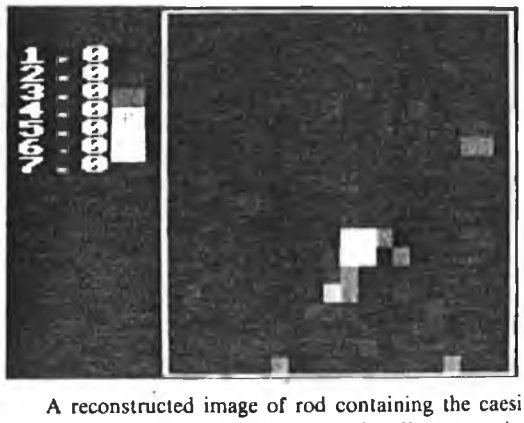

A reconstructed image of rod containing the caesium. No correction has been made for matrix effects (maximum concentration: 9 kg/m^3).

Reconstructed image of 55Caesium.

FIGURE 5.13

the energy of the K absorbtion edge of 46 Palladium. Figure 5.12d is the absorbtion of the higher energy Silver K_β X-rays in which the dominant feature is the two Palladium rods when the X-ray energy is above the K absorbtion edge of Palladium.

Figures 5.12e and f are images of 46Palladium only formed by the differential absorbtion of Silver K_α and K_β X-rays, uncorrected and corrected respectively for the effect of the matrix, which includes the 55Caesium rod. The maximum value of the Palladium concentration is increased in Figure 5.12f due to the correction for the matrix effect.

Figure 5.13 shows a reconstructed image of the 55Caesium rod scanned with 56Barium K_α and K_β X-rays from the variable energy X-ray source, in which no correction for the matrix effect was made. The background level is higher because fewer X-ray photons were used in the Caesium scan.

The images of Figures 5.12 and 5.13 may be compared with Plate 5.2. Table 5.1 is a comparison of the maximum equivalent thickness and concentrations of the analyte elements measured by static differential absorbtion and from the scanning measurements to check the accuracy of the results. In the static measurements the X-ray beam was transmitted through the epoxy glue rods alone with and without the analyte element present. The equivalent thickness t_a of the analyte element of mass attenuation coefficient μ_a was determined from the equation

$$t_a = \ln[(N_l/N_h)(N_{mh}/N_{ml})]/(\mu_{ah}-\mu_{al}) \qquad (5.3)$$

ROD	Concentration (kg/m³)		Equivalent thickness (10^{-2} kg.m^2)	
	by Differential Absorption	from reconstructed image	by differential absorption	from projection data *
a) palladium	15 ± 0.6	16	6.2 ± 0.3	6 ± 0.5
b) palladium	7 ± 0.6	8	3.2 ± 0.3	3 ± 0.5
c) caesium	5 ± 2.5	9	2.5 ± 1.2	3.8 ± 2

Comparison of equivalent thickness and concentrations.
They were obtained in static differential absorption measurements and from the scan data.

* measurements made at the maximum of the scan data.

TABLE 5.1

where N is the number of transmitted X-ray photons, l,h refer to the low and high energy sides of the K absorbtion edge, and a,m refer to analyte and matrix. The equivalent thicknesses are taken from Figures 5.10c and 5.11. The errors in the equivalent thickness are due to statistical variation in X-ray photon counts. There is good agreement for the Palladium analyte showing that the correction for the matrix was effective. Poor counting statistics gave larger errors for Caesium.

The final concentration in the reconstruction image depends also on the relaxation constant R in the iteration equation.

$$C_{jk}\ (\text{new}) = C_{jk}\ (\text{old}) + R f_{jk}^{rs} \epsilon \qquad (5.4)$$

where $$\epsilon = (t_{ao}^{rs} - t_{ai}^{rs}) \Big/ \sum_{jk} (f_{jk}^{rs})^2 \qquad (5.5)$$

and C_{jk} is the concentration of the analyte element in the jk pixel, f_{jk} is the fractional area of overlap between the simulated X-ray beam path for the r^{th} rotation angle and the s^{th} linear step with the jk pixel of the reconstruction grid and t_{ao}^{rs} is the analyte equivalent thickness as determined from the object, t_{ai}^{rs} is its equivalent thickness as calculated from the assumed image. This is shown in Figure 5.14 and Table 5.2 for the higher concentration Palladium rod.

The total number of K_α and K_β photons was about 5×10^7 and 10^7 for Palladium, and 5×10^6 and 10^6 for Caesium, respectively.

A CRYSTAL TRANSMISSION FILTER FOR X-RAYS.

The continuum spectrum from an X-ray tube is too broad for imaging one or more consecutive atomic elements in the Periodic Table of the

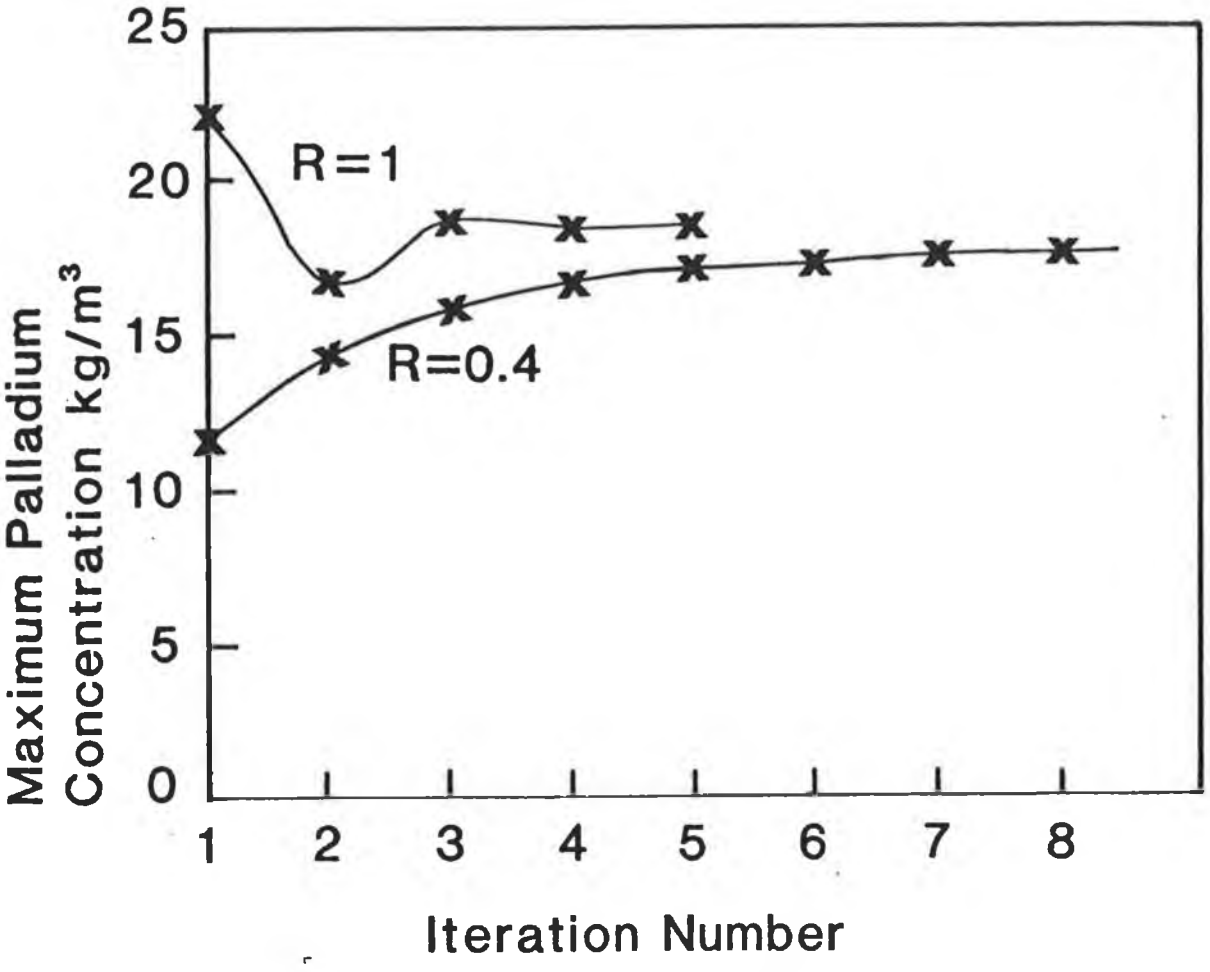

Relaxation constant in imaging 46Palladium.

The variation of the maximum concentration of 46Palladium with iteration number. The curves are for a relaxation constant R = 1 and R = 0.4.

[14]

FIGURE 5.14

Relaxation Constant R	Final iteration number	Maximum Palladium Concentration kg/m^3
1	5	18.4
0.4	8	17.7
0.2	11	16.9
0.1	17	16.0

The relaxation constant and analyte element concentration. The variation of the maximum 46Palladium concentration with relaxation constant R. The final iteration is the one for which the change in standard deviation of the concentration is less than 1% different from the succeeding iteration.

TABLE 5.2

Elements. Only a narrow band of X-rays of about 1keV to 8keV wide is needed in the region of the K absorbtion edge(s) of the atomic element(s) being analysed. The spectrum outside this band effectively reduces the counting efficiency of the scanning machine in the pass band of the spectrum which is the region of interest.

A single crystal of Lithium fluoride, taken from the Philips PW1270 X-ray spectrometer, was tried as a transmission filter, comparing calculated and experimental results.

The very low count rate, 1 photon in 3 seconds, showed that only a small fraction of the beam was transmitted through the crystal and the transmission at the peak was about 1%.

The transmission crystal was not suitable as a filter for X-rays herein because the relative attenuation outside the region of interest was low, and due to the limited range of peak wavelength in the relation between the variables in the transmission crystal equation. Thus this filter method was not used. Instead, filters made of pure metals of a particular thickness were found by calculation and experiment to be very suitable. These transmission filters are described in Chapter 4 and used in the main experiment of Chapter 6. The BASIC computer program SPECTRA for calculation of the band pass X-ray spectra is listed in Annexe D.

CHAPTER VI

A X-RAY SCANNING MACHINE FOR IMAGING ATOMIC ELEMENTS

Three consecutive atomic elements, 46Palladium, 47Silver and 48Cadmium of the Periodic Table of the Elements each of two different concentrations in an object were imaged using the X-ray machine. Differential K absorbtion edge tomography produced images of each atomic element separately. Computer axial tomography produced images which depended on the general absorbtion of X-rays by the object so that these images depended on the atomic number of the absorber and on its density. Thus one complete scan of the object can do both kinds of tomography [15].

Image reconstruction for imaging three consecutive atomic elements was done by the Algebraic Reconstruction Technique for imaging a specific element by differential K absorbtion edge tomography, and Backprojection incorporating a Ramachandran filter was used for imaging the internal structure of the whole object by computer axial tomography. The images were displayed on a colour monitor screen and also printed on paper.

Figure 6.1 is a schematic diagram of the scanning machine used to image 46Palladium, 47Silver and 48Cadmium, whose K absorbtion edges are at 24.35keV, 25.52keV, and 26.71keV. Each element at two different known concentrations, Palladium dust in powdered charcoal, Silver nitrate

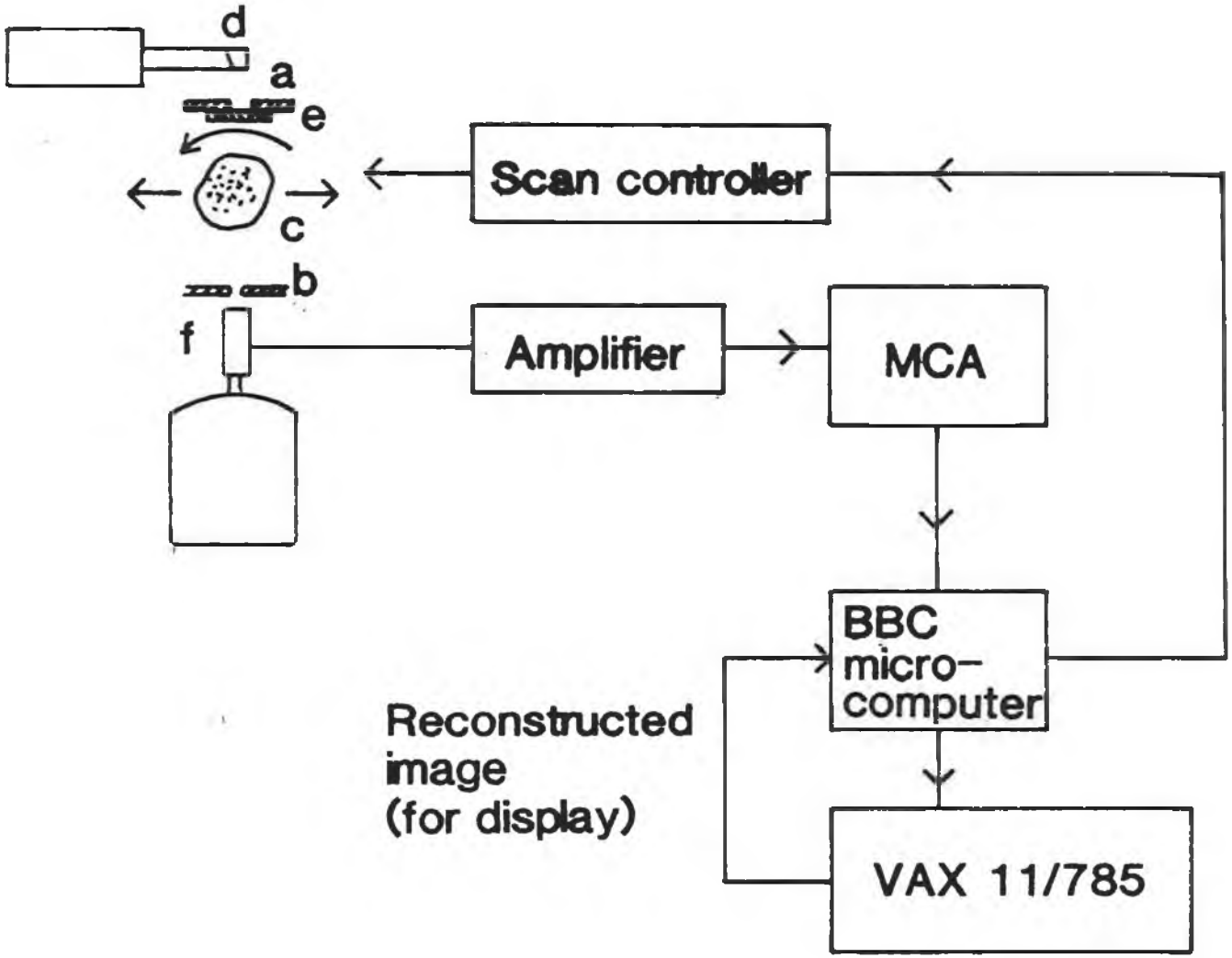

Schematic diagram of the differential K absorbtion edge scanning machine.

[15]

FIGURE 6.1

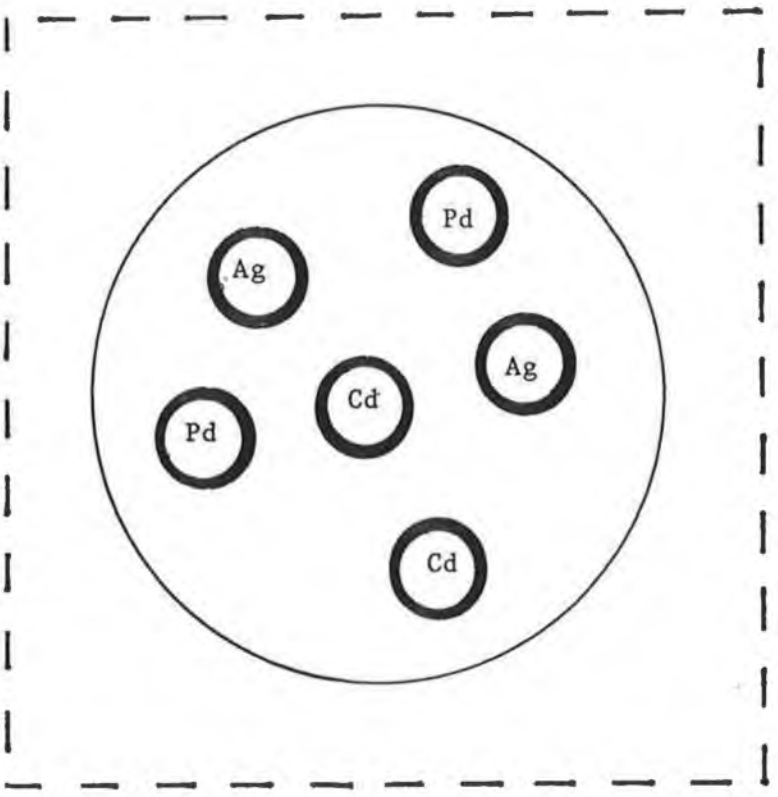

Cork matrix and 3 analyte elements.

The 30mm diameter cork matrix containing the 46Palladium, 47 Silver and 48Cadmium analyte elements, each at two different concentrations in 5mm diameter test tubes set within the 40 x 40 scanning grid.

FIGURE 6.2

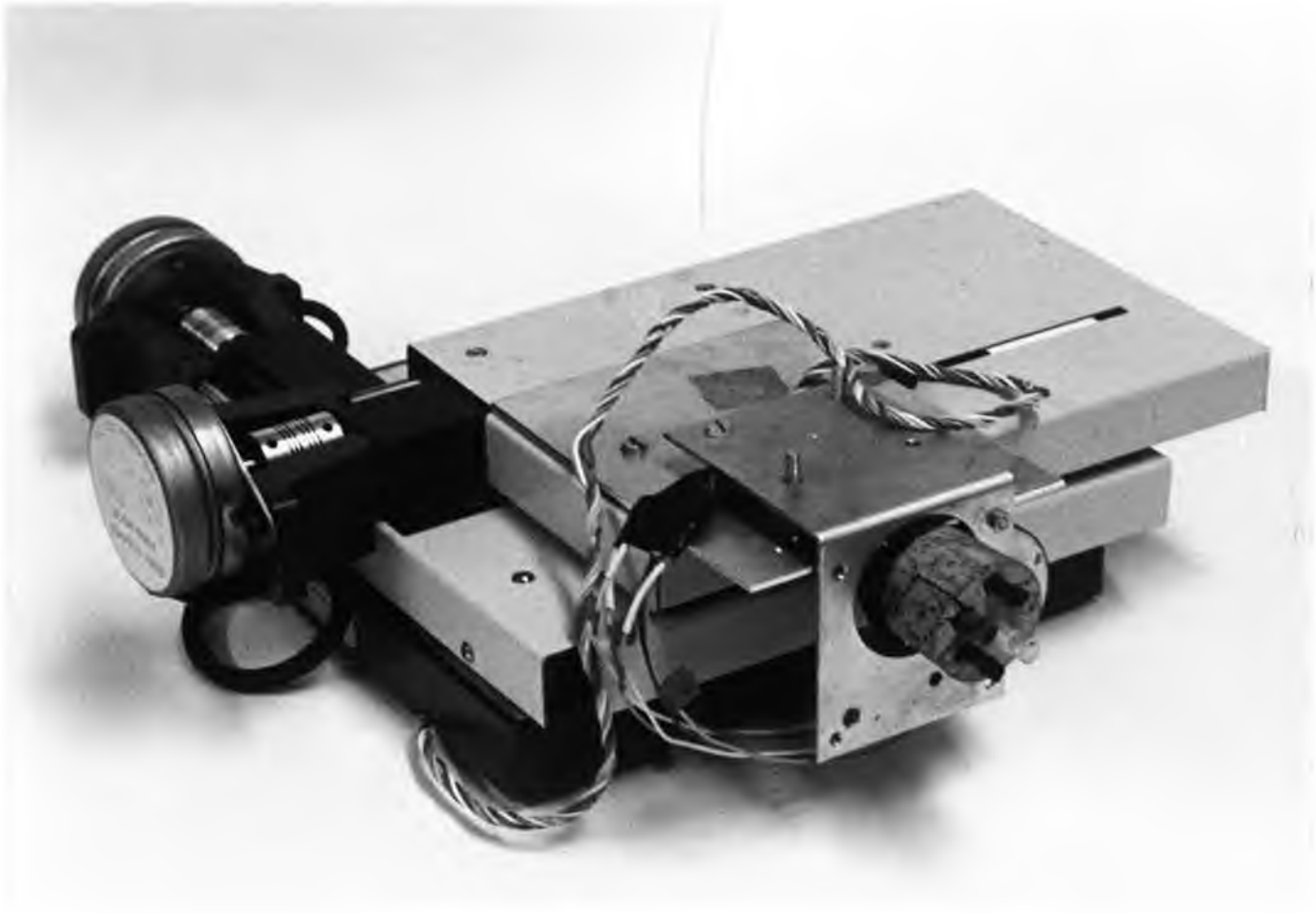

The three analyte elements and cork matrix on the coordinate table.

PLATE 6.1

$AgNO_3$, and Cadmium sulphate $3CdSO_4.8H_2O$, was mixed in epoxy resin and individually sealed in 5mm diameter test tubes. The six test tubes were set, spaced apart and axially parallel, in a 30mm diameter cork as shown in Figure 6.2 and Plate 6.1. The cork was attached to a bush wheel mounted on the rotation or ϕ-axis stepping motor.

The X-ray tube d having a 1mm thick Beryllium window provides a broad X-ray spectrum in a pencil beam defined by a 1mm circular aperture a in the floor of the steel box in the Lead analysing chamber and a 1mm square aperture b below the floor of the analysing chamber. a is the fixed collimator and b is the adjustable collimator of the machine. The X-ray beam is detected by the Si(Li) detector f and the output pulses are amplified by the EG & G Ortec 575 main amplifier, gain set at 200. The amplified pulses of height, or voltage, proportional to the X-ray photon energy are selected and counted according to energy by the EG & G Ortec 7100 multichannel analyser to produce an energy spectrum, a graph of number of pulses against pulse energy, on the colour display monitor. Plates 4.1 to 4.4 show the X-ray machine.

The BBC microcomputer controls the scan controller and the multichannel analyser, and counts and stores on disc the X-ray photon counts, the photon count data. When a complete scan of an object is made the photon count data is sent to the VAX 11/785 computer which reconstructs the image of the object. The reconstructed image data is sent to the BBC microcomputer and stored on disc. This image data is then displayed on a colour monitor using a BASIC display program. A block diagram of the BASIC computer programming procedure is shown in Figure 6.3 and Figure 6.4.

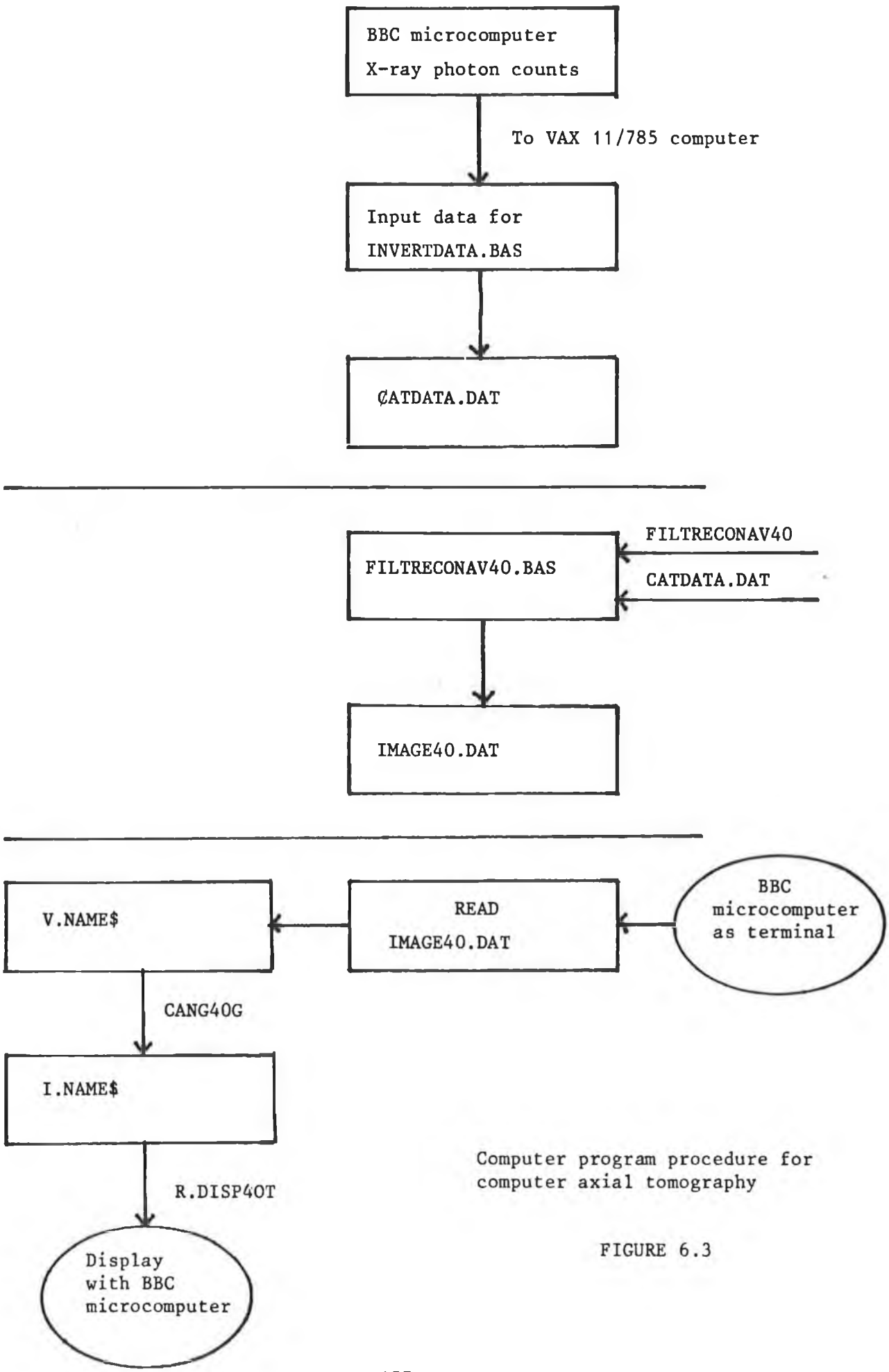

Computer program procedure for computer axial tomography

FIGURE 6.3

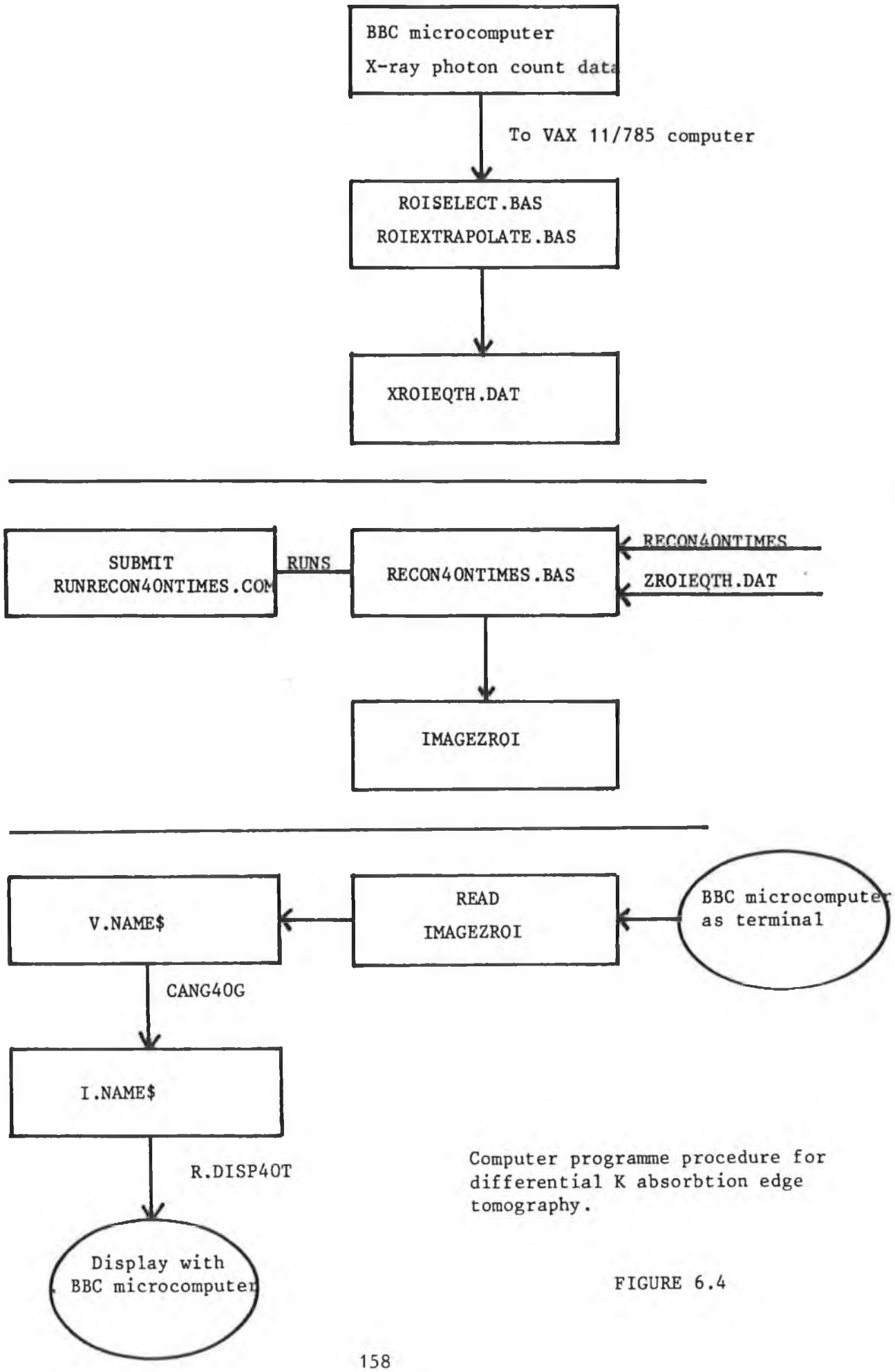

Computer programme procedure for differential K absorbtion edge tomography.

FIGURE 6.4

The cork matrix containing the three analyte elements was scanned in 40 x 1mm linear steps and 40 x 4.5° angular steps between 0° and 175.5°, for a step scanning real time of 60 seconds. The X-ray tube was run at 40kV, and 5mA. At the end of each 40 step linear scan which took one hour, the photon count data was accessed to the BBC microcomputer memory by BBC microcomputer command. The cork was incremented by a 4.5° rotation and another 40 step linear scan made in the opposite direction. This procedure was continued until the cork was rotated through 175.5° in 40 angular steps; 40 hours for a complete scan of the object.

The intensity of the X-ray beam needed to be reduced by about 100 so that the maximum count rate was not greater than about 2×10^4 counts per second, and the width of the X-ray spectrum should be reduced so as to include an energy range encompassing the energy of the K absorbtion edge of the analyte elements. A 0.29mm thick Tin filter was placed below the aperture in the steel box which narrowed the X-ray pass band to between 21 and 29.5keV, which is below the K absorbtion edge energy of Tin, 29.19keV. Figure 6.5 shows the variation in the mass attenuation coefficient of Tin near its K absorbtion edge energy, and Figure 6.6 shows the calculated normalised curves for various Tin filters against the background of the X-ray tube spectrum, curve a. The curve for a 0.3mm thick Tin filter which reduces the intensity by a 4×10^{-2} is shown at c, which is close to the experimentally measured curve. The X-ray absorbtion spectrum as measured is shown in Figure 6.7, a graph of number of counts per electron volt against X-ray energy in keV. Absorbtion of X-rays at the K absorbtion edge energies of 46Palladium, 47Silver, and 48Cadmium, marked by the arrows, are shown by the dips in the curve at these X-ray energies. The shaded parts of the graph are

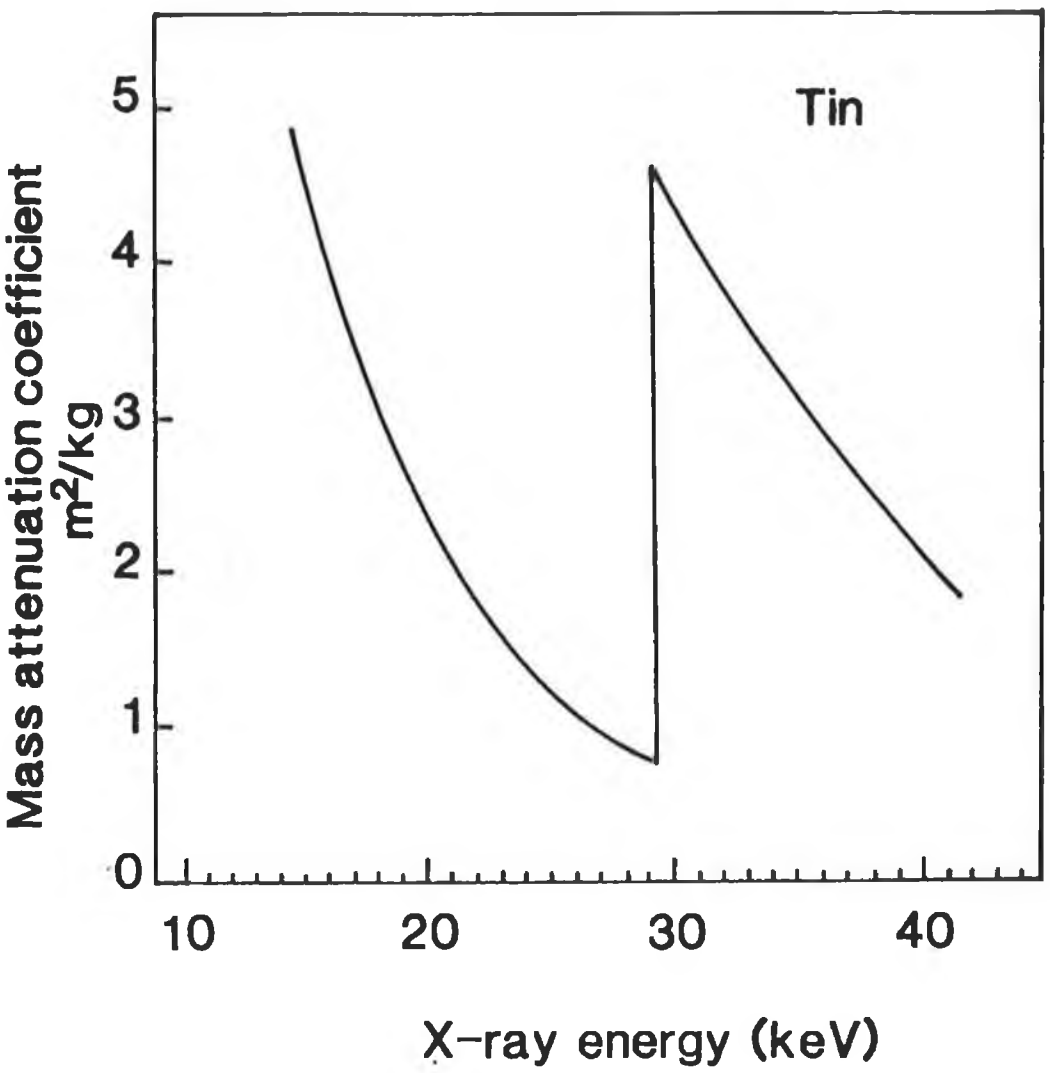

The mass attenuation coefficient of 50Tin.

This shows the variation of the mass attenuation coefficient of 50Tin in the vicinity of its K absorbtion edge at 29.19keV.

[15]

FIGURE 6.5

	Filter	Calculated Transmission
a	none	1
b	0.2mm	9×10^{-2}
c	0.3mm	4×10^{-2}
d	0.5mm	8.4×10^{-3}

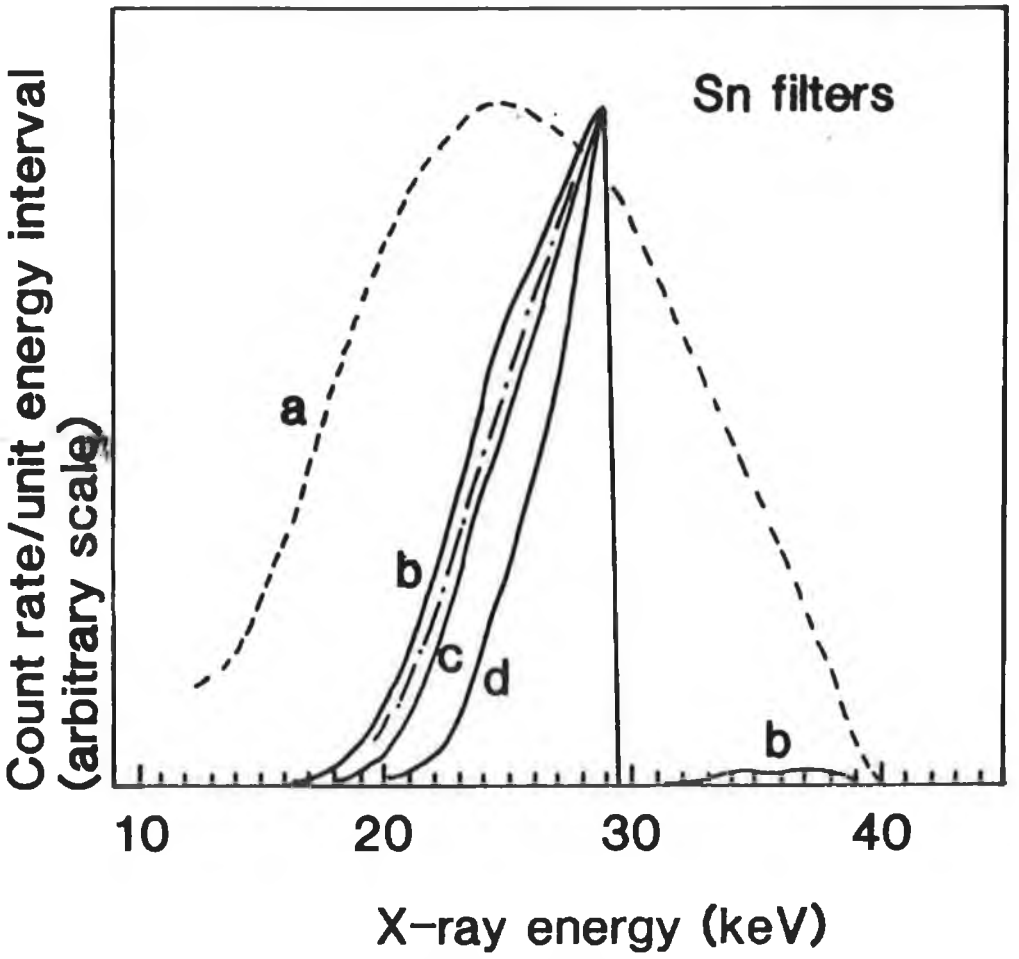

50Tin filter transmission.

This shows the calculated effect of a 50Tin filter on the X-ray spectrum. The dot-dash line is the measured spectrum for 0.29mm of Tin.

[15]

FIGURE 6.6

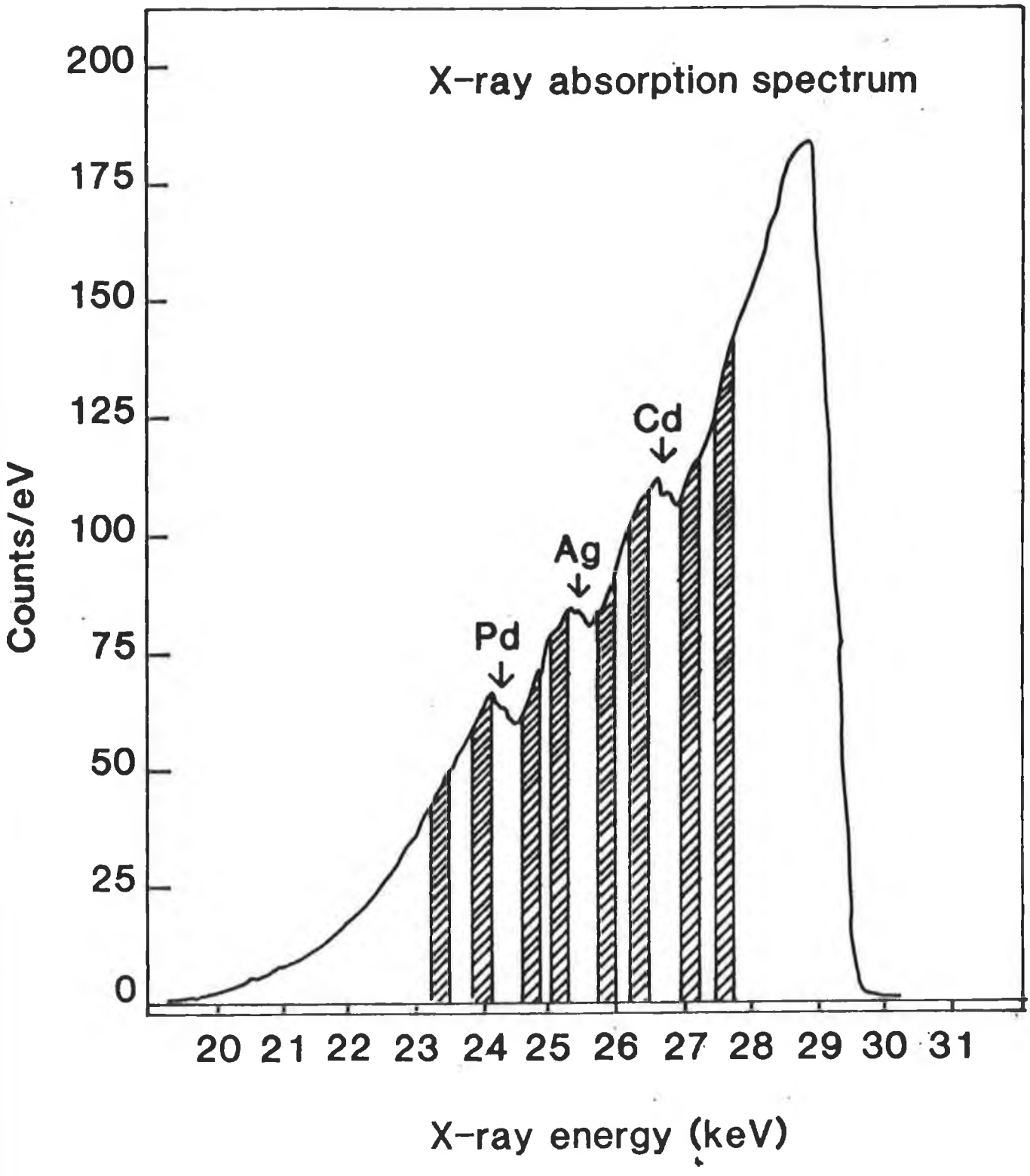

An X-ray spectrum after transmission through the object.
The K absorbtion edges are marked with the arrows.

[15]

FIGURE 6.7

the calibrated energy bands 300 electron volts wide selected in the multichannel analyser, each about 10 channels wide. These eight energy bands or regions of interest 300 electron volts wide were chosen experimentally from a graph of K absorbtion edge energy against element atomic number as shown in Figure 6.8. The K absorbtion edge energy difference between the atomic elements chosen for scanning is about 1.2keV, so that choosing two energy bands 300 electron volts wide spaced apart equally, and from the K absorbtion edges of the elements leaves three energy band gaps of 200 electron volts. These band gaps space the regions of interest from the fine structure of the K absorbtion edges of the elements.

The multichannel analyser was calibrated in X-ray photon energy by using the Amersham International 241 Americium variable energy X-ray source. The K_α line of 56Barium of energy 32.19keV was used to fix the high energy end of the spectrum at channel number 958 so that 958/32.19 = 30 channels per 1keV, 33 volts per channel, or 10 channels is equivalent to 330 electron volts. The low energy end of the spectrum of the multichannel analyser was fixed using the K_α line of 29Copper of energy 8.05keV. The calibration was tested using K_α lines provided by the variable energy X-ray source of intermediate energy. The calibration should be checked each time an object is scanned.

The resolution of the Si(Li) detector and of the multichannel analyser for the Silver K_α line emitted by the 241 Americium variable X-ray source given by Resolution = $\frac{\text{Full width of peak at half maximum}}{\text{multichannel analyser channel number}} \times 100$ was 370 electron volts and 1.8 channels, where the K_α maximum appeared at channel number 659 and the width was 12 channels.

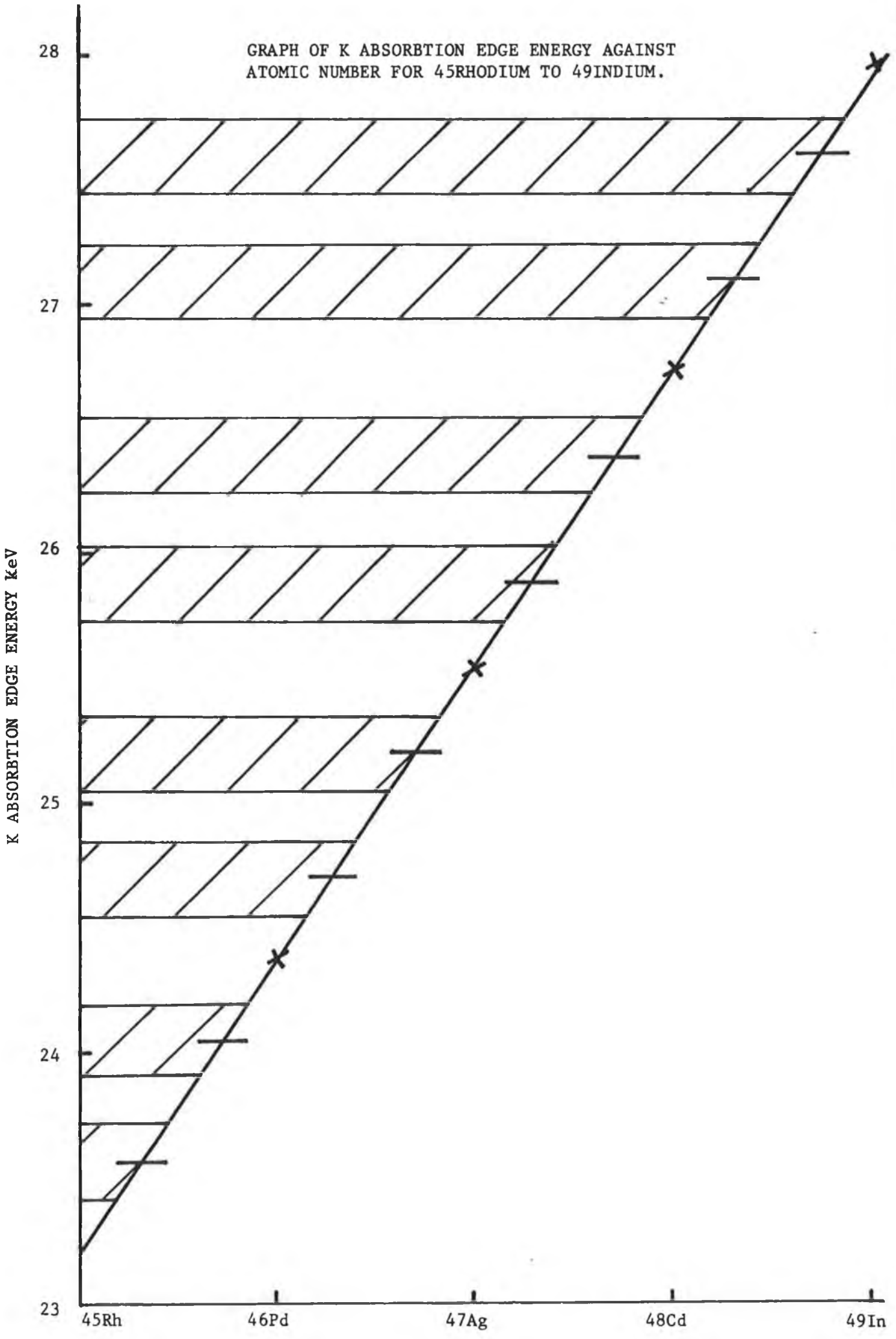

Selection of the 8 regions of interest for scanning.
FIGURE 6.8

Detected photons within these selected energy bands were stored in the memory of the multichannel analyser. The average number of photons counted per linear scan was $\approx 10^6$ for each chosen energy band, so that the total photon count was $10^6 \times 40 \times 8 \approx 3 \times 10^8$. Figure 6.9 represents the projection data profile across the object for 46Palladium, a graph of $\ln(N_o/N)$ against the linear scan position for rotation 39 which is the last scan, 175.5° from the start and the second region of interest which is the X-ray energy band at about 24keV, just below the K absorbtion edge of Palladium, as shown in Figure 6.7.

Figure 6.10 shows the equivalent thickness of Palladium for rotation 39, corrected 2, and uncorrected 1, for the presence of the matrix which is the cork and the other elements, Silver and Cadmium. The matrix effectively reduces the equivalent thickness of the analyte element, and in a non linear way, because lines 1 and 2 are not displaced from one another by a constant. Part of line 2 for the corrected value of the equivalent thicknes is close to zero and within the error bar, as shown, which indicates that the correction for the matrix is excellent.

As shown in Chapter 3 the equivalent thickness of the analyte element a corrected for the effect of the matrix m is given by equation 3.7:

$$t_a = \ln[(N_1/N_h)(N_1/N_{o1})] /(\mu_{ah}-\mu_{a1}) - t_m(\mu_{mh} - \mu_{m1})/(\mu_{a1} - \mu_{a1})$$

where N_o, N are the incident and transmitted X-ray photon fluxes. μ is the mass attenuation coefficient, t_m is the equivalent thickness of the matrix and 1, h refer to the X-ray energies below and above the K absorbtion edge of the analyte element. The equivalent thickness is the sum of the concentrations of the analyte elements in the voxels of the

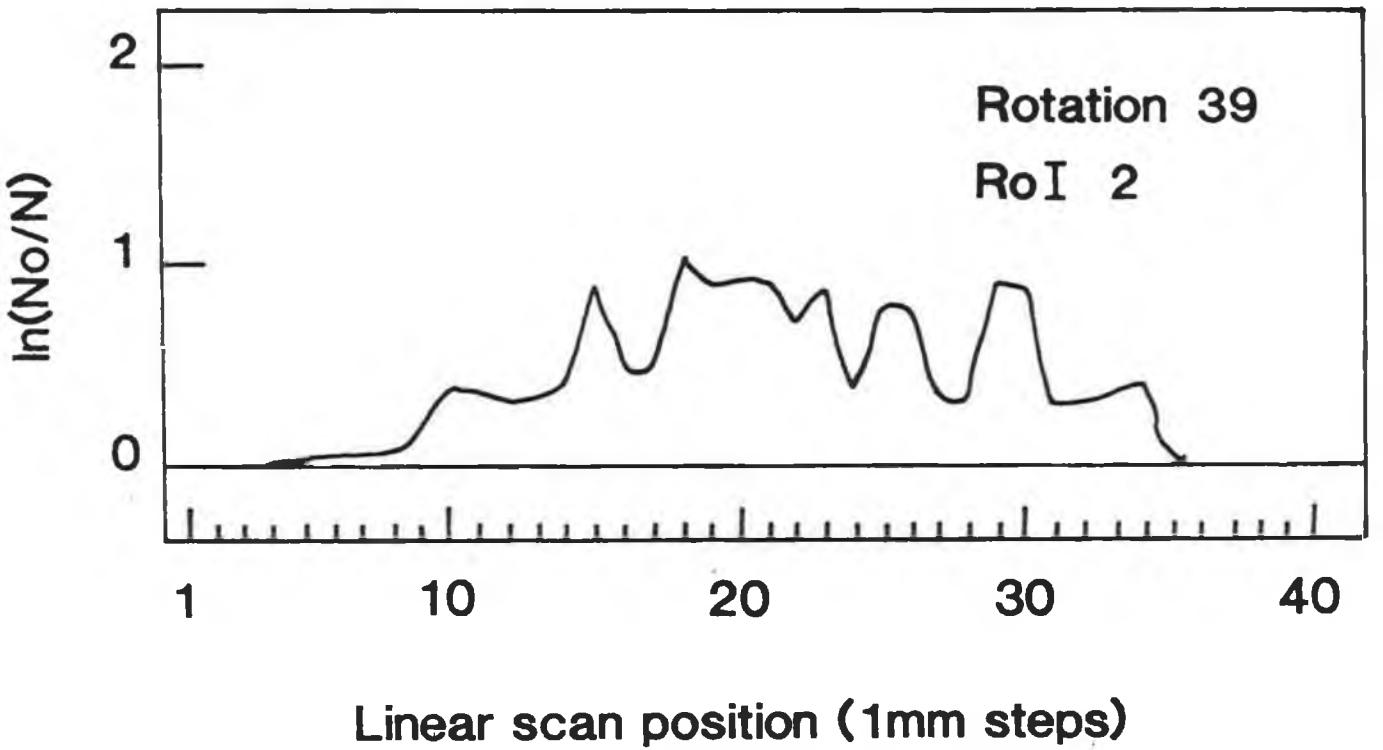

The projection data profile across the object.

This shows the computer axial tomography projection data for the narrow spectral region of interest 2 in Figure 6.5 using the equation $\ln(N_o/N) = \int \mu(\Omega) dy$ for producing tomographs as shown in Figure 6.11 and Plate 6.2.

[15]

FIGURE 6.9

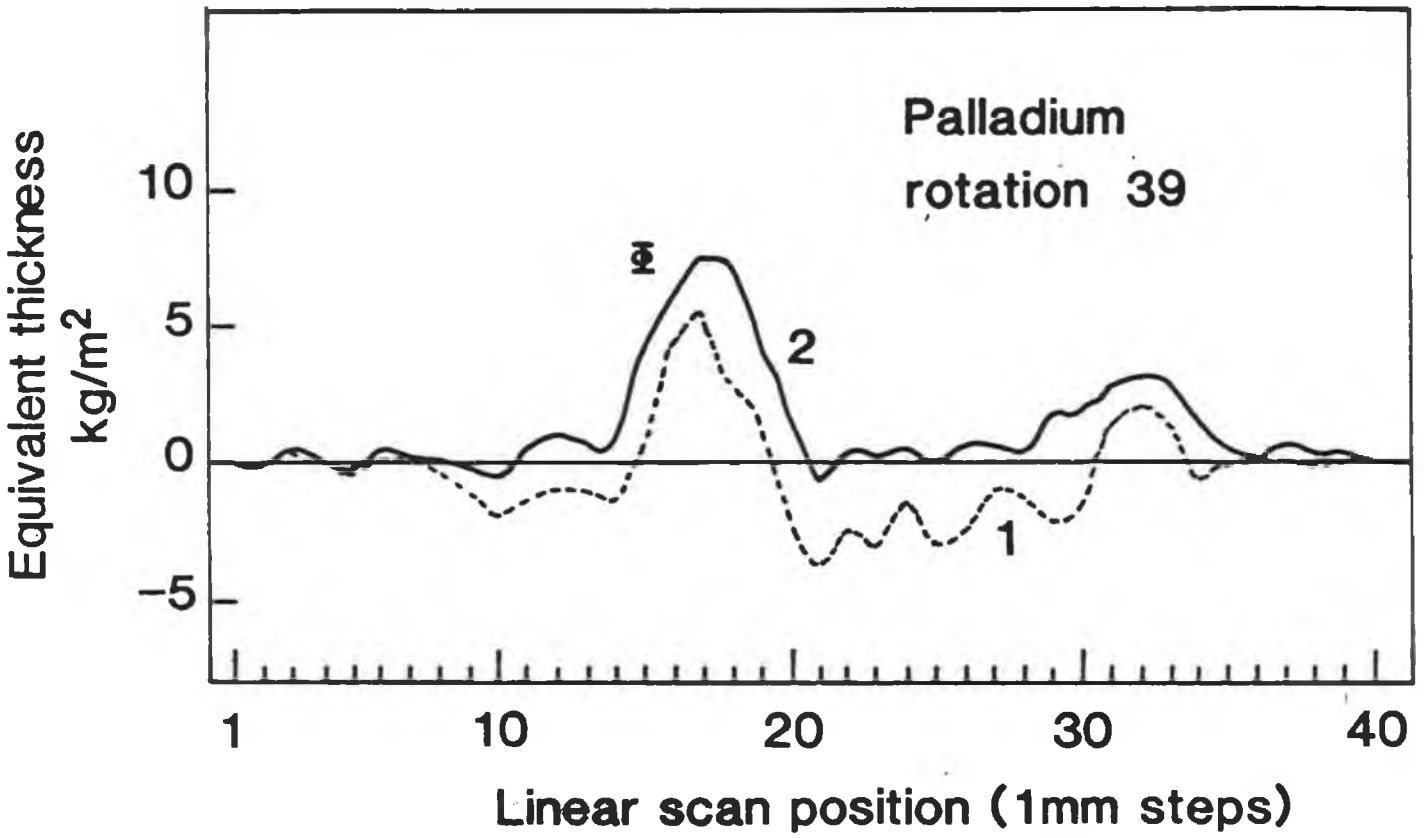

The equivalent thickness profile of 46Palladium.

This shows the variation in the equivalent thickness of 46Palladium in a cork matrix. Curve 1 is uncorrected for the effect of the matrix using regions of interest 2 and 3 of Figure 6.5. Curve 2 has been corrected by extrapolating to the K absorbtion edge.

[15]

FIGURE 6.10

scanning grid intercepted by the X-ray beam, and this provides the projection data used to build up an image of the concentration of the analyte in the reconstruction grid by differential K absorbtion edge tomography. The correction for the effects of the matrix is made by extrapolating the X-ray photon counts in two narrow bands from the centre of each band on each side of the K absorbtion edge of an analyte element and using the equation 3.8 for the transmitted flux

$$N = N_o \exp [-(\mu_a t_a + \mu_m t_m)]$$

which gives $\ln(N_o/N) = \mu_a t_a + \mu_m t_m$

and so, equation 3.8, $t_a = (Y_h - Y_l)/(\mu_{ah} - \mu_{al})$

where Y is the extrapolated value of $\ln(N_o/N)$ as described before.

Figure 6.11 is a graph of $\ln(N_o/N)$ against X-ray energy keV in the region of the K absorbtion edges of the three analyte elements for one of the scanning positions, at step 21 and rotation 4, to show the linear extrapolation to the absorbtion edges using two points between each absorbtion edge. $N_o > N$ so that the extrapolation slopes are alternately negative and positive. Each point chosen for the extrapolation is at the centre of the corresponding 300eV wide energy band selected by the multichannel analyser. Figure 6.7 shows that the linear extrapolation slopes for each pair of 300 electron volt wide energy bands is alternately positive and negative because the ordinate is given in X-ray photon counts per electron volt. The pair of energy bands between two consecutive atomic elements is extrapolated to the K absorbtion edges of those elements. Thus for imaging three consecutive elements of the Periodic Table of the Elements eight narrow X-ray energy bands are required, a pair on either side of a K absorbtion edge.

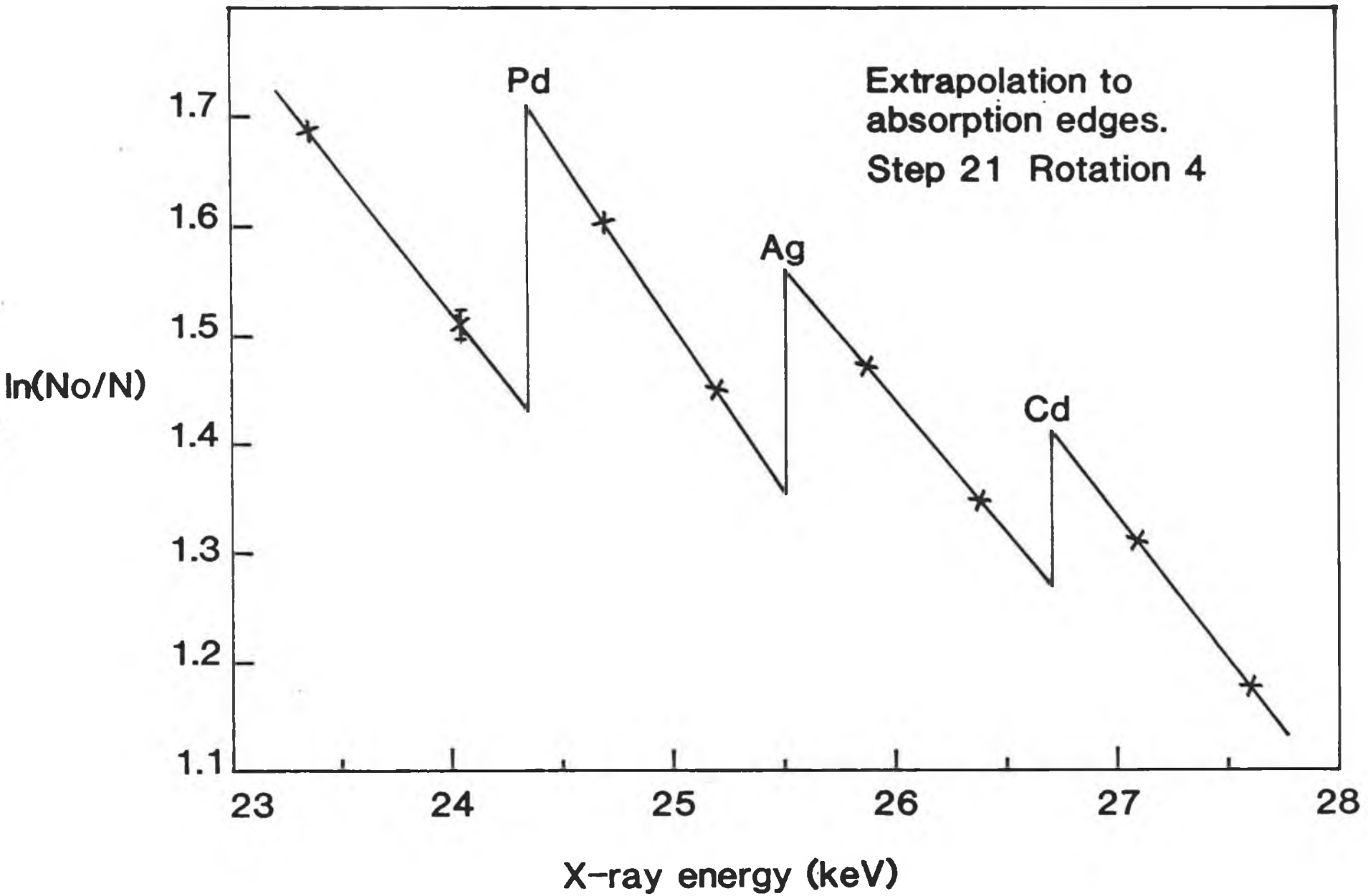

[15]

FIGURE 6.11

Theory confirmed by experiment showed that the photon counting dead time, the time for which the slowest counting instrument is unable to register the next detected photon, does not affect the extrapolation intersection with the K absorbtion edge of an analyte element. From the equation 3.15

$$\ln(N_o/N) = \mu_a t_a + \mu_m t_m$$

the equation including the counting dead-time is

$$\mu_a t_a + \mu_m t_m = \ln(N_o/N) + \text{constant}$$

A pair of lines extrapolated to the K absorbtion edge of an analyte element is equally shifted on the ordinate axis by an equal amount as the count rates N_o/N change. Thus the measured equivalent thickness of the analyte element is not influenced by counting dead-time. Herein, the multichannel analyser is the slowest counting instrument having a dead-time of about 50% at a count rate of 2×10^4 s^{-1}: the Si(Li) detector can count at over 10^5 s^{-1}. The maximum count rate in the experiment was $\approx 10^4$ s^{-1} with a 1mm square collimator, direct source to detector X-ray beam having a 0.29mm Tin transmission filter, and the X-ray tube operating at 40kV and 5mA. Thus the dead-time was less than 15%. Long dead-times will give unreliable counting statistics because a large fraction of the photons will not be included in the photon count data stored in the BBC microcomputer memory, so a compromise between fast count rate and dead-time needs to be found. The dead-time was reduced by using the low level discriminator of the multichannel analyser to eliminate detected photon counts at the low energy side of the lowest energy band selected by the multichannel analyser, i.e. below 23keV. A graph of percentage dead-time against measured count rate for the multichannel analyser is shown in Figure 6.12.

Graph of % dead-time against count rate for the EG & G Ortec 7100 multichannel analyser.

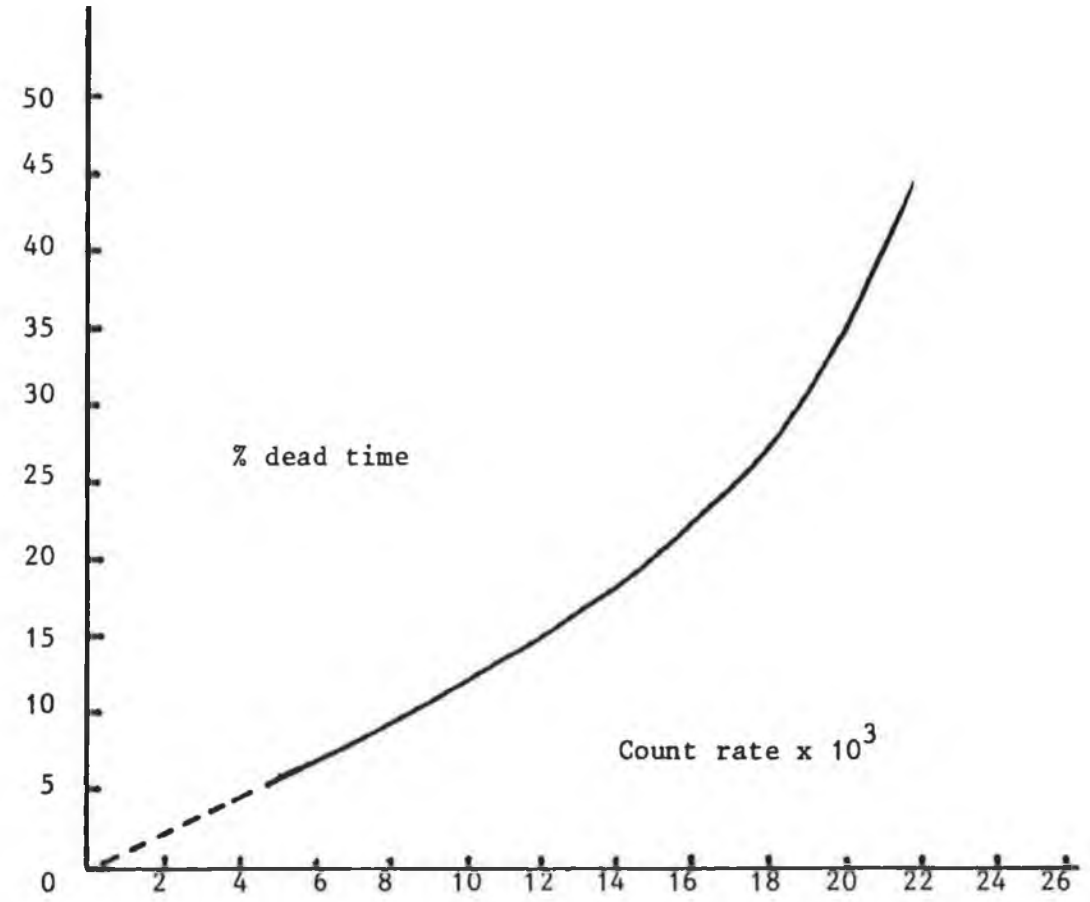

The dead-time of the multichannel analyser.

FIGURE 6.12

Element	Concentration kg/m^3	
	maximum from image	expected from amounts added
Pd	21	15
Pd	10	7
Ag	17	25.4
Ag	12	12.7
Cd	15	22
Cd	10	11

The concentrations of analyte elements.

The measured concentrations of 46Palladium, 47Silver, and 48Cadmium from the differential K absorbtion edge tomography image compared with that of the analyte elements added to the epoxy glue.

FIGURE 6.17

Reconstruction of the image of the object by Backprojection is faster than by the Algebraic Reconstruction Technique in the VAX 11/785 computer. Both methods can be used for computer axial tomography to image the whole object as image density variations corresponding to the general absorbtion of X-rays and for differential K absorbtion edge tomography to image a specific element, but at present, only the Algebraic Reconstruction Technique can measure the concentration of analyte element. To obtain better image resolution by Backprojection each pixel is mathematically divided in four squares and the X-ray beam representation divided into two equal parts in the computer program. The time taken for the central processing unit of the VAX 11/785 computer to reconstruct the image of the whole object by Backprojection as shown in Figure 6.13 was about 30 seconds, using the 300eV energy band at 24keV as shown in Figure 6.7 selected on the multichannel analyser as the photon count data. The BASIC program for Backprojection run on the VAX 11/785 computer is listed in Annexe D.

The BASIC program run on the VAX 11/785 computer for the Algebraic Reconstruction Technique is listed in Annex D. The areas of overlap of the pixels in the reconstruction grid with the X-ray beam representation, about 13×10^4 is too large a number to be held in the VAX 11/785 computer memory, so they are accessed one by one from disc. The method described in Chapter 3 is also more complicated than that for Backprojection. Using floating point arithmetic for the values of the overlap areas and in the reconstruction, the central processing unit time of the VAX 11/785 computer was 34 minutes for one iteration. The number can be determined by the computer program itself so that the maximum concentration of analyte element is within a chosen value of the limit, herein <1% , at which iteration the program stops. R is a

relaxation constant, $0<R\leq1$ which damps the oscillations of the maximum concentration value. When R is small, say $R<0.1$, the damping is too great, and many iterations are needed as the concentration rises towards a limit, as shown in Figure 3.7. R is best chosen between 0.2 and 0.5.

The BASIC computer program sequence for scanning an object and reconstruction of its iamge by the Algebraic Reconstruction Technique is as follows. The rotation axis of the object is centred with the X-ray beam, the object is scanned automatically in 40 x 1mm linear steps and 40 x 4.5° angular steps, and detected photons counted in 8 x 300eV wide regions of interest selected by the calibrated multichannel analyser, whose memory is accessed after each linear scan by the BBC microcomputer, and the photon count data stored on disc. When scanning is complete, the BBC microcomputer photon data count is sent to the VAX 11/785 computer and inverted to the form $\ln(N_o/N) = \mu t$, the equivalent thickness of the object for each step. The image is then reconstructed to form the image data which is returned to the BBC microcomputer, stored on disc, and displayed using a BASIC display program.

Figure 6.13 and Plate 6.2 show a computer axial tomography image of the 30mm diameter cork matrix and analyte elements shown in the eight colour scale 0 to 80, which shows absorbtion of X-rays as image density variations and with no discrimination between elements. The cork does not appear in the image because it absorbs relatively little of the X-rays, being composed of light elements: it is a water like matrix. The dark pixels approximate to circles, which is the absorbtion of X-rays due to the 5mm diameter glass test tubes. Intermediate density variations are due to the presence of the three analyte elements. The outline of the image corresponds to a 40mm square scanning area in the

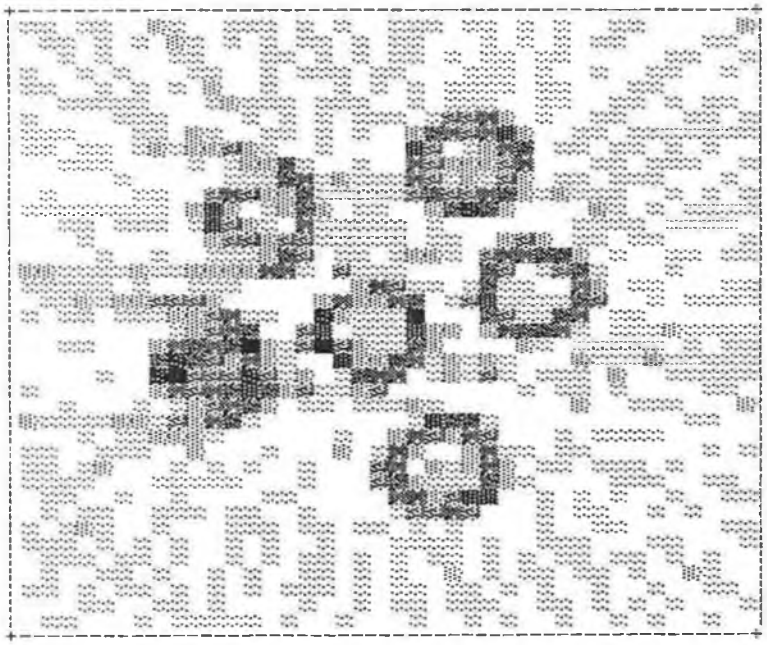

A computer axial tomography image.

This shows the variation of the linear attenuation coefficient measured within the region of interest 2 of Figure 6.9. There is no analyte element discrimination within the six test tubes.

[15]

FIGURE 6.13

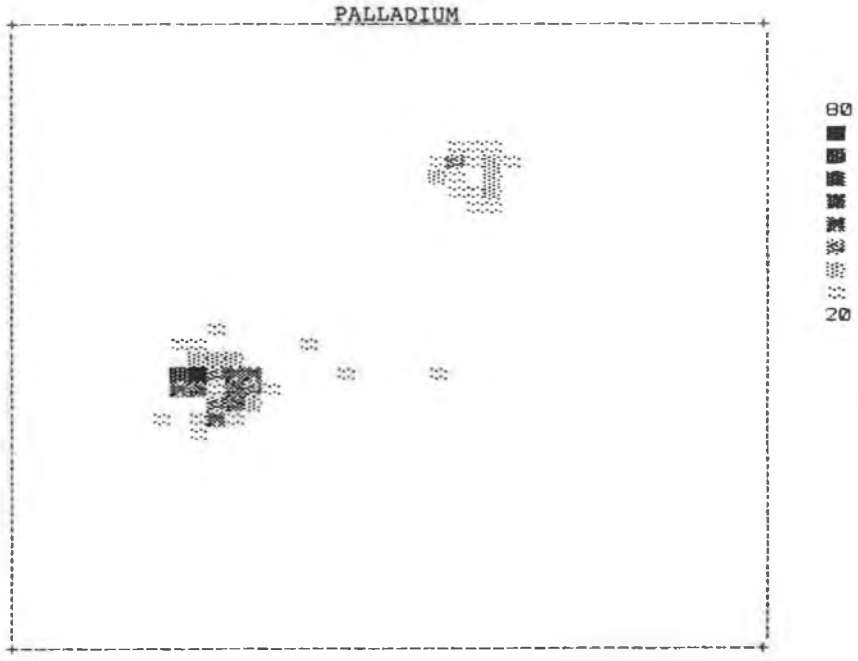

Differential K absorbtion edge tomography scan of 46Palladium. This shows the two images of concentration 21 kg/m^3 and 10 kg/m^3 of 46Palladium alone.

[15]

FIGURE 6.14

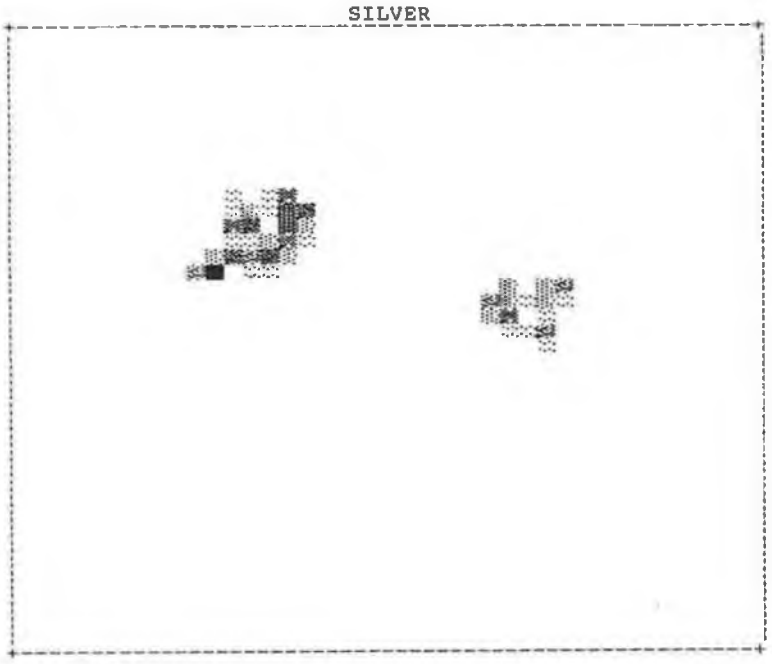

Differential K absorbtion edge tomography scan of 47Silver. This shows the two images of concentration 17 kg/m^3 and 12 kg/m^3 of 47Silver alone.

[15]

FIGURE 6.15

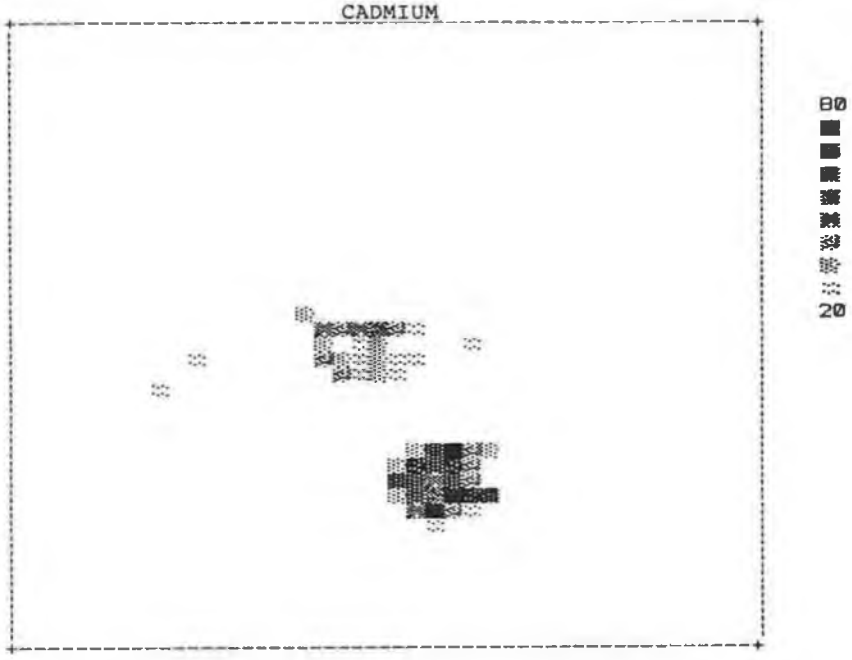

Differential K absorbtion edge tomography scan of 48Cadmium. This shows the two images of concentration 15 kg/m^3 and 10 kg/m^3 of 48Cadmium alone.

[15]

FIGURE 6.16

X-ray machine, but the ordinate has been reduced a little in the printer; the outline of the image should be square. The graph below the image is the image density in the pixels intercepted by the line cursor set for rotation 0 and step 20 in the image display.

Figures 6.14, 6.15 and 6.16 and plates 6.3, 6.4 and 6.5 are the images of the 46Palladium, 47Silver, and 48Cadmium, each at two different densities which have been separately imaged by differential K absorbtion edge tomography, and which have been reconstructed by the Algebraic Reconstruction Technique. These images are located at the same position as in the image shown in Figure 6.13 and Plate 6.2. The lower limit of the image density has been set at 20 in order to delete the background to show the images clearly. The glass test tubes do not appear in these images although they absorb X-rays more strongly than the analyte elements, as shown in Figure 6.13 and Plate 6.2. Streaked artefacts in the computer axial tomography scan for the low density Cadmium and the high density Palladium analytes, on the left hand side of Figure 6.13 and plate 6.2 may have been due to non exact centering of the rotation axis with the X-ray beam.

Figure 6.17 shows the values of the two different concentrations in kg/m^3 of each atomic element. The third column shows the concentration of analyte element expected from the amount added to the epoxy glue. The second column is the maximum concentration measured from the images formed by the Algebraic Reconstruction Technique. This maximum concentration was read off the colour monitor concentration display by selecting the pixels of maximum concentration shown on the eight colour scale by means of the point cursor of the display. The cursor was moved over the image by the two (x,y) edit command keys of the BBC microcomputer until the value of the concentration in kg/m^3 was a maximum.

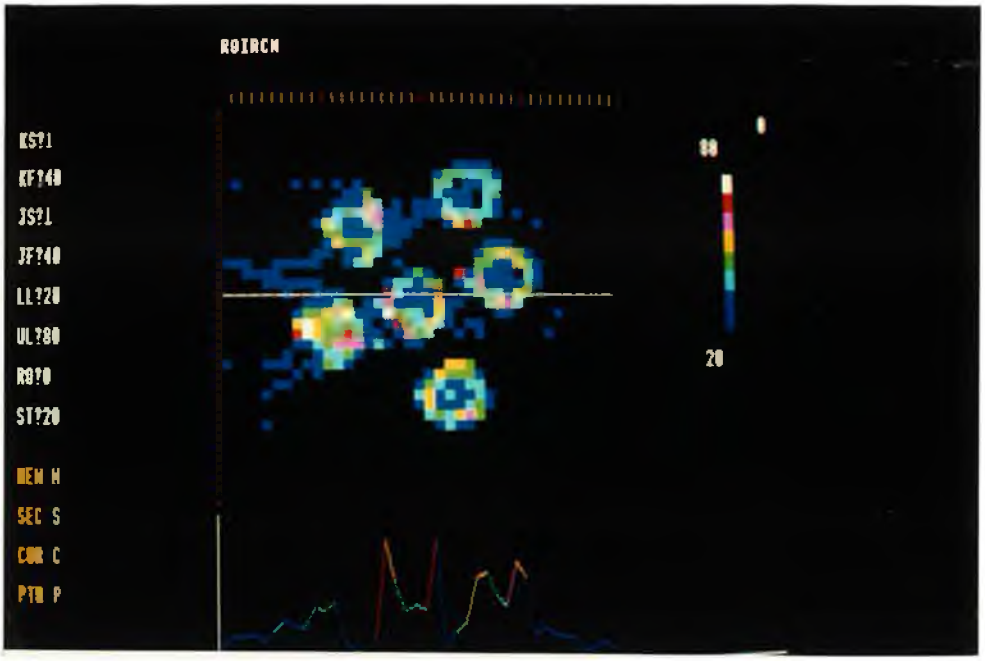

Computer axial tomography image.

PLATE 6.2

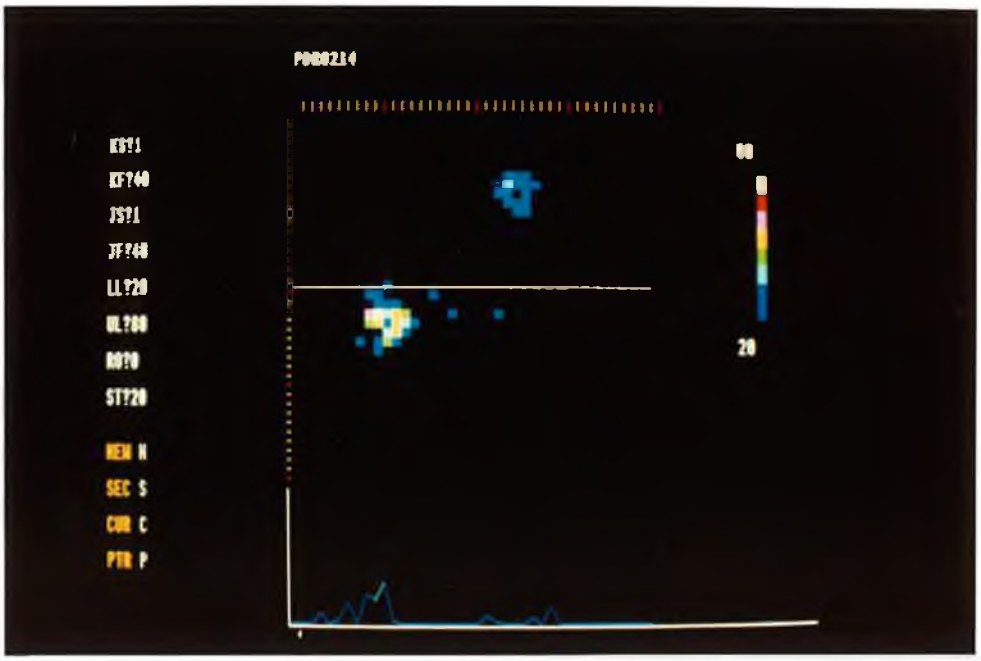

Differential K absorbtion edge tomogram of 46Palladium.

PLATE 6.3

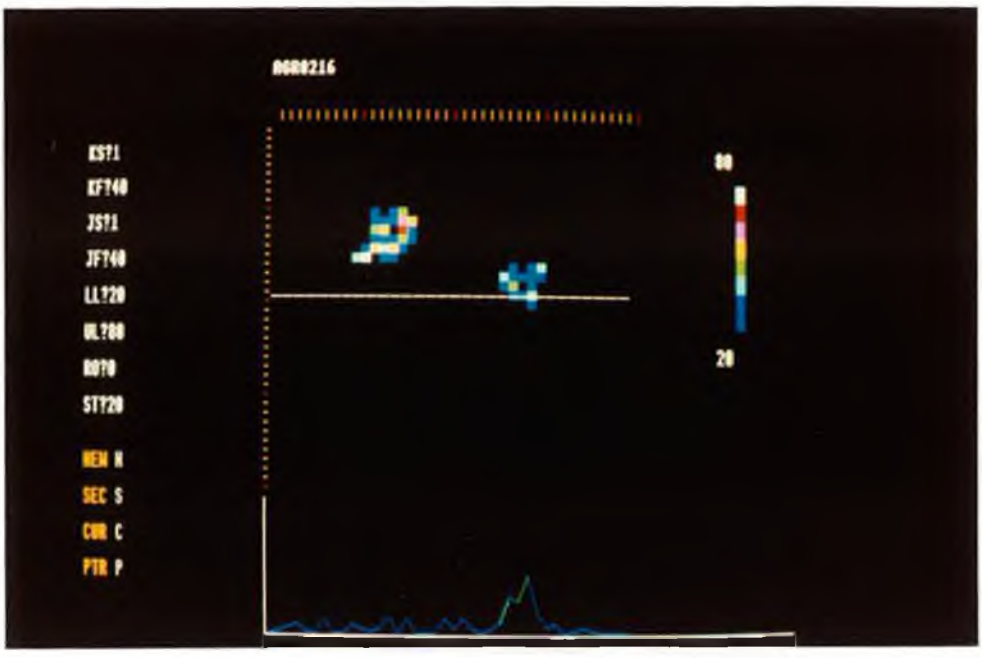

Differential K absorbtion edge tomogram of 47Silver.

PLATE 6.4

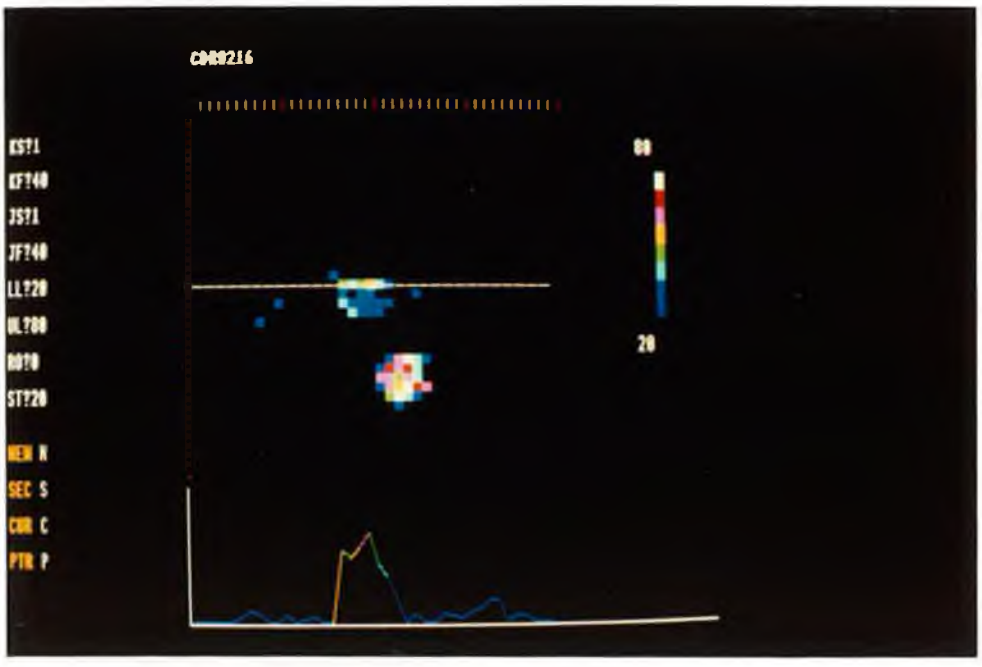

Differential K absorbtion edge tomogram of 48Cadmium.

PLATE 6.5

CHAPTER VII

CONCLUSION

The X-ray absorbtion edge energies uniquely identify each atomic element in the Periodic Table of the Elements because a definite quantity of energy unique to each element is required to remove an electron from an inner electron shell of the atom. Thus the mass attenuation coefficient of an element abruptly increases at each absorbtion edge energy.

The flux N of photons transmitted through an object irradiated with a monochromatic collimated beam of N_o X-ray photons is $N = N_o e^{\mu_1 x}$, where μ_1 is the linear attenuation coefficient of the object and x is its thickness. If p is the density of the object then the equivalent thicknes is $t = px$ and $N = N_o e^{-\mu t}$, where μ is the mass attenuation coefficient of the object. At low X-ray energies and for heavy atomic elements photoelectric absorbtion is dominant, and at higher X-ray energies and for light elements Compton scattering is dominant. Thus the attenuation of a monochromatic collimated beam of X-rays of less than 1.02MeV is due almost entirely to photoelectric absorbtion and Thomson and Compton scattering, and the attenuation coefficient is larger than the absorbtion coefficient.

There is an abrupt decrease in the transmitted flux N of X-rays at an absorbtion edge of an atomic element. The projection data from which an image of an object from X-ray linear attenuation coefficients can be reconstructed is given by $\ln(N_o/N) = \mu t$ is obtained by counting the incident and transmitted flux N_o, N, where μ is the mass attenuation coefficient of the object, equivalent thickness t in the X-ray beam path. The projection data for a specific element due to photoelectric absorbtion at an absorbtion edge is given by $\ln(N_o/N)$ extrapolated to the K absorbtion edge of an analyte element.

The object is made up of one or more analyte elements and a matrix, which is the material of the object and all analyte elements except the one chosen for analysis, so that $\ln(N_o/N) = \mu_a t_a + \mu_m t_m$, where a, m refer to analyte element and matrix. The matrix attenuates X-rays to an extent which depends on the atomic number of its elements and on their density.

This work used two methods for correcting for the effects of the matrix. One method [14] is to scan the matrix of the object alone and then do an identical scan containing the analyte elements. This method works only if the analyte elements can be added to the object after an initial scan; the incident X-ray photon counts N_o for the scan of the object containing the analyte elements being taken from transmission through the matrix. The second method of correcting for matrix effects [15] also allows for absorbtion edge fine structure.

The absorbtion edges of the atomic elements have fine structure due to small energy differences in energy state of the atom, and due to atomic isotopes. In order to correct for these two effects the differential measurement at the absorbtion edge of an analyte element

is made by measuring the transmitted flux N in four narrow X-ray pass bands, two on each side of the absorbtion edge, and from the centre of each pass band, extrapolating the value of $\ln(N_o/N)$ to each side of the absorbtion edge to give a value for the equivalent thickness t_a of the analyte element. The calculation is done using the equation:

$$t_a = (Y_h - Y_l)/(\mu_{ah} - \mu_{al}) \qquad (7.1)$$

where Y is the extrapolated value of $\ln(N_o/N)$, μ_a is the mass absorbtion coefficient of the analyte element, and h,l refer to the high and low energy sides of the absorbtion edge.

An image of the internal structure of an object through a chosen disc of the same width as the collimated X-ray beam can be made by computer axial tomography using an X-ray beam of fixed energy distribution. The reconstructed image shows an image density distribution map of linear attenuation coefficient in the scanned disc. The image reconstruction depends on the general attenuation of the X-ray beam by the object which is due to its density and the average atomic number of its elements, the spatial resolution of the scanning, the sensitivity of the X-ray photon detector and counting instruments, and the computer reconstruction algorithm, Filtered Backprojection or the Algebraic Reconstruction Technique.

Differential absorbtion edge tomography scans the object in a simliar manner to computer axial tomography, but with an energy dispersive detector and X-ray photon counting instruments which have an energy resolution of about 300eV or less, which is a fractional energy spread of about 10^{-2}. The image reconstruction can be done by the same algorithms as for computer axial tomography, but at present only the

Algebraic Reconstruction Technique can give a quantitative measurement of the analyte element concentration. L. Grodzins [9] predicted that this method could be used to image analyte element concentrations of $10^{-3}kg/m^3$ in small samples.

A.C. Thompson et al [10] used a synchrotron to make a tomographic image of a 53Iodine analyte in an excised pig heart. The intensity of the white X-ray beam was sufficiently great that a reflection double crystal monochromator could be used to select a narrow X-ray pass band with a fractional energy spread of about 5×10^{-4}. The 53Iodine was imaged with incident X-ray photon energies 25eV above and below the 53Iodine K absorbtion edge at 33.17keV, using a multielement Si(Li) detector cooled to -30°C to detect the transmitted X-rays.

Element specific X-ray tomography is possible provided the fractional energy spread of detected X-ray photons is less than about 10^{-2} in the range of absorbtion edge energies of the analyte elements being imaged. The required energy resolution herein was achieved using an EG & G Ortec Si(Li) detector and a pair of EG & G Ortec single channel analysers for imaging a single analyte element, and an EG & G Ortec 7100 multichannel analyser for imaging three consecutive elements of the Periodic Table of the Elements.

Using a synchrotron it is possible to do differential absorbtion edge tomography using a non-energy-dispersive detector provided a single narrow pass band of X-rays having a fractional energy spread of less than 10^{-2} can be scanned across at least part of the X-ray spectrum corresponding to the absorbtion edge energies of the analyte elements, and measuring the change in transmitted X-ray flux as an absorbtion edge is crossed.

This work started with a simple manually operated scanning machine which showed that differential K absorbtion edge tomography is able to locate an analyte element within a matrix, a 2mm diameter 55Caesium hydroxide sample in a 20mm diameter cork with reference to an arbitrary radius, and draw on paper an 'image' or concentration shape of the analyte element from the measured value of the equivalent thickness of the analyte element. The differential absorbtion of the K_α and K_β 56Barium X-rays emitted by an Amersham International 241 Americium variable energy X-ray source located on either side of the K absorbtion edge of 55Caesium identified the analyte element, and the amount of absorbtion measured its equivalent thickness to be 0.30 ± 0.02 kg/m^2. The 2mm diameter 55Caesium sample was located 5mm from the centre of the cork 90° from the reference radius by means of the locus of maximum equivalent thickness of analyte element on a graph of angle of rotation against horizontal linear position.

This machine was developed to a semiautomatic machine on which the object to be scanned was mounted on a (x,z,ϕ) scanning coordinate table controlled in the x-direction by a BBC microcomputer via a controller interface. The 20 9° angular steps were adjusted manually. The X-ray photon count data was collected and stored at each scanning step by the BBC microcomputer. A BASIC programme run on a BBC microcomputer drew graphs shown in Figure 5.8 of the equivalent thickness profile of the 55Caesium, a 6mm x 1mm flat and a 2mm diameter round sample within a 30mm diameter cork matrix. The 55Caesium analyte was located and its equivalent thickness measured by the K_α and K_β 56Barium X-rays from the Amersham International variable energy X-ray source. The maximum equivalent thickness was about 8kg/m^2.

The semiautomatic scanning machine was fully automated so that it could image 46Palladium and 55Caesium analytes made into 5mm diameter epoxy glue rods by computer axial tomography and differential absorbtion edge tomography in a 20 x 20 image reconstruction grid [14]. The (x,z,ϕ) scanning coordinate table could be moved in the 3 directions using the two controllers of the interface by the BBC microcomputer and the images of the analyte elements are shown in Figures 5.12 and 5.13. The maximum concentrations are shown in Table 5.1

A Philips PW1270 X-ray spectrometer was converted to a X-ray computer axial tomography machine and a Lead analysing chamber was constructed for scanning objects on a (x,z,ϕ) scanning coordinate table. The spectrometer had been overhauled and tested by Philips previously so that current and voltage stability tests were not made. The X-ray machine was used as a X-ray source in place of the Amersham International variable energy X-ray source. The X-ray attenuation and band pass width for 40keV X-rays of a 50Tin transmission filter were calculated with a BASIC program run on a BBC microcomputer. A selected filter was used to attenuate and narrow the X-ray pass band beam for scanning the elements 46Palladium, 47Silver, and 48Cadmium using the EG & G Ortec Si(Li) detector and 7100 multichannel analyser, as shown in Figure 6.6.

BASIC computer programs, listed in Annexe D, were written and run on the BBC microcomputer for automatically scanning the object. The program MDPOINT was written in order to centre the X-ray beam as accurately as possible with the centre of the linear scan with the ϕ-axis at the start of scanning. This was required so as to make a unique reference point for the image reconstruction so that there was

a one to one correspondence between the image and the disc in the object scanned. Streaked artefacts around the image appear when the centering was not exact, as shown in Plate 6.2. The image reconstruction was calculated by a VAX 11/785 computer by two alternative methods.

Excellent qualitative images of the distribution of linear attenuation coefficients within an object displayed on a colour monitor or printed on paper were obtained by Backprojection incorporating a Ramachandran filter, as shown in Plate 6.2. Quantitative images of analyte elements within an object were obtained by the Algebraic Reconstruction Technique giving the concentration at a point in the analyte element in kg/m^3 down to a few kg/m^3. The cork matrix is composed of light elements, mostly 1Hydrogen, 6Carbon and 8Oxygen, a water like matrix, does not absorb X-rays much and is not seen in Plate 6.2. The heavier analyte elements, 46Palladium, 47Silver and 48Cadmium more strongly absorb X-rays, depending on the concentration. There is still stronger absorbtion of X-rays by the relatively dense glass of the 5mm diameter test tubes, composed mostly of 8Oxygen, 11Sodium, 13Aluminium, and 14Silicon, as shown in Plate 6.2. The computer axial tomography scan image shows the absorbtion of X-rays in an object in which the heavier elements are surrounded by lighter elements. A computer axial tomograhy scan of a heavy element matrix containing light elements may not show a clear image of the light elements due to strong absorbtion of X-rays by the heavy elements, but selective absorbtion of X-rays by the K absorbtion edge should make it possible to image a light analyte element within a heavy element matrix, or a low concentration of analyte element within a relatively dense absorber, the glass test tubes, which was done herein, as shown in Plates 6.3, 6.4 and 6.5.

The practical limits for measurement with the method hereinbefore described is of the order of a few kg/m^3 for an analyte element located in a relatively small region of the matrix of the object. For a 5mm diameter analyte in a 30mm diameter cork matrix the analyte is dispersed in a scanned disc of only about 3% by area of the matrix. The sensitivity [16] increases to about $2 \times 10^{-4} kg/m^3$ when the analyte element is evenly dispersed in the matrix. The reason for this is that over the path length of X-ray beam there is more analyte and thus more absorbtion due to analyte element because the fraction of analyte becomes bigger.

The total number of photons needed to image the three analyte elements in the cork matrix was about 3×10^8, and this is about 100 times less than that required for a conventional computer axial tomography scan of a water like object [15].

An X-ray tube or a radioactive line source of X-rays can be used to scan an object by differential absorbtion edge tomography and computer axial tomography, and both Filtered Backprojection and the Algebraic Reconstruction Technique can be used for reconstruction of the image of the object for both kinds of tomography [14, 15].

Theory predicted, and experiment confirmed, that it was not necessary to correct for dead-times, the time for which a pulse counting instrument is inoperative, for differential absorbtion edge tomography, because at an absorbtion edge the extrapolated value of the equivalent thickness of an analyte element stays constant because $\ln(N_o/N)$ at the high and low energy sides of the absorbtion edge changes equally. Dead-times of up to 15% were allowed, but longer dead-times would introduce errors into the counting statistics. This

intrinsic correction for dead-times applies only to differential absorbtion edge tomography by extrapolation, not to computer axial tomography. In this work, the multichannel analyser was the slowest counting instrument so that the X-ray beam was attenuated sufficiently by the Tin transmission filter to limit the incident X-ray beam flux to about 10^4 s^{-1}.

This experiment is not affected by beam hardening, the relatively greater transmission, and thus count rate, of higher energy photons than lower energy photons due to their greater penetrating power through an object, because the X-ray beam has a narrow energy spread and an energy dispersive detector is used.

CHAPTER VIII

POSSIBLE FUTURE DEVELOPMENT

The 60kV X-ray scanning machine used in this work may be developed further for scanning a range of atomic elements from 11Sodium to 68Erbium using their K absorbtion edges and from 42Molybdenum to 92Uranium using their LIII absorbtion edges for differential absorbtion edge tomography. The internal structure of objects may also be imaged by computer axial tomography.

To image objects of maximum size 230mm diameter and 230mm wide with this machine, a new analysing chamber is required in which the X-ray beam is centrally located. For easier access to the chamber a new (x,z,ϕ) scanning coordinate table is needed, one which moves the object in the linear scans parallel to the door of the analysing chamber. Alternatively, a purpose built machine may be made similar in design to the Hewlett Packard Faxitron X-ray photography machine, in which the scanning coordinate table and object to be scanned are located in an upper cabinet beneath a centrally mounted X-ray tube, and the Si(Li) detector is located vertically below in a lower cabinet. The Faxitron can generate X-rays of up to 120keV energy at a maximum of 3mA X-ray tube current, and this would be suitable for imaging atomic elements from 11Sodium to 92Uranium using their K absorbtion edges only.

The X-ray pass band energy overlapping the absorbtion edges of one or more selected analyte elements may be chosen by specially designed transmission filters whose X-ray characteristics are calculated by computer and tested experimentally.

The scanning procedure, from placing the object to be scanned inside the machine to display of reconstructed images of all the elements it has found in the object, may be automated, and a computer print of the analytes and their concentrations in the object may be produced.

The main disadvantage of the present scanning machine is that it takes a long time to do a complete scan of an object, in the main experiment herein about 40 hours.

The X-ray photon flux is limited by the narrowness of the collimated beam, and there is only one energy dispersive detector useable because the energy resolution must be better than about 300eV for atomic elements around number 40. The energy resolution needs to be better than about 200eV for light elements and better than about 1keV for heavy elements. Thus the scanning is done in linear steps at each angular step between 0° and 180°, so that the time taken is proportional to the square of the number of linear scan steps. The scanning time may be shortened to 1 or 2 seconds for each scanned plane in water like objects using a ring of 360 detectors located around the object and a high intensity X-ray tube movable around the ring for computer axial tomography scanning, but these detectors do not need to be energy dispersive. It may be possible to shorten the scanning time for differential absorbtion edge tomography, say by 10 times, by using a narrow fan X-ray beam and 10 energy dispersive

detectors mounted in a line, and move the object in 10 linear steps at a time corresponding to the 10 detectors. Energy dispersive detectors are very expensive, and it may not be possible to make 10 identical detectors. Artefacts may be introduced into the image because the X-ray beam is divergent. Also, each detector requires its own X-ray photon counting instrument set.

A STEEL ANALYSING CHAMBER.

The Lead analysing chamber containing the steel box had sufficient space to image objects of maximum size 120mm diameter and 30mm wide, but the largest object scanned was the 30mm diameter cork 25mm wide in a 40 x 40mm square grid in 40 linear steps corresponding to the 40 x 40 grid of the image reconstruction.

Figures 8.1 and 8.2 are drawings of an analysing chamber designed to scan objects of up to 230mm diameter and 230mm wide in a 240 x 240mm scanning grid. The linear step size in mm for the largest object which can be scanned is then 240/N, where N is the number of steps in the scanning and in the reconstruction grid.

The analysing chamber, external dimensions 50cm wide x 35cm high x 55cm deep, is made of mild steel 4mm thick in which the the joins are closely fitting as shown and butt welded together on the inside and outside to ensure there is no leakage of X-rays. The barrel of the X-ray tube is supported in the Aluminium clamp of the X-ray machine attached to the raised web of the left hand side of the analysing chamber. The anode of the X-ray tube is enclosed in a cubical brass box of side 15cm and 10mm thick, joins brazed together, and the box is

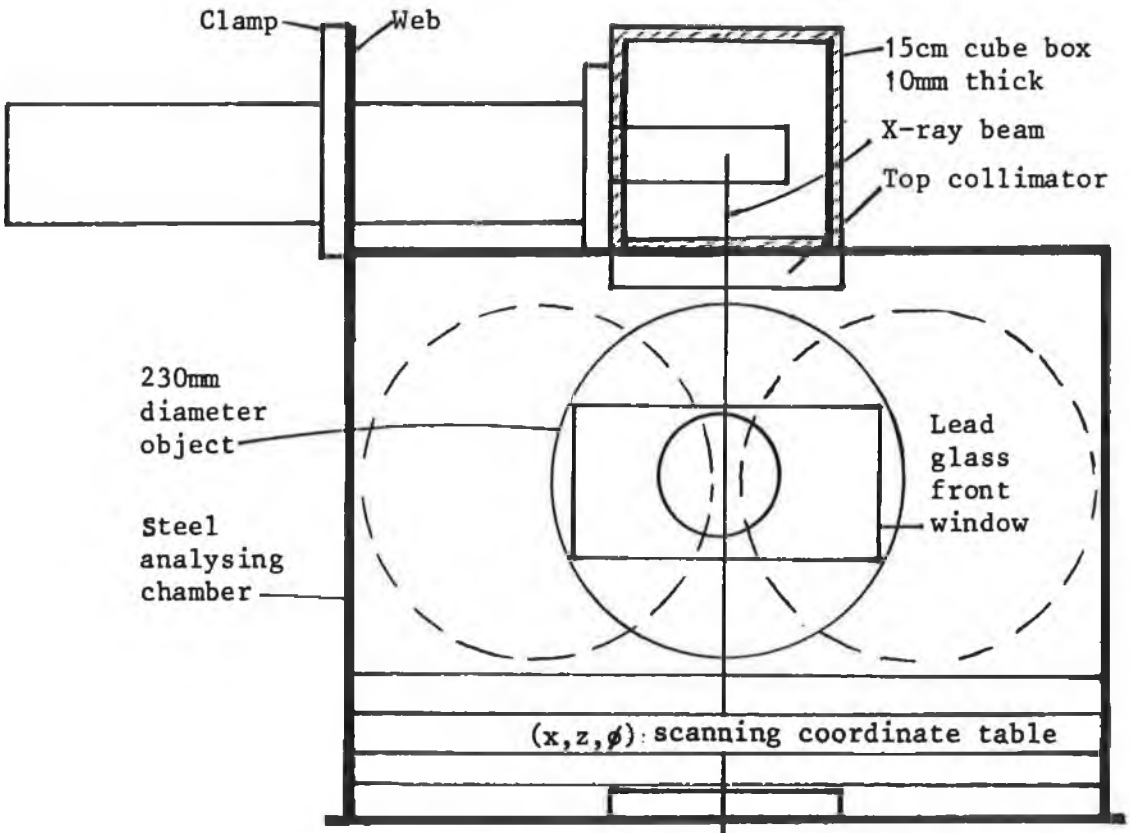

Front view of a steel analysing chamber.

FIGURE 8.1

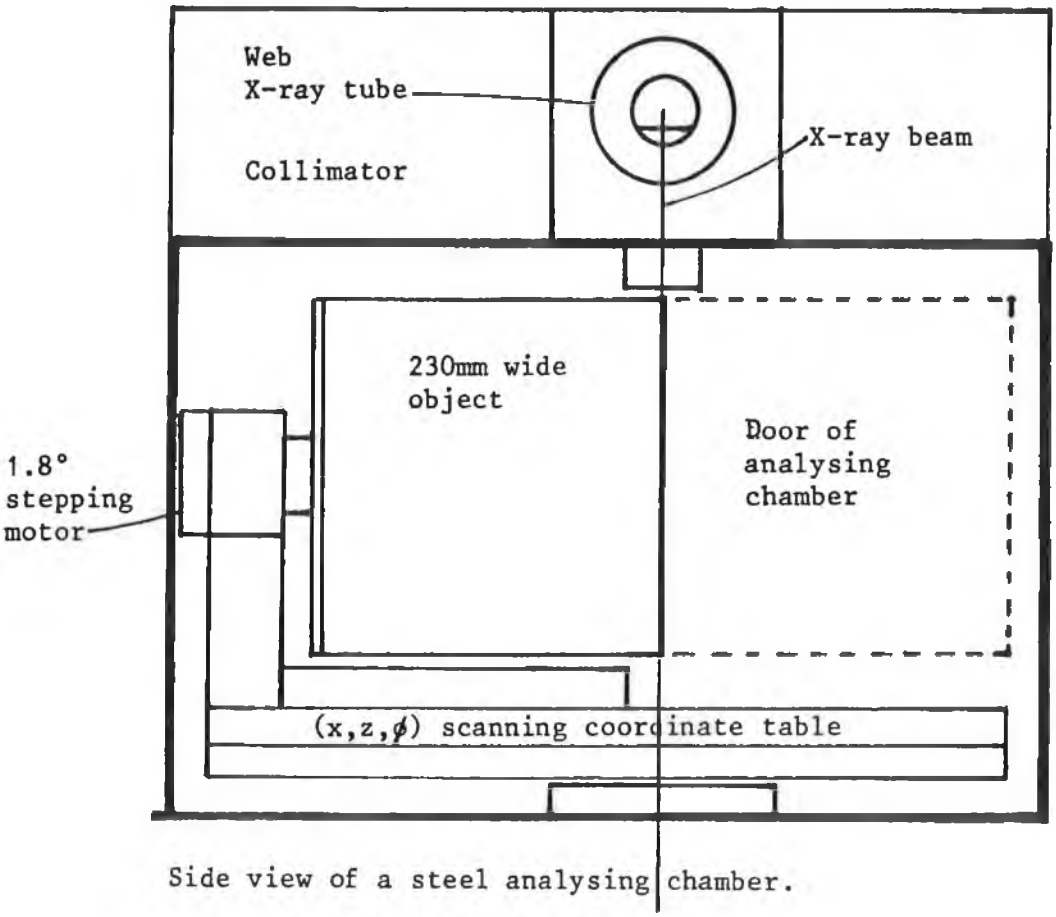

Side view of a steel analysing chamber.

FIGURE 8.2

covered with 3mm of lead sheet having overlapping seams soldered together. The brass box is attached to the top of the steel box with 4 studs, threads tapped into the brass. Alternatively, a similar box may be made of bright mild steel, joins welded together, welded to the top of the steel box, and covered on the five exposed sides with 3mm Lead sheet. The brass box absorbs most of the radiation from the X-ray tube.

The steel analysing chamber is hermetically closed on five sides. The front, which is fully open, is closed by a 4mm thick steel door attached by hinges to the floor of the analysing chamber so as to open downwards. The door closes flat against the four exposed edges of the analysing chamber, and is sealed by a closely fitting 10mm square steel strip attached around the edges of the back of the door by studs. The door has a Lead glass window for viewing the inside of the analysing chamber, which is illuminated by four miniature electric lamps mounted at the front corners of the inside thereof.

The X-ray beam is defined by two collimators located vertically below the anode of the X-ray tube so that the centres of the anode, detector and collimators are in straight line. The top collimator covers a 6mm diameter aperture in the top of the steel analysing chamber and bottom of the brass box, and the lower collimator covers a 15mm diameter aperture in the floor of the analysing chamber. The top collimator consists of a 10mm thick brass plate 20mm wide and 140mm long having circular collimator apertures spaced apart 10mm in a straight line of diameters 6, 5, 4, 3, 2, 1.5, 1, 0.7, 0.4 and 0.2mm, and movable in a linear enclosure in the x-direction by a lead screw so as to locate a chosen collimator aperture in the X-ray beam. The enclosure is

attached to the top of the analysing chamber with studs tapped into the brass. A compression spring maintains the plate in contact with the end of the lead screw which is driven by a 1.8° stepping motor bolted to the outside of the analysing chamber. The lower collimator is attached to the floor of the analysing chamber by means of countersunk studs threaded into the brass mounting of the collimator. This collimator is similar to the top one but is wider and in addition has a 15mm z-direction movement set by adjusting screws and screw clamp in order that it may be aligned to define a vertical line between the anode centre of the X-ray tube and the centre of the detector. Alternatively the z-direction movement may be controlled by a lead screw driven by a 1.8° stepping motor. The lower collimator may have square apertures, or there may be a row of square apertures parallel to the row of circular ones which may be moved by the z-direction movement into the X-ray beam. The size of aperture chosen is the same as that of the linear step size.

A (x,z,ϕ) precision scanning coordinate table extends over the floor area of the analysing chamber, and is mounted on rails so that it may be drawn half way out through the open door of the analysing chamber. The x-direction linear stepping movement at right angles to the ϕ-coordinate is crosswise of the door of the analysing chamber, and the z-direction is parallel to the ϕ-axis. The z-coordinate may be chosen to locate a particular plane in the object being scanned, or several axial planes may be chosen in steps of the same size as those of the x-coordinate to scan the object in axial planes to reconstruct a three dimensional image of the object. The (x,z) coordinates are chosen by lead screws operated by 1.8° stepping motors, and the ϕ-coordinate is chosen by a 1.8° stepping motor: the object is mounted

in a chuck on the axle of the motor. The (x,z) coordinates can move 240mm, and the ϕ-coordinate can rotate through any number of half or complete rotations.

X-RAY BEAM TRANSMISSION FILTERS.

Figure 8.3 shows a stepped wedge filter 8mm wide and 100mm long in twelve steps of thickness 0.1, 0.2, 0.3, 0.5, 0.75, 1, 1.25, 1.5, 2, 2.5, 3 and 4mm made of a chosen atomic element such as Tin. Figure 8.4 shows twelve stepped wedge filters mounted side by side made of single elements such as 13Aluminium, 26Iron, 29Copper, 42Molybdenum, 50Tin, 82Lead, or two elements such as Aluminium and Copper, Aluminium and Tin, Aluminium and Lead, Copper and Lead, or alloys such as brass or bronze. The thickness of the steps of each filter is empirically chosen and the filtered X-ray spectra calculated by means of the SPECTRA BASIC computer program in Annexe D. This may be compared with the experimentally measured filtered spectrum produced by the X-ray tube and displayed on the EG & G Ortec 7100 multichannel analyser. Thus, a filter may be chosen from 144 combinations of filter material and thickness to select a X-ray band pass spectrum anywhere in the energy range of 1keV to 60keV of a chosen energy span and X-ray photon attenuation to suit a particular scan, size of object, width of collimated X-ray beam, and X-ray tube voltage and current. The filters are mounted in a carriage, bolted to the top of the analysing cabinet under the top collimator, which may be moved in the (x,z) directions by means of lead screws and 1.8° stepping motors bolted to the outside of the analysing cabinet. The filters made of two elements or alloys can be arranged to form a pass two band filter, one band at low energy to image a water like matrix and the other at high

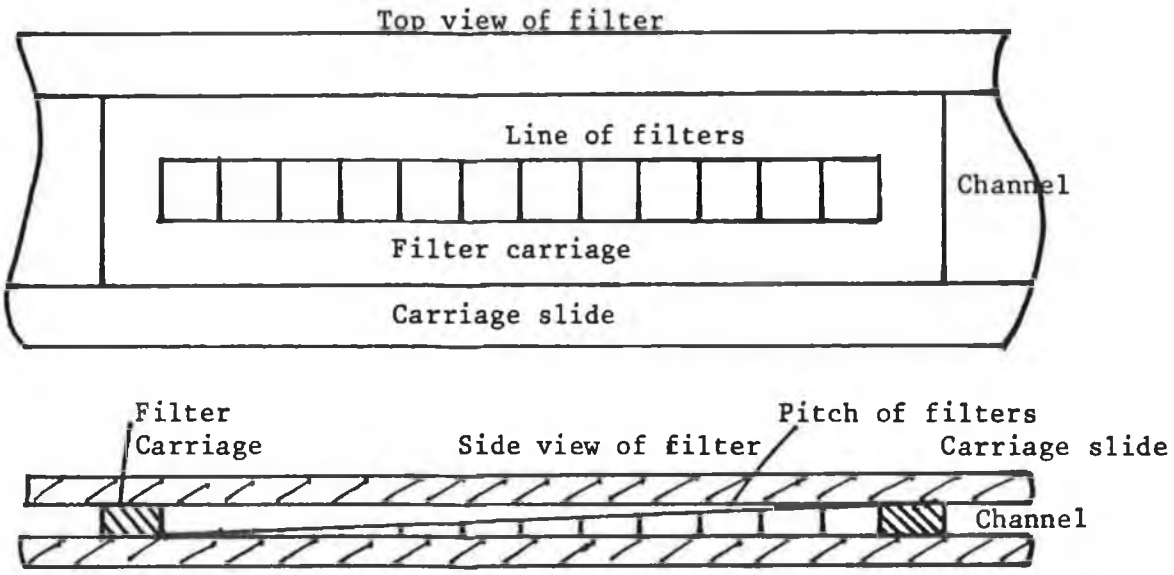

A stepped wedge X-ray filter.

FIGURE 8.3

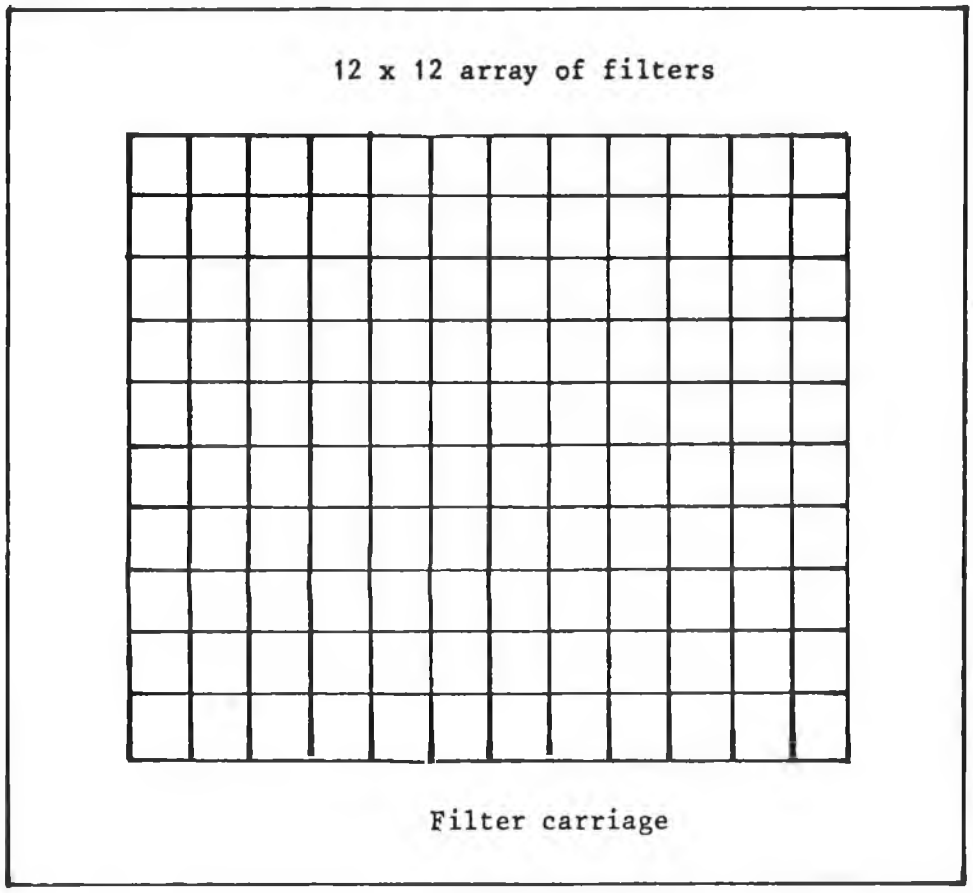

12 x 12 stepped wedge X-ray filter.

FIGURE 8.4

X-ray photon energy to image analyte elements. Figure 8.5 shows normalised spectra for 8 filters calculated by the SPECTRA computer program: 13Aluminium, 29Copper, 42Molybdenum, and 50Tin.

SCANNING AND IMAGE RECONSTRUCTION.

The scanning procedure herein was to count transmitted X-ray photons for a given time at each of 20 or 40 linear steps of 2mm or 1mm step size and after each linear scan rotate the object by 9°, 7°, or 4.5° for 20, 24, or 40 angular steps between 0° and 180°. In the experiments the linear scans were all done in the same direction: the linear scans started from the same starting point. In scanning three analyte elements, the linear scans were made from both ends of the 40 step scan, and the X-ray photon count data reversed for every second scan so that the data sequence was from the same starting position. In this way time taken to move the x-coordinate table to one starting position was saved. Another scanning method is to make all the angular steps of 4.5° from 0° to 180° at each linear scan step: rotation-linear scanning instead of linear-rotation scanning. In this case either the object needs to be rotated from 180° to 0° after each linear step, or to save time, the X-ray photon count data is reversed for angles between 180° and 0° to keep the data sequence in the correct order, and the object is rotated in 4.5° angular steps only. This method should give an identical image to that herein because only the scanning procedure is changed, not the X-ray photon count data, and a computer axial tomography scan using Filtered Backprojection produced an image of the three analyte elements in the cork matrix, which confirmed this is so.

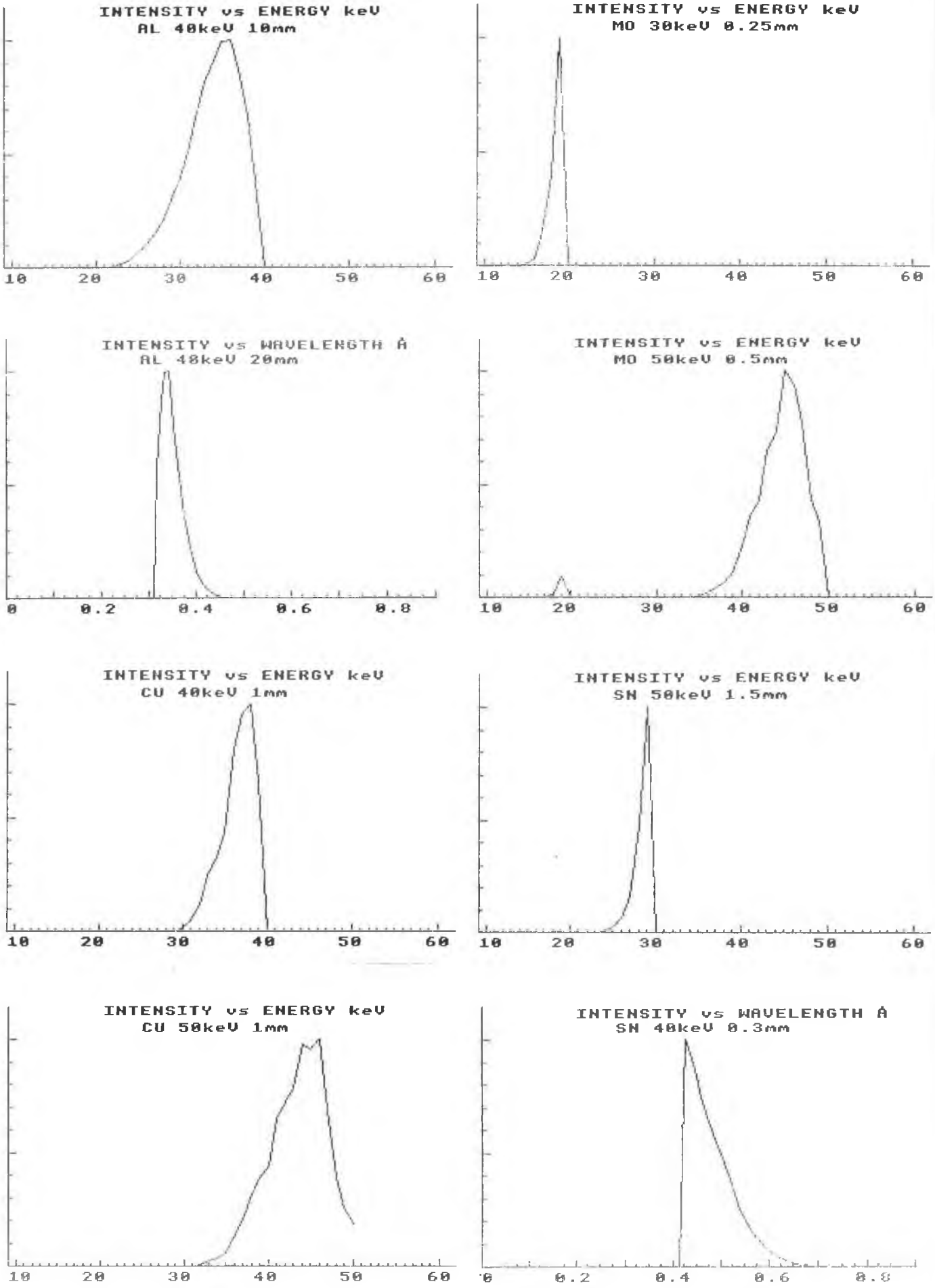

NORMALISED X-RAY SPECTRA CALCULATED BY SPECTRA.

FIGURE 8.5

The Algebraic Reconstruction Technique builds up an image from the measured values of the equivalent thickness of the analyte element and compares the value calculated for the image at each iteration with the experimental value, so that it is a quantitative method. The iterations are stopped when the difference is less than a chosen value, say 1%. Filtered Backprojection is a qualitative method of image reconstruction because the image of the object is built up in layers of backprojected image data on to the image plane, but since the image formed is the same as that for the Algebraic Reconstruction Technique, it may be possible to turn this into a quantitative method by calibration either by use of a multiplying scaling factor in the Backprojection computer program, or by comparing the analyte image with the image of a reference concentration analyte element during scanning. Image reconstruction by Backprojection is about 60 times faster than the Algebraic Reconstruction Technique in the computer.

It was necessary to centre the linear scan and thus the rotation axis of the object with the X-ray beam as precisely as possible, and the MDPOINT BASIC computer program was written to do this in order to prevent artefacts being incorporated in the image of the object. One kind is the streaked blurring of one side of the image shown in Plate 6.2 when the rotation ϕ-axis is not centred with the X-ray beam, even by half of one linear step. This may be compensated for by shifting the X-ray photon count data by a fraction of one or more linear steps by means of a calculation done on each count in the Backprojection BASIC computer program, until the sharpest image is obtained. This was confirmed empirically with the computer program, but should not be necessary with a scanning machine which has a precision scanning coordinate table correctly aligned with the X-ray beam.

X-RAY K, L AND M ABSORBTION EDGES.

An atomic element has a X-ray absorbtion edge whenever an electron can be removed from an electron shell inside another electron shell.

Thus all elements from 3Lithium have K absorbtion edges of increasing photon energy and decreasing wavelength. Similarly, elements from 12Magnesium have L absorbtion edges, and from 17Chlorine they have M absorbtion edges. Herein atomic elements are analysed by their X-ray K absorbtion edges, but it may not be possible to image elements lighter than 16Sulphur, K absorbtion edge energy 2470eV, wavelength 5.02A due to strong absorbtion of low energy X-rays by a matrix which cannot be isolated from the analyte element, and amplified detector electrical noise at the low energy end of the X-ray spectrum. 6Carbon and 14Silicon have K absorbtion edge energies of 280, 1840eV, and wavelength 43.89, 6.75A respectively, which possibly would be useful to be able to image for differential K absorbtion edge microtomography of plants or Silicon chip integrated circuits.

In a similar way the scanning machine should be able to image atomic elements using the strong LIII absorbtion edges from 42Molybdenum, energy 2520eV and wavelength 0.491nm to 92Uranium, energy 17.17keV and wavelengt

0.0722nm, or the MV absorbtion edges from 80Mercury, energy 2290eV wavelength 0.541nm, to 92Uranium, energy 3530eV, wavelength 0.351nm.

The heaviest elements which can be imaged with 60keV X-rays, which is the upper energy of the X-ray machine, using their K absorbtion edges is 68Erbium, so that the K absorbtion edge range of the scanning

machine herein is 16Sulphur to 68Erbium, 53 atomic elements, and if the LIII absorbtion edge is used thereon, the range can be extended to 92Uranium.

To image all of the atomic elements by K absorbtion edge spectroscopy from 11Sodium to 92Uranium requires an X-ray machine which can operate at up to 120kV to overlap the K absorbtion edge of Uranium of energy 114.78keV, wavelength 0.0108nm and a very low electrical noise detector and amplifier to be able to detect the low energy photons around the K absorbtion edge of Sodium of energy 1080keV, wavelength 1.18nm. The EG & G Ortec Lithium drifted Silicon detector has a photon detection range of 1keV to 60keV, so that with a 60kV X-ray machine and the best experimental conditions it should be possible to image all of the atomic elements from 11Sodium to 92Uranium using the K and LIII absorbtion edges.

ADVANCED SCANNING MACHINE.

Figure 8.6 shows a block diagram of a scanning machine entirely operated by a computer program. The object to be scanned is clamped in a chuck on the ϕ axis of a (x,z,ϕ) scanning coordinate table. The analyte elements to be imaged are selected by entering the highest and lowest atomic number Z into the computer program which selects the required X-ray band pass filter from the array of filters shown in Figure 8.4 by matching it with the calculated X-ray pass band. The filter is automatically moved into position in the X-ray beam by means of its (x,z) stepping motors. The X-ray tube operating voltage is selected automatically at the voltage setting above the K or L absorbtion edge of the filter element selected, or if a two element or

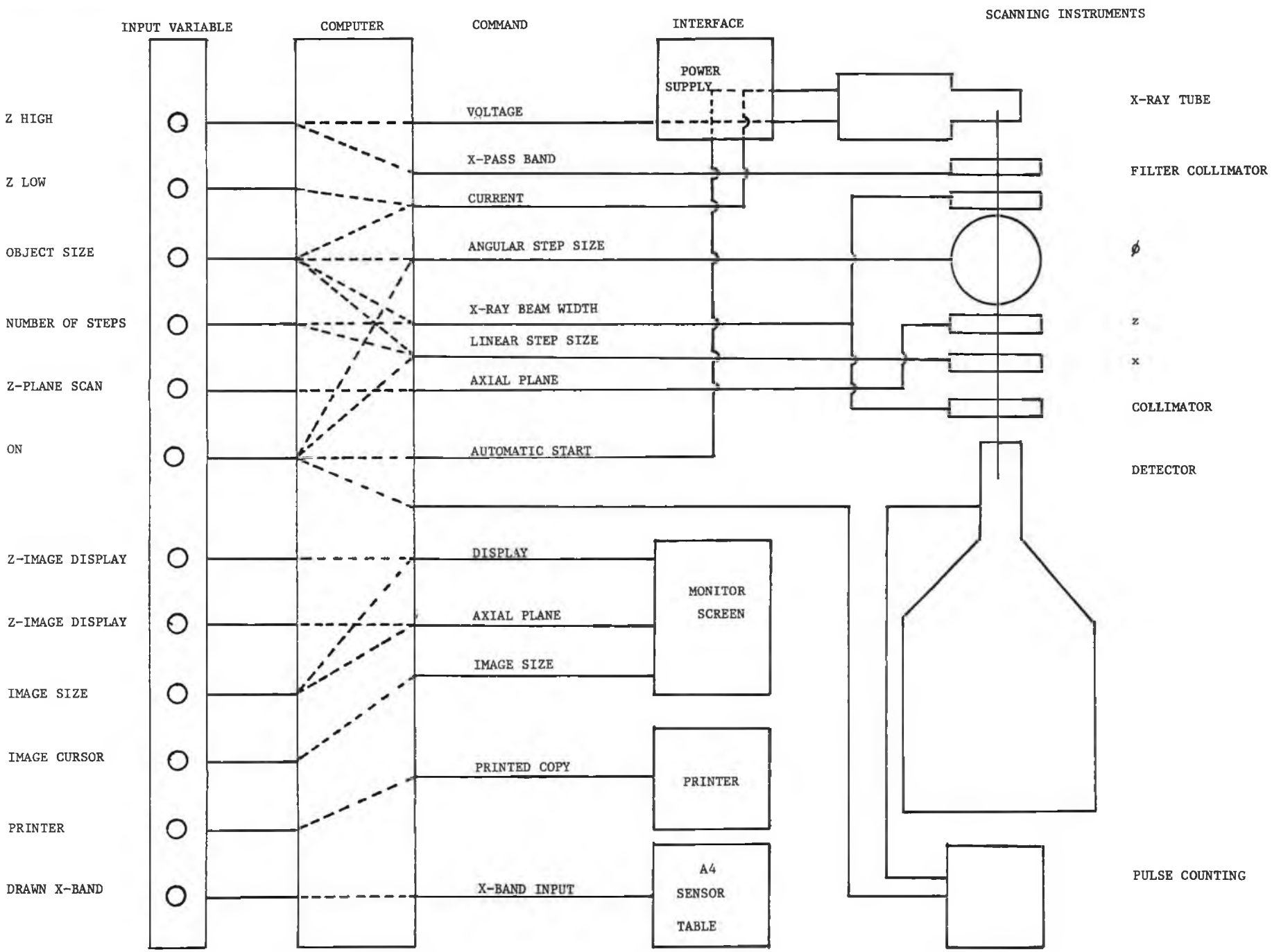

A BLOCK DIAGRAM OF AN ADVANCED SCANNING MACHINE

FIGURE 8.6

alloy filter is chosen, above the absorbtion edge of the heaviest element of the filter. Thus the incident beam intensity I_o profile is fixed. The size of the object to be scanned and the number of scanning steps is entered into the program. This selects the spatial resolution of the scan, the length of the linear scan, the linear step size, the angular step size and causes the stepping motors to move the two X-ray beam collimators into position in the X-ray beam to select the diameter of the beam. The machine is switched on, and one or a few preliminary linear scans select the optimum X-ray tube current setting so that at maximum photon absorbtion by the object there is a sufficient count rate to give good results. The machine may automatically select a different filter having less attenuation but similar energy band pass if necessary. The complete scan is then started automatically, the object being rotated in the selected equal angular steps through the required number of complete rotations equal to half the number of linear steps, and at alternate half rotations, the X-ray photon count data is reversed to keep the correct order in the scanning sequence. The X-ray photon count data is stored on disc, and when scanning is finished, the data is sent to another computer to reconstruct the image and display it on a colour monitor. If more than one plane in the object is to be scanned, the number and their axial position is entered into the computer before starting. If a three dimensional image of the object is to be made, then many consecutive image planes are scanned, and the X-ray photon count data stored on disc.

The X-ray energy pass band selected by the computer may be displayed on the colour monitor, together with the regions of interest on each side of the absorbtion edges of the analyte elements. Instead of the

computer selecting the pass band, it may be drawn on an A4 sheet of paper placed on an array of sensors which has the same number of pixels as the colour monitor. The drawn pass band stored in computer memory can be displayed on the monitor together with the pass band of the closest matching X-ray filter in the scanning machine, and then the (x,y) stepping motors select the required filter.

The image of an analyte element in an object found by differential absorbtion edge tomography may be displayed on a colour monitor by entering into the display computer program the atomic number of the element. The images of several analyte elements may be displayed in different colours, or the concentration of one analyte element displayed in different colours to show the distribution by concentration in the object. A computer axial tomography scan of the object may be displayed by entering 0 into the computer program. A region of interest such as the distribution of an analyte in an object may be magnified or diminished on the display.

The computer may print out a table of analyte elements found in the object together with their maximum measured concentrations.

The display monitor may have a mm and cm measurement grid and (x,z) line cursors overlaying the picture to measure the image size, and multiplied by a scaling factor determined by the computer program in order to measure the physical size of the object and analyte element distribution.

MEDICAL AND INDUSTRIAL USES OF DIFFERENTIAL ABSORBTION EDGE TOMOGRAPHY.

Differential absorbtion edge tomography is a method of non-invasive non-destructive testing. Any object which can fit into the scanning machine may be analysed. In general, the limitations on the size of object are determined by the absorbtion of X-rays by the object, the intensity of the X-ray beam, the time required for scanning, the spatial resolution, and the maximum safe limit for X-radiation exposure to the object during scanning. Thus the size of object is mainly limited by the atomic number of the elements of which it is composed, and its density. L. Godzins [9] gave theoretical limits for the quantitative distribution of analyte elements as a function of spatial resolution, object size and material, and X-ray photon flux. K.J. McCarthy [16] showed theoretically, confirmed by experiment, that the sensitivity of scanning an object with a given X-ray photon flux increases as the analyte element is dispersed throughout the matrix. For a 30mm diameter 48Cadmium sulphate in water object, the theoretical lower limit detectable with 10^7 photons is $10^{-5}kg/m^3$. and experimentally $2 \times 10^{-4}kg/m^3$. A greater number of photons would be required to image an analyte element at a lower concentration than this. The change in detectable concentration is approximately proportional to $\sqrt{N}$; if N is increased by 100 the limit of detectability can be lowered by 10 for an evenly dispersed analyte element.

This experiment was done using two regions of interest on each side of the absorbtion edge of 48Cadmium, and an image of the Cadmium analyte made by differential K absorbtion edge tomography. A computer axial tomography image was made using one of the regions of interest, and of

the water matrix alone, because the attenuation of the matrix has to be known as the analyte concentration is increased.

Medical applications of differential absorbtion edge tomography may be detection of 82Lead in bones, accumulation of analyte elements in particular regions such as 53Iodine in thyroid gland, distribution of elements such as 20Calcium or 38Strontium in bones. The K and LIII absorbtion edge energies for these elements are 82Lead, 88.01 and 13.04; 53Iodine, 33.17 and 4.35; 38Strontium, 16.11 and 1.94; and 20Calcium 4.03, keV.

Industrial and scientific applications of differential absorbtion edge tomography may be testing machine parts such as bearings and gears, analysis of pipes for corrosion and mineral depositions, analysis of rocks, fossils and meteorites.

DIFFERENTIAL ABSORBTION EDGE TOMOGRAPHY WITH A NON-ENERGY-DISPERSIVE DETECTOR.

A possible method in principle of differential absorbtion edge tomography using a non-energy-dispersive detector such as a scintillation detector or even a proportional counter may be investigated to find out if this method is feasible in practice. The Electromagnetic Spectrum is scanned from 115keV to 0.9keV in discrete narrow X-ray pass bands at each scanning step of an object, and the X-ray photons are counted for a chosen time in each pass band. The narrow X-ray pass bands are chosen from a continuum spectrum by carefully designed and matched transmission filters which can be moved sequentially into the X-ray beam.

A collimated beam of X-rays from an X-ray tube operating at 120kV and anode current chosen according to the attenuation of the object irradiates the object mounted on a (x,z,ϕ) scanning coordinate table. The transmitted beam is detected by the detector via a second collimator. The X-ray beam is intercepted by transmission filters set in a circle on a metal disc opaque to X-rays which is rotated continuously at a steady speed by an electric motor. The object is scanned in linear and angular steps as hereinbefore described on the (x,z,ϕ) scanning coordinate table, and the X-ray photons are detected and counted to provide an array of X-ray photon count data to make an image of the internal structure of the object in a reconstruction grid of pixels.

The X-ray photon counting instruments operate in synchronisation with the rotating metal disc. The output pulses from the scintillation detector are gated so that they are accepted by the multichannel analyser only for a short time whilst a particular filter is in line with the X-ray beam collimators. Thus for a short fixed time interval each filter allows a narrow pass band of X-rays to irradiate a scanned object held between the collimator on the (x,z,ϕ) scanning coordinate table.

A scanning machine which uses this principle may have 300 scintillation detectors located in a ring around the object. The filter elements are equally spaced apart in a metal band which is opaque to X-rays. The metal band is mounted on bearings and spins around the object inside the array of detectors so that consecutive detectors are exposed to a narrow pass band of X-rays in turn, as the X-ray tube irradiated the object with a wide fan beam of X-rays as it

rotates 360° around the ring of detectors. The metal band rotates once around the object for each scanning step, and the X-ray photon counting instruments operate in synchronisation with the rotating metal band.

ANNEXE A

X-RAY MACHINE SPECIFICATION

The X-ray machine is a modified Philips PW1270 automatic simultaneous X-ray spectrometer, and consists of a power supply, analysing cabinet, and 3kW Philips PW 2184/00 X-ray tube.

*****

X-RAY TUBE.

3kW maximum, single phase A.C. E.S.B. 32A maximum circuit-breaker-protected against overload.

Ranges: kV 20, 30, 40, 50, 60 constant potential

mA 5, 20, 30, 40, 50, 60, 70, 80; subject to kV x mA $\leq$ 3kVA and 1.8mA $\leq$ kV.

The 74Tungsten target is set at 66° to the axis of the X-ray tube and the X-radiation is emitted through a 1mm thick Berillium window.

Mains cold water-cooled, protected by one internal and one external flow switch.

The voltage and current stability for electricity mains fluctuation from +10% to -15%, and for ambient temperature variations of ±15 C° is better than 0.03%.

LEAD BOX ANALYSING CHAMBER.

The external dimensions are 45cm wide x 49cm high x 50cm deep, formed of two layers of 1.5mm thick Lead wrapped around a light box section steel frame, with 5cm wide soldered overlapped seams, fitted with a push-on 7cm flanged 3mm thick Lead door, protected by one internal microswitch.

Internal 10mm thick bright mild steel welded box, external dimensions 17cm wide x 27cm heigh x 44cm deep.

X-ray beam apertures: of 2mm diameter in the steel box and of 15mm diameter in the Lead box, vertically below the anode of the X-ray tube, and covered by Lead collimators of 2mm maximum diameter.

Optional X-ray beam attenuator for 2mm diameter collimators: 3mm thick bright mild steel, transmission = 10^{-5}.

The inside of the analysing cabinet has a 1.5mm thick Lead shield surrounding the liquid Nitrogen dewar, 64cm wide x 75cm high and 54cm deep. The front part of the shield is in the steel cabinet door overlapping the sides of the shield.

X-RADIATION FLUX AND EXPOSURE RATE AT 3kW.

The data used in the calculations is taken from British Standard 4094: Part 1: 1966 and 4094: Part 2: 1971, which are measured in RAD and REM. The following calculations were sent to the Nuclear Energy Board.

The maximum current at 60kV is 50mA.

The distance of the Berillium window vertically above the floor of the steel box is 18cm, and above the floor of the Lead box it is 38cm.

The X-ray tube output at 60kV constant potential is 10 R/mA.min at 1m target distance. (Part 2 page 13).

The conversion factor at 60keV is 1.2×10^{-4} mR/h per photon/cm^2.sec. (Part 1 page 48)

10 R/mA.min at 1m target distance for 50mA is

$$50 \times 10 \times 60 \times 10^3 = 3 \times 10^7 \text{ mR/h}$$
$$= 3 \times 10^7 / 1.2 \times 10^{-4}$$
$$= 2.5 \times 10^{11} \text{ photons/cm}^2\text{sec. max}$$

The X-radiation below the floor of the Lead box with no aperture and in the absence of the steel box is

$$2.5 \times 10^{11} \times 6 \times 10^{-12} = 15 \text{ photons/sec/cm}^2$$
$$= 10^{-3} \text{ mR/h}$$

because the transmission through 3mm of Lead is 6×10^{-2} (Part 2, page 35).

The X-radiation calculations are summarised in Figure A.1 for the Lead and steel boxes without apertures, and in Figure A.2 for the boxes with apertures.

The maximum scattered radiation to the front door of the cabinet is calculated from a maximum of 0.05% incident exposure rate scattered to

X-RAYS AT 60kV AND 50mA

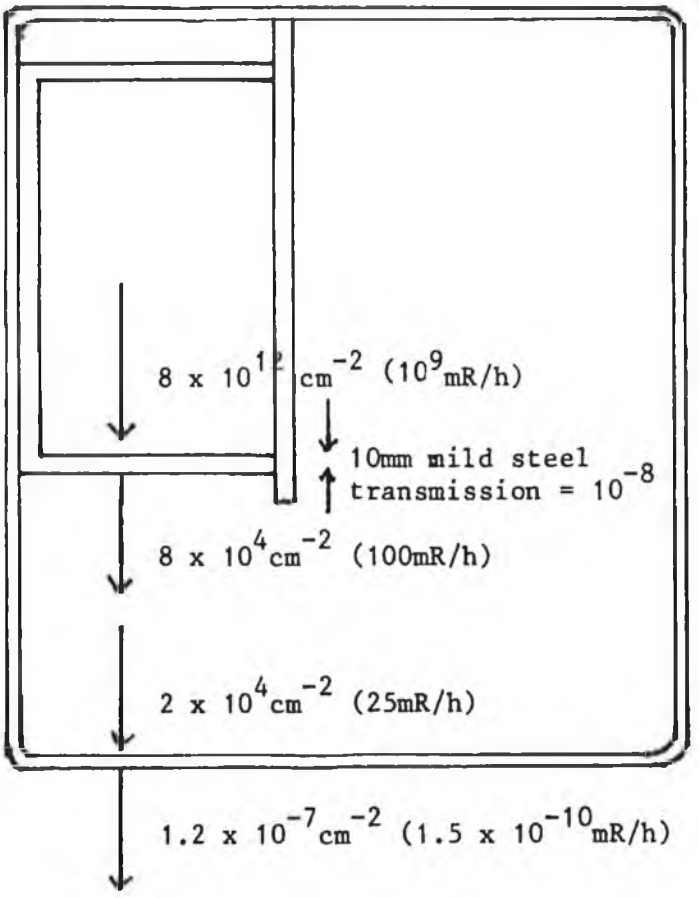

APERTURES CLOSED.

FIGURE A.1

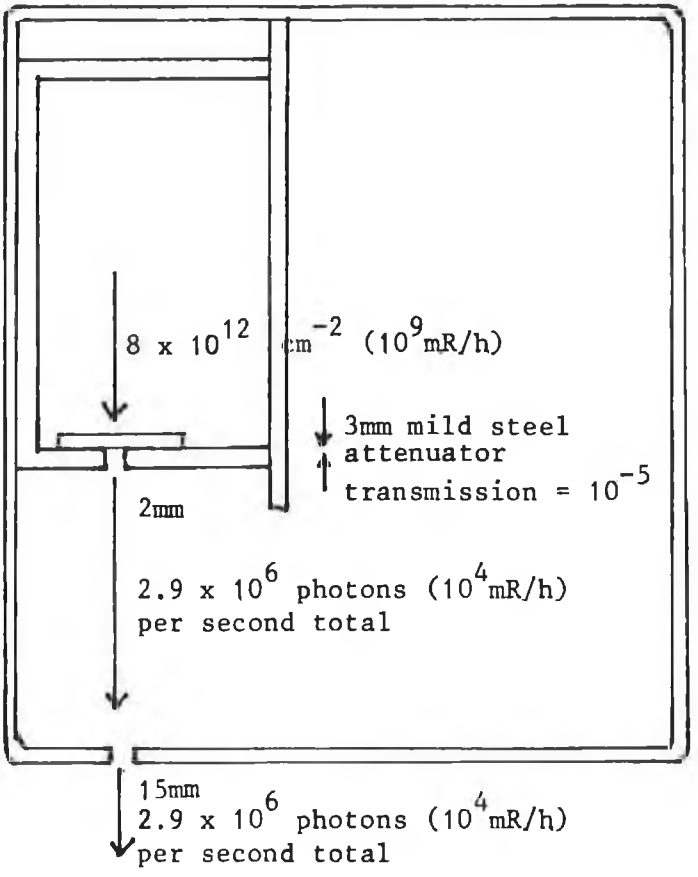

APERTURES OPEN.

FIGURE A.2

1m per $100cm^2$ irradiated area for 45°/45° scatter angle. (Part 2, page 50).

The maximum exposure-rate of the scattered beam on the inside of the Lead shield of the cabinet door is

$$2.5 \times 10^3 \times \frac{\pi \times (0.02)^2}{100} \times 5 \times 10^{-4} = 1.5 \times 10^{-4} \text{ mR/h}$$

The maximum exposure-rate of the scattered beam outside the door of the cabinet having a 1.5mm thick Lead shield, transmission = 3×10^{-6} is

$$1.5 \times 10^{-4} \times 3 \times 10^{-6} = 5 \times 10^{-10} \text{ mR/h}$$

The average background radiation exposure rate at sea level is about 0.05 mR/h.

ANNEXE B

THE X-RAY BEAM PROFILE

To show that $\mu t = \ln(I_o/I)$ is a constant independent of the X-ray projection beam profile.

*****

Figure A.3 illustrates a X-ray beam of width 1mm crossing one pixel of side 1mm of the (j,k) grid. Figure A.4 shows the X-ray beam profile which is a graph of X-ray beam intensity P(x) against distance x normal to the beam direction.

Consider a longitudinal section of the X-ray beam at a rotation angle of length l_{jk} bounded by the (j,k) pixel, and of infinitesimal width dx_r, and let I^o_{xr} be the incident number of X-ray photons in the beam path of width dx_r.

The number of photons incident to the pixel is

$$I_{xr} = I_o \, P(x) \, dx_r$$

where I_o is the total flux of collimated incident X-rays.

The number of photons emergent from the pixel is

$$I_{xr} = I^o_{xr} \exp \left(-\sum_k \bar{\mu}_k l_{jk} \, (x_r)\right.$$

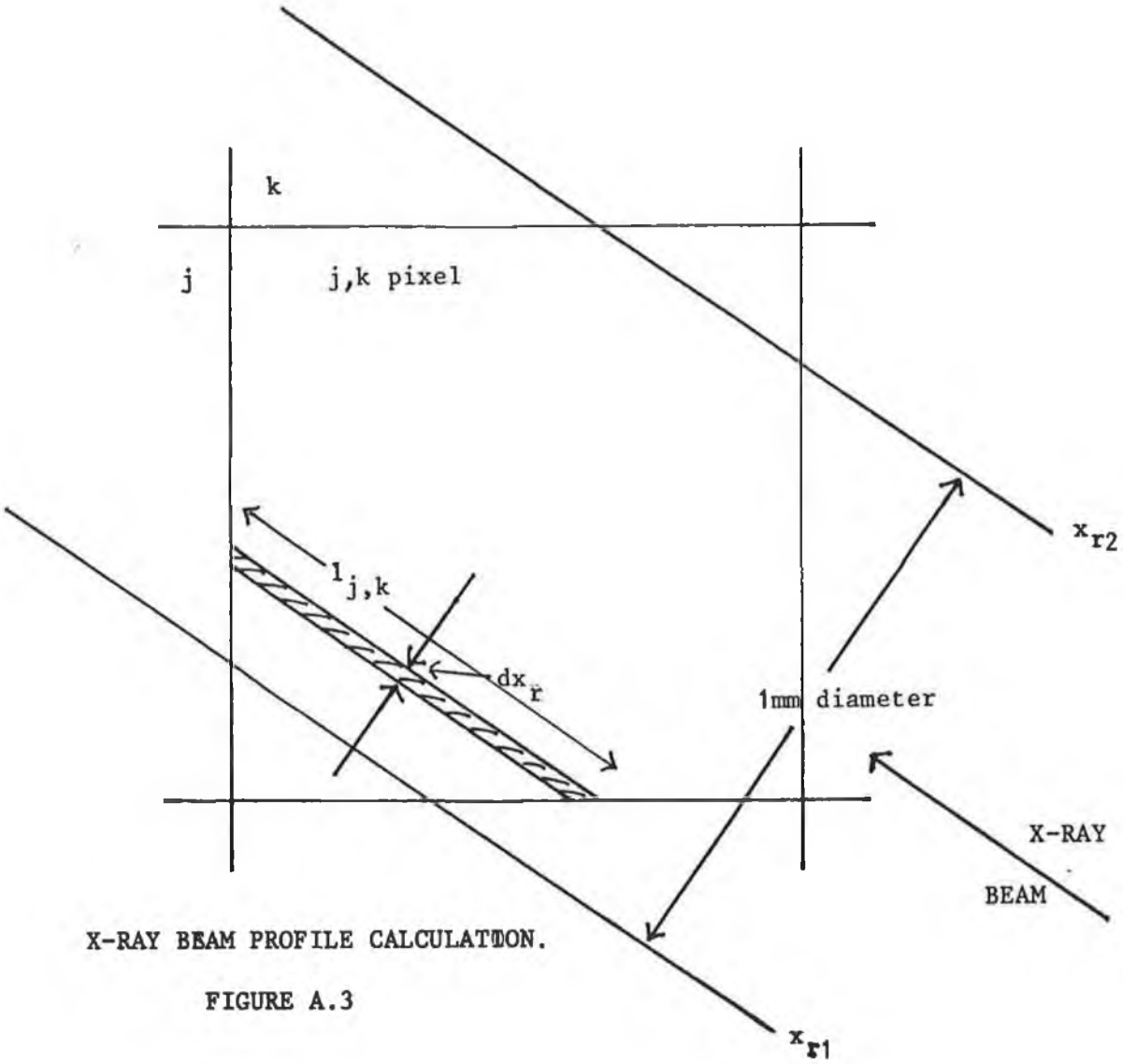

X-RAY BEAM PROFILE CALCULATION.

FIGURE A.3

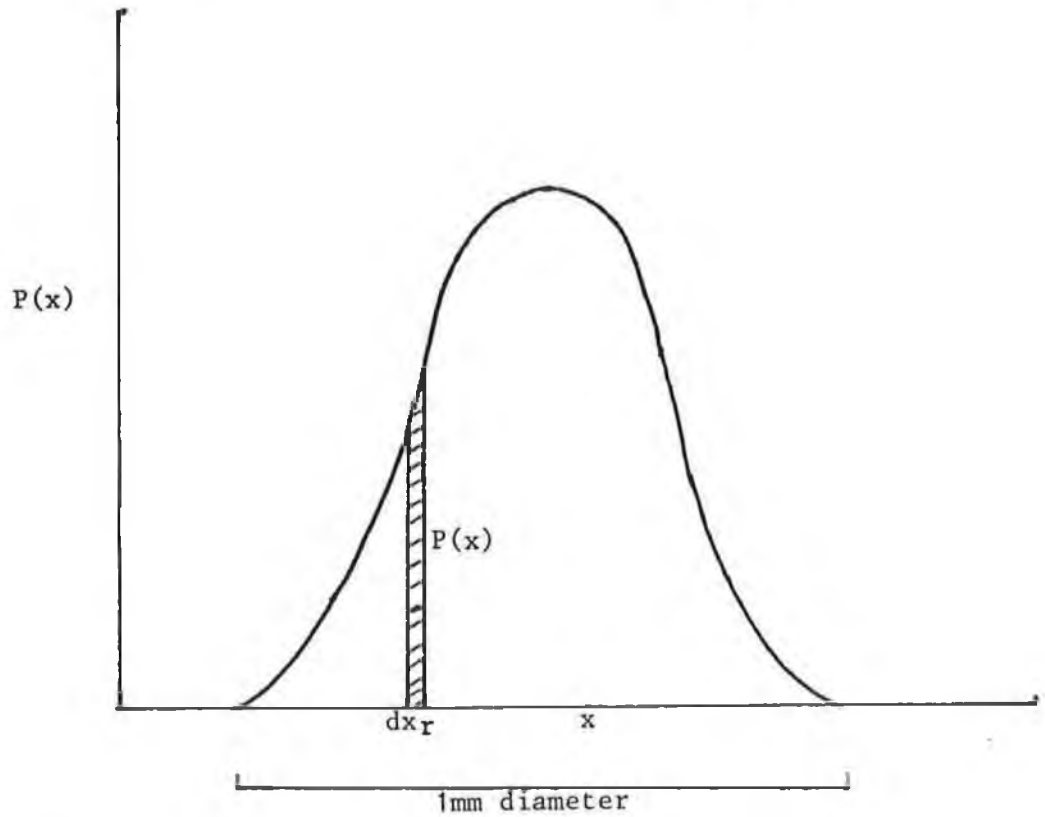

X-RAY BEAM PROFILE.

FIGURE A.4

where μ_k is the mean linear attenuation coefficient of the pixel.

$$I_{xr} = I_o P(x) \exp\left(-\sum_k \bar{\mu}_k l_{jk}(x_r)\right) dx_r$$

$$\alpha_j = I/I_o = \int_{x_{r1}}^{x_{r2}} \left(P(x) \exp\left(-\sum_k \bar{\mu}_k l_{jk}(x_r)\right) dx_r\right.$$

where I is the total flux of emergent X-rays.

If the average length of a beam section is $\bar{l}_{jk}$, then

$$l_{jk}(x_r) = \bar{l}_{jk} + \Delta l_{jk}(x_r)$$

and so $$\alpha_j = \int_{x_{r1}}^{x_{r2}} P(x) \exp\left(-\sum_k \bar{\mu}_k \left(\bar{l}_{jk} + \Delta l_{jk}(x_r)\right)\right) dx_r$$

$$= \int_{x_{r1}}^{x_{r2}} P(x) \exp\left(-\sum_k \bar{\mu}_k \bar{l}_{jk}\right) \exp\left(-\sum_k \bar{\mu}_k \Delta l_{jk}(x_r)\right) dx_r$$

$$= \exp\left(-\sum_k \bar{\mu}_k \bar{l}_{jk}\right) \int_{x_{r1}}^{x_{r2}} P(x) \left(\exp -\sum_k \bar{\mu}_k \Delta l_{jk}(x_r)\right) dx_r$$

$$= \exp\left(-\sum_k \bar{\mu}_k \bar{l}_{jk}\right) \int_{x_{r1}}^{x_{r2}} P(x) \left(1 - \sum_k \bar{\mu}_k \Delta l_{jk}(x_r)\right) dx_r$$

to a first approximation

$$= \exp\left(-\sum_k \bar{\mu}_k \bar{l}_{jk}\right) \int_{x_{r1}}^{x_{r2}} P(x)\, dx_r$$

because $\sum_k \bar{\mu}_k \Delta l_{jk}(x_r)$ is very small, and

$$\alpha_{jk} = \exp -\sum_k \bar{\mu}_k l_{jk}$$

because $\int_{x_{r1}}^{x_{r2}} P(x)\, dx_r = 1$

$$\ln(I_o/I) = \sum_k \bar{\mu}_k l_{jk}$$

$$= \mu t$$

where μ is the linear attenuation coefficient and t is the thickness of the object in the X-ray beam path, is a constant and independent of the X-ray beam profile.

ANNEXE C

Periodic Table of the Elements and some of their absorbtion edge energies.

The Periodic Table of the Elements showing atomic number Z and wavelengths of selected X-ray emission lines.
[E.P. Bertin, Principles and Practice of X-ray Spectrometric Analysis].

Atomic number and element	K-*series*						L-*series*								
	K *edge*	KN_{III}	KM_{III}	KM_{II}	KL_{III}	KL_{II}	L_I *edge*	L_IN_{III}	L_IM_{III}	L_{II} *edge*	$L_{II}N_{IV}$	$L_{II}M_{IV}$	L_{III} *edge*	$L_{III}N_V$	$L_{III}M_V$
		$K\beta_2$	$K\beta_1$	$K\beta_3$	$K\alpha_1$	$K\alpha_2$		$L\gamma_3$	$L\beta_3$		$L\gamma_1$	$L\beta_1$		$L\beta_2$	$L\alpha_1$
Intensity	—	~5	~30	~12	100	~50	—	~2	~6	—	~10	~50	—	~20	100
4 Be	0.115				0.109								0.006		
5 B	0.188				0.183								0.005		
6 C	0.282				0.277								0.005		
7 N	0.397				0.393								0.004		
8 O	0.533				0.525								0.008		
9 F	0.692				0.677								0.015		
10 Ne	0.874		0.858		0.848								0.026		
11 Na	1.080		1.071		1.041								0.039		
12 Mg	1.309		1.302		1.253		0.062						0.056		
13 Al	1.562		1.557		1.487	1.486	0.087			0.076			0.075		
14 Si	1.840		1.836		1.740	1.739	0.118			0.101			0.100		
15 P	2.143		2.139		2.014	2.013	0.153			0.130			0.129		
16 S	2.471		2.464		2.308	2.307	0.193			0.164			0.163		
17 Cl	2.824		2.816		2.622	2.620	0.237			0.204			0.202		
18 Ar	3.203		3.190		2.958	2.956	0.286			0.247			0.245		
19 K	3.607		3.590		3.314	3.311	0.340			0.296			0.293		
20 Ca	4.034		4.013		3.692	3.688	0.403			0.346			0.342		
21 Sc	4.486		4.461		4.090	4.086	0.462			0.400		0.400	0.396		0.395[4]
22 Ti	4.965		4.932		4.511	4.505	0.529			0.460		0.458	0.454		0.452[4]
23 V	5.463		5.427		4.952	4.944	0.626		0.585[3]	0.519		0.519	0.511		0.511[4]
24 Cr	5.987		5.947		5.415	5.405	0.694		0.654[3]	0.582		0.583	0.572		0.573[4]
25 Mn	6.537		6.490		5.899	5.888	0.768		0.721[3]	0.649		0.649	0.638		0.637[4]
26 Fe	7.112		7.058		6.404	6.391	0.846		0.792[3]	0.721		0.719	0.708		0.705[4]
27 Co	7.712		7.649		6.930	6.915	0.929		0.870[3]	0.797		0.791	0.782		0.776[4]
28 Ni	8.339		8.265		7.478	7.461	1.016		0.941[3]	0.878		0.869	0.861		0.852[4]
29 Cu	8.993		8.905	8.903	8.048	8.028	1.109		1.023[3]	0.965		0.950	0.945		0.930[4]
30 Zn	9.673	9.658[1]	9.572	9.567	8.639	8.616	1.208		1.107[3]	1.057		1.035	1.034		1.012[4]
31 Ga	10.386	10.366[1]	10.271	10.261	9.252	9.231	1.316		1.197[3]	1.155		1.125	1.134		1.098[4]
32 Ge	11.115	11.101[1]	10.983	10.978	9.887	9.856	1.426		1.294	1.259		1.218	1.228		1.188[4]
33 As	11.877	11.864[1]	11.727	11.721	10.544	10.509	1.536		1.386	1.368		1.316	1.333		1.282[4]
34 Se	12.666	12.652[1]	12.496	12.489	11.222	11.181	1.662		1.492	1.485		1.419	1.444		1.379[4]
35 Br	13.483	13.470[1]	13.292	13.285	11.924	11.878	1.791		1.600	1.605		1.523	1.559		1.480[4]
36 Kr	14.330	14.315[1]	14.113	14.105	12.650	12.598	1.923		1.706	1.732		1.637	1.680		1.586[4]
37 Rb	15.202	15.185[1]	14.962	14.952	13.396	13.336	2.067	2.051[2]	1.827	1.866		1.752	1.806		1.694
38 Sr	16.106	16.085[1]	15.836	15.826	14.166	14.098	2.217	2.197[2]	1.947	2.008		1.872	1.940		1.806
39 Y	17.037	17.015[1]	16.737	16.725	14.958	14.882	2.372	2.347[2]	2.072	2.155		1.996	2.079		1.923
40 Zr	17.997	17.963[1]	17.662	17.649	15.770	15.692	2.535	2.503[2]	2.200	2.305	2.292	2.118	2.227	2.215	2.043
41 Nb	18.985	18.947[1]	18.623	18.606	16.615	16.521	2.698	2.660[2]	2.336	2.464	2.449	2.257	2.370	2.357	2.166
42 Mo	20.002	19.960	19.608	19.590	17.479	17.374	2.867	2.825[2]	2.473	2.628	2.611	2.396	2.523	2.508	2.295
43 Tc	21.048	21.002	20.619	20.599	18.367	18.251	3.047	3.001[2]	2.618	2.797	2.778	2.537	2.681	2.664	2.424
44 Ru	22.123	22.072	21.656	21.637	19.279	19.150	3.230	3.179[2]	2.763	2.973	2.952	2.683	2.844	2.825	2.556
45 Rh	23.229	23.173	22.723	22.698	20.216	20.073	3.421	3.365[2]	2.915	3.156	3.132	2.835	3.013	2.992	2.698

Atomic number and element	K-*series*						L-*series*								
	K *edge*	KN_{III}	KM_{III}	KM_{II}	KL_{III}	KL_{II}	L_I *edge*	L_IN_{III}	L_IM_{III}	L_{II} *edge*	$L_{II}N_{IV}$	$L_{II}M_{IV}$	L_{III} *edge*	$L_{III}N_V$	$L_{III}M_V$
		$K\beta_2$	$K\beta_1$	$K\beta_3$	$K\alpha_1$	$K\alpha_2$		$L\gamma_3$	$L\beta_3$		$L\gamma_1$	$L\beta_1$		$L\beta_2$	$L\alpha_1$
Intensity	—	~5	~30	~12	100	~50	—	~2	~6	—	~10	~50	—	~20	100
46 Pd	24.365	24.303	23.819	23.792	21.178	21.021	3.619	3.557	3.073	3.344	3.318	2.990	3.187	3.163	2.838
47 Ag	25.531	25.463	24.943	24.912	22.163	21.991	3.822	3.754	3.234	3.540	3.511	3.151	3.368	3.342	2.985
48 Cd	26.727	26.653	26.095	26.061	23.173	22.985	4.034	3.960	3.402	3.742	3.710	3.319	3.554	3.525	3.134
49 In	27.953	27.872	27.275	27.237	24.209	24.002	4.250	4.169	3.572	3.951	3.915	3.487	3.744	3.712	3.288
50 Sn	29.211	29.122	28.491	28.439	25.272	25.044	*4.475*	*4.377*	*3.750*	4.167	4.127	3.661	3.939	3.903	3.442
51 Sb	30.499	30.402	29.725	29.677	26.359	26.110	4.706	4.609	3.932	4.389	4.345	3.843	4.140	4.101	3.604
52 Te	31.817	31.712	30.995	30.944	27.472	27.201	4.942	4.837	4.120	4.616	4.568	4.030	4.345	4.302	3.770
53 I	33.168	33.054	32.295	32.239	28.612	28.317	5.186	5.072	4.313	4.851	4.799	4.221	4.556	4.509	3.938
54 Xe	34.551	34.428	33.625	33.562	29.779	29.459	5.442	5.319	4.516	5.092	5.035	4.415	4.772	4.720	4.110
55 Cs	35.966	35.833	34.985	34.918	30.973	30.625	5.700	5.567	4.719	5.341	5.278	4.619	4.993	4.936	4.289
56 Ba	37.414	37.270	36.378	36.303	32.194	31.817	5.964	5.820	4.928	5.597	5.529	4.827	5.220	5.153	4.470
57 La	38.894	38.739	37.802	37.721	33.442	33.034	6.235	6.080	5.143	5.860	5.786	5.037	5.452	5.385	4.651
58 Ce	40.410	40.243	39.258	39.170	34.720	34.279	6.516	6.349	5.364	6.131	6.051	5.261	5.690	5.617	4.839
59 Pr	41.958	41.778	40.748	40.653	36.026	35.550	6.802	6.622	5.592	6.408	6.321	5.485	5.932	5.853	5.034
60 Nd	43.538	43.345	42.272	42.166	37.361	36.847	7.095	6.902	5.829	6.691	6.597	5.722	6.177	6.091	5.231
61 Pm	45.152	44.947	43.825	43.713	38.725	38.171	7.398	7.193	6.071	6.981	6.880	5.962	6.427	6.334	5.433
62 Sm	46.801	46.584	45.413	45.289	40.118	39.523	7.707	7.490	6.319	7.278	7.169	6.205	6.683	6.582	5.635
63 Eu	48.486	48.256	47.036	46.902	41.542	40.902	8.024	7.794	6.574	7.584	7.467	6.455	6.944	6.835	5.843
64 Gd	50.207	49.964	48.696	48.554	42.996	42.309	8.343	8.100	6.832	7.898	7.772	6.713	7.211	7.034	6.058
65 Tb	51.965	51.709	50.382	50.228	44.481	43.744	8.679	8.423	7.096	8.221	8.086	6.976	7.484	7.358	6.273
66 Dy	53.761	53.491	52.119	51.956	45.999	45.208	9.013	8.743	7.371	8.553	8.409	7.249	7.762	7.627	6.496
67 Ho	55.593	55.308	53.878	53.707	47.547	46.699	9.365	9.080	7.650	8.894	8.740	7.529	8.046	7.901	6.719
68 Er	57.464	57.164	55.681	55.491	49.128	48.221	9.725	9.425	7.942	9.243	9.078	7.813	8.336	8.180	6.951
69 Tm	59.374	59.059	57.513	57.303	50.742	49.773	10.097	9.782	8.236	9.601	9.426	8.103	8.632	8.465	7.181
70 Yb	61.322	60.991	59.374	59.157	52.389	51.354	10.479	10.148	8.531	9.968	9.781	8.402	8.933	8.755	7.415
71 Lu	63.311	62.960	61.286	61.049	54.070	52.965	10.869	10.518	8.844	10.346	10.144	8.709	9.241	9.049	7.655
72 Hf	65.345	64.973	63.236	62.979	55.790	54.611	11.262	10.890	9.153	10.734	10.517	9.016	9.555	9.348	7.891
73 Ta	67.405	67.011	65.221	64.946	57.533	56.277	11.672	11.278	9.488	11.128	10.894	9.345	9.872	9.649	8.147
74 W	69.517	69.100	67.244	66.951	59.318	57.982	12.092	11.675	9.819	11.535	11.284	9.671	10.199	9.959	8.396
75 Re	71.670	71.230	69.309	68.994	61.140	59.718	12.522	12.082	10.161	11.952	11.682	10.006	10.530	10.273	8.651
76 Os	73.869	73.404	71.416	71.077	63.001	61.487	12.968	12.503	10.515	12.382	12.092	10.349	10.868	10.592	8.905
77 Ir	76.111	75.620	73.560	73.203	64.896	63.287	13.416	12.925	10.865	12.824	12.514	10.705	11.215	10.919	9.175
78 Pt	78.400	77.883	75.751	75.364	66.832	65.123	13.880	13.363	11.231	13.277	12.944	11.073	11.568	11.251	9.439
79 Au	80.729	80.182	77.985	77.580	68.804	66.990	14.353	13.806	11.609	13.739	13.383	11.432	11.925	11.585	9.705
80 Hg	83.109	82.532	80.261	79.822	70.819	68.894	14.835	14.258	11.987	14.215	13.834	11.823	12.290	11.927	9.999
81 Tl	85.532	84.924	82.575	82.384	72.872	70.832	15.344	14.736	12.387	14.700	14.293	12.217	12.660	12.272	10.271
82 Pb	88.008	87.367	84.936	84.450	74.969	72.804	15.863	15.222	12.791	15.204	14.769	12.618	13.039	12.625	10.555
83 Bi	90.540	89.866	87.354	86.831	77.118	74.815	16.391	15.717	13.205	15.725	15.261	13.031	13.422	12.981	10.836
84 Po	93.113	92.403	89.801	89.250	79.301	76.863	16.940	16.230	13.628	16.250	15.756	13.452	13.812	13.342	11.131
85 At	95.730	94.983	92.302	91.722	81.523	78.943	17.495	16.748	14.067	16.787	16.262	13.882	14.207	13.708	11.427

Atomic number and element	K-series						L-series								
	K *edge*	KN_{III}	KM_{III}	KM_{II}	KL_{III}	KL_{II}	L_I *edge*	L_IN_{III}	L_IM_{III}	L_{II} *edge*	$L_{II}N_{IV}$	$L_{II}M_{IV}$	L_{III}	$L_{III}N_V$	$L_{III}M_V$
		$K\beta_2$	$K\beta_1$	$K\beta_3$	$K\alpha_1$	$K\alpha_2$		$L\gamma_3$	$L\beta_3$		$L\gamma_1$	$L\beta_1$	*edge*	$L\beta_2$	$L\alpha_1$
Intensity	—	~5	~30	~12	100	~50	—	~2	~6	—	~10	~50	—	~20	100
86 Rn	98.402	97.617	94.866	94.246	83.793	81.065	18.047	17.262	14.511	17.337	16.777	14.323	14.609	14.079	11.727
87 Fr	101.131	100.306	97.477	96.807	86.114	83.231	18.630	17.805	14.976	17.900	17.307	14.775	15.017	14.456	12.031
88 Ra	103.909	103.039	100.130	99.432	88.476	85.434	19.222	18.352	15.443	18.475	17.848	15.238	15.433	14.839	12.340
89 Ac	106.738	105.837	102.846	102.101	90.884	87.675	19.823	18.922	15.931	19.063	18.402	15.711	15.854	15.227	12.652
90 Th	109.641	108.690	105.611	104.831	93.358	89.952	20.449	19.498	16.419	19.689	18.993	16.215	16.283	15.622	12.970
91 Pa	112.599	111.606	108.435	107.606	95.883	92.287	21.088	20.095	16.924	20.312	19.581	16.715	16.716	16.022	13.300
92 U	115.606	114.561	111.303	110.424	98.440	94.659	21.757	20.712	17.454	20.947	20.167	17.219	17.166	16.429	13.614
93 Np	118.678	117.591	114.243	113.312	101.068	97.077	22.427	21.340	17.992	21.601	20.785	17.751	17.610	16.840	13.944
94 Pu	121.818	120.703	117.261	116.277	103.761	99.552	23.097	21.982	18.540	22.266	21.417	18.293	18.057	17.256	14.279
95 Am	125.027	123.891	120.360	119.317	106.523	102.083	23.773	22.637	19.106	22.944	22.065	18.852	18.504	17.676	14.617
96 Cm	128.220	127.066	123.423	122.325	109.290	104.441	24.460	23.306	19.663	23.779		19.552	18.930		14.959
97 Bk	131.590	130.355	126.663	125.443	112.138	107.205	25.275	24.040	20.348	24.385		20.019	19.452		15.320
98 Cf	135.960	134.681	130.851	129.601	116.030	110.710	26.110	24.831	21.001	25.250		20.763	19.930		15.677
99 Es	139.490	138.169	134.238	132.916	119.080	113.470	26.900	25.579	21.648	26.020		21.390	20.410		16.036
100 Fm	143.090	141.724	137.693	136.347	122.190	116.280	27.700	26.334	22.303	26.810		22.044	20.900		16.402
101 Md	146.780	145.370	141.234	139.761	125.390	119.170	28.530	27.120	22.984	27.610		22.707	21.390		16.768
102 No	150.540	149.092	144.852	143.295	128.660	122.100	29.380	27.932	23.692	28.440		23.403	21.880		17.139
103 Lw	154.380	152.900	148.670	146.920	132.020	125.100	30.240	28.760	24.530	29.280		24.130	22.360		17.500

Unresolved lines:
1– K $N_{II,III}$ ($K\beta_2$); 2—L_I $N_{II,III}$ ($L\gamma_{2,3}$); 3—L_I $M_{II,III}$ ($L\beta_{3,4}$); 4—L_{III} $M_{IV,V}$ ($L\alpha_{1,2}$).
Depending on the resolving power of the dispersing system used (e.g. crystal spectrometer, solid state energy dispersive detector) line pairs shown separately in the table may not be resolved and the effective energy of the doublet will be close to the mean value weighted by the relative intensity of the components.

The K and L absorbtion edge energies of the atomic elements.
[G.W.C. Kaye and T.H. Laby, Tables of Physical and Chemical Constants and some Mathematical Functions].

ANNEXE D

BASIC COMPUTER PROGRAMS

The fifteen computer programs are listed in the order in which they are used in computing, together with their authors. Most were developed from simpler computer programs during the work.

POSSCAN	To position the scanning coordinate table.	K.J.McC.
MDPOINT	To find the mid point of the linear scan.	K.J.McC.
MCASCAN	Counter program to scan an object.	K.J.McC.
COMPILE	To convert random access numbers to ASCII code.	K.J.McC.
ROISELECT	To sort serial data into 8 Regions of Interest.	K.J.McC.
ROIEXTRAPOLATE	To extrapolate to an absorbtion edge of an element.	K.J.McC.
CALAREA40	Overlap areas for 40 steps and 40 rotations.	J.F.
RECON40NTIMES	Algebraic Reconstruction Technique.	J.F., K.J.McC.
INVERTDATA	To invert the X-ray photon count data.	K.J.McC.
CALAR40	To select overlap areas as 1 or 0.	J.F., K.J.McC.
FILTRECONAV40	Filtered Backprojection.	K.J.McC., J.F.
CANG40G	To convert ASCII code to random access numbers.	J.F.
R.DISP40T	Image display on the monitor screen.	J.F.
SPECTRA	X-ray spectral shapes.	A.F., K.J.McC.
FRACION	L. Grodzin's equation calculation.	J.F.

POSSCAN

This program, run on the BBC microcomputer, is used to position the (x,z,ϕ) scanning coordinate table on the chosen (x,z,ϕ) coordinates at the start complete scan of an object.

****

Lines 20 to 250 is the part of the program for moving the x-coordinate table using the cursor EDIT keys, and for changing the linear scan step size. The scanning linear step size is chosen at line 40; for a 1mm step with a 1mm wide X-ray beam, S = 48.

When the x-coordinate has been chosen Q is pressed and the program diverts to lines 260 to 450. This section is for changing the ϕ-coordinate, and choosing the angular setting of the object at the start of a scan, using the cursor EDIT keys. When S = 15, each angular step is 4.5° the step size for a 40 x 40 scan.

When ϕ is set, Q is pressed and the program diverts to lines 460 to 860, which moves the z-coordinate table. This direction is parallel to the axis of the scan, the direction of the ϕ-axis. The cursor EDIT keys can adjust z, 48 pulses per mm, and the step size may be changed.

When z has been chosen, which determines the plane through which the X-ray beam passes in the object being scanned, Q is pressed and the program, MDPOINT, which centres the linear scan with the X-ray beam, may be selected.

The scanning coordinate table has three stepping motors for the (x,z,ϕ) coordinates, but the scanning controller has only two stepping motor interfaces between the BBC microcomputer and the stepping motors. Thus the z-stepping motor and the ϕ-stepping motor plugs are exchanged at line 540.

```
  5 REM****POSSCAN****
 10 REM PROGRAM TO POSITION THE SCANNING TABLE
 20 *FX4,1
 30 CLS
 40 INPUT TAB(2,12) "SIZE OF STEP IN X-DIRECTION (48 PULSES/mm)",S
 50 CLS
 60 PRINT "USE EDIT KEYS TO POSITION SCAN"
 70 PRINT "SMALL STEP LEFT", CHR$(93)
 80 PRINT "SMALL STEP RIGHT", CHR$(91)
 90 PRINT "CHANGE STEP SIZE",     "C"
100 PRINT "          (QUIT)",     "Q"
110 Q$=GET$
120 IF Q$<>CHR$(&8B) AND Q$<>CHR$(&89) AND Q$<>"Q" AND Q$<>"C" THEN GOTO 50
130 IF Q$="Q" THEN GOTO 260
140 IF Q$="C" THEN GOTO 30
150 IF Q$=CHR$(&89) THEN PROCDEF1
160 IF Q$=CHR$(&88) THEN PROCDEF2
170 PROCSTEP(S)
180 *FX21,0
190 GOTO 50
200 DEF PROCDEF2
210 D=112:R=96
220 ENDPROC
230 DEF PROCDEF1
240 D=48:R=32
250 ENDPROC
260 *FX4,1
270 CLS
280 INPUT TAB(1,12) "ANGLE STEP SIZE (3 DEGREES=10 PULSES)",S
290 CLS
300 PRINT "USE EDIT KEYS TO ROTATE SCAN"
310 PRINT "CLOCKWISE ROTATION", CHR$(93)
320 PRINT "ANTICLOCKWISE ROTATION", CHR$(91)
330 PRINT "CHANGE ANGLE STEP",     "C"
340 PRINT "RETURN TO X-DRIVE",     "R"
350 PRINT "          (QUIT)",     "Q"
360 Q$=GET$
370 IF Q$<>CHR$(&8B) AND Q$<>CHR$(&89) AND Q$<>"Q" AND Q$<>"C" AND Q$<>"R" THE
N GOTO 290
380 IF Q$="Q" THEN GOTO 460
390 IF Q$="C" THEN GOTO 270
400 IF Q$="R" THEN GOTO 30
410 IF Q$=CHR$(&89) THEN PROCROT1
420 IF Q$=CHR$(&88) THEN PROCROT2
430 PROCSTEP(S)
440 *FX21,0
450 GOTO 290
460 CLS
470 INPUT TAB(1,12) "SIZE OF Z-STEP(48PULSES/mm)",S
480 CLS
490 PRINT "USE EDIT KEYS TO MOVE TABLE FOWARD OR BACKWARDS"
500 PRINT "TABLE FOWARDS", CHR$(86)
510 PRINT "TABLE BACKWARDS", CHR$(94)
520 PRINT "CHANGE STEP SIZE",     "C"
530 PRINT "RETURN TO X-DRIVE",     "X"
540 PRINT "RETURN TO Y-DRIVE",     "Y"
550 PRINT "          (QUIT)",     "Q"
560 Q$=GET$
570 IF Q$<>CHR$(&8B) AND Q$<>CHR$(&8A) AND Q$<>"Q" AND Q$<>"C" AND Q$<>"X" AND
Q$<>"Y" THEN GOTO 480
580 IF Q$="Q" THEN GOTO 870
590 IF Q$="C" THEN GOTO 460
600 IF Q$="X" THEN GOTO 30
610 IF Q$="Y" THEN GOTO 270
620 IF Q$=CHR$(&8B) THEN PROCROT1
630 IF Q$=CHR$(&8A) THEN PROCROT2
640 PROCSTEP(S)
650 *FX21,0
660 GOTO 480
670 DEF PROCSTEP(S)
680 B=&FE60
690 ?(B+2)=255
700 FOR N=1 TO S
710 ?B=D
720 Q=TIME+5
730 REPEAT
740 UNTIL TIME>=Q
750 ?B=R
760 Q=TIME+5
770 REPEAT
780 UNTIL TIME>=Q
790 NEXT N
800 ENDPROC
810 DEF PROCROT1
820 D=14:R=12
830 ENDPROC
840 DEF PROCROT2
850 D=6:R=4
860 ENDPROC
870 *FX4,0
880 CLS
890 PRINT TAB(5,12) "DO YOU WANT TO CHAIN FIND MIDPOINT PROGRAM Y/N?":Q$=GET
900 IF Q$="Y" THEN CHAIN "Mdpoint"
910 IF Q$="N" THEN END ELSE GOTO 880
```

MDPOINT

This BBC microcomputer program is used to find the mid point of the ϕ-coordinate stepping motor axle so as to centre the ϕ-axis with the centre of the X-ray beam, and to find the starting position for the linear scan. The mid point is the primary reference point for the scanning coordinate table: the ϕ-axis, the centre of the linear scan and the centre of the X-ray beam are coincident. The centering ensures that blurring artefacts or distortion are not introduced into the reconstructed image of the object, because the centre of rotation in the reconstruction is at the centre of the reconstruction grid. Coincidence of the two centres containing the (x,ϕ) reference fixes the image to the scanned object like two triangulation points at the same height fix the reference for an ordnance survey contour map. The X-ray photon count scanning data is the linear transformation from the object space to the image space provided the two centres are coincident.

*****

The main part of the program consisting of twelve procedures and a CHAIN statement is listed in lines 20 to 260. The program is used immediately after the scanning coordinate table has been positioned at the correct (x,z,ϕ) coordinates using the POSSCAN program from which it may be loaded into the BBC microcomputer memory and run by a CHAIN statement. The main part of the program is executed in line number order and calls the procedures in sequence.

The program starts at line 20 by calling PROCQUESTIONS, defined at lines 270 to 440, which asks for the number and length in mm of the steps for the linear scan, the voltage setting for the X-ray tube and X-irradiation time in seconds at each step, and the number of angular steps for the ϕ-axis scanning motor. Line 290 is the distance the z-coordinate table is to be moved in order for the X-ray beam to scan the chosen plane in the object. PROCSAVEDATA, defined at lines 450 to 490, stores the answers to these questions on disc for later use.

PROCVARIABLES, defined at lines 3810 to 3850 is to set up the allocation of variable names to memory addresses in the BBC microcomputer. PROCASSEMB is defined at lines 3860 to 4350. This procedure is used to store the X-ray photon count data, input to the BBC microcomputer through the RS423 serial port, in the memory addresses as assembly language using the variables defined in PROCVARIABLES. Lines 3820 to 4350 are the commands for the BBC microcomputer to store in its memory the incoming X-ray photon count data, otherwise the data is lost as it is printed to the monitor screen.

PROCsetup, defined at lines 2920 to 2980, connects the BBC microcomputer to the EG & G Ortec 7100 multichannel analyser via the RS423 serial port. The multichannel analyser sends and receives ASCII code, and it has a serial remote control option so that it can be controled by the BBC microcomputer PROCSETPHA, defined at lines 2990 to 3130, are the commands for the multichannel analyser to do a pulse height analysis for a chosen time. When the multichannel analyser has been enabled by the BBC microcomputer, all of the multichannel analyser keys are inoperative, and the BBC microcomputer is used to set up and run commands, and clear the multichannel analyser memory after the X-ray photon count data has been

received by the BBC microcomputer. PROCSETIO, defined at lines 3140 to 3310, are the commands for the multichannel analyser to send the X-ray photon count data to the BBC microcomputer memory. PROCclear, defined at lines 3320 to 3370, clears the multichannel analyser memory after the X-ray photon count data for one scanning step has been received by the BBC microcomputer. Lines 3380 to 3410 define PROCstartpha to start the pulse height analysis and lines 3430 to 3480 define PROCrunio which sends the X-ray photon count data in the multichannel analyser memory to the BBC micrcomputer memory. All the procedures in lines 2920 to 3480 are for controlling the multichannel analyser automatically from the BBC micromputer. When the procedures of lines 40 to 90 have been run to enable the BBC micromputer to communicate with the multichannel analyser, line 100 disenables the multichannel analyser.

PROCZFORWARDDRIVE is defined at lines 500 to 570. This procedure asks whether or not the scanning coordinate table is to be moved forwards so that the axle of the stepping motor intercepts the X-ray beam. If the answer is YES the program diverts to PROCSTEP(S) otherwise it diverts to line 120.

PROCSTEP(S), defined at lines 700 to 830, are the commands for moving the scanning coordinate table.

When the z-coordinate table has been moved forwards, and the answer chosen at line 120 is NO, the program diverts to line 160, PROCX5mmDRIVE, which is defined at lines 630 to 690. This procedure calls PROCSTEP(S) to move the x-coordinate table forwards by 5mm to take up the backlash in the lead screw. The scanning coordinate table is now ready to scan the stepping motor axle in order to find its axis.

PROCFINDMIN is defined at lines 840 to 1000, and contains twelve procedures listed from lines 1010 to 2910. Some of these procedures divert to further procedures. The BBC microcomputer starts the scan of the stepping motor axle in 0.125mm steps, and at each step the multichannel analyser counts detected X-ray photons in a chosen energy band for a chosen time. The photon count rate drops sharply as the stepping motor axle begins to intercept the X-ray beam, stays fairly steady whilst the axle intercepts the X-ray beam, and rises sharply as the X-ray beam reappears at the other side of the axle. The slopes of the graph of X-ray photon count against z-coordinate scan step where the X-ray beam disappears from, and reappears in view of, the detector are determined by the method of least squares to find the best fit line by PROCSLOPES, defined at lines 2330 to 2400. The mid point of the scan is determined by PROCLINEIntercept, defined at lines 2710 to 2740, using the intercepts of the slopes with the line parallel to the abscissa which has been determined from the average maximum count of X-ray photons not intercepted by the stepping motor axle by PROCAVERAGETOP, defined at lines 1690 to 1790. These procedures print to the monitor screen, and on paper, the X-ray photon counts detected at each step, the calculated values of variables listed in the procedures, and the distance of the mid point in mm from the origin, x=0.

The program returns to PROCFINDSTART, which is defined at lines 1210 to 1310. This procedure uses the midpoint x-coordinate calculated by PROCFINDMIN as reference, and moves the x-coordinate table to the starting position for the scan, having taken up the backlash in the lead screw.

PROCZBACKDRIVE, defined at lines 580 to 620 moves the z-coordinate table back to the position in which the X-ray beam can scan the chosen plane in the object.

The BBC microcomputer program COUNTER which counts the X-ray photon data for the complete scan of the object can be loaded into the BBC microcomputer memory and run by the CHAIN command at line 250.

```
  5 REM ****MDPOINT****
 10 REM PROGRAM TO FIND THE MIDPOINT OF THE LINEAR SCAN
 20 PROCQUESTIONS
 30 DIM COUNT1(8,2,8)
 40 PROCSAVEDATA
 50 PROCVARIABLES
 60 PROCASSEMB
 70 PROCsetup
 80 PROCSETPHA
 90 PROCSETIO
100 VDU3
110 PROCZFORWARDDRIVE
120 CLS:PRINT TAB(2,12) "DO YOU WANT A HARD COPY Y/N":Q$=GET$
130 IF Q$<>"Y" AND Q$<>"N" THEN 120
140 IF Q$="Y" THEN 150 ELSE 160
150 VDU2
160 PROCX5mmDRIVE
170 PROCFINDMIN
180 VDU3
190 PROCFINDSTART
200 PROCZBACKDRIVE
210 VDU3
220 CLS:PRINT TAB(1,12) "DO YOU WANT TO CHAIN COUNTER PROGRAM Y/N":Q$=GET$
230 IF Q$<>"Y" AND Q$<>"N" THEN 220
240 IF Q$="Y" THEN 250 ELSE END
250 CHAIN"COUNTER"
260 END
265 ****
270 DEF PROCQUESTIONS
280 CLS
290 INPUT TAB(1,12) "Z-POSITION mm FROM END OF AXLE (MAX 75 mm)",Z
300 IF Z>75 GOTO 280
310 CLS
320 INPUT TAB(4,12) "NUMBER OF STEPS/STEPS (20 OR 40)",NUMSTEPS
330 IF NUMSTEPS<>20 AND NUMSTEPS<>40 THEN 310
340 CLS
350 INPUT TAB(4,12) "STEP SIZE (MAX 2mm)",SIZESTEP
360 IF SIZESTEP>2 GOTO 340
370 CLS
380 INPUT TAB(8,12) "MAXIMUM X-RAY ENERGY (keV)",EMAX
390 CLS
400 INPUT TAB(4,12) "TIME FOR EACH STEP",TT%
410 CLS
420 INPUT TAB(2,12) "NUMBER OF ROTATIONS (24 OR 40)",NUMROTS
430 IF NUMROTS<>24 AND NUMROTS<>40 THEN 410
440 ENDPROC
450 DEF PROCSAVEDATA
460 X=OPENOUT "NUMBERS"
470 PRINT #X,Z,NUMSTEPS,NUMROTS,SIZESTEP,EMAX,TT%
480 CLOSE#X
490 ENDPROC
495 ****
500 DEF PROCZFORWARDDRIVE
510 CLS: PRINT TAB(1,12) "DO YOU WANT Z-FOWARD DRIVE Y/N":Q$=GET$
520 IF Q$<>"Y" AND Q$ <>"N" THEN 510
530 IF Q$="Y" THEN 540 ELSE 570
540 CLS:PRINT"PROCZFORWARDDRIVE"
550 S=Z*48:D=6:R=4
560 PROCSTEP(S)
```

```
  570 ENDPROC
  580 DEF PROCZBACKDRIVE
  590 S=Z*48:D=14:R=12
  600 PROCSTEP(S)
  610 CLS:PRINT TAB(1,12) "CHANGE PLUG ON STEPPER INTERFACE AND HIT ANY KEY":Q$=
GET$
  620 ENDPROC
  630 DEF PROCX5mmDRIVE
  640 CLS:PRINT"PROCX5mmDRIVE"
  650 S=5*48:D=112:R=96
  660 PROCSTEP(S)
  670 S=10:D=48:R=32
  680 PROCSTEP(S)
  690 ENDPROC
  700 DEF PROCSTEP(S)
  710 B=&FE60
  720 ?(B+2)=255
  730 FOR X= 1 TO S
  740 ?B=D
  750 Q=TIME+5
  760 REPEAT
  770 UNTIL TIME>=Q
  780 ?B=R
  790 Q=TIME+5
  800 REPEAT
  810 UNTIL TIME>=Q
  820 NEXT X
  830 ENDPROC
  835 ****
  840 DEF PROCFINDMIN
  850 NUMsteps=NUMSTEPS*8
  860 DIM Step(NUMsteps):A%=0
  870 PRINT "PROCFINDMIN"
  880 PROCFIRST3
  890 PROCCOMPAREDOWNSLOPE:IF A%=1 THEN GOTO 910
  900 PROCCONTINUEX
  910 PROCFINDUP
  920 PROC5MORESTEPS
  930 PROCAVERAGETOP
  940 PROCAVERAGEBOTTOM
  950 PROCSETSTDBOTTOM
  960 PROCSETLIMITS
  970 PROCFINDPOINTS
  980 PROCCHECK
  990 PROCSLOPES
 1000 ENDPROC
 1005 ****
 1010 DEF PROCCOMPAREDOWNSLOPE
 1020 PRES=0:PAST1=0:PAST2=0:A%=0:AVERPRES=0
 1030 PRES=Step(T-1):PAST1=Step(T-2):PAST2=Step(T-3)
 1040 AVERPRES=(PRES+PAST1+PAST2)/3:PRINT"AVERAGE=",AVERPRES
 1050 IF AVERPRES<AVERPAST-(1.5*SQR(AVERPRES)) THEN 1060 ELSE 1080
 1060 POSITION1=T-3:SLOPE0=PAST2:SLOPE1=PAST1:A%=1
 1070 PRINTPOSITION1,     SLOPE0 ,SLOPE1
 1080 AVERPAST=AVERPRES
 1090 ENDPROC
 1100 DEF PROCFIRST3
 1110 T=1:S=3:D=48:R=32
 1120 REPEAT
 1130 PROCCOUNT
```

```
1140 PROCINTERPRET
1150 PROCSTEP(S)
1160 T=T+1
1170 UNTIL T>3
1180 AVERPAST=0:AVERPAST=(Step(T-1)+Step(T-2)+Step(T-3))/3
1190 PRINT"AVERPAST=",AVERPAST
1200 ENDPROC
1210 DEF PROCFINDSTART
1220 REM TO FIND NO OF STEPS TO START
1230 PRINT "FINDING START"
1240 S=((NUMSTEPS-1)*SIZESTEP*24)-((T-Midpoint)*3)+142
1250 PRINT"No Pulses to Start="S
1260 D=48:R=32
1270 PROCSTEP(S)
1280 S=144:D=112:R=96
1290 PROCSTEP(S)
1300 CLS:PRINT TAB(6,12) "SCAN AT STARTING POSITION"
1310 ENDPROC
1320 DEF PROCCONTINUEX
1330 S=3:D=48:R=32
1340 REPEAT
1350 PROCCOUNT
1360 PROCINTERPRET
1370 T=T+1
1380 PROCCOMPAREDOWNSLOPE
1390 PROCSTEP(S)
1400 UNTIL A%=1
1410 ENDPROC
1420 DEF PROCFINDUP
1430 S=3:D=48:R=32
1440 REPEAT
1450 PROCCOUNT
1460 PROCINTERPRET
1470 T=T+1
1480 PROCCOMPAREUPSLOPE
1490 PROCSTEP(S)
1500 UNTIL B%=1
1510 ENDPROC
1520 DEF PROCCOMPAREUPSLOPE
1530 PRES=0:PAST1=0:PAST2=0:PAST3=0:B%=0
1540 PRES=Step(T-1):PAST1=Step(T-2):PAST2=Step(T-3):PAST3=Step(T-4)
1550 IF PRES<PAST1+(3*SQR(PAST1)) AND PRES>PAST1-(SQR(PAST1)) AND PAST2<PAST1
.5*SQR(PAST1)) AND PAST3<PAST2-(1.5*SQR(PAST2)) AND PRES>Step(1)/2 THEN 1560
E 1580
1560 POSITION2=T-2:SLOPEUP0=PAST2:SLOPEUP1=PAST1:B%=1
1570 PRINT POSITION2    ,SLOPEUP0 ,SLOPEUP1
1580 ENDPROC
1590 DEF PROC5MORESTEPS
1600 FOR MORE= 1 TO 5
1610 S=3:D=48:R=32
1620 REPEAT
1630 PROCCOUNT
1640 PROCINTERPRET
1650 T=T+1
1660 PROCSTEP(S)
1670 NEXT MORE
1680 ENDPROC
1690 DEF PROCAVERAGETOP
1700 SUMTOPL=0:SUMTOPR=0
1710 FOR TPL= 1 TO POSITION1
```

```
1720 SUMTOPL=SUMTOPL+Step(TPL)
1730 NEXT TPL
1740 FOR TPR= POSITION2 TO (T-1)
1750 SUMTOPR=SUMTOPR+Step(TPR)
1760 NEXT TPR
1770 AVERAGE=(SUMTOPL+SUMTOPR)/(TPL+((T-1)-POSITION2))
1780 PRINT "TOP AVERAGE=";AVERAGE
1790 ENDPROC
1800 DEF PROCAVERAGEBOTTOM
1810 min=1000000
1820 FOR val= 1 TO (T-1)
1830 IF Step(val)<min THEN min =Step(val)
1840 NEXT val
1850 PRINT "min ",min
1860 ENDPROC
1870 DEF PROCSETSTDBOTTOM
1880 DIM AV(T)
1890 SDB1=Step(1)/6000
1900 SDB2=0
1910 IF SDB2<0 THEN SDB2=0
1920 C=0
1930 FOR P= 1 TO (T-1)
1940 IF Step(P)<SDB1 AND Step(P)>SDB2 THEN  1960 ELSE AV(P)=0
1950 GOTO 1970
1960 AV(P)=Step(P):C=C+1
1970 NEXT P
1980 SUMAV=0
1990 FOR P=1 TO (T-1)
2000 SUMAV=SUMAV+AV(P)
2010 NEXT P
2020 AVBOTTOM=SUMAV/C
2030 PRINT"BOTTOM AVERAGE=";AVBOTTOM
2040 ENDPROC
2050 DEF PROCSETLIMITS
2060 TopLIMIT=AVERAGE-(18*SQR(AVERAGE))
2070 BOTTOMLIMIT=AVBOTTOM+(12*SQR(AVERAGE))
2080 PRINT"TOPLIMIT",TopLIMIT,"BOTTOMLIMIT",BOTTOMLIMIT
2090 ENDPROC
2100 DEF PROCFINDPOINTS
2110 NoPTS=1:Nopts=1
2120 DIM DWNPTS(T/2):DIM UPPTS(T/2):DWNPTS(0)=1000000
-( 2130 FOR PTS=2 TO (T-1)
EL 2140 IF Step(PTS)<TopLIMIT AND Step(PTS)>BOTTOMLIMIT AND Step(PTS)<Step(PTS-1)
  AND Step(PTS)<DWNPTS(NoPTS-1) THEN 2180
 2150 IF Step(PTS)<TopLIMIT AND Step(PTS)>BOTTOMLIMIT AND Step(PTS)>Step(PTS-1)
 THEN 2200
 2160 NEXT PTS
 2170 GOTO 2230
 2180 DWNPTS(NoPTS)=Step(PTS) :PRINT"DOWNPTS", DWNPTS(NoPTS):NoPTS=NoPTS+1:t=PTS
 -(NoPTS-1)
 2190 GOTO 2150
 2200 UPPTS(Nopts)=Step(PTS):Nopts=Nopts+1:tt=PTS-Nopts+1
 2210 PRINT"UPPTS",UPPTS(Nopts-1)
 2220 GOTO 2160
 2230 ENDPROC
 2240 DEF PROCCHECK
 2250 IF NoPTS=Nopts THEN GOTO 2320
 2260 IF NoPTS>Nopts THEN GOTO 2310
 2270 IF NoPTS<Nopts THEN GOTO 2280
 2280 FOR I= 1 TO NoPTS
```

```
2290 UPPTS(I)=UPPTS(I+1):PRINTUPPTS(I)
2300 NEXT I:tt=tt+(Nopts-NoPTS):Nopts=NoPTS:GOTO 2320
2310 NoPTS=Nopts
2320 ENDPROC
2330 DEF PROCSLOPES
2340 PROCDownIntercept
2350 PROCUpIntercept
2360 Intercept1=Intercept1+t
2370 Intercept2=Intercept2+tt
2380 PRINT"Intercept1= ",Intercept1,"Intercept2= ",Intercept2
2390 PROCLINEIntercept
2400 ENDPROC
2410 DEF PROCDownIntercept
2420 a=0:b=0:c=0:d=0:e=0
2430 FOR h= 1 TO (NoPTS-1)
2440 a=a+DWNPTS(h)
2450 b=b+h
2460 c=c+(h*DWNPTS(h))
2470 d=d+(DWNPTS(h)^2)
2480 NEXT h
2490 h=h-1
2500 a=a/h:b=b/h:c=c/h:d=d/h:e=a*a
2510 slope1=((a*b)-c)/(e-d)
2520 Intercept1=-((d*b)-(a*c))/(e-d)
2530 PRINT "Intercept1= " ,Intercept1
2540 PRINT "slope1= ",slope1
2550 ENDPROC
2560 DEF PROCUpIntercept
2570 a=0:b=0:c=0:d=0:e=0
2580 FOR g= 1 TO (Nopts-1)
2590 a=a+UPPTS(g)
2600 b=b+g
2610 c=c+(g*UPPTS(g))
2620 d=d+(UPPTS(g)^2)
2630 NEXT g
2640 g=g-1
2650 a=a/g:b=b/g:c=c/g:d=d/g:e=a*a
2660 slope2=((a*b)-c)/(e-d)
2670 Intercept2=-((d*b)-(a*c))/(e-d)
2680 PRINT "Intercept2= " ,Intercept2
2690 PRINT "slope2= ",slope2
2700 ENDPROC
2710 DEF PROCLINEIntercept
2720 Midpoint=(Intercept1+((Intercept2-Intercept1)/2))
2730 PRINT"Midpoint=",Midpoint
2740 ENDPROC
2750 DEF PROCCOUNT
2760 PROCsetup
2770 PROCclear
2780 PROCstartpha
2790 VDU3
2800 TIME=0
2810 REPEAT
2820 UNTIL TIME=1300
2830 PROCTRANSFER
2840 ENDPROC
2850 DEF PROCTRANSFER
2860 PROCsetup
2870 PROCrunio
2880 CALL INIT
```

```
2890 ?MEMLOC=00:?(MEMLOC+1)=&48:?STORE=255
2900 VDU3
2910 ENDPROC
2915 ****
2920 DEF PROCsetup
2930 *FX5,2
2940 *FX8,6
2950 *FX7,6
2960 VDU2
2970 VDU1,7
2980 ENDPROC
2990 DEF PROCSETPHA
3000 VDU1,67:FOR tt=1 TO 1000:NEXT tt
3010 VDU1,83:FOR tt=1 TO 1000:NEXT tt
3020 VDU1,80:FOR tt=1 TO 1000:NEXT tt
3030 VDU1,78:FOR tt=1 TO 1000:NEXT tt
3040 VDU1,64:FOR tt=1 TO 1000:NEXT tt
3050 VDU1,43:FOR tt=1 TO 1000:NEXT tt
3060 VDU1,78:FOR tt=1 TO 1000:NEXT tt
3070 VDU1,65:FOR tt=1 TO 1000:NEXT tt
3080 VDU1,78:FOR tt=1 TO 1000:NEXT tt
3090 VDU1,90:FOR tt=1 TO 1000:NEXT tt
3100 VDU1,49:FOR tt=1 TO 1000:NEXT tt
3110 VDU1,48:FOR tt=1 TO 1000:NEXT tt
3120 VDU1,78:FOR tt=1 TO 1000:NEXT tt
3130 ENDPROC
3140 DEFPROCSETIO
3150 VDU1,67:FOR tt=1 TO 1000:NEXT tt
3160 VDU1,83:FOR tt=1 TO 1000:NEXT tt
3170 VDU1,73:FOR tt=1 TO 1000:NEXT tt
3180 VDU1,78:FOR tt=1 TO 1000:NEXT tt
3190 VDU1,64:FOR tt=1 TO 1000:NEXT tt
3200 VDU1,88:FOR tt=1 TO 1000:NEXT tt
3210 VDU1,78:FOR tt=1 TO 1000:NEXT tt
3220 VDU1,64:FOR tt=1 TO 1000:NEXT tt
3230 VDU1,49:FOR tt=1 TO 1000:NEXT tt
3240 VDU1,78:FOR tt=1 TO 1000:NEXT tt
3250 VDU1,64:FOR tt=1 TO 1000:NEXT tt
3260 VDU1,85:FOR tt=1 TO 1000:NEXT tt
3270 VDU1,78:FOR tt=1 TO 1000:NEXT tt
3280 VDU1,64:FOR tt=1 TO 1000:NEXT tt
3290 VDU1,71:FOR tt=1 TO 1000:NEXT tt
3300 VDU1,78:FOR tt=1 TO 1000:NEXT tt
3310 ENDPROC
3320 DEF PROCclear
3330 VDU1,67:FOR tt=1 TO 1000:NEXT tt
3340 VDU1,48:FOR tt=1 TO 1000:NEXT tt
3350 VDU1,62:FOR tt=1 TO 1000:NEXT tt
3360 VDU1,65:FOR tt=1 TO 1000:NEXT tt
3370 ENDPROC
3380 DEF PROCstartpha
3390 VDU1,67:FOR tt=1 TO 1000:NEXT tt
3400 VDU1,82:FOR tt=1 TO 1000:NEXT tt
3410 VDU1,80:FOR tt=1 TO 1000:NEXT tt
3420 ENDPROC
3430 DEF PROCrunio
3440 VDU1,67:FOR tt=1 TO 1000:NEXT tt
3450 VDU1,82:FOR tt=1 TO 1000:NEXT tt
3460 VDU1,73:FOR tt=1 TO 1000:NEXT tt
3470 VDU3
```

```
3480 ENDPROC
3485 ****
3490 DEF PROCINTERPRET
3500 MEM=18922
3510 FOR mem=MEM TO MEM+12
3520 IF ?(mem)>=48 AND ?(mem)<=57 THEN 3530 ELSE 3600
3530 A$=A$+CHR$(?(mem))
3540 NEXT mem
3550 Step(T)=VAL(A$)
3560 A$=" "
3570 PRINT Step(T),T
3580 MEM=MEM+31
3590 GOTO 3720
3600 IF ?(mem)=69 OR ?(mem)=43 OR ?(mem)=46 OR ?(mem)=32 THEN 3530 ELSE 36
3610 GOTO 3720
3620 PROCclearMEM
3630 PROCsetup
3640 PROCclear
3650 PROCstartpha
3660 VDU3
3670 TIME=0
3680 REPEAT
3690 UNTIL TIME=1300
3700 PROCTRANSFER
3710 GOTO 3500
3720 PROCclearMEM
3730 ENDPROC
3740 DEF PROCclearMEM
3750 MEM=18600
3760 REPEAT
3770 ?MEM=0
3780 MEM=MEM+1
3790 UNTIL MEM=19000
3800 ENDPROC
3810 DEF PROCVARIABLES
3820 CONREG=&FE08:STATREG=&FE08:RECREG=&FE09
3830 MEMLOC=&70:STORE=&72:NUMCHR=&73:COMPARE1=&74:COMPARE2=&75
3840 ?MEMLOC=00:?(MEMLOC+1)=&48:?STORE=255:?COMPARE1=&49:?COMPARE2=&F7
3850 ENDPROC
3860 DEF PROCASSEMB
3870 FOR N=0 TO 2 STEP 2
3880 P%=30000
3890 [OPT N
3900.INIT   LDA #03
3910        STA CONREG
3920        LDA #&12
3930        STA CONREG
3940.LOOP   LDY #00
3950        LDA #01
3960        BIT STATREG
3970        BEQ LOOP
3980        LDA RECREG
3990        CMP #22
4000        BEQ LOOP
4010        CMP #23
4020        BEQ LOOP
4030        CMP #13
4040        BEQ LOOP
4050        CMP #0
4060        BEQ LOOP
```

```
4070          CMP #10
4080          BEQ LOOP
4090          BEQ LOOP
4100          CMP #25
4110          BEQ LOOP
4120          LDY STORE
4130          STA (MEMLOC),Y
4140          CMP #04
4150          BEQ QUIT
4160          INY
4170          STY STORE
4180          CPY NUMCHR
4190          BEQ LOOP2
4200          JMP COMP
4210          JMP INIT
4220.LOOP2    INC (MEMLOC +1)
4230          JMP INIT
4240.COMP     LDX (MEMLOC +1)
4250          CPX COMPARE1
4260          BEQ CONP
4270          JMP INIT
4280.CONP     LDX STORE
4290          CPX COMPARE2
4300          BEQ QUIT
4310          JMP INIT
4320.QUIT     RTS
4330]
4340 NEXT N
4350 ENDPROC
```

MCASCAN

This is a BBC microcomputer program to scan an object using the EG & G Ortec 7100 multichannel analyser to count detected X-ray photons. The program may be loaded into the BBC microcomputer memory and run by a CHAIN command in the MDPOINT program. After each scanning step, the X-ray photon count data is transferred from the multichannel analyser memory to the BBC microcomputer memory, and the multichannel analyser memory is cleared whilst the x-coordinate table is moved to the next step.

*****

The main part of the program is listed at lines 20 to 130, and is executed in line number order. The main controls for the scanning coordinate table are PROCLOADDATA and PROCSCAN, defined at lines 140 to 190, and 200 to 390.

PROCLOADDATA loads the BBC microcomputer memory from the file on disc, NUMBERS, containing the scan settings such as linear and angular step size and number of steps. The BBC and multichannel analyser are set up ready to communicate with one another by PROCVARIABLES, PROCASSEMB, PROCsetup, PROCSETPHA, and PROCSETIO, defined at lines 1280 to 1600 and 2120 to 2660, as in the FINDMIN program.

PROCSCAN directs the entire scanning of the object, and counting and collection of X-ray photon count data for the BBC microcomputer. It includes five procedures to which it diverts as required, and some of these procedures divert to other procedures, defined at lines 400 to 1270, and 1610 to 2110.

PROCRETURN, defined at lines 990 to 1030, sets the scanning coordinate table at the starting position when the complete scan is finished.

```
  5 REM ****MCASCAN****
 10 REM COUNTER PROGRAM TO SCAN AN OBJECT
 20 CLEAR:CLS
 30 PROCLOADDATA
 40 DIM COUNT1(8,2,NUMSTEPS):DIM STORE(8,NUMSTEPS):REF=-1
 50 PROCVARIABLES
 60 PROCASSEMB
 70 PROCsetup
 80 PROCSETPHA
 90 PROCSETIO
100 VDU3
110 PROCSCAN
120 PROCRETURN
130 END
135 ****
140 DEF PROCLOADDATA
150 X=OPENIN"NUMBERS"
160 INPUT #X,Z,NUMSTEPS,NUMROTS,SIZESTEP,EMAX,TT%
170 PRINTZ,NUMSTEPS,NUMROTS,SIZESTEP,EMAX,TT%
180 CLOSE#X
190 ENDPROC
200 DEF PROCSCAN
210 FOR scan%=0 TO NUMROTS-1
220 D=124:R=108
230 dir=0
240 PROCSTEPX
250 S=600/NUMROTS
260 PROCROTATE
270 S=(SIZESTEP*48)+11:D=60:R=44
280 PROCSTEP(S)
290 scan%=scan%+1
300 dir=1
310 PROCSTEPX
320 PROCINVERT
330 PROCSAVEDATAX
340 S=(SIZESTEP*48)+11:D=124:R=108
350 PROCSTEP(S)
360 S=600/NUMROTS
370 PROCROTATE
380 NEXT scan%
390 ENDPROC
395 ****
400 DEF PROCSTEP(S)
410 B=&FE60
420 ?(B+2)=255
430 FOR X=1 TO S
440 ?B=D
450 Q=TIME+5
460 REPEAT
470 UNTIL TIME>=Q
480 ?B=R
490 Q=TIME+5
500 REPEAT
510 UNTIL TIME>=Q
520 NEXT X
530 ENDPROC
540 DEF PROCSTEPX
550 CLS
560 PRINT TAB(4,2)"ANGLE=";scan%*180/NUMROTS"DEGREES"
```

```
570 PRINT TAB(7,3)"step"
580 PRINT TAB(15,3)"COUNT"
590 FOR step%=1 TO NUMSTEPS
600 S=SIZESTEP*48
610 IF step%=1 AND dir=0 THEN S=(SIZESTEP*48)+1
620 PROCCOUNT
630 PROCINTERPRET
640 PROCSTEP(S)
650 NEXT step%
660 ENDPROC
670 DEF PROCSAVEDATAX
680 REF=REF+1
690 NAME$="DATA"+STR$(scan%-REF)
700 X=OPENOUT NAME$
710 FOR H%=0 TO 1
720 FOR G%=1 TO NUMSTEPS
730 FOR F%=1 TO 8
740 PRINT #X,COUNT1(F%,H%,G%)
750 PRINT COUNT1(F%,H%,G%)
760 NEXT F%
770 NEXT G%
780 NEXT H%
790 CLOSE#X
800 ENDPROC
810 DEF PROCROTATE
820 D=14:R=12
830 PROCSTEP(S)
840 ENDPROC
850 DEF PROCINVERT
860 IF dir=0 THEN 980
870 FOR R%= 1 TO NUMSTEPS
880 FOR QQ%=1 TO 8
890 STORE(QQ%,NUMSTEPS-R%+1)=COUNT1(QQ%,1,R%)
900 NEXT QQ%
910 NEXT R%
920 FOR W%= 1 TO NUMSTEPS
930 FOR QQ%=1 TO 8
940 COUNT1(QQ%,1,W%)=STORE(QQ%,W%)
950 PRINT COUNT1(QQ%,1,W%)
960 NEXT QQ%
970 NEXT W%
980 ENDPROC
990 DEF PROCRETURN
1000 S=600+(600/NUMROTS)
1010 PROCSTEP(S)
1020 CLS:PRINT TAB(2,12) "SCAN FINISHED AND ROTOR ANGLE=0 DEGREES
1030 ENDPROC
1040 DEF PROCCOUNT
1050 PROCsetup
1060 PROCclear
1070 PROCstartpha
1080 VDU3
1090 TIME=0
1100 REPEAT
1110 UNTIL TIME=6300
1120 PROCTRANSFER
1130 ENDPROC
1140 DEF PROCTRANSFER
1150 PROCsetup
1160 PROCrunio
```

```
1170 CALL INIT
1180 ?MEMLOC=0:?(MEMLOC+1)=&40:?STORE=255
1190 VDU3
1200 ENDPROC
1210 DEF PROCsetup
1220 *FX5,2
1230 *FX8,6
1240 *FX7,6
1250 VDU2
1260 VDU1,7
1270 ENDPROC
1280 DEF PROCSETPHA
1290 VDU1,67:FOR tt=1 TO 1000:NEXT tt
1300 VDU1,83:FOR tt=1 TO 1000:NEXT tt
1310 VDU1,80:FOR tt=1 TO 1000:NEXT tt
1320 VDU1,78:FOR tt=1 TO 1000:NEXT tt
1330 VDU1,64:FOR tt=1 TO 1000:NEXT tt
1340 VDU1,43:FOR tt=1 TO 1000:NEXT tt
1350 VDU1,78:FOR tt=1 TO 1000:NEXT tt
1360 VDU1,65:FOR tt=1 TO 1000:NEXT tt
1370 VDU1,78:FOR tt=1 TO 1000:NEXT tt
1380 VDU1,88:FOR tt=1 TO 1000:NEXT tt
1390 VDU1,54:FOR tt=1 TO 1000:NEXT tt
1400 VDU1,48:FOR tt=1 TO 1000:NEXT tt
1410 VDU1,78:FOR tt=1 TO 1000:NEXT tt
1420 ENDPROC
1430 DEFPROCSETIO
1440 VDU1,67:FOR tt=1 TO 1000:NEXT tt
1450 VDU1,83:FOR tt=1 TO 1000:NEXT tt
1460 VDU1,73:FOR tt=1 TO 1000:NEXT tt
1470 VDU1,78:FOR tt=1 TO 1000:NEXT tt
1480 VDU1,64:FOR tt=1 TO 1000:NEXT tt
1490 VDU1,88:FOR tt=1 TO 1000:NEXT tt
1500 VDU1,78:FOR tt=1 TO 1000:NEXT tt
1510 VDU1,64:FOR tt=1 TO 1000:NEXT tt
1520 VDU1,49:FOR tt=1 TO 1000:NEXT tt
1530 VDU1,78:FOR tt=1 TO 1000:NEXT tt
1540 VDU1,64:FOR tt=1 TO 1000:NEXT tt
1550 VDU1,85:FOR tt=1 TO 1000:NEXT tt
1560 VDU1,78:FOR tt=1 TO 1000:NEXT tt
1570 VDU1,64:FOR tt=1 TO 1000:NEXT tt
1580 VDU1,71:FOR tt=1 TO 1000:NEXT tt
1590 VDU1,78:FOR tt=1 TO 1000:NEXT tt
1600 ENDPROC
1610 DEF PROCclear
1620 VDU1,67:FOR tt=1 TO 1000:NEXT tt
1630 VDU1,48:FOR tt=1 TO 1000:NEXT tt
1640 VDU1,62:FOR tt=1 TO 1000:NEXT tt
1650 VDU1,65:FOR tt=1 TO 1000:NEXT tt
1660 ENDPROC
1670 DEF PROCstartpha
1680 VDU1,67:FOR tt=1 TO 1000:NEXT tt
1690 VDU1,82:FOR tt=1 TO 1000:NEXT tt
1700 VDU1,80:FOR tt=1 TO 1000:NEXT tt
1710 ENDPROC
1720 DEF PROCrunio
1730 VDU1,67:FOR tt=1 TO 1000:NEXT tt
1740 VDU1,82:FOR tt=1 TO 1000:NEXT tt
1750 VDU1,73:FOR tt=1 TO 1000:NEXT tt
1760 VDU3
```

```
1770 ENDPROC
1780 DEF PROCINTERPRET
1790 MEM=18705
1800 FOR NUM=1 TO 8
1810 FOR mem=MEM TO MEM+12
1820 IF ?(mem)>=48 AND ?(mem)<=57 THEN 1830 ELSE 1910
1830 A$=A$+CHR$(?(mem))
1840 NEXT mem
1850 COUNT1(NUM,dir,step%)=VAL(A$)
1860 A$=" "
1870 PRINT COUNT1(NUM,dir,step%),NUM,dir,step%
1880 MEM=MEM+31
1890 NEXT NUM
1900 GOTO 2030
1910 IF ?(mem)=69 OR ?(mem)=43 OR ?(mem)=46 OR ?(mem)=32 THEN 1830 ELSE 1930
1920 GOTO 2030
1930 PROCclearMEM
1940 PROCsetup
1950 PROCclear
1960 PROCstartpha
1970 VDU3
1980 TIME=0
1990 REPEAT
2000 UNTIL TIME=6300
2010 PROCTRANSFER
2020 GOTO 1790
2030 PROCclearMEM
2040 ENDPROC
2050 DEF PROCclearMEM
2060 MEM=18600
2070 REPEAT
2080 ?MEM=0
2090 MEM=MEM+1
2100 UNTIL MEM=19000
2110 ENDPROC
2120 DEF PROCVARIABLES
2130 CONREG=&FE08:STATREG=&FE08:RECREG=&FE09
2140 MEMLOC=&70:STORE=&72:NUMCHR=&73:COMPARE1=&74:COMPARE2=&75
2150 ?MEMLOC=00:?(MEMLOC+1)=&48:?STORE=255:?COMPARE1=&49:?COMPARE2=&F7
2160 ENDPROC
2170 DEF PROCASSEMB
2180 FOR N=0 TO 2 STEP 2
2190 P%=30000
2200[OPT N
2210.INIT   LDA #03
2220        STA CONREG
2230        LDA #&12
2240        STA CONREG
2250.LOOP   LDY #00
2260        LDA #01
2270        BIT STATREG
2280        BEQ LOOP
2290        LDA RECREG
2300        CMP #22
2310        BEQ LOOP
2320        CMP #23
2330        BEQ LOOP
2340        CMP #13
2350        BEQ LOOP
2360        CMP #0
```

```
2370          BEQ LOOP
2380          CMP #10
2390          BEQ LOOP
2400          BEQ LOOP
2410          CMP #25
2420          BEQ LOOP
2430          LDY STORE
2440          STA (MEMLOC),Y
2450          CMP #04
2460          BEQ QUIT
2470          INY
2480          STY STORE
2490          CPY NUMCHR
2500          BEQ LOOP2
2510          JMP COMP
2520          JMP INIT
2530.LOOP2    INC (MEMLOC +1)
2540          JMP INIT
2550.COMP     LDX (MEMLOC +1)
2560          CPX COMPARE1
2570          BEQ CONP
2580          JMP INIT
2590.CONP     LDX STORE
2600          CPX COMPARE2
2610          BEQ QUIT
2620          JMP INIT
2630.QUIT     RTS
26401
2650 NEXT N
2660 ENDPROC
```

COMPILE

This program is used to convert random access numbers which the X-ray photon count data in the BBC microcomputer memory to ASCII code for transfer to the VAX 11/785 computer in wich the image of an object which has been scanned is reconstructed.

*****

Lines 20 to 60 select a single or dual disc drive for the X-ray photon count data and the ASCII code. Lines 90 to 210 are to set up a file in the BBC microcomputer memory of dimension 1680 for the X-ray photon count data C and the corresponding rotation step R and linear step S, COU, in the scan, of dimension 80, 40 angular steps and 40 linear steps.

Lines 310 to 350 is the special program to convert the random access numbers to ASC11 code, held in a read only memory in the BBC microcomputer.

The program is loaded into the BBC microcomputer memory and listed. Line 310 is selected and the name of the file, "FILNAME", on disc holding the random access numbers is entered after *SPOOL, so that the SPOOL program can select this file. The program is run and the BBC microcomputer prints the X-ray photon count numbers for rotation R and linear step S to the monitor screen as they are compiled to ASCII code. A key is pressed to save the ASCII code data, on a new disc if required, as suggested at line 220.

```
  5 REM ****COMPILE****
 10 PROGRAM TO CONVERT RANDOM ACCESS NUMBERS TO ASCII CODE
 20 CLS:PRINT TAB(7,9) "SINGLE OR DUAL DRIVE  S/D":Q$=GET$
 30 IF Q$<>"S" AND Q$<>"D" THEN GOTO 20
 40 IF Q$="S" THEN 50 ELSE 60
 50 CLS:PRINT TAB(7,9) "PUT DATA DISK IN DRIVE no.0":GOTO 80
 60 CLS:PRINT TAB(7,9) "PUT DATA DISK IN DRIVE no.1"
 70 *DRIVE 1
 80 REM PROGRAM TO COMPILE SINGLE DATA FILES AND EQUIVALENT THICKNESS FILES
 90 DIM C(1680) :DIM COU(80)
100 PRINT TAB(7,11)"IS DISC IN DRIVE Y/N":Q$=GET$
110 IF Q$="Y" THEN GOTO 120 ELSE GOTO 100
120 FOR R%= 1 TO 20
130 PRINT R%
140 NAME$="DATA"+STR$(R%)
150 X=OPENIN NAME$
160 FOR S%=0 TO 79
170 INPUT #X,COU(S%)
180 C((R%*80)+S%)=COU(S%)
190 NEXT S%
200 CLOSE #X
210 NEXT R%
220 PRINT "PUT NEW DISC IN DRIVE"
230 PRINT
240 PRINT
250 PRINT "HIT ANY KEY TO SAVE DATA"
260 Q$=GET$
270 PROCSAVEDATA
280 *DRIVE 0
290 END
300 DEF PROCSAVEDATA
310 *SPOOL FILNAME
320 FOR F=80 TO 1679
330 PRINT C(F)
340 NEXT F
350 *SPOOL
360 ENDPROC
```

ROISELECT

This VAX 11/785 program is for sorting the ASCII code serial data, the X-ray photon count data, sent from the BBC microcomputer into an array of eight blocks of data corresponding to the eight regions of interest for imaging the three analyte elements 46Palladium, 47Silver, 48Cadmium.

ROIEXTRAPOLATE

This VAX 11/785 program is used to calculate the equivalent thickness of an analyte element for each scan step by extrapolating the X-ray photon count data in pairs of regions of interest on either side of the absorbtion edge of the element to the absorbtion edge. The extrapolated value of the equivalent thickness of the analyte element is then used in the reconstruction program.

*****

The ASCII code file containing the X-ray photon count data in eight arrays is input to the VAX 11/785 memory at line 150 and a pair of regions of interest on either side of an absorbtion edge is selected for calculation at lines 200 to 240. I_o, the incident X-ray beam photon count is calculated at line 250, and $\ln(I_o/I) = \mu t$ = ratio is calculated at line 270. The equivalent thickness is calculated from the extrapolation equation at line 310 and put into the equivalent thickness file at line 320.

```
 50 !ROISELECT
100 !To sort serial data into 8 Regions Of Interest
110 input "input data file name", name$
120 input "input file title name for roi's",names$
130 open name$ for input as file #9
140 for times= 1 to 8
150 nmes$=names$+str$(times)+".dat"
160 open nmes$ for output as file #times
170 next times
180 for t= 1 to 1600
190 for r=1 to 8
200 input #9,cat
210 print cat,r,t
220 print #r,cat
230 next r
240 next t
250 close #9
260 for t=1 to 8
270 close#t
280 next t
```



```
 50 !ROIEXTRAPOLATE
100 !To extrapolate to an absorbtion edge of an element
110 dim roi(40),ratio(160),eqth(40)
120 input"general name for files",name$
130 input" file name for equivalent thicknesses",nme$
140 open nme$ for output as file #9
150 input " regions of interest first/last", fir, last
160 for t= fir to last
170 names$=name$+str$(t)+".dat"
180 open names$ for input as file #t
190 next t
200 for s=1 to 40
210 for r=0 to 3
220 for t=1 to 40
230 input#(r+fir),roi(t)
240 next t
250 avroi=(roi(1)+roi(2)+roi(39)+roi(40))/4
260 for g= 1 to 40
270 ratio((r*40)+t)=log(avroi/roi(g))
280 next g
290 next r
300 for t=1 to 40
310 eqth(t)=((((ratio(120+t)-ratio(80+t))/.5)*(-.34)+ratio(t+80))
-ratio(t))/.68)*.32+ratio(t+40)))/4.95
320 print #9,eqth(t)
330 next t
340 next s
350 close#9
360 for d= fir to last
370 close#d
380 next d
```

-(((ratio(40+t)

CALAREA40

This VAX 11/785 computer program is for calculating the areas of overlap between the pixels of the 40 x 40 reconstruction grid and the simulated X-ray beam path. The width of the beam path is the same as the size of the pixels. The overlap areas, about 1.3×10^4, are stored in a disc file in about 5500 blocks of memory space, and are read into the computer memory one at a time when called by the Algebraic Reconstruction Technique program. The file name is AREA40.DAT.

******

Figure A.5 shows the simulated X-ray beam path at a particular step S intercepting at an angle θ a pixel P of the (k,j) reconstruction grid set against (x,y) coordinates. The area of overlap between the beam path and the pixels is calculated to 0.02 of a pixel.

According to the geometry of the drawings the equations of the edges of the beam path are:

$$x_A = x\tan\theta + CEPTA$$

$$y_A = x\tan\theta + CEPTB$$

at lines 330 and 340 of the computer program, where θ is the slope of the lines, $\theta = \pi R/40$ for 40 rotational steps R, and CEPTA, CEPTB are the intercepts of y_A, y_B with the ordinate. For a given angle of rotation R, beam step S, and k column of the reconstruction grid, the program steps down the grid from J = 0, one pixel at a time, through the column of 40 pixels until it reaches the pixel p.

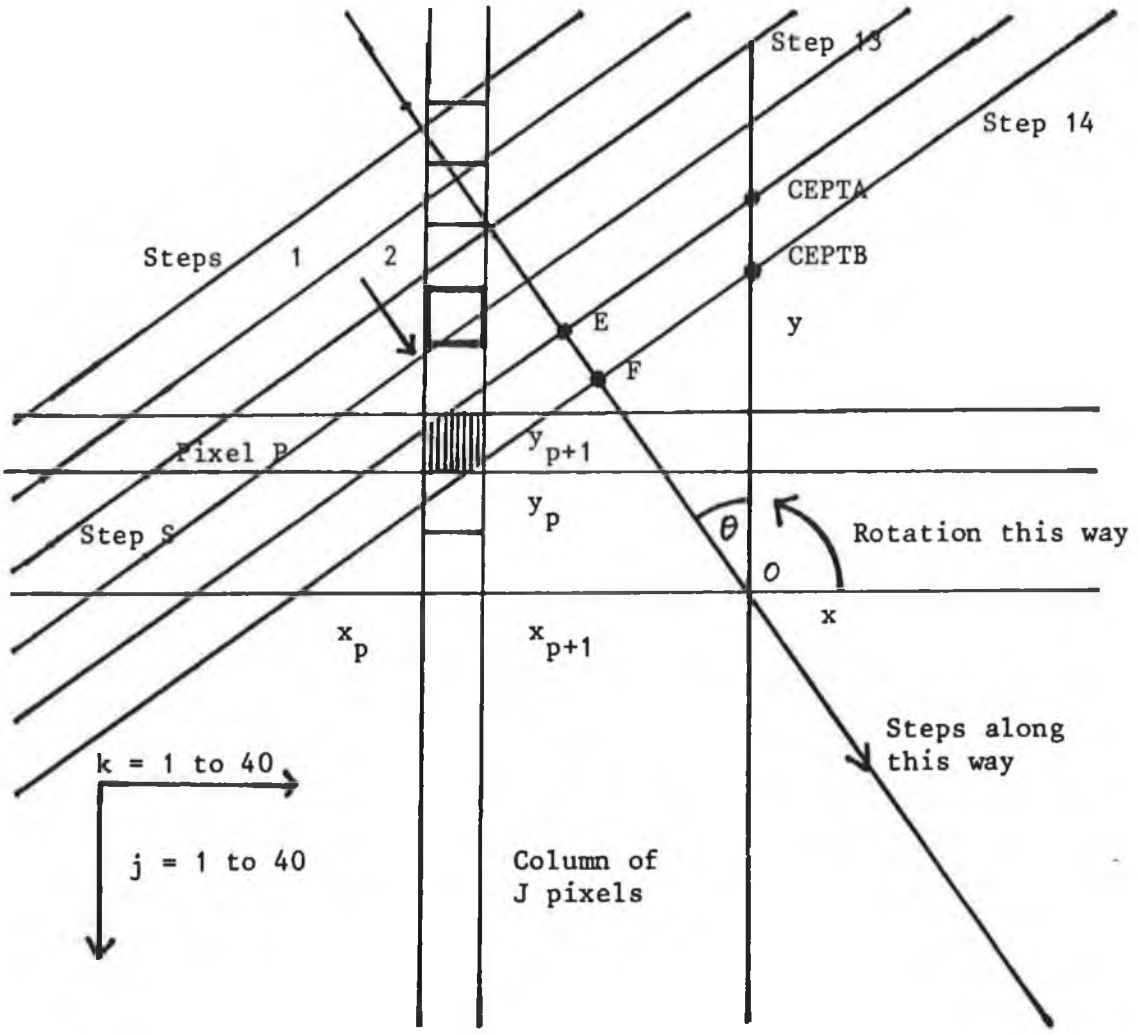

$$y_A = x\tan\theta + CEPTA$$

$$y_B = x\tan\theta + CEPTB$$

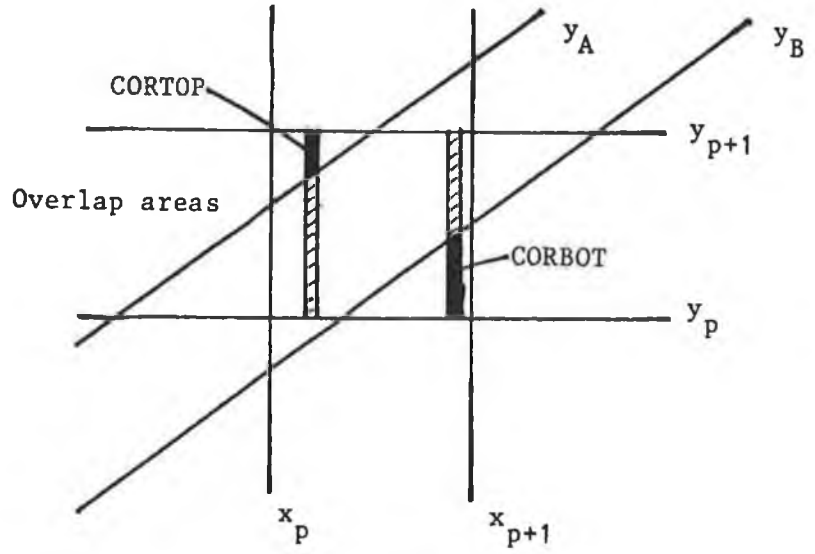

To calculate the overlap areas to 2% by CALAREA40.

FIGURE A.5

$E0 = (21 - S)$ and $F0 = (20 - S)$

Thus, at lines 190 and 210, CEPTA = $(21 - S)/\cos\theta$ and CEPTB = $(20 - 5)/\cos\theta$. $\tan\theta$ is an odd function so $\tan(-\theta) = -\tan\theta$, and $\tan\theta$ is set equal to $-\tan\theta$ at lines 170 and 180. $\cos\theta$ is an even function so $\cos(-\theta) = \cos\theta$. Thus when $\cos\theta$ is negative CEPTA is -CEPTA and CEPTB is -CEPTB, at lines 200 and 220.

The pixel p, of side unity, is bounded by the lines whose equations are x_p, x_{p+1} and y_p, y_{p+1}, so that the top and bottom of the pixel is y_p and y_{p+1}, and the sides are x_p and x_{p+1}.

$$\text{If} \quad y_p > x_p \tan\theta + \text{CEPTA}$$

$$\text{and} \quad y_p > x_{p+1} \tan\theta + \text{CEPTA}$$

then the bottom edge of the pixel is above the line y_A, or in stepping j down one pixel at a time in the FOR NEXT loop between lines 240 and 490, the bottom of the pixel has not reached the top edge of the beam path, so J is stepped down to the next pixel, at lines 270 and 490.

$$\text{If} \quad y_{p+1} < x_p \tan\theta + \text{CEPTB}$$

$$\text{and} \quad y_{p+1} < x_{p+1} \tan\theta + \text{CEPTB}$$

then the top edge of the pixel is below the line y_B, or in stepping J down one pixel at a time, the top edge of the pixel is below the lower edge of the beam path, so j is stepped down to the next pixel, at lines 280 and 490.

If these two conditions are not true, then the beam path defined by the lines y_A and y_B intercepts the pixel p, and the variable AREA is set equal to zero at line 290. The area of overlap of the beam with the pixel p is summed in vertical strips 0.02 times the width of the pixel, bounded by the edges of the beam y_A, y_B, and the edges of the pixel x_p, x_{p+1}. This is summed in a FOR NEXT loop at lines 300 to 430 starting at $(x_p + 0.01)$ and finishing at $(x_p + 0.99)$ in 50 steps of width 0.02, at line 300.

The program uses the variables CORTOP and CORBOT for the area of width 0.02 enclosed between the edge of the pixel and the edge of the beam which is to be excluded from the overlap area, or the correction to the overlap area.

If $y > y_{p+1}$ and $y_B > y_{p+1}$, then the excluded area CORTOP = 0 at line 350 because y_A is above and y_B is below the top of the pixels, so the top of the pixel lies within the beam path.

If $y_A \leq y_{p+1}$, and $y_A \geq y_p$, then Y_A lies between y_p and y_{p+1}, so CORBOT = $(y_{p+1} - y_A)$x0.02, at line 360, and so the area overlap of this slice is 1 x 0.02 - CORTOP.

If $y_B \geq y_p$ and $y_B \leq y_{p+1}$, the y_B lies between y_p and y_{p+1}, so CORTOP = $(y_B - y_p)$ x 0.02 at line 370 and so the overlap area of this slice is 1 x 0.02 - CORBOT.

If $y_B < y_p$ and $y_A > y_p$, then the excluded area COROBT = 0 because y_B lies between the top and the bottom of the pixel, at line 380.

The area of overlap of each slice is

1 x 0.02 - CORTOP - CORBOT, at line 390.

If $y_B > y_{p+1}$ and if $y_A < y_p$, the SLICEAREA is zero because the beam path is either above or below the pixel p at lines 400 and 410.

The area of each slice is added to the previous ones for each 0.02 step that x makes to sum the area of overlap of the beam path with the pixel p by

AREA = AREA + SLICEDAREA, at line 420.

If the AREA is zero then j steps down to the next pixel at line 490. The overlap area of each pixel p is stored in a string array AREA$ at line 450.

When j = 40, K is incremented by 1 to select the next column in the FOR NEXT loop between lines 230 and 500, j steps down this column 1 pixel at a time and the program calculates the area of overlap between the beam path and its next intersection with a pixel p. When Θ is a large angle, the beam path intercepts many pixels.

A is a line counter or file position number for AREA$, set to 0 at line 120 and incremented by 1 at line 480 as each overlap area is calculated. The zeros of the array are not stored in memory: there are about $2N^3$ finite overlap areas and about N^4 zeros, where N is the grid pitch.

The VAX 11/785 computer prints the string array as

AREA, J, K, S, R

at lines 450 and 460 as the program proceeds. When the program is completed, the computer prints out

100, 1, 1, 1, 1,

at line 550 to show that all of the overlap areas have been calculated, and the file is closed at line 560.

The computer calculations were checked and validated for several overlap areas of the beam path with pixel p for different angles θ and step s, against a large scale graph grid in which 1mm squares were manually counted.

```
 50 !CALAREA40
100 !Overlap Areas for  40 steps and 40 rotations
110 OPEN "AREA40.DAT" FOR OUTPUT AS FILE #1
120 A%=0
130 FOR W%=0 TO 1
140 FOR R%=0 TO 19
150 THETA=PI*R%/40
160 FOR S%= 1 TO 40
170 SLOPE=TAN(THETA)
180 IF SLOPE<0 THEN SLOPE=-SLOPE
190 CEPTA=(21-S%)/COS(THETA)
200 IF COS(THETA)<0 THEN CEPTA=-CEPTA
210 CEPTB=(20-S%)/COS(THETA)
220 IF COS(THETA)<0 THEN CEPTB=-CEPTB
230 FOR K%=1 TO 40
240 FOR J%=1 TO 40
250 XP=(K%-21)
260 YP=(20-J%)
270 IF YP>SLOPE*XP+CEPTA AND YP>SLOPE*(XP+1)+CEPTA THEN GOTO 490
280 IF YP+1<SLOPE*XP+CEPTB AND YP+1<SLOPE*(XP+1)+CEPTB THEN GOTO 490
290 AREA=0
300 FOR X=XP+0.01 TO XP+0.99 STEP 0.02
310 CORTOP=0
320 CORBOT=0
330 YA=SLOPE*X+CEPTA
340 YB=SLOPE*X+CEPTB
350 IF YA>YP+1 AND YB>YP+1 THEN CORTOP =0
360 IF YA<=YP+1 AND YA>=YP THEN CORTOP=(YP+1-YA)*0.02
370 IF YB>=YP AND YB<=YP+1 THEN CORBOT=(YB-YP)*0.02
380 IF YB<YP AND YA<YP THEN CORBOT=0
390 SLICEAREA=0.02-CORTOP-CORBOT
400 IF YB>YP+1 THEN SLICEAREA=0
410 IF YA<YP THEN SLICEAREA=0
420 AREA=AREA+SLICEAREA
430 NEXT X
440 IF AREA =0 THEN GOTO 490
450 IF W%=0 THEN AREA$=STR$(AREA)+","+STR$(K%)+","+STR$(J%)+","+STR$(S%)+","+STR
$(R%)
460 IF W%=1 THEN AREA$=STR$(AREA)+","+STR$(J%)+","+STR$(41-K%)+","+STR$(S%)+","+
STR$(R%+20)
470 PRINT #1,AREA$
480 A%=A%+1
490 NEXT J%
500 NEXT K%
510 NEXT S%
520 PRINT R%
530 NEXT R%
540 NEXT W%
550 PRINT #1,"100,1,1,1,1"
560 CLOSE #1
570 END
```

RECON4ONTIMES

This VAX 11/785 computer program is to reconstruct the image of an object scanned by X-rays by the Algebraic Reconstruction Technique.

For differential absorbtion edge tomography the program takes the extrapolated values of the equivalent thickness of an analyte element from a selected file which has been named by the ROIEXTRAPOLATE program, and the calculated values of the areas of overlap between the simulated X-ray beam path and the pixels in the reconstruction grid held in the file AREA40.DAT, and combines the two sets of data by means of an algorithm to form the image data, from which the image of the object can be displayed.

For computer axial tomography scanning of an object, this program takes the equivalent thickness data held in the file catdata.dat of the scanned object calculated by the program INVERTDATA and the overlap areas held in AREA40.DAT and combines the two sets of data by means of an algorithm and sends the image data to an image storage file, from which the image of the scanned object may be displayed.

*****

The main part of the program is listed between lines 110 and 390 following which there are nine subroutines between lines 400 and 1180. The algorithm for calculating the concentration of the analyte element is contained in lines 330 to 390.

The program opens the input file FILENAME.dat at line 130 which is entered into the program at the start. For the Algebraic Reconstruction Technique this is the name of the file chosen in the ROIEXTRAPOLATE program which contains the values of the equivalent thickness of the analyte element extrapolated to its X-ray K absorbtion edge, $\ln(I_o/I) = \mu t$.

For computer axial tomography reconstruction the name of the file is catdata.dat which contains the values of the equivalent thickness of the object at each scan step calculated by the INVERTDATA program, $\ln(I_o/I) = \mu t$.

The data from FILENAME.dat is stored in an array lambda(s,r) at line 170, in the FOR NEXT loop between lines 150 and 210. All of the equivalent thickness data, $\mu t = \ln(I_o/I)$ is added together using the variable all with x as a dummy variable, at line 190. The total is divided by 64000 at line 230 to give a resultant average called all, which is allocated to each pixel in the image reconstruction array in the FOR NEXT loop between lines 240 and 280 as the estimated concentrations, f(k,j) = all, of each pixel at line 260.

The maximum number of image iterations for image reconstruction is chosen as 20 which is set at line 290. The program repeats the image reconstruction by N image iterations until the average maximum concentration of analyte element estimated by the program is within 1% of the measured maximum concentratin as shown at lines 300 and 370, 380. This calculation is made in GOSUB (1020, 1180) selected in GOSUB (580, 600) at line 360. Then a, which is a counter, is set at 0 at line 310, and increments by 1 each time the beam path moves by 1 step s. Also at

line 310, s is set at 1 for the first step and the scanning position start, rotation r = 0.

The program opens the file AREA40.DAT which contains the areas of overlap between the beam path and the pixels of the reconstruction grid at line 320, and they are input one at a time in the input loop between lines 330 and 380 to the computer memory in a string array a$ at line 340 made up of the variables v, k, j, s, r, where v is the area of overlap between the beam path at the s step, r rotation and the k,j pixel in the reconstruction grid. Each time a line a$ is input to the computer memory the beam path step and rotation number s,r are checked at line 350 with the previous one, and if it is the same, which is the same beam path, the program diverts GOSUB (400, 440) and then GOSUB (620, 730) to decode the areas aS. This section of the program looks at a$ along the length of the string to find the position of the commas, and sets the variables k, j, s to the corresponding values in the string. The variable b$ at line 650 is used to read each character in the a string in turn. Each number is selected one at a time by diverting GOSUB (740, 790). The program returns to line 410 and diverts GOSUB (800, 830) to sum the concentrations of analyte element for this beam path if the end of the array has not been reached. Thus at line 810

$$SUM1 = SUM1 + (W*f(k,j))$$

where W is the overlap area of the k,j pixel, and f(k,j) is the concentration of the analyte element in that pixel estimated by the algorithm, and

$$SUM2 = SUM2 + W^2$$

SUM1 and SUM2 are stored in the array area$(a) at line 420. The counter a is incremented by 1, and the program returns to line 330 if the

end of the array a$ is not reached, and a new value of k,j is input to the memory. Each time the value of s and r change, which is a new step of the beam path, the program diverts GOSUB (450, 570) and then GOSUB (840, 900) to correct the f(k,j) values of the estimated concentration by putting the new values of f(k,j) into the array area$(a) instead of the previous values. The program calculates the new values at line 880 by the algorithm formula

$$f(k,j) = f(k,j) + W*(\text{lambda}(s,r) - \text{Sum1})/\text{Sum2}$$

If the program has iterated through all the beam path steps for 40 rotations, and the end of the program has not been reached at line 360, the program diverts GOSUB (580, 610). After checking for the difference between the average concentration estimated for consecutive images at GOSUB (1020, 1180) the program saves the image on disc file, named imageFILENAMEtimes.dat at line 910 by diverting GOSUB (910, 1010) at line 600 if the difference is $\geq$1% the program repeats the image reconstruction at line 370. If the difference is <1% the program stops reconstructing images at line 1160, but if the difference is not less than 1%, the program stops at line 390.

Thus starting with a low average value for all the pixels the concentration of analyte element is built up in particular pixels which corresponds to regions of absorbtion of X-rays by the analyte element.

```
 50 !RECON40NTIMES
100 !Algebraic Reconstruction Technique for 40 steps and 40 rotations
110 dim area$(160),f(40,40),lambda(40,40)
120 all=0
130 OPEN "FILENAME.dat" FOR INPUT AS FILE #1
140 print "opening file"
150 for r=0 to 39
160 for s=1 to 40
170 input #1,x
180 lambda(s,r)=x
190 all=all+x
200 next s
210 next r
220 close #1
230 all=all/64000\print"Average=";all
240 for j=1 to 40
250 for k=1 to 40
260 f(k,j)=all
270 next k
280 next j
290 times=1 \ ti=20
300 until times=ti
310 a=0\s1=1\r1=0\sum1=0\sum2=0
320 open "area40.dat" for input as file #1
330 input #1,v,k,j,s,r
340 a$=str$(v)+","+str$(k)+","+str$(j)+","+str$(s)+","+str$(r)
350 if s=s1 and r=r1 then gosub 400 else gosub 450
360 if a$<>"100,1,1,1,1" then goto 330 else gosub 580
370 times=times+1
380 next
390 stop
400 gosub 620
410 gosub 800
420 area$(a)=a$
430 a=a+1
440 return
450 c$=a$
460 gosub 840
470 for a=0 to 160
480 area$(a)=" "
490 next a
500 a$=c$
510 gosub 620 \ !decode a$
520 if a$="100,1,1,1,1" then return
530 s1=s\r1=r\a=0\sum1=0\sum2=0
540 gosub 800
550 area$(a)=a$
560 a=a+1
570 return
580 close #1
590 gosub 1020
600 gosub 910
610 return
620 !DECODE AREAS
630 p1com=0\p2com=0\p3com=0\p4com=0\h=1
640 for i=1 to len(a$)
650 b$=mid$(a$,i,1)
660 if b$="," then gosub 740
```

```
670 next i
680 k=val(mid$(a$,p1com+1,p2com-p1com-1))
690 j=val(mid$(a$,p2com+1,p3com-p2com-1))
700 s=val(mid$(a$,p3com+1,p4com-p3com-1))
710 r=val(mid$(a$,p4com+1,len(a$)-p4com))
720 w=val(mid$(a$,1,p1com-1))
730 return
740 if h=1 then p1com=i
750 if h=2 then p2com=i
760 if h=3 then p3com=i
770 if h=4 then p4com=i
780 h=h+1
790 return
800 !SUM THE CONCENTRATIONS
810 if a$<>"100,1,1,1,1"then sum1=sum1+(w*f(k,j))
820 if a$<>"100,1,1,1,1" then sum2=sum2+(w^2)
830 return
840 !CORRECT THE f VALUES
850 for z=0 to a-1
860 a$=area$(z)
870 gosub 620\ !DECODE AREAS
880 f(k,j)=f(k,j)+0.2*w*(lambda(s1,r1)-sum1)/sum2
890 next z
900 return
910 !SAVE IMAGE TO FILE
920 name$="imageFILENAME"+str$(times)+".dat"
930 open name$ for output as file #1
940 for j=1 to 40
950 for k=1 to 40
960 print #1,f(k,j)
970 next k
980 next j
990 print #1,"sigma=",standev
1000 close #1
1010 return
1020 mean=0
1030 for k=1 to 40
1040 for j=1 to 40
1050 mean=mean+f(k,j)
1060 next j
1070 next k
1080 mean=mean/1600
1090 diff=0
1100 for k=1 to 40
1110 for j=1 to 40
1120 diff=diff+(f(k,j)-mean)^2
1130 next j
1140 next k
1150 standev=sqr(diff)/40
1160 if abs(oldstandev-standev)<oldstandev/100 then stop
1170 oldstandev=standev
1180 return
```

INVERTDATA

This VAX 11/785 computer program is for inverting the X-ray photon count data in the absorbtion equation $I = I_o e^{-\mu t}$ to the form $\ln(I_o/I) = \mu t$. μt is the variable used for reconstruction of the image of an object by the Algebraic Reconstruction Technique and by Filtered Backprojection for computer axial tomography scanning.

*****

The program opens the input file containing the X-ray photon count data at line 140, and the data I is read in to the VAX 11/785 computer memory in the array A(I) at line 160. The program searches through A(I) for the biggest value of I, which is the incident X-ray photon count I_o, and sets it equal to BIG. BIG is found for each linear scan of 40 steps because I_o may change during the complete scan.

The program opens the file catdata.dat, goes through the array A(I) calculating each value of $\ln(BIG/A(I)) = \ln(I/I_o) = \mu t$, and sends the result to the file catdata.dat.

```
 50 !INVERTDATA
100 !To invert the X-ray photon count data
110 BIG=0
120 DIM A(1600)
130 input "file to invert",name$
140 open name$ for input as file #1
150 for i=1 to 1600
160 INPUT #1,A(I)
170 IF A(I)>BIG THEN BIG=A(I)
180 NEXT I
190 CLOSE #1
200 open "catdata.dat" for output as file#1
210 FOR I=1 TO 1600
220 PRINT #1,LOG(BIG/A(I))
230 NEXT I
240 CLOSE #1
250 STOP
260 END
```

```
  5 REM ****CALAR40****
 10 REM PROGRAM TO SELECT OVERLAP AREAS AS 1 OR 0
 20 THETA=PI/40
 30 X=OPENOUT"AREA40"
 40 FOR R=0 TO 39
 50 phi=R*THETA
 60 cosphi=COS(phi)
 70 tanphi=TAN(phi)
 80 IF R<>20 THEN PROCNOT20 ELSE PROCTWENTY
 90 NEXT R
100 CLOSE #X
110 END
120 DEF PROCNOT20
130 FOR S=1 TO 40
140 CEPT=(20.5-S)/cosphi
150 FOR x=-19.5 TO 19.5
160 y=(x*tanphi)+CEPT
170 K=21+INT(x)
180 J%=20-INT(y)
190 IF J%>40 OR J%<1 THEN J%=0
200 BPUT #X,J%
210 PRINT J%,K,S,R
220 NEXT x
230 NEXT S
240 ENDPROC
250 DEF PROCTWENTY
260 FOR M%=1 TO 40
270 FOR N%=1 TO 40
280 BPUT#X,N%
290 NEXT N%
300 NEXT M%
310 ENDPROC
```

CALAR40

This BBC+ microcomputer program does not calculate the areas of overlap between the simulated X-ray beam path and the pixels of the reconstruction grid, but instead counts a pixel area as 1 if the centre of the beam path intercepts the pixel and 0 if it does not. The program stores the intercepted pixels as 1.

This program is not useable with the Algebraic Reconstruction Technique because for good image reconstruction the areas of overlap between beam path and pixels need to be calculated accurately as the concentration of analyte element estimated for each pixel is compared with the measured concentration at each iteration of the reconstruction program. This program was incorporated in the reconstruction program by Filtered Backprojection, FILTRECONAV40, because good image reconstruction is possible with this method without accurate calculation of overlap areas.

*****

Figure A.6 shows the centre of the simulated X-ray beam path at a step S and rotation R at angle Θ to the ordinate intercepting the j,k pixels of the reconstruction grid set against (x,y) coordinates.

The main part of the program is listed from lines 20 to 100, which calls two procedures at line 80. The centre of the beam path has equation of the form $y = mx + c$, where m is the slope and c is a constant. Θ, $\cos\Theta$, and $\tan\Theta$ are calculated for each rotation R in the FOR NEXT loop between lines 40 and 90.

CALAR40

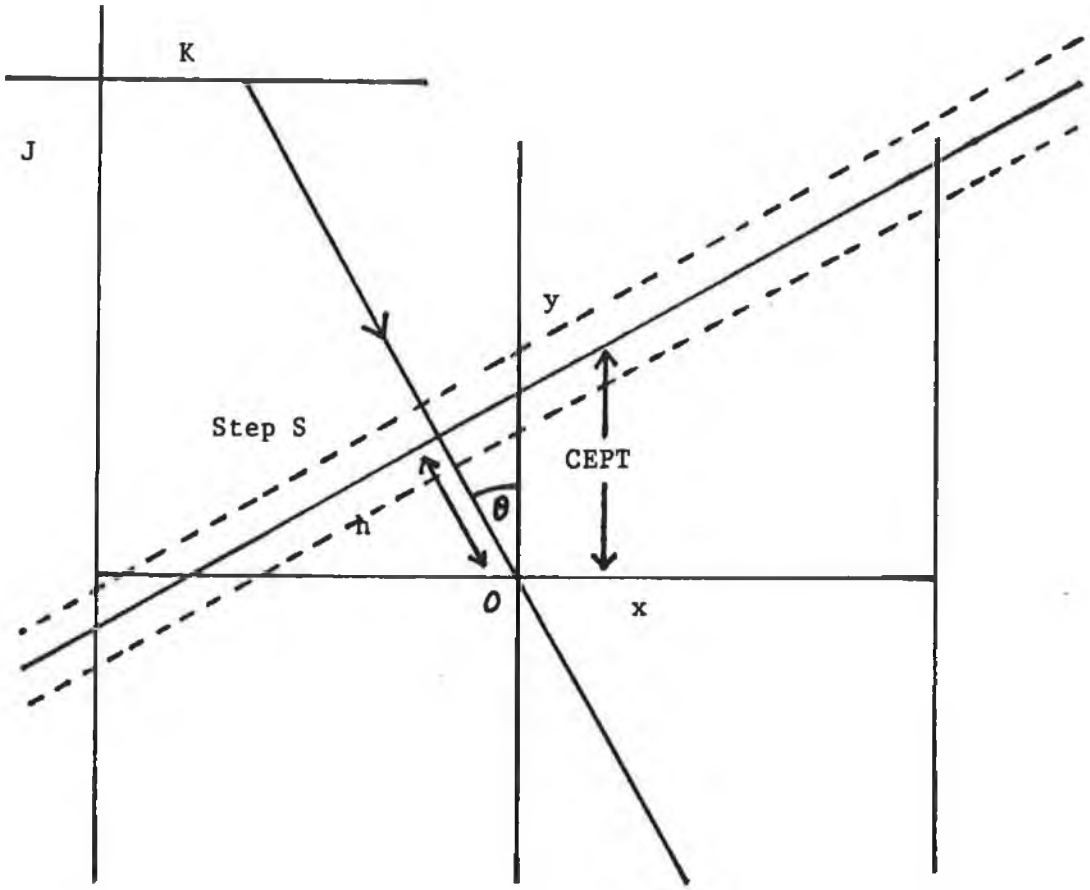

$$y = x\tan 0 + CEPT$$

$$CEPT = (20.5 - S)/\cos\theta$$

To select the overlap areas as 1 or 0 by CALAR40.

FIGURE A.6

For all angular steps except R = 20, the program diverts at line 80 to PROCNOT20 defined at lines 120 to 240. The intercept of the beam path centre with the ordinate is CEPT = h/cosθ, which is the number of steps the beam centre moves from step S to the origin. This is calculated for each step, CEPT = (20.5 - S)/cosθ, in the FOR NEXT loop between lines 130 and 230, as K goes from 1 to 40. The centre of the beam path moves from x = -19.5 to x = 19.5 as K moves from 1 to 40. For each K position of a pixel on the x-axis, its position on the y-axis, which is its J position, is calculated from the equation of the beam path centre.

$$y = x\tan\theta + CEPT$$

at line 160 in the FOR NEXT loop between lines 150 and 220. The values of K, J corresponding to (x,y) are calculated at lines 170 and 180. Only values of J from 1 to 40 are needed because all others are outside the 40 x 40 reconstruction grid, which are set equal to zero at line 190. J is stored on disc file at line 200, and the values for J, K, S, K are printed to the monitor screen at line 210 and stored on disc file.

When R = 20, $\theta = \pi/2$, and $\tan\theta = \infty$, so it is not possible to calculate y. Instead the program diverts to PROCTWENTY defined at lines 250 to 310, which stores on disc file all the pixels of the grid as bits, because the beam path centre intercepts all the pixels for R = 20.

FILTRECONAV40

This VAX 11/785 computer program is to reconstruct the image of a scanned object by Filtered Backprojection using a Ramachandran filter, for computer axial tomography, and it may also be used for differential absorbtion edge tomography.

To reconstruct the image of an object the measured equivalent thickness at each scanning step $\mu t = \ln(I_o/I)$, which is the beam profile one pixel wide, is projected back on to the reconstruction grid by allocating $\ln(I_o/I)$ to each pixel of the grid in the direction in which the measurement was made. For N projection angles, the beam profiles reinforce qualitatively the image density by $N\ln(I_o/I)$. Every beam profile is modified before backprojection by convolving it with a Ramachandran filter in order to multiply non zero values of the backprojection which are not part of the image. Only the pixels intersected by the centre of the beam path are selected to have the modified values of the equivalent thickness added to them. Each pixel is divided in four and the beam path is divided in two in order to improve the image definition.

*****

The program inputs at line 130 to the computer memory the equivalent thickness data, lambda(s,r) stored as bits, of each step of the scanned object produced by the INVERTDATA program for computer axial tomography, or the extrapolated values of the equivalent thickness produced by the ROIEXTRAPOLATE program for differential absorbtion edge tomography.

The Ramachandran filter starts the convolution with the beam profiles five steps before the centre of the filter function reaches a chosen pixel, so that in the two FOR NEXT loops between lines 160 and 210 values of K represented by the dummy variable T not in the reconstruction grid, 1 to 5 and 46 to 50 have their beam step set at 0. The array is set up in the FOR NEXT loop between lines 220 and 250.

The filter correction factors C are made in the FOR NEXT loop between lines 280 and 300 for every rotation R, and then multiplied by the beam profile equivalent thickness $\mu t = \ln(I_o/I)$ in the FOR NEXT loop between lines 330 and 350.

The pixels in the reconstruction grid through which the centre of the beam path passes are selected between lines 380 and 520. For each angular step, Θ, $\cos\Theta$, and $\tan\Theta$ are calculated, except when $\Theta = \pi/2$ for rotation 20. The range = $0.5/\cos\Theta$, defined at line 440, is the length of the ordinate in each column of pixels specified by its K value for each rotation R. Each beam path is divided in two at line 460, and each pixel in four at line 480. The intercept of the centre of a beam path with the ordinate is calculated at line 470, and the equation of its line at line 490. The range counter, jc, is set at 41-y at line 510, and if it is not on the reconstruction grid, the program selects the next value of x at line 570. The pixel numbers j% which the beam centre intersects are calculated in the FOR NEXT loop between lines 530 and 570, which are on both sides of the range counter by the ordinate length of the range. The backprojection algorithm, $f(k,j) = \sum_{r,s} W_{k,j}$,s is at line 560, where $W_{k,j} = 1$ when the beam path centre intersects the k,j pixel and is the filtered projection value. When $\Theta = \pi/2$ for R = 20, the program diverts GOSUB (720, 790) at line 420 to do a similar calculation.

The reconstructed image data is summed into a 40 x 40 array from the 80 x 80 array at line 650 and sent to file at line 670.

```
 50 !FILTRECONAV40
100 !Filtered Backprojection for 40 steps and 40 rotations
110 INPUT"NAME OF DATA STORAGE FILE",NAME$
120 INPUT"NAME OF IMAGE STORAGE FILE",NAME2$
130 OPEN NAME$  FOR INPUT AS FILE #1
140 DIM Stp(2100), CORRCT(2110),lambda(40,40),f(80,80),finalim(40,40)
150 FOR R=0 TO 39
160 FOR T=(R*50)+1 TO (R*50)+5
170 Stp(T)=0
180 NEXT T
190 FOR T=(R*50)+46 TO (R*50)+50
200 Stp(T)=0
210 NEXT T
220 FOR T=(R*50)+6 TO (R*50)+45
230 INPUT#1,Stp(T)
240 NEXT T
250 NEXT R
260 CLOSE#1
270 FOR R= 0 TO 40
280 FOR K=(R*50)+6 TO (R*50)+45
290 CORRCT(K)=Stp(K)*.25-((Stp(K-1)*.101)+(Stp(K+1)*.101))-((Stp(K-3)*.0112)+
p(K+3)*.0112))-((Stp(K-5)*4E-3)+(Stp(K+5)*4E-3))
300 NEXT K
310 NEXT R
320 FOR r%=0 TO 40
330 FOR N%=(r%*50)+6 TO (r%*50)+45
340 lambda((n%-(r%*50)-5),r%)= CORRCT(N%)
350 NEXT N%
360 NEXT r%
370 theta=pi/40
380 for r%= 0 to 39
390 phi=r%*theta
400 cosphi=cos(phi)
410 tanphi=tan(phi)
420 if r%=20 then gosub 720
430 if r%=20 then goto 600
440 range=abs(0.5/cosphi)
450 if range>40 then range=40
460 for s=1 to 80
470 cept=(40.5-s)/cosphi
480 for x=-39.5 to 39.5
490 y=(x*tanphi)+cept
500 k%=41+int(x)
510 jc=41-y
520 if jc>87 or jc<-7 then goto 580
530 for j%=jc-range to jc+range
540 if j%<=0 or j%>80 then goto 570
550 s%=int((s+1)/2)
560 f(k%,j%)=f(k%,j%)+(lambda(s%,r%)/80)
570 next j%
580 next x
590 next s
600 print r%
610 next r%
620 open name2$ for output as file#1
630 for j%= 1 to 80 step 2
640 for k%= 1 to 80 step 2
650 sum1=f(k%,j%)+f(k%+1,j%)+f(k%,j%+1)+f(k%+1,j%+1)
```

```
660 finalim((k%+1)/2,(j%+1)/2)=sum1
670 print#1,finalim((k%+1)/2,(j%+1)/2)
680 next k%
690 next j%
700 close#1
710 goto 800
720 for s= 1 to 80
730 k%=s
740 s%=int((s+1)/2)
750 for j%= 1 to 80
760 f(k%,j%)=f(k%,j%)+(lambda(s%,r%)/80)
770 next j%
780 next s
790 return
800 stop
810 end
```

(St

CANG40G

This BBC microcomputer program is for changing ASCII code sent from the VAX 11/785 computer to the BBC microcomputer into random access numbers. The ASCII code contains the reconstructed image data of the scanned object, and the change is required in order that the R.DISP40T program can display the image on the monitor screen.

*****

The program asks at line 70 for a file to be selected from the disc file catalogue, and when the name is entered, this file is opened at line 110. PROCBGET, defined at lines 420 to 450, takes the ASCII code one byte at a time from the disc file. Each ASCII byte is converted into the corresponding random access number at line 470, denoted by the variable ALL$, by a read only memory in the BBC microcomputer. The random access number VAL$(ALL) is printed to the monitor screen at line 150, and stored in the BBC microcomputer memory. The file is closed at line 190 when all the ASCII code is converted.

A new disc is used for storing the image data as random access numbers, as requested at line 300, the file name has G. placed in front of it for the catalogue, and the random access numbers are read into the disc file at lines 330 to 400.

```
  5 REM ****CANG406****
 10 REM PROGRAM TO CONVERT ASCII CODE TO RANDOM ACCESS NUMBERS
 20 DIM A(40,40)
 30 MAX=0
 40 CLS
 50 *.
 60 RESTORE
 70 INPUT"FILE NAME (*. Catalog) ",name$
 80 IF name$<>"*." THEN GOTO 110
 90 *.
100 GOTO 70
110 X=OPENIN name$
120 FOR J%=1 TO 40
130 FOR K%=1 TO 40
140 PROCBGET
150 PRINTVAL(ALL$)
160 A(J%,K%)=VAL(ALL$)
170 NEXT K%
180 NEXT J%
190 CLOSE#X
200 FOR J%=1 TO 40
210 FOR K%=1 TO 40
220 IF A(J%,K%)>MAX THEN MAX=A(J%,K%)
230 NEXT K%
240 NEXT J%
250 FOR J%=1 TO 40
260 FOR K%=1 TO 40
270 IF A(J%,K%)>=0 THEN A(J%,K%)=A(J%,K%)*255/MAX ELSE A(J%,K%)=0
280 NEXT K%
290 NEXT J%
300 PRINT "INSERT DISC. HIT C TO CONTINUE.";:Q$=GET$
310 IF Q$<>"C" THEN 300
320 name$="G."+name$
330 X=OPENOUT name$
340 PRINT#X,MAX
350 FOR J%=1 TO 40
360 FOR K%=1 TO 40
370 BPUT#X,A(J%,K%)
380 NEXT K%
390 NEXT J%
400 CLOSE#X
410 END
420 DEF PROCBGET
430 Y=BGET#X
440 IF Y=&20 OR Y=&2D THEN PROCNUMBER ELSE GOTO 430
450 ENDPROC
460 DEF PROCNUMBER
470 ALL$=CHR$(Y)
480 REPEAT
490 Y=BGET#X
500 ALL$=ALL$+CHR$(Y)
510 UNTIL Y=&20
520 ENDPROC
```

R.DISP40T

This BBC microcomputer program is for displaying on the monitor screen in colour, or in grey shades, as required, the image of a scanned object reconstructed by the Algebraic Reconstruction Technique or by Filtered Backprojection. The image is in the form of random access numbers held in a disc file which may be called by the program by name from the catalogue. There are eight image colours, or grey shades, on a scale of 0 to 80 so that the image depth profile can be represented as contours. The scale range can be changed to intermediate numbers such as 20 to 80 in order to eliminate the low level background, or the matrix.

The program also has a line cursor which may be set at any position across the display, and a graph of image depth profile against linear position along the line is drawn underneath the image. There is also a single pixel cursor which may be moved to any of the 1600 pixels on the image graphics using the BBC microcomputer EDIT keys, and the concentration in kilograms per cubic metre of analyte element at the cursor position is printed as a digital indicator on the monitor screen. Both cursors read out from the BBC microcomputer memory the values of image depth profile corresponding to the pixel location on the monitor screen which they intercept. The display appears as shown in Plates, 6.2, 6.3, 6.4, and 6.5.

*****

The main part of the program is listed from lines 20 to 1440; the rest of the program from lines 1450 to 2940 consists of thirteen procedures to which the main program diverts as required.

Lines 30 and 90 select the Teletext MODE7 for a colour text and graphics display. Line 110 prints on the monitor screen the disc file catalogue from which the image data is to be accessed at line 130. The graphics heading is printed at line 130. At lines 270, 280 the disc file selected by name is loaded into the BBC microcomputer memory, and PROCESSING DATA is printed to the monitor screen. The data for display is normalised to the 0 to 80 scale at line 380. PROCSHOWCODE, defined at line 1690 to 1770, selects colour or grey shades for the display by diverting to PROCSELECTCOL or to PROCSELECTSHADE, defined at lines 1450 to 1540 and 1550 to 1640. PROCSCALES, defined at lines 1820 to 1910 draws the colour scale at the right hand side of the monitor screen. PROCINFO, defined at lines 1920 to 2040, prints the K,J coordinate limits for the display, the upper and lower limits for the graphics scales, and the rotation and linear step numbers for the line cursor selection.

PROCSECTION, defined at lines 2050 to 2270, draws the image of the object in the graphics part of the monitor screen line by line. Lines 540 to 1440 are for printing the line cursor or the monitor screen by diverting to PROCPLOTLINE defined at lines 2410 to 2590, and for printing the pixel cursor on the monitor screen by diverting to PROCCURSOR, defined at lines 2640 to 2940.

```
  5 REM ****R.DISP40T****
 10 REM PROGRAM TO DISPLAY A RECONSTRUCTED IMAGE IN COLOUR OR GREY SCALE
 20 *SHADOW
 30 MODE7
 40 DIM A(40,40):MAX=255:PIXEL=0.002:LI%=0
 50 VDU23,248,255,255,255,255,255,255,255,255
 60 PRINTTAB(6,10)"COLOUR";CHR$(131);"C";CHR$(135);"OR B/W";CHR$(131);"B";CHR$
(135);:Q$=GET$
 70 IF Q$<>"C" AND Q$<>"B" THEN 50
 80 IF Q$="C" THEN CODE=0 ELSE CODE=1
 90 MODE7
100 STP%=16:KS%=1:KF%=40:JS%=1:JF%=40:LL%=0:UL%=80:RO%=0:ST%=20
110 *.
120 MAX=255:RESTORE
130 INPUT"FILE NAME (*. Catalog) ",NAME$
140 IF NAME$<>"*." AND NAME$<>"*.:0" AND NAME$<>"*.:1" THEN GOTO 250
150 IF NAME$="*." THEN *.
160 IF NAME$="*.:0" THEN *.:0
170 IF NAME$="*.:1" THEN *.:1
180 GOTO 130
190 PRINTTAB(8)CHR$(130);"**********";CHR$(135)
200 INPUT"HEADING1",HEAD1$
210$
220 IF LEN(HEAD1$)>11 THEN 200
230 INPUT"HEADING2",HEAD2$
240 IF LEN(HEAD2$)>11 THEN 230
250 CLS
260 VDU23;8202;0;0;0;
270 PRINTTAB(0,10)CHR$(136);CHR$(131);CHR$(157);CHR$(132);"     LOADING FILE "
;NAME$
280 X=OPENIN NAME$
290 INPUT#X,max
300 FOR J%=1 TO 40
310 FOR K%=1 TO 40
320 NUM=BGET#X
330 A(K%,J%)=NUM
340 NEXT K%
350 NEXT J%
360 CLOSE#X
370 PRINTTAB(0,10)CHR$(136);CHR$(132);CHR$(157);CHR$(131);"  PROCESSING DATA"
380 Factor=80/MAX
390 FOR J%=1 TO 40
400 FOR K%=1 TO 40
410 A(K%,J%)=A(K%,J%)*Factor-.001
420 NEXT K%
430 NEXT J%
440 MODE2:PRINTTAB(1,5)
450 VDU23;8202;0;0;0;
460 VDU5
470 MOVE350,1023:PRINTNAME$
480 PROCSHOWCODE
490 PROCSCALES
500 PROCINFO
510 PROCSECTION(RO%,ST%)
520 VDU4:COLOUR0:PRINTTAB(0,22)"      "
530 COLOUR0:PRINTTAB(0,24)"      "
540 VDU4:COLOUR3:PRINTTAB(0,26)"END ";:COLOUR12:PRINT"E":VDU5
550 FOR J%=JS% TO JF%
560 FOR K%=KS% TO KF%
```

```
570 KEY$=INKEY$(0)
580 IF KEY$<>"E" THEN 600
590 J%=JF%:K%=KF%
600 PROCGETA(UL%,LL%)
610 IF CODE=0 THEN PROCSELECTCOL(A) ELSE PROCSELECTSHADE(A)
620 GCOL 0,HUE
630 MOVE((K%-KS%)*STP%)+352,900-((J%-JS%)*STP%):PRINT CHR$(248)
640 NEXT K%
650 GCOL0,0:MOVE((K%-KS%)*STP%)+352,900-((J%-JS%)*STP%):PRINT CHR$(248)
660 VDU13
670 NEXT J%
680 GCOL0,0
690 FOR K%=KS% TO KF%
700 MOVE((K%-KS%)*STP%)+352,900-((J%-JS%)*STP%):PRINT CHR$(248)
710 NEXT K%
720 GCOL0,7
730 VDU4
740 COLOUR3:PRINTTAB(0,26)"CUR ";:COLOUR12:PRINT"C"
750 COLOUR3:PRINTTAB(0,22)"NEW ";:COLOUR12:PRINT"N"
760 COLOUR3:PRINTTAB(0,24)"SEC ";:COLOUR12:PRINT"S"
770 IF RO%<>20 THEN PROCPLOTLINE(RO%,ST%)
780 IF RO%=20 THEN PROCPLOT90(ST%)
790 KSO%=KS%:COLOUR12:PRINTTAB(3,5)STR$(KS%):COLOUR7:INPUTTAB(0,5)"KS",KS$:KS%
=VAL(KS$):IF KS%=0 THEN KS%=KSO%
800 PRINTTAB(3,5)STR$(KS%);:IF KS%<10 THEN PRINT" "
810 IF KS$="N" THEN 90
820 IF KS$="S" AND RO%<>20 THENPROCPLOTLINE(RO%,ST%)
830 IF KS$="S" AND RO%=20 THENPROCPLOT90(ST%)
840 IF KS$="C" THEN PROCCURSOR
850 IF KS$="S" OR KS$="C" THEN 790
860 KFO%=KF%:COLOUR12:PRINTTAB(3,7)STR$(KF%):COLOUR7:INPUTTAB(0,7)"KF",KF$:KF%
=VAL(KF$):IF KF%=0 THEN KF%=KFO%
870 PRINTTAB(3,7)STR$(KF%);:IF KF%<10 THEN PRINT" "
880 IF KF$="N" THEN 90
890 IF KF$="S" AND RO%<>20 THENPROCPLOTLINE(RO%,ST%)
900 IF KF$="S" AND RO%=20 THENPROCPLOT90(ST%)
910 IF KF$="C" THEN PROCCURSOR
920 IF KF$="C" OR KF$="S" THEN 860
930 JSO%=JS%:COLOUR12:PRINTTAB(3,9)STR$(JS%):COLOUR7:INPUTTAB(0,9)"JS",JS$:JS%
=VAL(JS$):IF JS%=0 THEN JS%=JSO%
940 PRINTTAB(3,9)STR$(JS%);:IF JS%<10 THEN PRINT" "
950 IF JS$="N" THEN 90
960 IF JS$="S" AND RO%<>20 THENPROCPLOTLINE(RO%,ST%)
970 IF JS$="S" AND RO%=20 THENPROCPLOT90(ST%)
980 IF JS$="C" THEN PROCCURSOR
990 IF JS$="C" OR JS$="S" THEN 930
1000 JFO%=JF%:COLOUR12:PRINTTAB(3,11)STR$(JF%):COLOUR7:INPUTTAB(0,11)"JF",JF$:J
F%=VAL(JF$):IF JF%=0 THEN JF%=JFO%
1010 PRINTTAB(3,11)STR$(JF%);:IF JF%<10 THEN PRINT" "
1020 IF JF$="N" THEN 90
1030 IF JF$="S" AND RO%<>20 THENPROCPLOTLINE(RO%,ST%)
1040 IF JF$="S" AND RO%=20 THENPROCPLOT90(ST%)
1050 IF JF$="C" THEN PROCCURSOR
1060 IF JF$="C" OR JF$="S" THEN 1000
1070 IF KF%-KS%>20 OR JF%-JS%>20 THEN STP%=16 ELSE STP%=32
1080 LLO%=LL%:COLOUR12:PRINTTAB(3,13)STR$(LL%):COLOUR7:INPUTTAB(0,13)"LL",LL$:L
L%=VAL(LL$):IFLL%=0 THEN LL%=LLO%
1090 PRINTTAB(3,13)STR$(LL%);:IF LL%<10 THEN PRINT" "
1100 IF LL$="N" THEN 90
1110 IF LL$="S" AND RO%<>20 THENPROCPLOTLINE(RO%,ST%)
```

```
 1120 IF LL$="S" AND RO%=20 THENPROCPLOT90(ST%)
 1130 IF LL$="C" THEN PROCCURSOR
 1140 IF LL$="C" OR LL$="S" THEN 1080
 1150 ULO%=UL%:COLOUR12:PRINTTAB(3,15)STR$(UL%):COLOUR7:INPUTTAB(0,15)"UL",UL$:U
L%=VAL(UL$):IFUL%=0 THEN UL%=ULO%
 1160 PRINTTAB(3,15)STR$(UL%);:IF UL%<10 THEN PRINT" "
 1170 IF UL$="N" THEN 90
 1180 IF UL$="S" AND RO%<>20 THENPROCPLOTLINE(RO%,ST%)
 1190 IF UL$="S" AND RO%=20 THENPROCPLOT90(ST%)
 1200 IF UL$="C" THEN PROCCURSOR
 1210 IF UL$="C" OR UL$="S" THEN 1150
 1220 ROO%=RO%:COLOUR12:PRINTTAB(3,17)STR$(RO%):COLOUR7:INPUTTAB(0,17)"RO",RO$:R
O%=VAL(RO$):IFRO$="" THEN RO%=ROO%
 1230 PRINTTAB(3,17)STR$(RO%);:IF RO%<10 THEN PRINT" "
 1240 IF RO$="N" THEN 90
 1250 IF RO$="S" AND RO%<>20 THENPROCPLOTLINE(RO%,ST%)
 1260 IF RO$="S" AND RO%=20 THENPROCPLOT90(ST%)
 1270 IF RO$="C" THEN PROCCURSOR
 1280 IF RO$="C" OR RO$="S" THEN 1220
 1290 STO%=ST%:COLOUR12:PRINTTAB(3,19)STR$(ST%):COLOUR7:INPUTTAB(0,19)"ST",ST$:S
T%=VAL(ST$):IFST%=0 THEN ST%=STO%
 1300 PRINTTAB(3,19)STR$(ST%);:IF ST%<10 THEN PRINT" "
 1310 IF ST$="N" THEN 90
 1320 IF ST$="S" AND RO%<>20 THENPROCPLOTLINE(RO%,ST%)
 1330 IF ST$="S" AND RO%=20 THENPROCPLOTL90(ST%)
 1340 IF ST$="C" THEN PROCCURSOR
 1350 IF ST$="C" OR  ST$="S" THEN 1290
 1360 IF (KF%=KFO% AND KS%=KSO% AND JS%=JSO% ANDJF%=JFO% AND UL%=ULO% ANDLL%=LLO
% AND RO%=ROO% AND ST%=STO%) AND KEY$<>"E" THEN 790
 1370 IF (KF%=KFO% AND KS%=KSO% AND JS%=JSO% ANDJF%=JFO% AND UL%=ULO% ANDLL%=LLO
% AND RO%=ROO% AND ST%=STO%) AND KEY$="E" THEN 440
 1380 IF (KF%<>KFO% OR KS%<>KSO% OR JS%<>JSO% OR JF%<>JFO% OR UL%<>ULO% OR LL%<>
LLO%) THEN 440
 1390 IF LI%=0 THEN 1420
 1400 IF ROO%<>20 THEN PROCPLOTLINE(ROO%,STO%)
 1410 IF ROO%=20 THEN PROCPLOT90(STO%)
 1420 IF RO%<>20 THEN PROCSECTION(RO%,ST%) ELSE PROCSECT20(ST%)
 1430 IF KEY$="E" THEN GOTO 520 ELSE GOTO 730
 1440 END
 1450 DEF PROCSELECTCOL(CLR)
 1460  IF CLR<=80 AND CLR>70 THEN HUE=7
 1470  IF CLR<=70 AND CLR>60 THEN HUE=1
 1480  IF CLR<=60 AND CLR>50 THEN HUE=5
 1490  IF CLR<=50 AND CLR>40 THEN HUE=3
 1500  IF CLR<=40 AND CLR>30 THEN HUE=2
 1510  IF CLR<=30 AND CLR>20 THEN HUE=6
 1520  IF CLR<=20 AND CLR>=0 THEN HUE=4
 1530  IF CLR<0 OR CLR>80 THEN HUE=0
 1540 ENDPROC
 1550 DEF PROCSELECTSHADE(CLR)
 1560  IF CLR<=80 AND CLR>70 THEN HUE=7
 1570  IF CLR<=70 AND CLR>60 THEN HUE=3
 1580  IF CLR<=60 AND CLR>50 THEN HUE=6
 1590  IF CLR<=50 AND CLR>40 THEN HUE=2
 1600  IF CLR<=40 AND CLR>30 THEN HUE=5
 1610  IF CLR<=30 AND CLR>20 THEN HUE=1
 1620  IF CLR<=20 AND CLR>=0 THEN HUE=4
 1630 IF CLR<0 OR CLR>80 THEN HUE=0
 1640 ENDPROC
 1650 DEF PROCGETA(ul%,ll%)
 1660 FACTOR2=80/(ul%-ll%)
 1670 A=(A(K%,J%)-ll%)*FACTOR2
 1680 ENDPROC
 1690 DEF PROCSHOWCODE
 1700 FOR V%=5 TO 75 STEP 10
 1710 IF CODE=0 THEN PROCSELECTCOL(V%) ELSE PROCSELECTSHADE(V%)
 1720 GCOL0,HUE
 1730 MOVE1168,550+V%*32/10:PRINTCHR$(248):GCOL0,0:MOVE1208,550+V%*32/10:PRINTCH
R$(248)
 1740 NEXT V%
 1750 GCOL0,7
 1760 MOVE1130,850:PRINTSTR$(UL%):MOVE1130,500:PRINTSTR$(LL%)
 1770 ENDPROC
 1780 DEF PROCENDLINE
 1790 IF KT%=0 THEN 1810
 1800 PRINTCHR$(248);CHR$(248)
 1810 ENDPROC
 1820 DEF PROCSCALES
 1830 FOR J%=JS% TO JF%
 1840 IF J%/10=INT(J%/10) THEN GCOL0,1 ELSE GCOL0,3
 1850 MOVE348,900-((J%-JS%+1)*STP%):DRAW345,900-((J%-JS%+1)*STP%)
 1860 NEXTJ%
 1870 FOR K%=KS% TO KF%
 1880 IF K%/10=INT(K%/10) THEN GCOL0,1 ELSE GCOL0,3
 1890 MOVE((K%-KS%+1)*STP%)+352,905:DRAW((K%-KS%+1)*STP%)+352,920
 1900 NEXT K%
 1910 ENDPROC
 1920 DEF PROCINFO
 1930 GCOL 0,7
 1940 VDU4
 1950 PRINTTAB(0,5)"KS?";KS%
 1960 PRINTTAB(0,7)"KF?";KF%
 1970 PRINTTAB(0,9)"JS?";JS%
 1980 PRINTTAB(0,11)"JF?";JF%
 1990 PRINTTAB(0,13)"LL?";LL%
 2000 PRINTTAB(0,15)"UL?";UL%
 2010 PRINTTAB(0,17)"RO?";RO%
 2020 PRINTTAB(0,19)"ST?";ST%
 2030 VDU5
 2040 ENDPROC
 2050 DEF PROCSECTION(ro%,st%)
 2060 GCOL0,7:MOVE 345,240:DRAW345,0:DRAW1279,0
 2070 VDU24,352;5;1200;260;
 2080 CLG
 2090 phi=ro%*PI/40
 2100 cosphi=COS(phi)
 2110 tanphi=TAN(phi)
 2120 CEPT=(20.5-st%)/cosphi
 2130 IND%=0
 2140 MOVE352,5
 2150 FOR x=-19.5 TO 19.5 STEP ABS(COS(phi))
 2160 y=(x*tanphi)+CEPT
 2170 K%=21+INT(x)
 2180 J%=21-y
 2190 IF J%>40 OR J%<1 THEN GOTO 2250
 2200 PROCGETA(80,0)
 2210 V%=A
 2220 IF CODE=0 THEN PROCSELECTCOL(V%) ELSE PROCSELECTSHADE(V%)
 2230 GCOL0,HUE:DRAW352+(STP%*IND%),V%*3+5
 2240 IND%=IND%+1
```

```
2250 NEXT x
2260 VDU26
2270 ENDPROC
2280 DEF PROCSECT20(st%)
2290 GCOL0,7:MOVE 345,240:DRAW345,0:DRAW1279,0
2300 VDU24,352;5;1200;260;
2310 K%=st%
2320 CLG
2330 FOR J%=1 TO 40
2340 PROCGETA(80,0)
2350 V%=A
2360 IF CODE=0 THEN PROCSELECTCOL(V%) ELSE PROCSELECTSHADE(V%)
2370 GCOL0,HUE:DRAW352+(STP%*J%),V%*3+5
2380 NEXT J%
2390 VDU26
2400 ENDPROC
2410 DEF PROCPLOTLINE(ro%,st%)
2420 GCOL0,7
2430 LI%=NOT(LI%)
2440 phi=ro%*PI/40
2450 cosphi=COS(phi)
2460 tanphi=TAN(phi)
2470 CEPT=(20.5-st%)/cosphi
2480 x=KS%-20.5
2490 y=(x*tanphi)+CEPT
2500 J=20-y
2510 MOVE352,900-(J*STP%)
2520 IFro%<20 THEN STP=1.3/(ro%+1)ELSE STP=1.3/(ABS(40-ro%))
2530 FOR K=KS% TO KF% STEP STP
2540 x=K-20.5
2550 y=(x*tanphi)+CEPT
2560 J=20-y
2570 IF J>0 AND J<40 THEN PLOT6,(K-KS%)*STP%+352,900-(J*STP%) ELSE MOVE(K-KS%
STP%+352,900-(J*STP%)
2580 NEXT K
2590 ENDPROC
2600 DEF PROCPLOT90(st%)
2610 LI%=NOT(LI%)
2620 MOVE352+(st%-KS%)*STP%,900:PLOT6,(st%-KS%)*STP%+352,250
2630 ENDPROC
2640 DEF PROCCURSOR
2650 *FX4,1
2660 XX0%=1:XX%=1:YY0%=1:YY%=1
2670 COLOUR0:PRINTTAB(0,22)"      "
2680 COLOUR0:PRINTTAB(0,24)"      "
2690 COLOUR12:PRINTTAB(0,26)"END E"
2700 PLOT70,((XX0%-KS%)*STP%)+352+STP%/2,900-((YY0%-JS%)*STP%)-STP%/2
2710 REPEAT
2720 XX0%=XX%:YY0%=YY%
2730 COLOUR7:PRINTTAB(0,22)"KC "STR$(XX%);:IF XX%<10 THEN PRINT" "
2740 COLOUR7:PRINTTAB(0,24)"JC "STR$(YY%);:IF YY%<10 THEN PRINT" "
2750 KEY=INKEY(0)
2760 IF KEY=136 THEN XX%=XX%-1
2770 IF KEY=137 THEN XX%=XX%+1
2780 IF KEY=138 THEN YY%=YY%+1
2790 IF KEY=139 THEN YY%=YY%-1
2800 IF XX%>KF% THEN XX%=KF%
2810 IF XX%<KS% THEN XX%=KS%
2820 IF YY%<JS% THEN YY%=JS%
2830 IF YY%>JF% THEN YY%=JF%
```

```
 2840 PLOT70,((XXO%-KS%)*STP%)+352+STP%/2,900-((YYO%-JS%)*STP%)-STP%/2
 2850 PLOT70,((XX%-KS%)*STP%)+352+STP%/2,900-((YY%-JS%)*STP%)-STP%/2
 2860 COLOUR3:IF A(XX%,YY%)>=0 THEN PRINT TAB(5,1)((A(XX%,YY%)/Factor)+0.001)*m
x/255;"       " ELSE PRINTTAB(5,1)"                                    "
 2870 UNTIL KEY=69
 2880 PLOT70,((XX%-KS%)*STP%)+352+STP%/2,900-((YY%-JS%)*STP%)-STP%/2
 2890 COLOUR3:PRINTTAB(5,1)"                                           "
 2900 COLOUR3:PRINTTAB(0,26)"CUR ";:COLOUR12:PRINT"C"
 2910 COLOUR3:PRINTTAB(0,22)"NEW ";:COLOUR12:PRINT"N"
 2920 COLOUR3:PRINTTAB(0,24)"SEC ";:COLOUR12:PRINT"S"
 2930 *FX4,0
 2940 ENDPROC
```

```
:)*
```

SPECTRA

This BBC microcomputer program is for calculating X-ray band pass spectra emergent from a metallic filter element such as 50Tin and the attenuation which the filter element causes to the incident X-ray beam for photon energies between 12keV and 50keV, and corresponding wavelength, in 1keV increments. The program can print the attenuation at each energy increment, calculate and print the total attenuation for the band pass spectrum, which is the ratio of the integral of the emergent beam intensity I to that of the incident beam intensity I_o, and draw a graph of the normalised intensity against X-ray photon energy or against photon wavelength.

*****

The main part of the program is listed between lines 30 and 610, followed by sixteen procedures.

The incident X-ray spectrum I_o, or the mass attenuation coefficients of a filter element for the photon energy range 12keV to 50keV may be entered into the program at line 60. If these values are already stored on disc file, the program can start at lines 100 to 130 by entering the chemical symbol and thickness of the filter element and the spectrum maximum voltage. The program calculates the intensity I of the X-ray beam for each X-ray photon energy in 1keV increments at line 290, and this filtered spectrum may be stored on disc at line 330 if required.

The array of X-ray photon energies and corresponding filtered beam intensities may be printed on paper at line 430. The total absorbtion by

the filter over the whole energy range is the ratio of the area under the graph of I against energy to that of I_o against energy, calculated between lines 440 and 530, which may be printed on paper at line 560.

A graph of X-ray intensity against energy or wavelength may be drawn by PROCGRAPH defined between lines 630 and 1740. The graph is normalised at line 1080. The graph may be printed on paper at line 1650; or a new spectrum may be selected, or the spectrum may be changed from energy to wavelength, or vice versa. It is also possible to print on paper all together the array of X-ray photon intensities and filtered beam intensities, the filter attenuation of X-rays, and the graph at line 1650. The title of the graph is selected at lines 1250, 1280, 1450 and 1490.

A graph of filter element mass attenuation coefficient, or the incident X-ray spectrum I_o, or the filtered spectrum I, against energy or against wavelength of X-ray photons may be selected at line 920.

```
  5 REM ****SPECTRA****
 10 REM TO CALCULATE X-RAY FILTER BAND SPECTRA
 20 VDU2,1,27,50
 30 VDU3
 40 CLEAR:DIM SPECT(40):DIM MAC(40):DIM FILTERD(40):DIM ENERGY%(40):DIM EQUIVT
HICK(39):DIM A$(70)
 50 MODE 3
 60 REPEAT:CLS:PRINT "DO YOU WANT TO TYPE IN DATA Y/N ?";:Q$=GET$:UNTIL Q$="Y"
 OR Q$="N"
 70 VDU3:CLG
 80 IF Q$="Y" THEN PROCGETDATA ELSE GOTO 100
 90 GOTO 40
100 CLS
110 REPEAT:INPUT"CHEMICAL SYMBOL FOR ELEMENT",ELEMENT$:UNTIL LEN(ELEMENT$)<3
120 INPUT "FILTER THICKNESS mm",T
130 INPUT "SPECTRUM VOLTAGE",kV
140 SPECTkV$="SPCTM"+STR$(kV)
150 X=OPENIN SPECTkV$
160 FOR A=1 TO 39
170 INPUT #X,SPECT(A)
180 NEXT A
190 CLOSE#X
200 X=OPENIN ELEMENT$
210 INPUT#X,F
220 FOR D=1 TO 39
230 INPUT #X,MAC(D)
240 PRINT MAC(D)
250 NEXT D
260 CLOSE#X
270 TH=F*T*0.1
280 REM TO CALCULATE INTENSIY DROP
290 FOR E=1 TO 39
300 FILTERD(E)=SPECT(E)*EXP(-TH*MAC(E))
310 PRINT FILTERD(E)
320 NEXT E
330 REM TO SAVE FILTERED SPECTRUM TO DISC
340 PRINT "DO YOU WANT TO SAVE FILTERED SPECTRUM   ON DISC Y/N ?":Q$=GET$
350 NME$=ELEMENT$+STR$(kV)+RIGHT$(STR$(T),3)
360 IF Q$="Y" THEN GOTO 380
370 IF Q$="N" THEN GOTO 430 ELSE GOTO 340
380 X=OPENOUT NME$
390 FOR F=1 TO 39
400 PRINT #X,FILTERD(F)
410 NEXT F
420 CLOSE#X
430 CLS:PRINT "DO YOU WANT A PRINT OF ENERGIES AND INTENSITIES Y/N ?":Q$=GET$
440 IF Q$="Y" THEN PROCPRINTEANDI
450 FOR X=1 TO 38
460 S1=(SPECT(X)+SPECT(X+1))/2
470 S2=(FILTERD(X)+FILTERD(X+1))/2
480 SUM1=SUM1+S1:SUM2=SUM2+S2
490 NEXT X
500 CLS
510 PRINT "AREA UNDER SPECTRUM=",SUM1
520 PRINT "AREA UNDER FILTER=",SUM2
530 RATIO=SUM2/SUM1
540 PRINT "ATTENUATION=",RATIO
550 VDU3
560 PRINT "DO YOU WANT PRINT OF ABSORBTION RATIOS Y/N ?":Q$=GET$
```

```
570 IF Q$="Y" THEN PROCDUMPABRATIO
580 CLS: PRINT "DO YOU WANT TO DRAW A GRAPH Y/N ?":Q$=GET$
590 IF Q$="Y" THEN GOTO 610
600 IF Q$="N" THEN GOTO 100
610 MODE4:PROCGRAPH
620 GOTO 40
630 DEF PROCGRAPH
640 HEAD$=ELEMENT$+" "+STR$(kV)+"keV"+" "+STR$(T)+"mm"
650 HED$=STR$(kV)+"keV"+" "+"SPECTRUM"
660 HAD$="MASS ABS COEFF vs ENERGY keV"
670 FOR I= 1 TO LEN(HEAD$)
680 A$(I)=MID$(HEAD$,I,1)
690 NEXT I
700 I=25:IF LEN(HEAD$)<=25 THEN GOTO 770
710 REPEAT
720 X$=A$(I)
730 I=I-1
740 UNTIL X$=" "
750 FIRST$=LEFT$(HEAD$,I)
760 SECLN$=RIGHT$(HEAD$,LEN(HEAD$)-I-1):GOTO 810
770 FIRST$=HEAD$
780 SECLN$=" "
790 GOTO 810
800 FIRST$=HED$
810 CLS
820 VDU28,0,29,39,28
830 VDU24,0;150;1279;1023;
840 C$="E":MAX=0
850 PRINT "ENERGY OR WAVELENGHT GRAPH E/W ?":B$=GET$
860 IF B$<>"E" AND B$<>"W" THEN GOTO 850
870 PRINT "DISC OR MEMORY D/M ?":C$=GET$
880 IF C$<>"D" AND C$<>"M" THEN GOTO 870
890 IF C$="D" THEN PROCINDATA
900 IF C$="M" THEN PROCMEMDATA ELSE GOTO 1120
910 DEF PROCMEMDATA
920 PRINT "GRAPH OF MAC A,SPECTRUM S, FILTER I ?":D$=GET$
930 IF D$<>"A" AND D$<>"S" AND D$<>"I" THEN GOTO 920
940 IF D$="A" THEN PROCMAC
950 IF D$="S" THEN PROCSPECTRUM
960 IF D$="I" THEN PROCFILTERED
970 IF D$="S" THEN FIRST$=HED$
980 IF D$="I" THEN FIRST$=HEAD$
990 IF D$="A" THEN FIRST$=HAD$
1000 GOTO 1120
1010 ENDPROC
1020 DEF PROCINDATA
1030 MAX=0
1040 X=OPENIN NME$
1050 FOR J%=1 TO 39
1060 INPUT#X,EQUIVTHICK(J%)
1070 IF EQUIVTHICK(J%)>MAX THEN MAX=EQUIVTHICK(J%)
1080 MAG=700/MAX
1090 NEXT J%
1100 CLOSE#X
1110 ENDPROC
1120 VDU5
1130 IF B$<>C$ THEN CLG
1140 MOVE 0,200:DRAW 1260,200
1150 MOVE 0,200:DRAW 0,1000
1160 FOR I%=0 TO 700 STEP 70
```

```
1170 MOVE 0,I%+200:DRAW 10,I%+200
1180 NEXT I%
1190 MOVE 0,900:DRAW 20,900
1200 MOVE 0,550:DRAW 20,550
1210 C$=B$
1220 IF B$="E" THEN GOTO 1240
1230 IF B$="W" THEN GOTO 1440 ELSE GOTO 850
1240 REM GRAPH OF INTENSITY vs ENERGY
1250 MOVE 250,1000:PRINT "INTENSITY vs ENERGY keV"
1260 GOTO 1290
1270 REM GRAPH OF MASS ABSORBTION COEFFICIENT vs ENERGY
1280 MOVE 250,1000:PRINT "MASS ABS COEFF vs ENERGY keV"
1290 FOR J%=51 TO 1 STEP-1
1300 G=9+J%
1310 MOVE((G*22)-200),200:DRAW((G*22)-200),210
1320 NEXT J%
1330 FOR J%=51 TO 1 STEP-10
1340 G=9+J%
1350 MOVE((G*22)-200),200:DRAW((G*22)-200),220
1360 NEXT J%
1370 MOVE 0,180:PRINT"10     20      30      40      50      60"
1380 MOVE 900,200+EQUIVTHICK(39)*MAG
1390 FOR J%=39 TO 1 STEP-1
1400 G=11+J%
1410 DRAW((G*22)-200),200+EQUIVTHICK(J%)*MAG
1420 NEXT J%
1430 GOTO 1620
1440 REM GRAPH OF INTENSITY vs WAVELENGHT
1450 MOVE 250,995:PRINT "INTENSITY vs WAVELENGTH A"
1460 MOVE 1018,1022:PRINT"."
1470 GOTO 1510
1480 REM GRAPH OF MASS ABSORBTION COEFFICIENT vs WAVELENGTH
1490 MOVE 250,995:PRINT "MASS ABS COEFF vs WAVELENGHT A"
1500 MOVE 1177,1022:PRINT"."
1510 FOR J%=10 TO 1 STEP -1
1520 MOVE J%*124,200:DRAW J%*124,220
1530 NEXT J%
1540 FOR K%=40 TO 1 STEP -1
1550 MOVE K%*31,200:DRAW K%*31,210
1560 NEXT K%
1570 MOVE 0,180: PRINT "0      0.2      0.4      0.6      0.8      1.0"
1580 MOVE (12.4*1240/12),200+EQUIVTHICK(1)*MAG
1590 FOR J%=1 TO 39
1600 DRAW (12.4*1240/(J%+11)),200+EQUIVTHICK(J%)*MAG
1610 NEXT J%
1620 MOVE 350,950:PRINT FIRST$
1630 MOVE 350,900:PRINT SECLN$
1640 VDU4
1650 CLS:PRINT"HARD COPY H,NEW SPECTRA N,CHANGE E&W C, HARD COPY ALL A";:W$=GET
$
1660 IF W$<>"H"AND W$<>"N"AND W$<>"C"AND W$<>"A"THEN GOTO 1650
1670 CLS:IF W$="H" THEN PROCDUMPGRAPH
1680 CLS:IF W$="N" THEN GOTO 40
1690 CLS:IF W$="C" THEN GOTO 850
1700 CLS:IF W$="A" THEN PROCALL
1710 CLS
1720 VDU2,1,12
1730 VDU3
1740 ENDPROC
1750 DEF PROCASSEMB
```

```
1760 M=22405:STORE1=M-10:STORE2=M-20:MEMST=&70:OSWORD=&FFF1
1770 VDU2
1780 FOR N=0 TO 2 STEP 2
1790 P%=M-150
1800 [OPT N
1810 .PLT       LDA #00
1820            TAY
1830 .LOOP1     LDA #00
1840            TAX
1850 .LOOP3     ROR STORE1,X
1860            ROL A
1870            INX
1880            CPX #08
1890            BMI LOOP3
1900            STA STORE2,Y
1910            INY
1920            CPY #08
1930          BMI LOOP1
1940            RTS
1950 ]
1960 NEXT N
1970 ENDPROC
1980 DEF PROCPRINTEANDI
1990 VDU2
2000 PRINT "ENERGY (keV)          WAVELENGHT (A)              Io                  I
 "
2010 FOR G=1 TO 39
2020 ENERGY%(G)=11+G
2030 PRINT ENERGY%(G)," ",(INT(12396/(11+G)))/1000," ",SPECT(G)," ",FILTERD(G)
2040 NEXT G
2050 VDU3
2060 ENDPROC
2070 DEF PROCDUMPGRAPH
2080 PROCASSEMB
2090 VDU2,1,27,1,65,8
2100 VDU2,1,27,1,79
2110 VDU1,13
2120 X%=M-30:Y%=X%DIV256
2130 FORYY%=0TO 8960 STEP 320
2140 VDU1,27,1,75,1,63,1,1
2150 FORXX%=0TO312 STEP8
2160 MEMST=(22528+XX%+YY%)
2170 FOR J%=0 TO 7
2180 STORE1?J%=FNREADIO(MEMST+J%)
2190 NEXT J%
2200 CALL PLT
2210 FORZ%=7TO0STEP -1
2220 VDU1,?(STORE2+Z%)
2230 NEXTZ%
2240 NEXTXX%
2250 VDU1,13
2260 NEXTYY%
2270 *FX21,3
2280 VDU 1,14
2290 VDU3
2300 ENDPROC
2310 DEF FNREADIO(addr):Y%=X%DIV256:!X%=addr:A%=5:CALL OSWORD
2320 =X%?4
2330 PROCALL
2340 VDU2
```

```
 2350 DEF PROCALL
 2360 PROCPRINTEANDI
 2370 PROCDUMPABRATIO
 2380 PROCDUMPGRAPH
 2390 VDU3
 2400 ENDPROC
 2410 DEF PROCGETDATA
 2420 REPEAT:CLS:PRINT "SPECTRUM OR MASS ATTENUATION COEFFICIENTS S/M ?";:Q$=GET
$:UNTIL Q$="S"OR Q$="M"
 2430 IF Q$="S" THEN PROCGETSPECT ELSE PROCGETCOEFF
 2440 ENDPROC
 2450 DEF PROCGETSPECT
 2460 PRINT:INPUT "SPECTRUM VOLTAGE",KV
 2470 SPECTKV$="SPCTM"+STR$(KV)
 2480 FOR A=1 TO 39
 2490 PRINT "INTENSITY AT ENERGY=";11+A;"KeV"
 2500 INPUT SPECT(A)
 2510 NEXT A
 2520 REPEAT:CLS:PRINT"DO YOU WANT TO CHANGE THESE Y/N ?";:Q$=GET$:UNTIL Q$="Y"
OR Q$="N"
 2530 IF Q$="Y" THEN 2460
 2540 X=OPENOUT SPECTKV$
 2550 FOR A=1 TO 39
 2560 PRINT #X, SPECT(A)
 2570 NEXT A
 2580 CLOSE#X
 2590 CLS
 2600 ENDPROC
 2610 DEF PROCGETCOEFF
 2620 CLS
 2630 REPEAT:INPUT"CHEMICAL SYMBOL FOR ELEMENT",ELEMENT$:UNTIL LEN(ELEMENT$)<3
 2640 INPUT "FILTER DENSITY g/cubic cm",F
 2650 FOR B=1 TO 39
 2660 PRINT "INPUT MASS ATTENUATION COEFF AT ENERGY="11+B
 2670 INPUT MAC(B)
 2680 NEXT B
 2690 REPEAT:CLS:PRINT "DO YOU WANT CHANGE THESE (Y/N) ?";:Q$=GET$:UNTIL Q$="Y"
OR Q$="N"
 2700 IF Q$="Y" THEN GOTO 2620
 2710 X=OPENOUT ELEMENT$
 2720 PRINT#X,F
 2730 FOR C=1 TO 39
 2740 PRINT #X,MAC(C)
 2750 CLOSE#X
 2760 CLS
 2770 ENDPROC
 2780 DEF PROCPRINTEANDI
 2790 VDU2
 2800 PRINT "ENERGY (KeV)          WAVELENGHT (A)          Io                I
  "
 2810 FOR G=1 TO 39
 2820 ENERGY%(G)=11+G
 2830 PRINT ENERGY%(G)," ",(INT(12396/(11+G)))/1000," ",SPECT(G)," ",FILTERD(G)
 2840 NEXT G
 2850 VDU3
 2860 ENDPROC
 2870 DEF PROCDUMPABRATIO
 2880 VDU2
 2890 PRINT "SPECTRUM=";SUM1,"FILTER=";SUM2,"  ","ATTENUATION=";RATIO
 2900 VDU3
 2910 ENDPROC
 2920 DEF PROCMAC
 2930 MAX=0
 2940 FOR J%=1 TO 39
 2950 EQUIVTHICK(J%)=MAC(J%)
 2960 IF EQUIVTHICK(J%)>MAX THEN MAX=EQUIVTHICK(J%)
 2970 NEXT J%
 2980 MAG=700/MAX
 2990 ENDPROC
 3000 DEF PROCSPECTRUM
 3010 MAX=0
 3020 FOR J%=1 TO 39
 3030 EQUIVTHICK(J%)=SPECT(J%)
 3040 IF EQUIVTHICK(J%)>MAX THEN MAX=EQUIVTHICK(J%)
 3050 NEXT J%
 3060 MAG=700/MAX
 3070 ENDPROC
 3080 DEF PROCFILTERED
 3090 MAX=0
 3100 FOR J%=1 TO 39
 3110 EQUIVTHICK(J%)=FILTERD(J%)
 3120 IF EQUIVTHICK(J%)>MAX THEN MAX=EQUIVTHICK(J%)
 3130 NEXT J%
 3140 MAG=700/MAX
 3150 ENDPROC
```



```
  5 REM ****FRACION****
 10 CLS
 20 PRINT "THIS PROGRAMME CALCULATES DETECTABLE"
 30 PRINT "FRACTIONS OF ANALYTE/MATRIX ATOMS" '
 40 PRINT "ACCORDING TO GRODZIN'S EQUATION 4 IN"
 50 PRINT "NUCL.INST.AND METH.206 547-52 1983."
 60 INPUT TAB(0,5)"SAMPLE DIAMETER (CM)",D
 70 INPUT "ATTEN. COEFF. OF ANALYTE (M^2/KG)",Ua
 80 INPUT "ATTEN. COEFF. OF MATRIX (M^2/KG)" ,Um
 90 INPUT "TOTAL NUMBER OF STEPS ",n
100 INPUT "TOTAL NUMBER OF PHOTONS",N
110 INPUT "ATOMIC WEIGHT OF ANALYTE",Aa
120 INPUT "ATOMIC WEIGHT OF MATRIX",Am
130 W=D/n
140 X=D*2*EXP(Um*D)
150 Y=(W^3)*(Ua^2*Aa^2*N)/Am^2
160 f=SQR(X/Y)
170 PRINT "THE FRACTION DETECTABLE IS",f
180 GOTO 60
190 END
```

This BBC microcomputer program calculates the minimum detectable fraction of analyte element to matrix atoms in an object scanned with X-rays by L. Grodzin's equation, 3.19.

$$f = \frac{1}{\frac{W\mu_m\mu_a A_a}{\mu_m A_m}} \sqrt{\frac{DBC\mu m}{n_o W}}$$

REFERENCES

[1] W.K. Rontgen, On a new form of radiation, Sitz. Phys. Med. Ges. Wurzburg, 137 (1895); The Electrician 36 (1896) 415.

[2] G.N. Hounsfield, Computerized transverse axial scanning (tomography): Part 1, description of system, Brit.J.Radiol. 46 (1973) 1016.

[3] A.M. Cormack, Representation of a Function by Its Line Integrals, with Some Radiological Applications, J. Appl. Phys. 34 (1963) 2722.

[4] A.M. Cormack, Representation of a Function by Its Line Integrals, with Some Radiological Applications. II, J. Appl. Phys. 35 (1964) 2908.

[5] C.G. Barkla and C.A. Sadler, The Absorbtion of Rontgen Rays, Phil. Mag. 17 (1909) 739.

[6] R. Glocker and W. Frohnmayer, Rontgen-spectroscopic determination of the quantity of an element in mixtures, Ann. Phys. 76 (1925) 369.

[7] S.J. Riederer and C.A. Mistretta, Selective iodine imaging using K-edge energies in computerized X-ray tomography, Med. Phys. 4 (1977) 474.

[8] L. Grodzins, Optimum energies for X-ray transmission tomography of small samples. Applications of synchrotron radiation to computerized tomography I, Nucl. Intr. and Meth. 206 (1983) 541.

[9] L. Grodzins, Critical absorbtion tomography of small samples. Proposed applications of synchrotron radiation to computerized tomography II, Nucl. Instr. and Meth. 206 (1983) 547.

[10] A.C. Thompson, J. Llacer, L. Campbell Finman, E.B. Hughes, J.N. Otis, S. Wilson, and H.D. Zeman, Nucl. Instr. and Meth. 222 (1984) 319.

[11] C.G. Barkla, Secondary Rontgen Radiation, Phil. Mag. 11 (1906) 812.

[12] C.G. Barkla, The Spectra of the Fluorescent Rontgen Radiations, Phil. Mag. 22 (1911), 396.

[13] W.D. Coolidge, A powerful Rontgen ray tube with a pure electron discharge, Phys. Rev. 2 (1913) 409.

[14] J. Fryar, K.J. McCarthy, and A. Fenelon, Differential X-ray absorptiometry applied to computerised X-ray tomography, Nucl. Instr. and Meth. 259 (1987) 557.

[15] J. Fryar, K.J. McCarthy and A. Fenelon, Multi-element imaging in computerised X-ray tomography, Nucl. Instr. and Meth. NIMA 04789.

[16] K.J. McCarthy, Private communication.

J. Yarwood, Volume II Atomic Physics, University Tutorial Press (1963).

T.A. Littlefield and N. Thorley, Atomic and Nuclear Physics, an Introduction, Van Nostrand Reinhold Company (1979).

E.P. Bertin, Principles and Practice of X-ray Spectrometric Analysis, Plenum Press (1975).

H.E. Johns and J.K. Cunningham, The Physics of Radiology, Charles C. Thomas (1983).

R. Jenkins, R.W. Gould, and D. Gedcke, Quantitative X-Ray Spectrometry, Marcel Dekker (1981).

H.W. Barrett and W. Swindell, Radiological Imaging Volume 2, The Theory of Image Formation, detection and Processing, Academic Press (1981).

G.W.C. Kaye and T.H. Laby, Tables of Physical and Chemical Constants and some Mathematical Functions, Longman (1973).

Philips, Automatic Simultaneous X-ray Spectrometer PW1270, Service Manual.

Philips, 22 Channeled simultaneous Spectrometer PW 1270/30 Operating Manual (1974)

DIVISION

This work was done by J. Fryar, K.J. McCarthy, and A. Fenelon at the School of Physical Sciences, National Institute for Higher Education, Dublin.

The three interdependent parts of the work were divided approximately.

J. Fryar - theory and planning

K.J. McCarthy - computing, image reconstruction and experiments

A. Fenelon - X-ray machine and experiments.

The work was shared as follows:

A.F. A simple X-ray K absorbtion edge scanning machine,
conversion of a Philips PW1270 automatic simultaneous X-ray spectrometer to a X-ray machine,
design and construction of the Lead analysing chamber and X-ray beam collimators for the X-ray machine,
design of a X-ray tube cooling water pressuriser with Pump Services Ltd., Dublin, who made the pressuriser,
Possible future development, except scanning and image reconstruction.

K.J.McC. Control of the (x,z,ϕ) scanning coordinate table and X-ray photon pulse counting,
image reconstruction by Filtered Backprojection and by the Algebraic Reconstruction Technique,

an automatic scanning machine with an X-ray line source, design of the steel box, within the Lead analysing chamber, made by T. Walsh, Mechanical Workshop, N.I.H.E.D., 12 BASIC programs for the BBC microcomputer and the VAX11/785 computer.

J.F. Differential absorbtion edge tomography with an X-ray tube, multielement imaging in computerised X-ray tomography, spatial profile of a collimated X-ray beam, 2 BASIC programs for the BBC microcomputer, Two papers published by Nucl. Instr. and Meth..

K.J.McC. A semiautomatic BBC microcomputer controlled scanning machine.
+ J.F.

J.F. Design of X-ray beam transmission filters with the BASIC computer
+ A.F. program SPECTRA.

A.F. SPECTRA computer program
+ K.J.McC

J.F. Areas of overlap between the simulated X-ray beam path and the
+ K.J.McC pixels of the reconstruction grid.
+ A.F. A X-ray scanning machine for imaging atomic elements.

ACKNOWLEDGEMENTS

Grateful acknowledgement is made to

the Research and Postgraduate Studies Committee of N.I.H.E.D. for partially funding this work,

publishers of books for reproduced drawings [referenced] underneath each drawing,

D. Kearney for drawings in two published papers of this work, referenced [14] and [15],

A. Devine for the photographs,

T. Walsh, Mechanical Technician, N.I.H.E.D.,

the Technicians, School of Physical Sciences, N.I.H.E.D.,

Eileen Colgan, for typing the manuscript,

Joseph Fryar, for his supervision and encouragement in this work.